

Atomic Archaeology and Beyond?
*Using gamma radiation survey methods
for the in-situ detection and mapping of
sub-surface deposits*

PhD

School of Archaeology, Geography and Environmental Science

Victoria Robinson

November 2024

Declaration

I confirm that this is my own work and the use of all material from other sources has been properly and fully acknowledged.

- Victoria Robinson

*“Archaeology is the one science that destroys its own lab –
no repeated experiments... it better be done right first time,
or not at all”*

J. W. Weymouth, 1985¹

¹ In: Wynn, J.C. (1986) A review of Geophysical Methods used in Archaeology, *Geoarchaeology*, 1 (3): 245 - 257

Abstract

This research explores the efficacy of gamma radiation surveys as a complementary tool to established geophysical methods used in non-intrusive archaeological investigations. It represents the first reported study of this portable methodology in an archaeological context, with results demonstrating alignment with, and providing additional insights that are complementary to, other traditional methods.

This research tests the hypothesis that historic human activities can influence concentrations of naturally occurring radionuclides in the ground, and that these changes can be measured using portable gamma radiation surveying methods. Data processing then enables the visualisation of these changes. Surveys were undertaken using Groundhog, a rugged gamma radiation detection system designed for the nuclear industry, at Bisham, Silchester and East Heslerton. These sites were chosen to test the technique on known targets with diverse characteristics.

Data was processed using ArcGIS and Geoplot to create gamma radiation distribution maps that enabled identification of anomalies corresponding to known archaeological features. XRF data from environmental and archaeological samples, as well as desktop study data, were analysed to help interpret and understand these observations.

Results indicate that larger features such as roads, ditches and historic field boundaries can be delineated in the gamma radiation data. Other contextual information, such as transitions in geological conditions can also be identified. Accrued data was used to develop a high level model to help predict the influence of different combinations of soil and target types on the effectiveness of the technique. This insight can be used to guide the selection of future sites used in further research.

Findings from this research project suggest that portable gamma radiation surveying could offer a novel complementary tool for archaeological prospection, providing additional interpretive value for existing geophysical outputs. Opportunities have been created for further investigation, particularly in refining the method and its application in diverse archaeological contexts.

Acknowledgements

I would like to express my deepest gratitude to my supervisors, Dr Stuart Black, Dr Rob Fry and Dr Helen Beddow, for their invaluable guidance, support and belief in this novel project from the start. The help you have provided; from assistance in setting up fieldwork opportunities to teaching me how to use Geoplot and XRF systems, amongst other things, is truly appreciated.

I am also grateful to Nuvia for the loan of the Groundhog equipment, without which, this research would not have been possible. Special thanks to Rob and Jonathan for their help and patience in showing me the ropes.

Thank you to my amazing husband, Philip, for your unrelenting support and encouragement, your constructive feedback and for travelling to the ends of the Earth (well, Yorkshire) with me to allow me to collect my data safely. Thank you for your consistent faith in me, especially when I doubted myself. I could not have done this without you!

Thank you to my friends, and especially Steve, Adrian, Kaya and John for your encouragement, enthusiasm and willingness to listen to many practice presentations, discussions on ideas and proof reading passages – it has meant so much.

Finally, I would like to thank my family for your unwavering support and for instilling in me, and encouraging, a life-long love of natural history and archaeology. This thesis is a testament to the foundation you provided.

List of Terms

Term	Definition
Becquerel (Bq)	SI unit of radioactivity. One becquerel is typically defined as the activity of a quantity of radioactive material in which one nucleus decays per second.
Collimator	The collimator (typically lead) shields the detector ensuring that it is sensitive only to radiation directly beneath it.
Counts per Second (cps)	<p>The number of radioactive disintegrations registered by the detector used per second. This provides an indication of the intensity of the radiation present.</p> <p>As detectors are not 100% efficient, this measurement is only broadly proportional to the activity of the material being surveyed. It is therefore important that 'cps' is not confused with Bq. The former records the number of decays that have been <i>measured</i> per second, whereas the latter is a precise number radioactive decays that <i>have occurred</i> per second.</p>
Daughter (isotope)	The resultant element/product generated following the radioactive decay of the parent radionuclide. The daughter product can also be a radionuclide (and itself undergo radioactive decay) or a stable element.
eU/eTh	Equivalent uranium/ thorium – Both U-235 and Th-232 decay through the emission of an alpha particle. This cannot be detected using gamma detectors. As a result, the gamma emissions of daughter isotopes is used. For example, the presence of uranium can be established through for high resolution gamma spectrometry, uranium is detected through its daughters Th-234, Pb-214 and Bi-214. The quantity/ concentration of these radionuclides is therefore typically presented as equivalent values.
Primordial Radionuclide	Radionuclides generated from the 'Big Bang'
Roentgen equivalent man (Rem)	Similar to sieverts, the Rem is a method of measuring exposure to an ionising radiation dose. This unit of radiation dose is typically used in the USA.
Scintillator/ Scintillation Detector	A material that luminesces (generates visible or near-visible light) following excitation by high energy incident radiation.
Sievert (Sv)	A sievert is an SI unit for measuring exposure to an ionising radiation dose and associated health effects.
Spectrometry	Analysis of the measured energies of gamma rays emitted from a sample, to identify the specific radionuclides present.

Acronyms and Abbreviations

Acronym/ Abbreviation	Definition
μR	Micro Rem
Bq	Becquerel
CPS	Counts Per Second
CsI(Tl)	(Thallium Activated) Caesium Iodide (detector)
CZT	Cadmium Zinc Telluride (detector)
FIDLER	Field Instrument for the Detection of Low-Energy Radiation
GIS	Geographic Information System
GPR	Ground Penetrating Radar
GPS	Global Positioning System
HBRNA	High Background Natural Radiation
HPGe	High Purity Germanium (detector)
HRGS	High Resolution Gamma Spectrometry
IAEA	International Atomic Energy Agency
ISOCS	In-Situ Object Counting System
LiDAR	Light Detection and Ranging
Nal(Tl)	(Thallium Activated) Sodium Iodide (detector)
NOR	Naturally Occurring Radionuclide
OUMNH	Oxford University Museum of Natural History
PCA	Principal Component Analysis
PGRS	Portable Gamma Ray Spectrometer
PVC	Polyvinyl Chloride
R/Rem	Roentgen equivalent man
Th/K	Thorium/Potassium
Th/U	Thorium/ Uranium
TNORM	Technologically Enhanced Naturally Occurring Radioactive Material
UMHK	Union Manière due Haut Katanga
UMPC	Ultra-Mobile Personal Computer
ZnS(Ag)	Silver-activated Zinc Sulphide (detector)

List of Isotopes

Isotope	Definition
Am-241	Americium-241
Bi-214	Bismuth-214
C-14	Carbon-14
Co-60	Cobalt-60
Cs-137	Caesium-137
K-40	Potassium-40
Pb-206	Lead-206
Pb-214	Lead-214
Po-210	Polonium-210
Pu-239	Plutonium-239
Ra-226	Radium-226
Rn-222	Radon-222
Tc-99m	Technetium-99 (meta-stable)
Th-232	Thorium-232
Th-234	Thorium-234
Tl-208	Thallium-208
U-235	Uranium-235
U-238	Uranium-238

Contents

1	Research Background and Rationale	14
1.1.1	The Importance of Multiple Non-Intrusive Survey Methods in Archaeology – Research in Context.....	14
1.1.2	Testing the Feasibility of Radiation Surveying Methods in Archaeology – Addressing the Knowledge Gap	16
1.1.3	Key Concept – An Introduction to Groundhog	19
1.2	Research Aim	24
1.3	Research Objectives.....	25
1.4	Thesis Scope and Outline.....	25
1.5	References	29
2	Literature Review	31
2.1	Introduction	31
2.1.1	Contribution of Gamma Spectrometry to Site Investigations – An Overview	32
2.2	Radioactivity in the Environment	33
2.2.1	Sources of Naturally Occurring Radioactivity.....	34
2.2.2	Influence of Geology on Radionuclide Concentrations in the Environment.....	35
2.3	Methods of Detecting Radioactivity in the Environment and their Applications.....	39
2.3.1	Alpha/ Beta Radiation Detection.....	40
2.3.2	Gamma Radiation Detection	40
2.3.3	Application of Gamma Radiation Surveys.....	51
2.4	Use of Gamma Radiation Surveys in an Archaeological Context	59
2.4.1	Existing Non-Intrusive Techniques in Archaeological Prospection	60
2.4.2	Gamma Radiation Surveying of Archaeological Sites.....	68
2.4.3	Advantages and Limitations of Gamma Radiation Surveying in an Archaeological Context.....	77
2.5	Conclusion: Gamma Radiation Surveying in the Geophysics Toolbox.....	82
2.6	References	84
3	RESEARCH PROJECT METHODOLOGY	95
3.1	Introduction	95
3.2	Addressing the Research Problem.....	96
3.3	Data Collection Method – What, Why and How?	98
3.3.1	Data Requirements and Management (What and Why).....	98

3.3.2	Data Collection in the Field – An Iterative Process (How)	102
3.3.3	Sampling and Analysis of Soil and Target Samples (How)	112
3.3.4	Benefits and Limitations of the Chosen Survey Methodologies.....	113
3.4	Data Collection Method – Where and When?	115
3.4.1	An Ideal Test Site – Silchester Roman Town, Hampshire	115
3.4.2	Looking Further Afield – Bisham, Berkshire and East Heselton	116
3.4.3	Challenges Faced and Mitigations	118
3.5	Data Analysis Methods (Why and How)	119
3.5.1	Data Preparation and Processing	119
3.5.2	Data Analysis and Interpretation.....	120
3.5.3	Benefits and Limitations of the Methods Used	123
3.6	Conclusions.....	124
3.7	References	125
4	Portable Gamma Ray Spectrometry for Archaeological Prospection: A Preliminary Investigation at Silchester Roman Town.....	127
4.1	Introduction to Paper (as published in Archaeological Prospection, Vol 29(3))	127
4.2	Confirmation of Candidate Contribution.....	129
4.3	Published Paper	130
4.3.1	Keywords.....	130
4.3.2	Abstract	130
4.3.3	Introduction.....	131
4.3.4	Study Site and Existing Data	137
4.3.5	Methodology	140
4.3.6	Results	144
4.3.7	Discussion.....	155
4.3.8	Conclusions.....	157
4.3.9	References.....	158
4.4	Paper Impact.....	158
4.5	Conclusions and Next Steps.....	161
4.6	References	162
4.7	Supplementary Data	167
5	Radiating Encouragement: Further Investigation into the Application of Gamma Ray Spectroscopy for archaeological prospection at the Roman Town of Silchester	170
5.1	Introduction to Paper (as published in Archaeological Prospection, Vol 31(3))	170

5.2	Confirmation of Candidate Contribution.....	171
5.3	Published Paper	172
5.3.1	Keywords.....	172
5.3.2	Abstract	172
5.3.3	Introduction.....	173
5.3.4	Building on a Preliminary Investigation at Silchester.....	175
5.3.5	Current Study Site and Existing Data.....	177
5.3.6	Methodology.....	180
5.3.7	Results	190
5.3.8	Discussion.....	199
5.3.9	Conclusions.....	203
5.3.10	References	205
5.4	Conclusions and Next Steps.....	205
5.5	References	207
6	Exploring the Value of Gamma Radiation Surveys in Archaeological Prospection – A Consolidating Study	211
6.1	Introduction to the Paper.....	211
6.2	Confirmation of Contribution	213
6.3	Published Paper	214
6.3.1	Keywords.....	214
6.3.2	Abstract	214
6.3.3	Introduction.....	215
6.3.4	Looking Further Afield – New Study Sites	219
6.3.5	Methodology.....	223
6.3.6	Results	231
6.3.7	Discussion.....	247
6.3.8	Conclusion	254
6.3.9	References.....	254
6.4	Conclusions and Next Steps.....	255
6.5	References	256
7	Discussion.....	260
7.1	Introduction	260
7.2	Key Findings	261
7.3	Limitations and Impacts of the Selected Methodology.....	265

7.4	Interpretation and Evaluation of Results.....	270
7.5	Implications of this Research and Recommendations for Future Work.....	275
7.5.1	Recommendations for Future Work	276
7.6	References	279
8	Conclusion	281
8.1	Answering the Research Question	281
8.2	Closing Comments	283
	Appendix 1 - Raw Data	285
	Appendix 2 – As Published Papers	287

List of Figures

No.	Title	Page
Figure 1.1	Geophysics in Archaeology: A Timeline.	18
Figure 1.2	Schematic Layout of the Groundhog Fusion System.	20
Figure 1.3	Example of a gamma radiation distribution map. Elevated areas of radioactivity are shown red and orange colours, moderate levels in light greens and blues, and low areas of activity in dark green and purple. Areas found to contain Cs-137 are flagged with a yellow triangle.	23
Figure 1.4	Example of a count rate distribution graph generated from Groundhog data. This chart shows a normal distribution.	23
Figure 1.5	Example of mapped Groundhog measurements and graph showing the measured spectrum. The graph confirms the presence of Bi-214 – a daughter product within the U-238 decay chain.	24
Figure 2.1	Global distribution of naturally occurring radionuclides in soil where data is available. Mean and maximum values for K-40 (A, B), U-238 (C, D), Th-232 (E, F) are presented	38
Figure 2.2	Overview of the Groundhog Processing System	45
Figure 2.3	Nuvia Groundhog System in Uncollimated (A) and Uncollimated (B) Configurations	46
Figure 2.4	Examples of some of the more common Groundhog configurations. The Fusion System (front) will be deployed as part of this study.	48
Figure 2.5	Sample Map Produced by ArcGIS Showing Dose Rate in $\mu\text{Sv/hr}$. The typical cell resolution is set at 0.25 m.	50
Figure 2.6	Measured Radioactivity (Total Gamma Counts Collected) in Counts Per Second (CPS). Inset graph focusses on spectra data for an area of interest, showing presence of Bi-214	50
Figure 2.7	Overview of the Typical Applications of Gamma Surveys	51
Figure 2.8	Gamma Flux (cps) Profiles for the D1 Spoil Heap at the Olen Metal Ore Processing Site	54
Figure 2.9	Gamma Flux (cps) Profiles for the Stort 1 Spoil Heap at the Olen Metal Ore Processing Site	55
Figure 2.10	Radiation Contour Map of Stort 1, Showing Gross Gamma Flux in Counts Per Second. These images were generated as part of an earlier Groundhog Survey undertaken in 2003	56
Figure 2.11	Red-green-blue composite generated by Keay, <i>et. al.</i> combining the geophysical responses from the multiple survey methods used. This image has supported identification of more subtle features that might otherwise have been missed	66
Figure 3.1	Relationship between naturally occurring radioactivity in buried targets, the surrounding substrate and the type of anomaly generated in mapped gamma radiation data. Approximate positions of targets from published studies that produced positive anomalies are plotted, along with the hypothesised position of a scenario expected to produce a negative anomaly.	97

No.	Title	Page
Figure 3.2	Overview of research variables explored when deploying the portable gamma radiation surveying system Groundhog	102
Figure 3.3	Operational view of the Groundhog UMPC. The radiation measurements (green bars), coordinates, velocity and alarm notices can be seen. Note: It is possible to see data being recorded for three detector units in this example. This photo was taken during a later vehicle based survey at Silchester.	108
Figure 3.4	1 metre transect survey pattern used for the preliminary Groundhog survey undertaken at Silchester.	109
Figure 3.5	Groundhog in a collimated configuration. The detector is shown sitting within lead shielding at the back of the trolley.	109
Figure 3.6	0.5 metre transect survey pattern used for the second Groundhog survey undertaken at Silchester during the follow-up study at the site, and latterly East Heselton. This figure highlights the significant impact utilising a 0.5 m grid has on measurement density, when compared to 1 m transects. Unfortunately, this method had a negative impact on data quality and was therefore discounted.	110
Figure 3.7	Left: View of the Groundhog in its vehicle-mounted configuration. Right: Fitting the mounting frame	111
Figure 3.8	Planned route of the Groundhog vehicle in a spiral pattern. The alternating colours for each pass demonstrates how an overlap is achieved.	111
Figure 4.1	NUVIA Groundhog [®] system in Uncollimated (a), collimated (b) and vehicle mounted (c) configurations. Sources: Personal photographs, NUVIA (2021)	134
Figure 4.2	Survey Locations (a, Urban Area; b, Cremation/ Inhumation Site; c, Temple Area, d, Kiln Area) in the context of the site of the Roman town of Calleva Atrebatum (Silchester).	139
Figure 4.3	Scheme diagram showing the Groundhog [®] detector in its collimated configuration.	142
Figure 4.4	Comparison of fluxgate gradiometer data (+/- 7nT) (a) against total gamma radiation data (b) collected at the Urban Area (Site A). Both collimated and uncollimated measurements are presented. Radiation data are displayed in cps. No clear anomalies have been identified. An area of increased activity in the bottom right corner of the survey area may be attributable to a modern feature (buried pipe). An area of elevated activity to the left of the survey area broadly aligns with the cross road. However, due to its distribution, it may be a naturally occurring feature.	146

No.	Title	Page
Figure 4.5	Frequency distribution graphs for Site A (Urban Area), uncollimated (a) and collimated (b); Site B (Cremation/ Inhumation Area) uncollimated (c); Site C (Temple Area), uncollimated (d); and Site D (Kilns Area, uncollimated (e) and collimated (f). Each chart shows a normal distribution of count rates with the exception of the uncollimated data collected for the Kilns area (e). This graph shows two distinctive activity distributions indicative of two different material types. This differentiation is likely attributable to the former clay pit (which has since been backfilled) in this area (Figure 4.9 and Figure 4.10).	147
Figure 4.6	Comparison of fluxgate gradiometry data (+/- 5nT) (a) against total gamma radiation data (b) collected at the Cremation/Inhumation Area (Site B). Uncollimated survey data are displayed in cps. No clear anomalies are observable. The area of elevated activity at the top of the survey area is expected to be naturally occurring.	148
Figure 4.7	Comparison of fluxgate gradiometry data (+/- 5nT) (a) against total gamma radiation data (b) collected at the Temple Area (Site C). Uncollimated survey data are displayed in cps. A clear linear anomaly of depleted radioactivity can be seen in the left-hand side of the survey area. This aligns with an anomaly visible in the fluxgate gradiometry data, which is known to be a Temenos wall.	149
Figure 4.8	Comparison of caesium magnetometry data (+/- 7nT) (a) against total gamma radiation data (b) collected at the Kiln Area (Site D). Both collimated and uncollimated measurements are presented. Radiation data are displayed in cps. An area of depleted radioactivity in the upper half of the Groundhog® survey area aligns with the clear anomaly present in the geophysics data. A 'P'-shaped anomaly in the bottom left corner of the survey area broadly aligns with one of the kilns but is assumed to be naturally occurring.	152
Figure 4.9	Ordnance Survey map from 1912 showing where the kiln survey area (blue square) overlaps the site of a disused modern claypit (shaded light red).	153
Figure 4.10	(a) 1947 aerial photo showing the sight of the Little London claypit (circled in red) infilled and covered with a well-established tree stand, (b) Modern satellite image of the same site showing absence of the tree stand and revealing a distinct discolouration of the grass covering the former claypit, (c) Modern satellite image overlayed with Caesium Magnetometer data revealing the Roman Kilns, modern clay pit (circled in red) and the area subject to Groundhog survey (red square).	154
Figure S4.1	Response Curve of Groundhog Detector GN08 to a 6 kBq Cs-137 Source as Part of Calibration Checks.	167
Figure 5.1	Survey areas one and two, highlighted in red and blue respectively, in the context of Silchester Roman Town and surrounding area. Inset: <i>Insulae</i> covered by the survey area.	178
Figure 5.2	Close-up view of the survey areas overlaying the fluxgate gradiometer data (+/- 7nT – black high to white low). The figure shows the targets present within Area A (outlined in red) and Area B (outlined in blue).	180

No.	Title	Page
Figure 5.3	View of the Nuvia survey vehicle, fitted with three Groundhog® Detectors and GPS system secured to the front. The detectors are spaced 1 m apart and positioned ~20 cm above ground level.	183
Figure 5.4	Plot of the GPS/ gamma radiation data points (blue) collected during the August 2022 survey, highlighting the area affected by missing GPS data (outlined in red).	185
Figure 5.5	Preliminary attempt at creating visualisations by combining the August 2022 and May 2023 datasets. This shows how the overlaid data is obscuring any anomalies, and indeed creates false positives as highlighted in the green oval.	186
Figure 5.6	Plot of the GPS/ gamma radiation data points collected during the August 2022 and May 2023 surveys. Areas 1 and 2 denote where data was sampled for statistical analysis.	187
Figure 5.7	Impact of different Geoplot processing tools on image quality for August 2022 total gamma counts (cps). The methods presented here are: 'No Processing' (A), 'GPS Gap Fill' (B), GPS Gap Fill + Wallis Filter (C), GPS Gap Fill + Median Filter (D), GPS Gap Fill + Low Pass Filter (E) and GPS Gap Fill + High Pass Filter (F). The GPS Gap Fill + Wallis Filter (C) was identified as the preferred processing method.	192
Figure 5.8	Count rate distribution graphs for the August 2022 (left) and May 2023 (right) datasets. The August 2022 chart indicates that the background radioactivity is not normally distributed.	193
Figure 5.9	Impact of different Geoplot processing tools on image quality for May 2023 total gamma counts (cps). The methods presented here are: 'No Processing' (A), 'GPS Gap Fill' (B), GPS Gap Fill + Wallis Filter (C), GPS Gap Fill + Median Filter (D), GPS Gap Fill + Low Pass Filter (E) and GPS Gap Fill + High Pass Filter (F). The GPS Gap Fill + Wallis Filter (C) was identified as the preferred processing method.	194
Figure 5.10	Application of the GPS Gap Fill + Wallis Filter to the following regions of interest within the August 2022 dataset, as per Table 5.2: Potassium (A), Uranium (B), Thorium (C), Caesium (D), Below Window (E) and Above Window (F).	196
Figure 5.11	Application of the GPS Gap Fill + Wallis Filter to the following regions of interest within the May 2023 dataset, as per Table 5.2: Potassium (A), Uranium (B), Thorium (C), Caesium (D), Below Window (E) and Above Window (F).	197
Figure 5.12	August 2022 (left) and May 2023 (right) Geoplot-processed data overlaid on existing Fluxgate Gradiometer data, demonstrating the alignment of observed anomalies. Gamma radiation data has been set at 25% transparency to reveal underlying anomalies. Data Source: Fluxgate Gradiometer Data from Creighton and Fry (2016).	198

No.	Title	Page
Figure 5.13	Combined August 2022 and May 2023 Geoplot-processed data overlaid on existing Fluxgate Gradiometer data, with previously mapped features overlaid demonstrating alignment of the anomalies in the gamma radiation data with known features. Overlaid data includes the Antiquaries Great Plan (pink lines), the Fluxgate Gradiometer interpretation of the roads (black outlines), positive linear anomalies in the Fluxgate Gradiometer data (blue lines) and historic field boundary from 1759 (red dotted line). Data Source: Fluxgate Gradiometer data and building overlays from Creighton and Fry (2016).	199
Figure 6.1	Silchester survey areas (inset) in the context of the surrounding area and local geology. Survey areas outlined in red are those from the 2022 study. The area outlined in blue denotes the location of the August 2022/ May 2023 surveys.	217
Figure 6.2	Bisham survey area (inset), outlined in red, in the context of the surrounding area and local geology.	221
Figure 6.3	East Heselton survey area (inset), outlined in red, in the context of the surrounding area and local geology.	222
Figure 6.4	Groundhog deployed at Bisham in a hand-held configuration. The detector unit is carried against the body with a straight arm, maintaining the face of the detector ~20 cm above the ground surface. The data logger (UMPC) is attached to the backpack enabling hands-free use.	225
Figure 6.5	Groundhog Configuration used at the East Heselton site. The three gamma detector units along with the GPS antennae can be seen fixed to the front of the vehicle.	226
Figure 6.6	(A) Magnetometer survey showing the features targeted in the gamma radiation survey; a chalk pit, Medieval burial and historic field boundary. The survey area is outlined in red. (B) Gamma radiation distribution map overlaying the existing magnetometer survey data for Bisham, highlighting a clear transition from an area of higher radioactivity towards the eastern side of the survey area to an area of lower activity in the west.	233
Figure 6.7	Composite figure revealing the impact of different energy windows on the clarity of the linear anomaly at the Bisham site. (A) Potassium (1400 – 1600 keV), (B) Uranium (1600 – 1900 keV), (C) Thorium (2500 – 3000 keV), (D) Above Window (760 – 3000 keV), (E) Below Window (0 – 530 keV) and (F) Caesium (581 – 740 keV) energy windows are shown against the Total Gamma data (G) image. All images utilised GPS Gap Fill + Wallis Filter.	234
Figure 6.8	Count rate distribution graph for the Bisham survey, suggesting the background radiation data are not normally distributed.	235
Figure 6.9	View of the Bisham survey area dating to c. 1805 – 1845. No field boundaries or other geological features aligning with the anomalies found in the gamma radiation or magnetometer survey data can be seen. The approximate location of the survey area in Bisham is outlined in red.	226

No.	Title	Page
Figure 6.10	Comparison of the Frequency Domain Electro Magnetic (FDEM) survey data (PRPHIP) (A) which reveals the Roman ladder settlement (bottom left) and transition in geological conditions (top right – circled in orange) within the survey area (outlined in red), with overlaid gamma radiation data for the East Heselton site in greyscale (B) and colour (C) palettes. Gamma radiation data (GPS Gap Fill + Wallis Filter) reveals linear anomalies on the western side of the survey area, broadly correlating with the ladder settlement evident in (A). These anomalies are more discernible in the greyscale palette (B) and are circled in blue. However, diagonal linear lines emanating from the corners of the survey area (circled in orange) likely result from vehicle manoeuvring and are considered artefacts. A distinct area of depleted radioactivity is observed in the northeastern corner of the survey area and is particularly pronounced in the colour palette (C). To further highlight this, the below window gamma data (D) is shown overlaying the ladder settlement at 65% transparency to highlight the relative locations of the linear anomalies in the gamma data and the ladder settlement.	239
Figure 6.11	Composite figure revealing the impact of different energy windows on the clarity of the linear anomaly at the East Heselton site. (A) Potassium (1400 – 1600 keV), (B) Uranium (1600 – 1900 keV), (C) Thorium (2500 – 3000 keV), (D) Above Window (760 – 3000 keV), (E) Below Window (0 – 530 keV) and (F) Caesium (581 – 740 keV) energy windows are shown against the Total Gamma (G) data image. All images applied GPS Gap Fill + Wallis Filter.	240
Figure 6.12	Composite figure revealing the impact of different energy windows on the clarity of the linear anomaly at the Silchester site (August 2022 survey). (A) Potassium (1400 – 1600 keV), (B) Uranium (1600 – 1900 keV), (C) Thorium (2500 – 3000 keV), (D) Above Window (760 – 3000 keV), (E) Below Window (0 – 530 keV) and (F) Caesium (581 – 740 keV) energy windows are shown against the Total Gamma data (G) image. All images applied GPS Gap Fill + Wallis Filter.	241
Figure 6.13	Composite figure revealing the impact of different energy windows on the clarity of the linear anomaly at the Silchester site (May 2023 survey). (A) Potassium (1400 – 1600 keV), (B) Uranium (1600 – 1900 keV), (C) Thorium (2500 – 3000 keV), (D) Above Window (760 – 3000 keV), (E) Below Window (0 – 530 keV) and (F) Caesium (581 – 740 keV) energy windows are shown against the Total Gamma data (G) image. All images applied GPS Gap Fill + Wallis Filter.	242
Figure 6.14	Count rate distribution graph for the East Heselton survey, suggesting the background radiation data are normally distributed.	243
Figure 6.15	Histogram showing the distribution of radionuclides of interest for this study across the Regions of Interest (ROI) in the Groundhog system. The absorption efficiency of the detector for each ROI is also presented. Most radionuclides are concentrated within the lower energy windows, where the Groundhog system demonstrates the highest efficiency.	251

No.	Title	Page
Figure 6.16	Model depicting optimal conditions for conducting gamma radiation surveys in archaeological prospection, along with a 'potential region of invisibility' where the contrast in naturally occurring radioactivity between archaeological targets and surrounding substrate is minimal. Approximate locations of Silchester, Bisham and East Heselton are shown. The figure demonstrates how the gravel/ flint roads of Silchester would yield a reasonable negative contrast relative to the surrounding soil, as seen in the gamma radiation surveys.	253
Figure 7.1	Overview of the iterative approach to developing the strategy and methodology for this project.	263
Figure 7.2	A comparison of the 'Total Gamma', 'Above Window' and 'Below Window' energy window representations of the negative anomaly delineating the main Roman road running through Silchester. All images applied GPS Gap Fill + Wallis Filter.	272
Figure 7.3	A comparison of the 'Total Gamma', 'Above Window' and 'Below Window' energy window representations of the positive anomaly associated with the ladder settlement at East Heselton. All images applied GPS Gap Fill + Wallis Filter.	273
Figure 7.4	Graphic showing the anticipated impact of burial depth of a point source, containing either a higher or lower concentration of radioactivity relative to the surrounding soil, on the strength of the anomaly generated.	274

List of Tables

No.	Title	Page
Table 2.1	List of Minerals Associated with Potassium, Uranium and Thorium, with Common through to Rare Incidences Considered	39
Table 2.2	Overview of Groundhog Systems Available for Carrying out Radiation Surveys and their Applications	47
Table 2.3	Overview of Viable Target Types and Areas of Susceptibility for the Common Geophysical Survey Methods	67
Table 2.4	Indicative values of radionuclide concentrations within common building materials	77
Table 2.5	Overview of Advantages and Limitations Associated with the Application of Gamma Radiation Detection Spectrometry (Groundhog) to Archaeological/ Palaeontological Surveys	78
Table 3.1	Overview of the Proposed Strategy for Collecting the Data Required to Address the Research Question	99
Table 4.1	Summary survey statistics for Sites A–D, showing the minimum, maximum and average total gamma (counts per second) and total number of measurements taken	151
Table S4.1	Descriptions of the Four Sites Subject to Groundhog Surveying	168
Table 5.1	Results from a two-tailed t-test for sub-sets of overlapping data from the August 2022 and May 2023 surveys as shown in Figure 5.6	187
Table 5.2	Regions of Interest Subject to Interrogation via Geoplot	189
Table 5.3	Summary statistics for the August 2022 and May 2023 surveys shown against the July 2019 Urban Area survey for comparison. This highlights the improved survey density achieved by the vehicle mounted	191
Table 6.1	Overview of the Results from the annual calibration checks for the three detectors used in the East Heselton Survey. Results are presented for the efficiency (net cps values) and energy resolution (FWHM) of the detectors.	227
Table 6.2	Summary Statistics from the gamma radiation survey of the Bisham Site. Values are provided for total gamma only.	235
Table 6.3	Summary statistics from the gamma radiation survey of the East Heselton Site. Values are provided for total gamma only.	238
Table 6.4	Results of pXRF analysis showing the average concentrations of naturally occurring uranium (U), thorium (Th) and potassium-40 (K-40) in environmental and archaeological samples from Silchester and East Heselton. For Silchester, mean concentrations (\pm error) are calculated from triplicate measurements per sample. For East Heselton, values represent average concentrations (\pm error) across each borehole. Mean soil concentrations of U, Th and K for the Bisham site (published data) are included for completeness. Isotope ratios (Th/K, Th/U and U/K) for all measurements are also presented.	246
Table 6.5	Overview of the gamma emitters and their peak energies from the potassium-40, uranium-238 and thorium-232 decay chains.	251
Table 7.1	Overview of challenges and limitations of the methodologies applied, impacts on the study and mitigation measures applied.	265



CHAPTER 1

General Introduction

1 RESEARCH BACKGROUND AND RATIONALE

This study offers a new body of research into the efficacy of portable gamma radiation surveying methods in the context of archaeological prospection, shedding light on a potential new tool in the existing collection of non-intrusive survey methods. The research findings, presented here principally as a collection of papers, include the first reporting of a vehicle-mounted gamma radiation survey at an archaeological site in the published literature.

1.1.1 The Importance of Multiple Non-Intrusive Survey Methods in Archaeology – Research in Context

The discovery of archaeological features through non-intrusive means dates back to c. 1919 and the application of aerial photography for military intelligence. One of the earliest examples identified is the discovery of the remains of an ancient city in Samarra, Mesopotamia by Lieutenant Colonel George Beazley (Beazley 1919). Without this intervention, it was noted by Lieutenant Beazley that the ancient city would likely have remained undiscovered (Beazley 1919).

Two decades later, the first targeted ground-based systematic survey took place using non-intrusive methods in Williamsburg Virginia, USA (Gaffney and Gater 2003). Whilst this initial survey was unsuccessful, it paved the way for the development of an ever-broadening array of geophysical methods for archaeological exploration. This culminated with the preliminary application of Ground Penetrating Radar (GPR) in archaeology in 1970 (Clark and Clark 1997). It would be another ~50 years before the application of gamma radiation survey methods for archaeological prospection would be tentatively explored. Figure 1.1 presents a timeline that situates the research presented in this thesis within the broader context of the development of traditional geophysical methods. It begins with an aerial photograph of Stonehenge – the first recorded example of an aerial image of an archaeological site in the UK (Barber 2006). It is highlighted that this research project represents the first in-depth study into the use of portable gamma radiation survey methods in this context.

Geophysical surveys add notable value to archaeological investigations and can be applied in isolation or as part of a phased approach to identifying historic man-made features. Their scalability and non-intrusive nature can facilitate the time- and cost-effective characterisation of

an entire site without disturbing the site, or destroying valuable data preserved within the soil strata (Barker 1993, Drewett 2011, Perrin *et. al.* 2014). This approach is particularly advantageous for culturally sensitive or agriculturally active sites.

In addition to generating archaeological data that is highly valuable in its own right, the output from geophysical surveys can be used to optimise the placement of excavations. This ensures the maximum amount of information is collected during an excavation, which, in contrast to a geophysical survey, is cost-, time-, and resource-intensive and, due to its destructive nature, unrepeatable (Barker 1993).

All geophysical methods rely on the presence of measurable differences in the physical properties of a target and the surrounding substrate, such as variations in magnetic field, density or conductivity. In consequence, the effectiveness of a technique can be influenced by the physical and chemical properties of the target and surrounding soil, target size and target burial depth (Ruffell and McKinley 2008). Further, some methods, such as magnetic techniques, can be susceptible to modern man-made features such as fences or pipelines. It is therefore crucial that the geological conditions of the site, characteristics of the anticipated target type(s) and local site conditions (e.g., presence of modern features) are considered to identify the most appropriate survey method. The ability to deploy a minimum of two geophysical techniques at a site, where practicable, may also be considered beneficial. This approach recognises that applying a single geophysical method will only provide a partial view, measuring variations in only one characteristic. Such an approach is at increased risk of incurring false positives, where an anomaly is wrongly identified as a feature of archaeological interest, or false negatives where it is wrongly concluded that there are no features of interest present. Additionally, it is acknowledged that the interpretation of geophysical data is subjective (Schmidt and Ernenwein 2022) and will be influenced by the expertise and past experience of the interpreter. By comparing data sets from contrasting but complementary survey methods, there is a greater chance of identifying and rejecting false positive and false negative conclusions, thereby increasing the confidence in data interpretation; particularly where anomalies are absent or indistinct in one of the data sets.

The value of applying optimally targeted geophysical survey methods, accounting for site-specific conditions, and applying multiple survey methods to aid data interpretation is recognised. This

research seeks to add further value by introducing a new, complementary tool to the toolbox of non-intrusive survey methods in the form of portable gamma radiation surveying. As explored within this thesis, measuring the radiological properties of an archaeological site offers a unique dataset to support characterisation by providing new insights into its physical and chemical properties. The distinct nature of gamma radiation data, when combined with other geophysical data sets, may increase interpretive value by enhancing or revealing features/ characteristics not visible through traditional survey methods. Consequently, overall understanding of the archaeological site can be improved.

1.1.2 Testing the Feasibility of Radiation Surveying Methods in Archaeology – Addressing the Knowledge Gap

Everything around us is radioactive; from the ground beneath our feet, to the food we eat and even the air we breathe. There are various mechanisms, both natural and man made that can influence the concentrations of this radioactivity. Changes in rock type, soil chemistry, vegetation cover and even recent rainfall can cause measurable changes in detectable radiation levels. Throughout history, humans have also influenced these concentrations by importing materials from other regions, concentrating materials naturally rich in radioactivity (such as clay in brick making) and through other industrial activities. This is explored in more detail in Chapter 2.4.3.

Based on this insight, this research tests the following hypothesis:

“Some past human activities have created measurable differences in concentrations of naturally occurring gamma radiation emitting radionuclides, enabling detection of buried structures and objects of archaeological interest using portable gamma radiation surveying methods”.

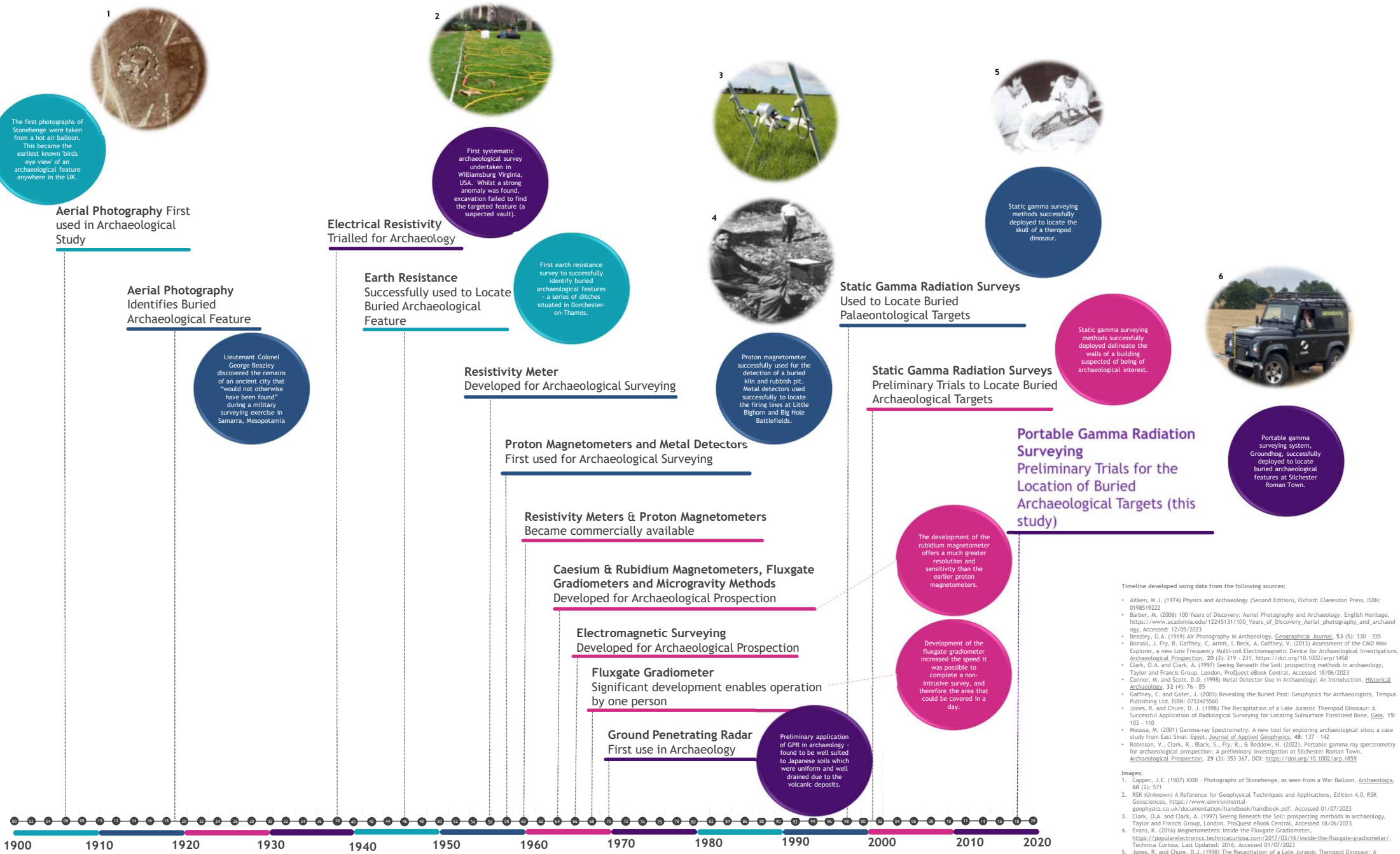
This hypothesis follows a similar principle to the geophysical methods discussed previously, which measure variations in other physical properties such as variations in magnetic field to delineate archaeological features. To test this hypothesis, extensive gamma radiation surveys have been conducted at several known archaeological sites. Evidence also suggests that the process of fossilisation can also create measurable differences in gamma radioactivity concentrations under the right conditions. Therefore, gamma survey methods could potentially be used to help locate

buried fossilised bone deposits. This aspect has been briefly explored as part of this research, with an aim to investigate this further in future work.

The findings presented within this thesis aim to address what is understood to be a significant knowledge gap. As explored in the literature review (Chapter 2) there appears to be fewer than ten papers examining the potential use of static gamma radiation methods in archaeological investigation. This research aims to build on these early studies by testing the efficacy of *portable* gamma radiation surveying methods which can be more easily be deployed at the scale of an archaeological site. This approach significantly increases the amount of data that can be collected and the area that can be realistically surveyed. Further, as demonstrated in this thesis, the data outputs are analogous to those generated by geophysical survey methods, enabling more effective comparisons.

The technology used to conduct this research is Nuvia Limited's Groundhog system, further discussed in Section 1.1.3. The use of Groundhog, an industrial technology developed for detecting man-made radioactive contamination, demonstrates how tools from the nuclear industry can be repurposed for the seemingly incongruous field archaeological research, potentially enhancing our ability to explore past human activities and their impact on the environment.

Geophysics in Archaeology: A Timeline



Timeline developed using data from the following sources:

- Aitken, M.J. (1974) Physics and Archaeology (Second Edition), Oxford: Clarendon Press, ISBN: 0198519222
- Barber, M. (2006) 100 Years of Discovery: Aerial Photography and Archaeology, English Heritage, https://www.academia.edu/12245131/100_Years_of_Discovery_Aerial_Photography_and_Archaeology, Accessed: 12/05/2023
- Beazley, G.A. (1919) Air Photography in Archaeology, *Geographical Journal*, 53 (5): 320 - 335
- Bonsall, J., Fry, R., Gaffney, C., Armit, L., Beck, A., Gaffney, V. (2013) Assessment of the CMD Mini Explorer, a new Low Frequency Multi-coil Electromagnetic Device for Archaeological Investigations, *Archaeological Prospection*, 20 (3): 219 - 231, <https://doi.org/10.1002/arp.1458>
- Clark, O.A. and Clark, A. (1997) Seeing Beneath the Soil: prospecting methods in archaeology, Taylor and Francis Group, London, ProQuest eBook Central, Accessed 18/06/2023
- Connor, M. and Scott, D.D. (1998) Metal Detector Use in Archaeology: An Introduction, *Historical Archaeology*, 32 (4): 76 - 85
- Gaffney, C. and Gater, J. (2003) Revealing the Buried Past: Geophysics for Archaeologists, Tempus Publishing Ltd. ISBN: 0752425560
- Jones, R. and Chure, D.J. (1998) The Recapitulation of a Late Jurassic Theropod Dinosaur: A Successful Application of Radiological Surveying for Locating Subsurface Fossilized Bone, *Gaia*, 15: 103 - 110
- Moussa, M. (2001) Gamma-ray Spectrometry: A new tool for exploring archaeological sites; a case study from East Sinai, Egypt, *Journal of Applied Geophysics*, 48: 137 - 142
- Robinson, V., Clark, R., Black, S., Fry, R., & Beddow, H. (2022). Portable gamma ray spectrometry for archaeological prospection: A preliminary investigation at Silchester Roman Town. *Archaeological Prospection*, 29 (3): 353-367, DOI: <https://doi.org/10.1002/arp.1859>

Images:

- Capper, J.E. (1907) XXIII - Photographs of Stonehenge, as seen from a War Balloon, *Archaeologia*, 60 (2): 371
- RSK (Unknown) A Reference for Geophysical Techniques and Applications, Edition 4.0, RSK Geosciences, <https://www.environmental-geophysics.co.uk/documentation/handbook/handbook.pdf>, Accessed 01/07/2023
- Clark, O.A. and Clark, A. (1997) Seeing Beneath the Soil: prospecting methods in archaeology, Taylor and Francis Group, London, ProQuest eBook Central, Accessed 18/06/2023
- Evans, K. (2016) Magnetometers: Inside the Fluxgate Gradiometer, <https://popular.electronics.technica.com/2017/03/16/inside-the-fluxgate-gradiometer/>, Technica Curiosa, Last Updated: 2016, Accessed 01/07/2023
- Jones, R. and Chure, D.J. (1998) The Recapitulation of a Late Jurassic Theropod Dinosaur: A Successful Application of Radiological Surveying for Locating Subsurface Fossilized Bone, *Gaia*, 15: 103 - 110
- Personal Image

1.1.3 Key Concept – An Introduction to Groundhog

The primary tool for conducting portable gamma radiation surveys for this research was the Groundhog Fusion system. This was made available through collaboration and support from Nuvia Limited – the designer and owner of this technology. A detailed insight into Groundhog is presented in Chapter 2 (Section 2.3) of this thesis. However, a brief overview is provided here for context.

Groundhog Fusion forms part of a family of portable gamma radiation measuring systems that are well established within the nuclear industry. Developed to meet the need for accurate characterisation of sites in a safe, efficient and time-efficient way, Groundhog systems are capable of supporting various projects from site declassification to drain surveys.

Each variant of Groundhog, whilst comprising the same basic elements, is built to accommodate the unique challenges posed by the environment in which it is used, and the purpose for which it is deployed. Groundhog Synergy for example consists of an array of detectors, developed specifically for the detection of low energy gamma emitters, fitted to a rugged off-road vehicle capable of operating within dynamic coastal environments. It is used for surveying beaches to look for and assist the recovery of tiny particles of radioactive material, often no bigger than a grain of sand. In contrast, Groundhog Fusion is a highly flexible system. This system is typically used for:

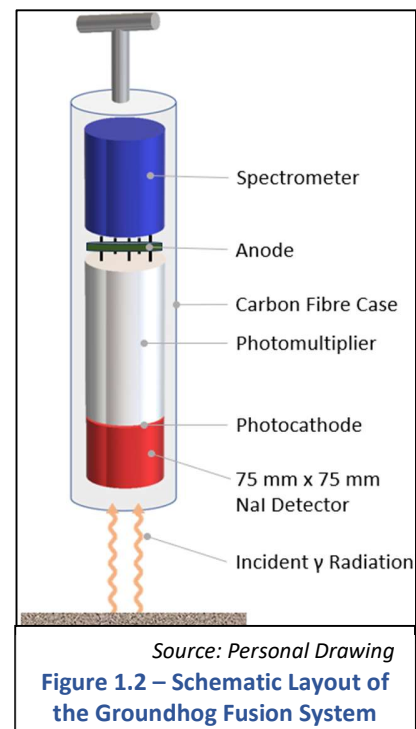
- Locating, and determining the nature and extent of, radioactive contamination present at a site, in support of the development of well targeted and effective remediation strategies.
- Undertaking reassurance monitoring to confirm the effectiveness of remedial works and/or that any radioactivity present is within acceptable limits.

Groundhog Fusion can be deployed either as a hand-held or vehicle mounted system. The hand-held system uses a single detector unit, and is capable of collecting thousands of radiation and Global Positioning System (GPS) measurements a day in an area of ~0.5 ha. It is therefore best suited to smaller or hard to access areas. The vehicle mounted system uses a bank of three detectors and can collect tens of thousands of measurements in a day, covering an area of ~3.5

ha. The hand-held system can also be deployed in a collimated (shielded) configuration. This ensures only those gamma rays directly beneath the unit reach the detector face. This improves accuracy of the measurements; particularly in scenarios where Groundhog may be deployed in areas with significant background radiation levels – e.g. close to a radioactive waste store.

Groundhog systems are equipped with all necessary components to automatically record high volumes of radioactivity measurements and positional data. The standard components within a Groundhog Fusion system (or ‘Groundhog’ as it is referred to for the remainder of this thesis) are as follows:

- Detector Unit – A carbon fibre case contains a thallium activated sodium iodide (NaI(Tl) or NaI) scintillation type detector, photocathode, photomultiplier, anode and spectrometer (Figure 1.2). The NaI detector is central to the Groundhog system, offering an optimal balance between ruggedness, efficiency, cost-effectiveness and resolution. The NaI detector captures the incident gamma photon and consequently emits a pulse of light. This strength of this light pulse is proportionate to the energy of the incident photon which is, in turn, unique to each radionuclide. The light pulse is converted to a photoelectron by the photocathode which is multiplied as it passes through the photomultiplier strengthening the signal. The electrons reach the anode creating an electrical pulse. The pulses are counted and analysed by the spectrometer, providing valuable insight into the number of events (counts) detected (i.e., the activity or intensity of the radiation source) and the radionuclides responsible.
 - When in a hand-held configuration, the unit is carried at the side of the body. When used in vehicle surveys, the units are secured to the front of the vehicle.
- GPS Unit – Groundhog has an integrated mapping grade GPS unit, enabling the positioning of each radiation measurement to centimetre



accuracy. The antennae is fitted to a backpack worn by the surveyor, with the supporting electronics and battery packs loaded in the backpack. For vehicle surveys, the antennae is fitted directly to the front of the vehicle.

- Data logger – An Ultra Mobile PC (UMPC) is used to automatically record radiation and GPS data during the survey. This is downloaded to a stand-alone desktop PC at the end of each survey for processing and interpretation. The UMPC is also secured onto the backpack during hand-held surveys, allowing hands-free operation and ensuring the surveyor can focus on safely navigating the site. During vehicle surveys, the UMPC is stowed in the cabin.

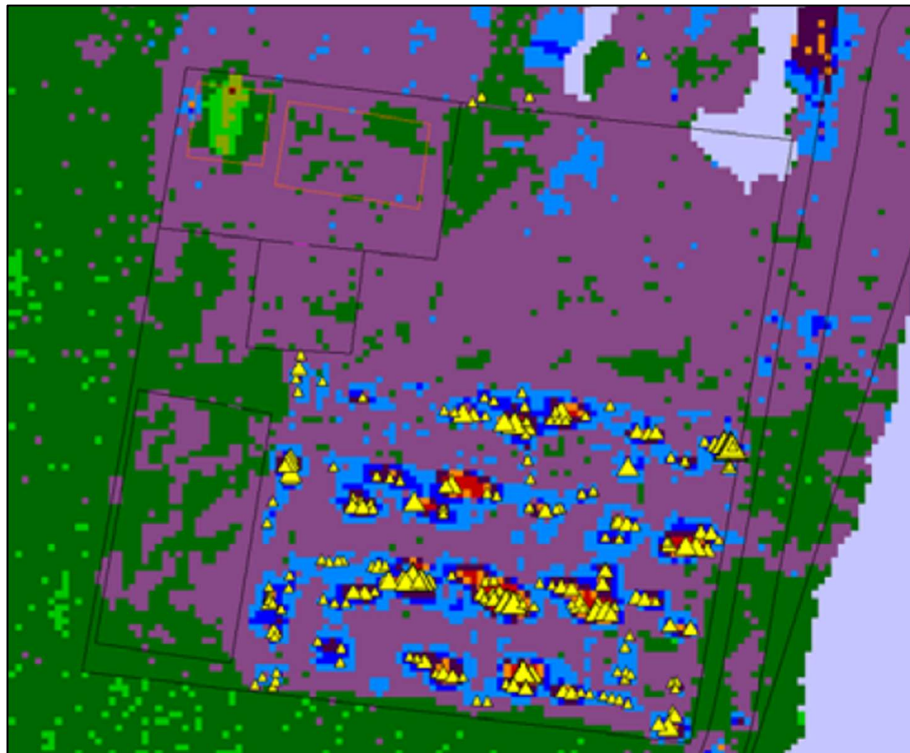
Data from the UMPC is downloaded to a desktop computer for processing. At this point, the data is checked for completeness and quality. A database application (MS Access) is used for collating GPS (.GHD and .GHE files) and spectrometric (.GHC) files. GrafNav is used for the post-processing of the GPS measurements, using base station data to help achieve centimetre accuracy. The key outputs from data processing are typically created using bespoke software within ArcGIS, developed by Nuvia Limited. The most important outputs used for data interpretation and action planning are:

- Gamma radiation distribution maps – these are effectively heat maps that highlight hotspots of radioactivity. In the example presented in Figure 1.3, areas of elevated radioactivity are presented in red, yellow and orange shades, moderate areas of radioactivity in light blue and light green, and lower levels in dark green and purple. Different colour ramps can be applied, as required, to better help draw out anomalies. In this example, hotspots of radioactivity that are attributable to caesium-137 are flagged with a yellow triangle. These maps allow the accurate targeting of remediation works and/ or provide reassurance that remediation has been successful by demonstrating removal of contamination hotspots.
- Count rate distribution graphs – these summarise the frequency of ‘counts per second’ (cps) measurements recorded in the field. One count per second is equivalent to one becquerel (Bq). A becquerel is defined as: *“the amount of ionising radiation released when an element (such as uranium) spontaneously emits energy as a result of the radioactive decay (or disintegration) of an unstable atom”* (US NRC 2021). The more becquerels (or cps) measured, the more active the source of the gamma radiation. For

remediation projects, the count rate distribution graph can be used to establish an action level that triggers further investigation and remedial work if exceeded. When the graph shows a normal distribution, as exemplified in Figure 1.4, the mean and standard deviation can be used to determine this action level.

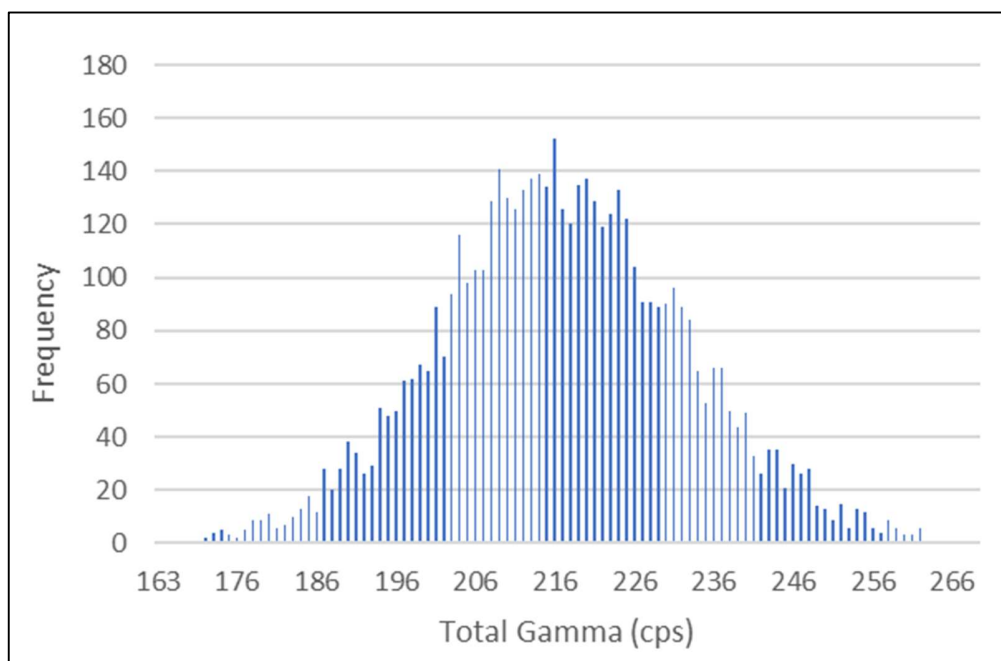
- Gamma spectrum – the energy spectra of the incident gamma radiation can be analysed to understand which radionuclides are responsible for the results observed in the gamma radiation distribution map. This is particularly valuable in characterisation projects where it is possible to determine whether an area of elevated radioactivity is attributable to naturally occurring radioactive material, or an anthropogenic contaminant of concern. In Figure 1.5 below, the spectral analysis has identified bismuth-214 (Bi-214) a daughter of natural uranium-238 (U-238). Summing spectra from a targeted area within the survey can improve the fidelity of the analysis.

Further detail on the processing of Groundhog data can be found in Chapters 3, 4 and 5 of this thesis.



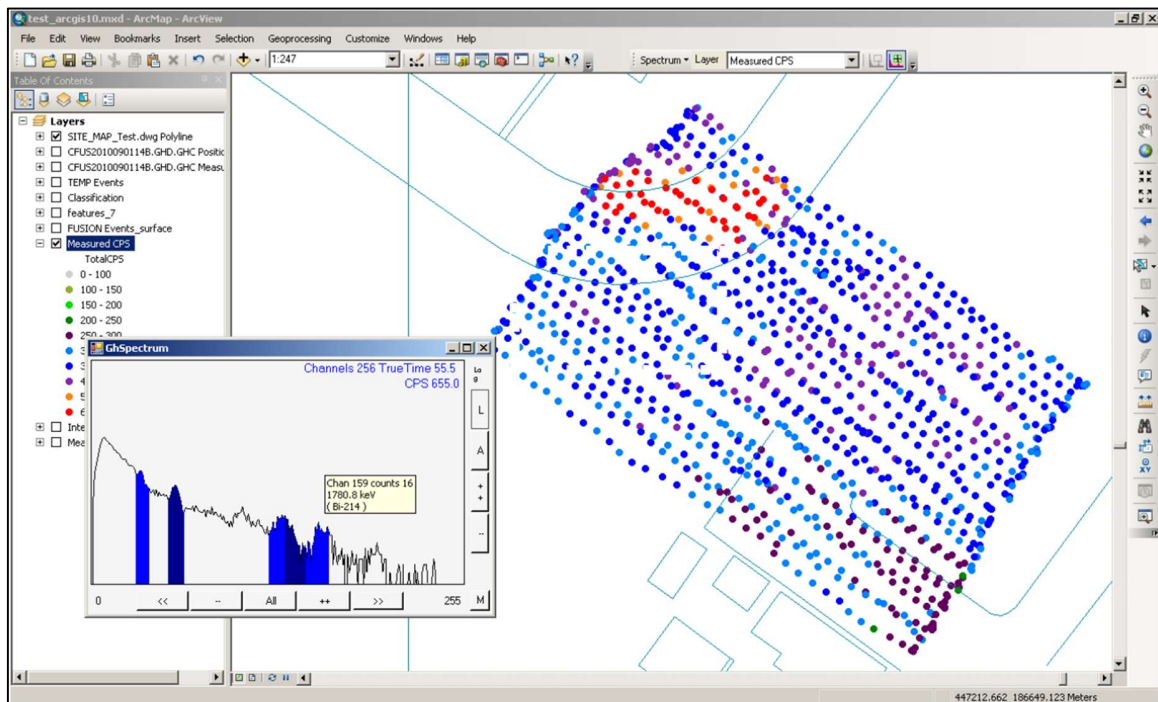
Source: Davies and Burgess (2011)

Figure 1.3 – Example of a gamma radiation distribution map. Elevated areas of radioactivity are shown red and orange colours, moderate levels in light greens and blues, and low areas of activity in dark green and purple. Areas found to contain Cs-137 are flagged with a yellow triangle.



Source: Created from original data

Figure 1.4 – Example of a count rate distribution graph generated from Groundhog data. This chart shows a normal distribution.



Source: Davies (2017)

Figure 1.5 – Example of mapped Groundhog measurements and graph showing the measured spectrum. The graph confirms the presence of Bi-214 – a daughter product within the U-238 decay chain.

1.2 Research Aim

As discussed in Section 1.1 the main aim of this research is to test the following hypothesis:

“Some past human activities have created measurable differences in concentrations of naturally occurring gamma radiation emitting radionuclides, enabling detection of buried structures and objects of archaeological interest using portable gamma radiation surveying methods”.

To test this hypothesis, multiple research methods have been implemented, including fieldwork and laboratory analyses which have been supported by desk-based research as required. Most notably, fieldwork has involved the deployment of gamma radiation survey methods, typically used in the nuclear industry, in the highly novel context of archaeological prospection. The effectiveness of these techniques in detecting buried archaeological features and their potential to complement traditional survey methods are tested.

1.3 Research Objectives

To achieve the project aims, the following objectives were identified and actioned:

- **Objective 1** – Interrogate existing literature to identify the extent of work undertaken to explore the efficacy of using gamma survey methods for archaeological and palaeontological prospection, and key gaps that need to be addressed.
- **Objective 2** – Generate datasets through the completion of gamma radiation surveys at various sites, including those of archaeological and, if possible, palaeontological interest. Surveys will be undertaken using a system known as Groundhog which is well established in the nuclear industry.
- **Objective 3** – Analyse datasets to test the feasibility of the technique and to classify the types of buried feature that are more amenable to detection via gamma-ray surveys and why.
- **Objective 4** – Process datasets using commercially available software, testing different methodologies to see which, if any, approaches generate high quality visual outputs.
- **Objective 5** – Test multiple variables – e.g. completion of collimated and uncollimated surveys, using Groundhog in both hand-held and vehicle mounted configurations, different site geologies and various target types.

1.4 Thesis Scope and Outline

The remainder of this thesis is structured as follows:

Chapter 2 provides context for the study by reviewing the importance of non-intrusive investigative techniques in archaeological prospection. It then identifies the sources of naturally occurring radioactive material and the mechanisms for its accumulation or depletion in archaeological artefacts. Potential strategies for conducting radiation surveys are discussed, followed by a review of existing literature relevant to this study. The review highlighted that only a very limited number of similar studies have tested the efficacy of gamma surveying in this unique context. The practical applications and added value of this technique therefore remain unclear and is something this research seeks to address. The literature review highlighted the

need for more rigorous testing of radiation survey techniques, testing different variables and target types.

As this thesis is principally presented as a collection of papers, it was considered prudent to present a separate, more detailed methodology chapter to underpin and rationalise the methodologies applied in the subsequent chapters. **Chapter 3** leads the reader through the process of identifying what data is required to address the research question, how this data can be obtained, and how it is stored/ processed. Further detail is also provided on the methodologies presented in the subsequent chapters, with a focus on the benefits, limitations and areas for improvement identified for each aspect.

In **Chapter 4**, the results of a preliminary investigation of the efficacy of gamma radiation surveying for archaeological investigation at the Roman Town of Silchester are presented. This chapter is presented as a paper, which was published in the journal *Archaeological Prospection*. Gamma radiation surveys were completed at Silchester using Groundhog in a hand-held configuration. Four different sites with varying target types were surveyed to establish which, if any, would generate measurable contrasts in radioactivity relative to the surrounding substrate. The impacts of a collimator, which limits the field of view of the detector, on data quality was also tested at two of the four sites. Completion of the surveys yielded some promising results. At two of the sites, no measurable difference between background radiation and the radiological properties of targets was found. However, in the two remaining sites, clear anomalies were visible in generated radiation heat maps. These anomalies aligned with known features and with anomalies identified in existing fluxgate gradiometry data for the same areas. The use of the collimator had no significant impact on data quality. It is noted that in this paper/ chapter, the term 'radiation heat maps' is used to describe the visual outputs generated. In subsequent chapters, this was revised to 'gamma radiation distribution maps' to provide a more accurate description.

The results from the preliminary investigation at Silchester were positive and highlighted several areas for improvement. These included exploring the scalability of the technique by deploying a vehicle mounted system and surveying the same or similar targets to confirm repeatability. These aspects are explored in **Chapter 5**. Here, the results from two further gamma radiation surveys at

Silchester are presented. In this scenario, Groundhog is deployed in a vehicle-mounted configuration, testing the scalability of the method. Surveys focussed on an area containing analogous target types to those in the preliminary study, demonstrating repeatability. Increased measurement density was achieved by overlapping vehicle passes. An equipment failure (and associated data loss) during the first survey, taken in very dry and hot conditions, necessitated a second survey at a later date. The second survey occurred after an extended period of rainfall. This provided a valuable opportunity to also briefly explore the impact of increased ground water on data quality. Results supported the findings from the preliminary study. Not all targets surveyed created measurable differences in gamma radiation intensities visible in the resultant gamma radiation distribution maps. However, the maps were capable of delineating three Roman roads, and drew out transitions in geochemical conditions across the site – potentially even identifying a historic field boundary. The positive results from this study support the hypothesis that gamma radiation surveying could be a complementary tool to traditional geophysical methods. However, it was noted that considerably more information is required to fully support this, and to understand the lack of consistency in results. At the time of writing, the manuscript presented has been published in *Archaeological Prospection*.

Chapter 6 begins to address the remaining data gaps highlighted in the previous chapter by presenting the findings from gamma radiation surveys at two further sites (Bisham and East Heslerton) offering contrasting geologies and target types. Groundhog was deployed in both hand-held and vehicle-mounted configurations for these surveys. To aid interpretation of the gamma radiation data collected, environmental and archaeological samples from Silchester and East Heslerton were subject to portable x-ray fluorescence (pXRF) analysis. The pXRF data, in conjunction with the output from the site surveys was used to create a model that can be used to plan optimised gamma radiation surveys as part of future research. Groundhog was successfully applied at both sites, with gamma radiation distribution maps revealing anomalies that broadly aligned with historic features. Again, changes in soil conditions not visible by eye or in the accompanying geophysical datasets were identified at both sites. At the time of writing, the manuscript presented here is in preparation for upload to *Archaeological Prospection* for consideration.

Chapters 7 and 8 complete this thesis by discussing the results across the three studies, what this research has revealed about gamma radiation surveying as an archaeological prospection tool and the wider implications of this research. Planned future activities are also explored.

Appendix 1 provides a link to access the raw data generated as part of this research, and Appendix 2 provides formatted versions of chapters published in *Archaeological Prospection*.

1.5 References

- Barber, M. (2006) 100 Years of Discovery: Aerial Photography and Archaeology, English Heritage, https://www.academia.edu/12245131/100_Years_of_Discovery_Aerial_photography_and_archaeology, Accessed: 12/05/2023
- Barker, P. (1993) (Third Edition) Techniques of Archaeological Excavation, Routledge, Taylor and Francis Group, UK.
- Beazley, G.A. (1919) Air Photography in Archaeology, *Geographical Journal*, 53 (5): 330 – 335
- Clark, O.A. and Clark, A. (1997) Seeing Beneath the Soil: prospecting methods in archaeology, Taylor and Francis Group, London, ProQuest E-book Central, Accessed 18/06/2023
- Davies, M. and Burgess, P. (2011) Integrating History and Measurement into a Case for Site Release, Proceedings of the 14th International Conference on Environmental Remediation and Radioactive Waste Management (ICEM 2011) September 25-29 2011, Reims, France, DOI: 10.1115/ICEM2011-59131
- Drewett, P. (2011) Field Archaeology: An Introduction, Second Edition, Routledge Taylor and Francis Group, UK, pp: 1 – 173, ISBN: 978-0-203-83087-1 (ebk)
- Davies, M. (2017) So, Just What is GROUNDHOG? Lunch and Learn Presentation for Nuvia Limited, Presented 8th June 2017, UNPUBLISHED
- Gaffney, C. and Gater, J. (2003) Revealing the Buried Past: Geophysics for Archaeologists, Tempus Publishing Ltd. ISBN: 0752425560
- Perrin, K. Brown, D.H. Lange, G. Bibby, D. Carlsson, A. Degraeve, A. Kuna, M. Larsson, Y. Palsdottier, S.U. Stoll-Tucker, B. Dunning, C. Rogalla von Beiberstein, A. (2014) A Standard and Guide to Best Practice for Archaeological Archiving in Europe, EAC Guidelines 1
- Ruffell, A. and McKinley, J. (2008) Geoforensics, Wiley, Blackwell, USA, ISBN: 978-0-470-05735-3
- Schmidt, A. and Ernenwein, E.G. (n.d.) Section 2 – The Life of Geophysical Data in n.e. Guide to Good Practice: Geophysical Data in Archaeology, 2nd Edition, Digital Antiquity, https://guides.archaeologydataservice.ac.uk/g2gp/Geophysics_2, created 10th January 2022, accessed 3rd May 2024
- US NRC (2021) Becquerel, <https://www.nrc.gov/reading-rm/basic-ref/glossary/becquerel-bq.html>, United States Nuclear Regulatory Commission (US NRC) Last Updated: 9th March 2021, Accessed: 15th June 2024



CHAPTER 2

Literature Review

2 LITERATURE REVIEW

2.1 Introduction

This chapter presents a review of available literature in the fields of gamma ray detection and spectrometry, its current applications, and more recently, its ability to detect features of archaeological interest. The chapter explores how gamma surveying and spectrometric techniques might be used as a supplementary approach to existing, well-established geophysical methods to improve the efficacy of non-intrusive surveying in this more novel context. The study focusses on the use of proprietary radiation monitoring tools with a long track record in the nuclear industry.

Section 2.2 explores sources of radioactivity in the environment, focussing on naturally occurring radionuclides and their presence in varying geologies. Interactions between naturally occurring radionuclides and buried anthropogenic artefacts are detailed. The following section (Section 2.3) then discusses the various methods used to measure and identify radioactive material in the environment and their common applications. The application of gamma radiation surveying in archaeological contexts is then explored in Section 2.4. This section begins by reviewing the application of traditional geophysical techniques in archaeological prospection. The advantages and limitations of different methods and the impact of applying complementary techniques on data integrity to improve interpretation are appraised. The section then focusses on the application of gamma radiation surveying techniques in the context of archaeological investigations. The methodologies applied in the available case studies are evaluated and compared against recognised good practices applied in the nuclear industry, where the technique was developed. Potential strategies for addressing identified shortfalls or data gaps in the reviewed studies are explored, with the output of this informing the methodologies applied throughout this research project. This chapter concludes with Section 2.5, which consolidates the information presented in previous sections and how these have informed the studies detailed in subsequent studies.

2.1.1 Contribution of Gamma Spectrometry to Site Investigations – An Overview

As discussed in Chapter 1, the aim of this research project is principally to test the efficacy of applying gamma radiation surveying techniques to support identification and mapping of sub-surface archaeology. To provide context for the following sections of this chapter, this sub-section presents a brief history of radiation survey techniques and the types of radiation they detect. Relevant aspects are covered in more detail in later sections.

The ability to undertake surveys has its foundations in the late 1920s and the development of the Geiger-Muller Tube; an ionisation-type detector (IAEA 1979). The device, whilst of limited sensitivity, particularly to gamma radiation, was physically robust, low cost and simple to use. It therefore supported effective detection of radioactive material (Flakus 1981, IAEA 1979). Its most common application was for radiation protection purposes within the controlled environment of a building. For example, detecting leaks in shielding, or identifying hotspots of contamination on surfaces/ equipment, although the system could also be used for site investigations (Flakus 1981, Holaday, 1948, IAEA 1979). The development of improved detectors using alternative methods of radiation ‘capture’ and measurement continues to progress, with the notable discovery of the thallium activated sodium iodide (NaI) detector in 1948. This was one of the first detectors to use a solid medium, the NaI crystal, to interact with radiation and support gamma spectrometric analyses (Flakus 1981). The efficacy of scintillation detectors, and in particular, those that use NaI crystals has not diminished over time. Rather, the NaI crystal remains one of the more common scintillation media due to it being one of the few materials capable of reliably generating a high number of visible photons for measuring (Flakus 1981, Mirion Technologies 2017). Finally, it is acknowledged that unlike cadmium zinc telluride (CZT) semiconductor type detectors or germanium detectors, NaI crystals can be made in different sizes, with larger crystals resulting in higher detection efficiencies. This is due to the increased probability of incident radiation dissipating its energy into the crystal that subsequently generates the measurable pulses of light (L’Annunziata 2012).

All radionuclides will generate either an alpha or beta particle during its decay (Podgorsak 2005). Where there is excess energy remaining, gamma radiation will also be produced (Podgorsak 2005, Steinberg and Rasmussen 2021). Gamma radiation rarely occurs in isolation and is typically associated with alpha or beta decay (Steinberg and Rasmussen 2021, Smidt and Warriner 2019). It

may therefore be reasonable to consider the detection of alpha and beta radiation through the use of dedicated surveying instrumentation as part of a site characterisation exercise. However, the use of such detectors in environmental surveys is severely limited due to the limited range of alpha and beta particles, susceptibility to shielding and fragility of the detector probe (IAEA 2012). Such non-intrusive surveys are therefore normally only carried out on smooth, solid surfaces in controlled environments (IAEA 2012). These limitations are discussed further in Section 2.3.1. In contrast, gamma radiation is far more amenable to detection and quantification using non-intrusive surveying methods. It is understood that methods of gamma detection and spectrometry are more diverse and can complement academic, commercial and safety investigations. The scale of a gamma survey can range from airborne surveys covering square kilometres of land with the aim of locating mineral deposits, through to the completion of high-density surveys on foot/ by hand to identify anthropogenic contamination over square metres within a building or over land. Further detail on the applications of gamma radiation and spectrometric techniques can be found in Section 2.3.2.

2.2 Radioactivity in the Environment

Radioactivity, and in particular its interaction with humans can elicit a sense of fear and deep mistrust; particularly since radiation cannot be directly seen, smelt, tasted or heard, making it impossible to know whether exposure has occurred. However, radioactivity is a naturally occurring phenomenon and is an important contributor to Earth's natural biogeochemical processes. Indeed, it is so ubiquitous one can reasonably expect to receive an annual radiation dose of approximately 2.4 mSv per year (IAEA 2019, Thorne 2003), depending on where an individual resides and their personal habits; time spent indoors/ outdoors, propensity for air travel or smoking for example.

The bulk of our radiation exposure, approximately 80% (IAEA 2017, Larivière and Guérin 2010), is of natural origin and is sourced from radionuclides present within rocks, building materials, the foods we eat, the air we breathe and cosmic radiation. A significantly smaller proportion, less than 1% (IAEA 2017, Larivière and Guérin 2010), is as a result of anthropogenic sources of radioactivity such as nuclear weapon testing/ deployment, nuclear accidents and nuclear power generation (and associated radioactive waste generation). The remainder (approximately 20%) is

as a result of medical interventions using ionising radiations, e.g., x-rays, or medical isotopes such as technetium-99m (IAEA 2017).

As this thesis concerns the accumulation of radioactivity in organisms and artefacts that were created long before the dawn of the nuclear age (broadly acknowledged to have started in 1945 with the detonation of the first atomic bomb (Shaw 2007)), it is the naturally occurring sources of radioactivity that are of relevance here and will therefore remain the focus of this study.

2.2.1 Sources of Naturally Occurring Radioactivity

Most naturally occurring radionuclides are of terrestrial origin (UNSCEAR 2008). Many were formed in the millennia immediately after the 'Big Bang' approximately 14 billion years ago and they "...have not stopped disintegrating since" (Liboutry 1999, page 182). There are 34 known primordial radionuclides found on Earth today (Ojovan and Lee 2013), some of the more significant being isotopes of uranium and thorium and potassium-40 (K-40) (UNSCEAR 2008). These radionuclides have half-lives of 1 billion years or more. The notable exception being uranium (U-235), which has a half-life of 704 million years, and hence its scarcity; accounting for less than 1% of the naturally occurring uranium on Earth (Ojovan and Lee 2013). Primordial radionuclides can be categorised into either 'series' or 'non-series' radionuclides. Non-series radionuclides decay directly into stable (non-radioactive) atoms. For example, K-40 will decay into either a stable form of calcium (via beta decay) or argon (via electron capture) (Jun *et. al.* 2010). Series radionuclides decay into other radioactive isotopes, 'daughters', which can also decay to form radionuclides. This process continues until a stable atom is finally reached. For example, the decay chain of uranium (U-238) generates a number of radionuclides including radium-226 (Ra-226), radon-222 (Rn-222) and polonium-210 (Po-210) with the decay chain concluding with the generation of the stable element lead-206 (Pb-206).

The Earth's mantle is the main sink of these primordial radionuclides, which eventually become entrained within various minerals and rocks during crustal formation (Plant, *et. al.* 1999, Landa 2007). Crustal rock predominantly comprises lighter elements such as silica, potassium, aluminium, sodium and magnesium as well as iron (Press and Siever 2002). As magma cools, minerals rich in magnesium and iron that crystallise at higher temperatures form first (generating mafic rock), followed by the formation of minerals rich in silica, aluminium, sodium and potassium

(felsic rock) (Press and Siever 2002, Ojovan and Lee 2013). Primordial radionuclides such as uranium and thorium-232 (Th-232) tend to mineralise towards the end of the cooling process, creating minor (accessory) minerals within igneous rock due to their incompatibility with silicate mineral structures (Landa 2007, Ojovan and Lee 2013). Formation of these accessory minerals has resulted in crustal concentrations of 8 – 12 mg/kg and 2.5 – 2.8 mg/kg of thorium and uranium respectively (Mahmood and Mohamed 2010, Rawlins, *et. al.* 2012, Vandenhove and Hurtgen 2010). To put this into context, in a representative sample of continental crust, uranium will account for just $1.6 \times 10^{-5}\%$ of the sample (Press and Siever 2002). In contrast, potassium is far more abundant in nature. Approximately 2.8% of the Earth's crust is potassium, of which 0.012% (120 mg/kg) is the radioactive K-40 (Peterson, *et. al.* 2007, Rawlins, *et. al.* 2012).

Naturally occurring radioactivity can also be cosmogenic in origin (Thorne 2003). Radionuclides such as carbon-14 (C-14) can be generated following interactions between cosmic rays and atoms within Earth's atmosphere or on its surface (IAEA 2017). Relative to other sources, the contribution of cosmogenic sources to Earth's radioactivity is relatively low.

Due to their relative abundance in the Earth's crust, long half-lives, potential for accumulation through technological enhancement, and their ability to generate gamma rays of sufficient energy and intensity to support gamma radiation mapping (IAEA 2003) this thesis focusses on the properties of three main primordial radionuclides – K-40, Th-232 and U-238.

2.2.2 Influence of Geology on Radionuclide Concentrations in the Environment

"There is no place on Earth without natural background radiation" (Dobrzyński, *et. al.* 2015, page 1). As discussed in Section 2.2.1, this natural radiation can either be terrestrial or cosmic in origin, with terrestrial being the dominant source. This radiation is not evenly distributed across the planet, as evident through the irregular distribution of average dose rates attributable to naturally occurring radioactivity. Approximately 65% of the global population will be exposed to an average dose rate of between 1 and 3 mSv/y (UNSCEAR 2000). However, occupants of areas identified as 'high background natural radiation areas' (HBRNAs) can be exposed to dose rates much higher than this, with approximately 10% of the global population receiving more than 3 mSv/y (UNSCEAR 2000, Aliyu and Ramli 2015).

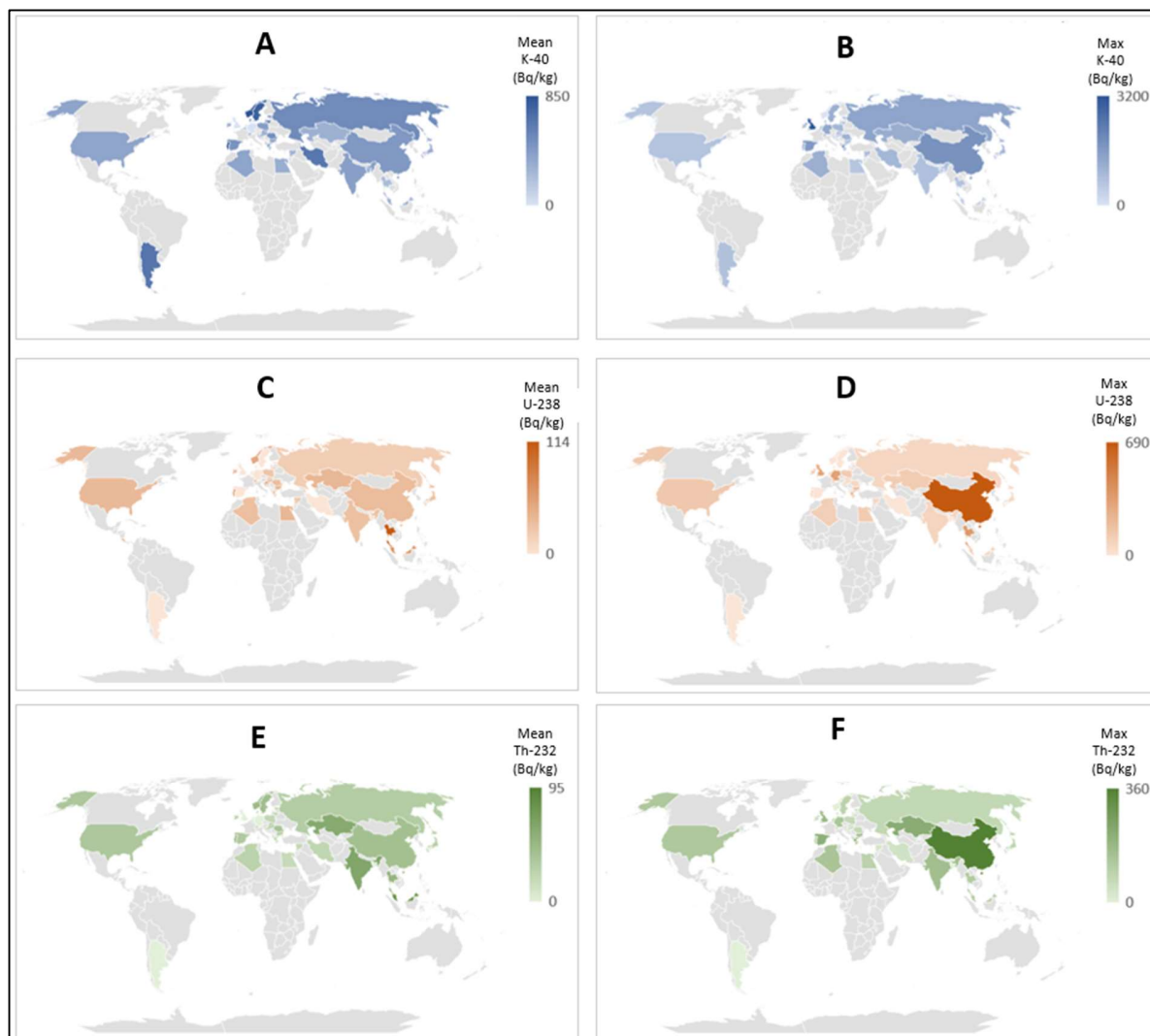
These global variations are attributable to the geology of each area, with higher dose rate areas characterised by igneous rocks such as granite, shales and phosphate rock (UNSCEAR 2000). These rocks can contain elevated concentrations of radionuclide containing minerals such as monazite; an accessory mineral in granitic rocks, which is naturally rich in uranium and thorium (Mindat.org 2022).

Minerals are crystalline, inorganic solids consisting of one or more elements and are the constituent components of rock (Press and Siever 2002). At the time of the Earth's formation 4.5 billion years ago, it is estimated that approximately 60 mineral species were in existence (Hazen, *et. al.* 2009). Exposure to multiple geochemical (and eventually, biological) processes, including volcanic activity, plate tectonics, oxidation-reduction, weathering, dissolution and hydrolysis resulted in a massive diversification of mineral species to the ~4300 known today (Hazen, *et. al.* 2009, Finch and Murakami 1999, Press and Siever 2002, Fayek and Kyser 1999). Of these known minerals, around 200 – 250 contain isotopes of uranium and/ or thorium (Burns 1999, Hazen, *et. al.* 2009). Some of the more significant uranium and thorium containing minerals are listed in Table 2.1.

As noted in Section 2.2.1, certain primordial radionuclides (and particularly thorium and uranium) were some of the last elements to mineralise, affecting where they appear in the Earth's crust (Plant, *et. al.* 1999, Landa 2007). This late crystallisation is due to incompatibility of these radionuclides with the structures of the main high-temperature forming minerals such as the silicates (Ojovan and Lee 2013, Plant, *et. al.* 1999). The main exception to this is zircon ($ZrSiO_4$) which is capable of accumulating uranium and thorium in its structure, through the incorporation of limited quantities of coffinite (U_2SiO_7) or thorite ($ThSiO_4$) in its end members (Hazen, *et. al.* 2009). This is possible due to the similar crystal structures of these minerals. Concentrations of uranium and thorium in zircon of 100 – 10,000 Bq/kg (IAEA 2003a) is therefore possible. More typically, these radionuclides accumulate preferentially in low temperature forming minerals (Plant, *et. al.* 1999) until they reach notable concentrations in igneous rocks such as granites. As the eighth most abundant element (Mindat 2019), potassium is more commonly distributed, with over 350 mineral species containing potassium as an essential component alone (Mindat 2019).

Once mineralised, the subsequent behaviour of these radionuclides is largely dependent on their chemical properties and the conditions to which they are exposed. Weathering of the parent rock can liberate radionuclide containing minerals (Ojovan and Lee 2013). These minerals are then more susceptible to transportation; initially via mechanical means, e.g. creep, saltation and suspension (Ojovan and Lee 2013). Once liberated from its parent material, the radionuclides can be susceptible to chemical alteration and transport mechanisms such as dissolution. For example, degrading uranium minerals within weathered igneous rock can become exposed to an oxidising environment causing it to change from a U^{4+} state, which is insoluble, to its soluble U^{6+} state (in the form of a uranyl ion) (Finch and Murakami 1999). This more mobile form of uranium can then migrate through hydrogeological systems until it encounters changing geochemical conditions (Cumberland *et. al.* 2016). This might include, for example, a reducing environment. This initiates the uranium's return to its U^{4+} state and subsequent precipitation, deposition and potential encasement in other insoluble solids (Finch and Murakami 1999). The mobilised uranium may also preferentially adsorb to other soil minerals such as clays. Thorium ions, which are generally less soluble than uranium remain reliant on mechanical transport mechanisms (Mahmood and Mohamed 2010) than chemical processes.

These mechanisms account for the massive variability in radionuclide concentrations across regions and geological formations, as exemplified in the maps shown in Figure 2.1. This figure shows indicative mean and maximum concentrations of some of the key primordial radionuclides (Thorium, Potassium and Uranium) globally distributed in soil. It is recognised that the map is far from complete, with significant data gaps across Africa, Australia, South America and Canada. Further, there is limited granularity in key areas such as the United States of America where there is notable variation in concentrations of naturally occurring radioactivity (USGS 2013). However, it can be seen that certain countries including China, Hong Kong, the United Kingdom and Greece consistently show elevated concentrations of naturally occurring radioactive isotopes, particularly when compared against the global average concentrations of 40 Bq/kg, 400 Bq/kg and 35 Bq/kg for Th-232, K-40 and U-238 respectively (Patnaik, *et. al.* 2016, European Commission 1999). The geological properties and location of a potential target site will therefore have a significant impact on the results of any gamma radiation surveys undertaken. In consequence, this must be carefully considered when planning a survey; particularly where naturally occurring radionuclides are of primary interest, as for this research project.



Source: Charts generated in Excel (version 2202) using data from UNSCEAR (2000)

Figure 2.1 – Global distribution of naturally occurring radionuclides in soil where data is available. Mean and maximum values for K-40 (Figures A, B), U-238 (Figures C, D), Th-232 (Figures E, F) are presented.

Table 2.1 – List of Minerals Associated with Potassium, Uranium and Thorium, with Common through to Rare Incidences Considered

Element	Minerals where Commonly Found	Minerals where Occasionally Found	Rocks/ Minerals where Rarely Found
Potassium	Orthoclase Muscovite Microcline Sylvite Carnallite Polyhalite	Plagioclases	Olivine Pyroxene
Uranium	Uraninite Carnotite Autunite Phosphate rock Monazite	Zircon Sphene Apatite Magnetite Olivine Tourmaline	Due to its incompatibility with silicate mineral structures, it is rarely found in felsic rocks and minerals.
Thorium	Thorite Thorianite Cheralite Monazite	Andesite Sphene Epidote Pyroxene Olivine	Due to its incompatibility with silicate mineral structures, it is rarely found in felsic rocks and minerals. Carbonate rock

Source: Table developed with information from Lliboutry (1999), Ojovan and Lee (2013), Vandenhove and Hurtgen (2010), Mahmood and Mohamed (2010), Rawlins *et. al.* 2012, Ojovan and Lee (2013), Banerjee, *et. al.* (2011), Mindat.org (2019)

2.3 Methods of Detecting Radioactivity in the Environment and their Applications

Unlike chemical contamination, the detection and quantification of radionuclides in an environment is not limited to physical sampling and analysis. Rather, the particles or radiation emitted during the radioactive decay of the contaminants permits the use of non-intrusive surveying and characterisation techniques as well as radiochemical analysis of samples in the laboratory. Alpha and beta particles emitted from decaying radionuclides can be detected using handheld probes when moved slowly across, and in close proximity to, the surface of interest (NPL 2014) as discussed in Section 2.1.1. Minimising the distance between the surface and the detector is necessary to maximise the probability of particles entering the detector window (NPL 2014). Radionuclides that also emit gamma rays can be surveyed via a greater range of detectors. The most common types of gamma radiation detector include gas chamber, scintillation, and solid state (Smith and Lucas 1991). As gamma radiation has a much larger range and is less susceptible

to shielding (Smith 2001), there is greater flexibility in the survey methods that can be applied. Aerial, vehicle mounted, and manual surveys as well as probe systems have all successfully been deployed (IAEA 2003). The most relevant surveying techniques and technologies are outlined in the following sub-sections.

2.3.1 Alpha/ Beta Radiation Detection

As alluded to in previous sections, the use of alpha and beta detection methods for environmental surveys is very limited. This is principally due to the limited range of alpha and beta particles. Even in air, alpha particles will travel just a few centimetres and beta particles between 1 and 3 metres (Mirion Technologies 2020). Further, these particles can be readily attenuated, with alpha particles unable to pass through a surface thickness of greater than 0.1 – 0.7 mm (Park 2001) and beta particles stopped by a thin sheet of metal (e.g. aluminium) or block of lower density material such as wood or plastic (Smith 2001). In consequence, any significant soil overburden would be impossible to penetrate; a key characteristic of the sites of interest within this study. Rough and porous surfaces also significantly reduce the detection efficiency of surface alpha/beta surveys undertaken using hand-held detectors (CNDNI 2009). Such surveys are therefore limited to contamination on hard, smooth surfaces that are free from moisture, dust and other debris. Contamination of bulk material contaminated with alpha and beta emitting isotopes is instead measured through a combination of destructive sampling/ radiochemical analysis and non-destructive bulk monitoring (CNDNI 2009). The results from radiochemical analysis are used to generate a ‘fingerprint’ for the material. This provides an estimate of the anticipated mix and ratios of radionuclides present (SDF 2017). Bulk monitoring is then undertaken to measure the gamma emitters, with the fingerprint used to calculate the quantity of alpha and beta emitters present.

For the reasons discussed above, it is evident that alpha and beta surveys would not be viable for supporting the detection of buried artefacts, either man-made or geological in nature, and are therefore not considered further.

2.3.2 Gamma Radiation Detection

Unlike alpha and beta radiations, which are emitted as particles with a limited range, gamma radiation comprises photons of energy and forms part of the electromagnetic spectrum (Smith 2001). Unabated (i.e. in air) gamma radiation can travel up to 700 m, up to 50 cm – 100 cm

through moderately dense materials such as soil and less than 10 cm through high density materials such as lead (IAEA 2003). It is this ability to penetrate through matter that makes gamma radiation suitable for studying radioactivity in the environment via non-intrusive survey methods. It is however noted that not all radionuclides, including those that are naturally occurring, emit gamma radiation. For example, U-238 and Th-232 both decay through the emission of alpha particles with no associated gamma radiation. In consequence it is their progenies, which do emit gamma radiation of sufficient energy and intensity to enable detection, that are measured to support calculation of uranium and thorium concentrations (IAEA 2003). Uranium detection can be achieved through its daughter Bi-214 (with a gamma energy of 1765 keV) and Th-232 via Thallium-208 (Tl-208) (with a gamma energy of 2615 keV) (Chiozzi, *et. al.* 2000a, Moussa 2001, IAEA 2003). However, different radionuclides can be used depending on the detector medium used and aims of the study. For example, for high resolution gamma spectrometry, U is detected through the Th-234 peak at 63 keV. For low resolution gamma spectrometry, the Pb-214 (with a gamma energy of 351 keV) and Bi-214 (with gamma energy of 609 keV – in addition to the peak at 1765 keV already mentioned) (IAEA 2003) are used. It is for this reason that concentrations of radionuclides such as U-238 and Th-232 established via non-intrusive surveys are often reported as ‘equivalent’ values; e.g. ‘ppm eU’ and ‘ppm eTh’. This technique assumes that parent and daughter are in secular equilibrium (Chiozzi, *et. al.* 2000a). In contrast, the radioactive isotope of potassium can be detected directly through its gamma radiation with an energy of 1461 keV (Moussa 2001).

Historically, non-intrusive portable gamma survey methods have been used for ‘screening’ a site. This is done with the aim of identifying areas of interest, ‘hotspots’, that warrant further investigation via excavation and the collection and radiochemical analysis of samples (CNDNI 2009). Over time however, technology improvements have resulted in the development of physically robust systems that are capable of generating real time data that are of sufficient quantity and quality to support various characterisation projects. This includes for example, the delicensing of a nuclear licensed site through to the identification of geological features such as soil-type distributions or identification of karst structures (Reinhardt and Hermann 2019, Putiška, *et. al.* 2014). The ability to collect vast numbers of samples (data sets comprising 10,000 – 100,000 individual measurements are typical for certain systems (Davies, *et. al.* 2003) over a short period of days or even hours). This makes gamma surveying a cost- and time-effective, low impact

characterisation technique (Chiozzi, *et. al.* 2000a). Incorporation of Global Positioning Systems (GPS) can further add value through generation of highly accurate radiation distribution maps.

There are multiple technologies available for conducting environmental gamma radiation surveys. Each technology has its own advantages and limitations, with selection of the optimal system dependent on a number of considerations:

- Anticipated radionuclides of interest, their dominant decay mechanism and their source.
- Size of survey area and terrain – informing deployment of hand-held, vehicle mounted or airborne methods.
- Planned use of data.
- Anticipated location of the radionuclides – near surface or at depth?

Radiation survey instruments used in gamma surveys can be broadly defined by the composition of the detector unit and be divided into three main groups: gas-filled, solid-state (or semi-conductor) and scintillation detectors (IAEA 2012). Gas filled detectors include ionisation chambers, proportional counters and Geiger-Müller Tubes. The latter is best suited for gamma radiation with the others more amenable to the detection of alpha and beta radiation (IAEA 2003, IAEA 2012, CNDNI 2009, NISDF 2017). Solid state detectors include systems, such as High Purity Germanium (HPGe) detectors, use a semi-conducting material as the detection medium; for example, a germanium or silicon crystal (IAEA 2003, IAEA 2012). Scintillation-type detectors are more diverse and are capable of utilising a variety of scintillant materials and detector configurations. However, there are limitations; particularly regarding the maximum size of crystal that can be grown and achieving optimal detector efficiency. A balance needs to be achieved between improving detection limits through increasing detector size (L'Annunziata 2012) and managing increasing interference from background radiation. For example, optimal efficiency for Cs-137 is typically achieved with an 7.5 cm wide by 7.5 cm thick NaI crystal (Mirion Technologies 2017).

Gas-filled detectors are less suitable for environmental monitoring due largely to their poor gamma detection efficiency; less than 2% for Geiger-Müller Tubes (IAEA 2012). Further, because

Geiger-Müller Tubes cannot differentiate between different radiation energies, the instrument does not support gamma spectrometry. Only count rate data is generated, limiting the amount of information that can be recovered from a survey. Due to the limitations described here, this type of detector would therefore be of limited value to the surveys proposed as part of this study and are not considered further.

Solid state detectors such as HPGe detectors operate similarly to gas-filled detectors in so far as the ionising properties of the incident radiation results in the generation of an electrical pulse which can be measured and interpreted (CNDNI 2009). Unlike gas-filled detectors however, solid-state detectors are capable of achieving very high energy resolution, thereby supporting the accurate determination of specific radionuclides present (IAEA 2003, Chiozzi *et. al.* 2000a, Reinhardt and Herrmann 2019). The sensitivity of these detectors is in part attributable to the significant cooling of the semi-conductor. For optimal performance, the unit is cooled to -196°C (IAEA 2003) through either a liquid nitrogen or electro-mechanical cooling system (NISDF 2017). The need for cooling not only increases operational time, it also reduces the mobility of the unit. In consequence, this type of system is better suited to static counting at pre-determined locations and laboratory work. In isolation, this type of detector is less suitable for the applications proposed in this study. Whilst it is capable of generating high-resolution data, the length of time required for each measurement – up to tens of minutes to generate a complete spectrum (IAEA 2003) and limited mobility of the system results in reduced data resolution over an entire survey area. However, solid state detectors could be used to obtain additional/ complementary information from samples collected from the field; particularly when used in conjunction with data collected from more portable (but lower energy resolution) system such as a scintillation-type detectors.

Scintillation-type detectors utilise a scintillant material to generate a pulse of light when it interacts with the incident radiation. This pulse of light is converted into an electron which is amplified before conversion to a voltage pulse which is recorded and analysed. As the intensity of the light pulses are influenced by the energy profile of the incident radiation, it is possible to determine the specific radionuclides involved. Scintillation-type detectors are more commonly used in environmental surveys due to their ruggedness, good detector efficiency, portability and ability to take rapid and accurate radiation measurements (IAEA 2003, IAEA 2012, Reinhardt and

Herrmann 2019, Chiozzi *et. al.* 2000a). Scintillation detectors are very flexible, with various scintillation materials, thicknesses and surface areas available to accommodate different radiation types and energies. For example, plastic scintillator and thicker thallium activated sodium iodide (NaI(Tl) or NaI) crystals are well suited to beta radiation, higher energy gamma and x-ray radiations (IAEA 2012). In contrast, thinner NaI and Cs(Tl) scintillator crystals are well suited to lower energy gamma radiation (Reinhardt and Herrmann 2019, IAEA 2012). Further, scintillation type detectors are amenable to multiple configurations depending on the source of the radioactivity of interest and the scale of the survey. They can offer a high resolution at a macro scale due to their ability to take a large number of measurements. Hand-held systems can be used for surveying areas of tens of square metres or locations only accessible by foot. Alternatively, vehicle mounted, or airborne systems can be deployed to survey hundreds of square metres if not square kilometres. Like solid-state detectors, scintillation detectors support spectrometric capability.

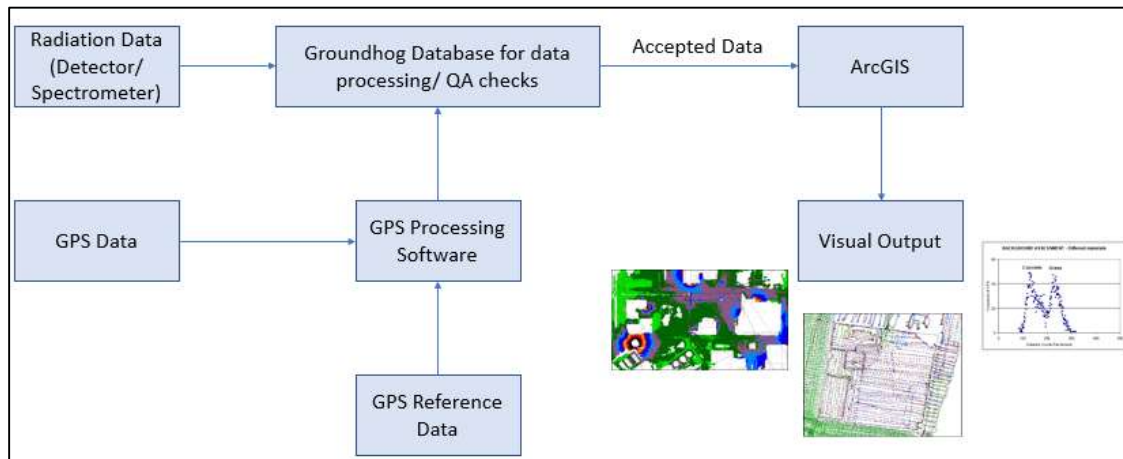
For the reasons discussed above, scintillation detectors are ideally suited to the applications proposed in this study. The use of NaI detectors is a proven method for identifying accumulations or even depletion of naturally occurring uranium, thorium and potassium in the environment as evidenced in studies by Chiozzi *et. al.* (2000a) – application of gamma spectrometry in geophysical surveys, Putiška *et. al.* (2014) – investigations into karst structures, Popp *et. al.* (2013) – characterisation of the subsurface of a series of hill slopes, Bezuidenhout (2015) – characterisation of a disused phosphate mine, de Quadros *et. al.* (2002) – gold exploration, Nemeth *et. al.* (2015) – mineral exploration and Tourlière *et. al.* (2003) – kaolin exploration.

Based on the conclusion that an NaI crystal scintillation-type detector is likely the most suitable technology for the application proposed as part of this study, an optimal radiation detection system – ‘Groundhog’ has been identified for use.

2.3.2.1 Groundhog

Groundhog is a proprietary radiation detection system designed, operated and owned by Nuvia Limited (Nuvia 2015). The system is used for detecting and quantifying the nature and extent of radioactive material on land, in buildings or within other structures such as drains and pipelines. The integrated use of a GPS supports the accurate plotting of the recorded data to centimetre

accuracy (Davies 2017). As summarised in Figure 2.2, data generated by the radiometric and GPS systems is processed by (adapted) commercially available software to generate visual outputs that can be used to inform decision making processes. The basic system comprises an NaI scintillation-type detector, gamma spectrometer, GPS system, supporting electronics, hand-held data logger and main PC processing unit (Nuvia 2018) as shown in Figure 2.3.



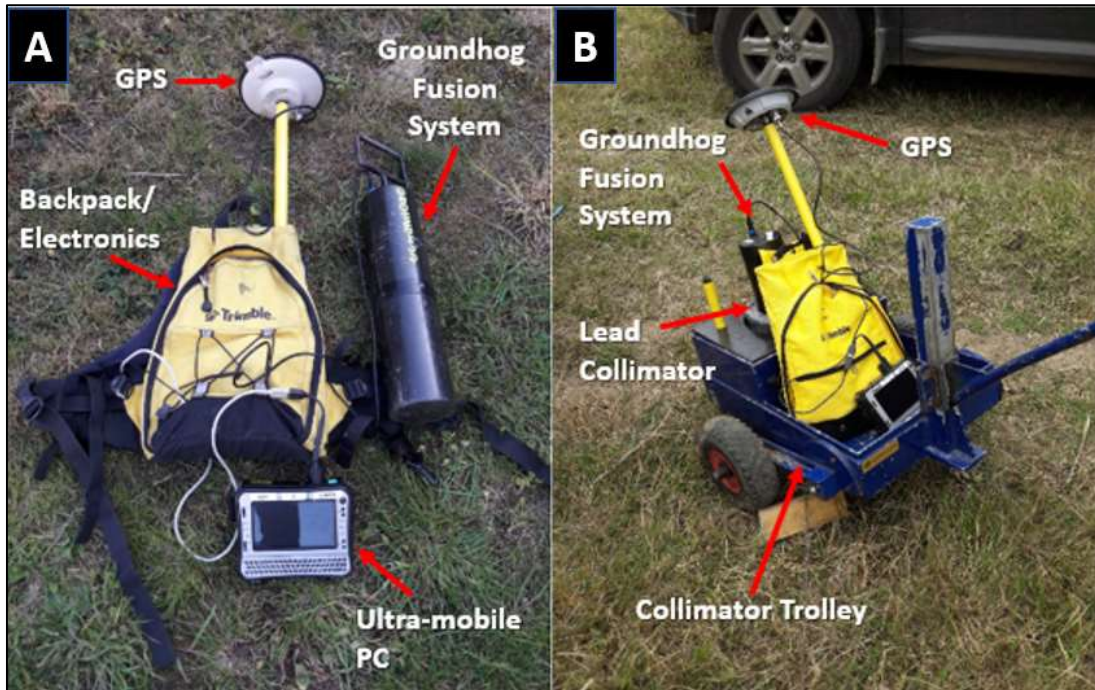
Source: Modified from Nuvia (2017)

Figure 2.2 – Overview of the Groundhog Processing System

A common configuration consists of a detection system encased in a robust, lightweight hand-held carbon fibre composite case. Supporting electronics and a GPS system are carried in a backpack (Figure 2.3a). This equipment can be loaded into a lightweight trolley or collimator trolley if required (Figure 2.3b). The hand-held or trolley-mounted system is typically deployed in smaller areas of tens of square metres. For larger areas, tens of thousands of square metres, banks of detectors and supporting GPS system can be vehicle mounted (Nuvia 2018).

In some applications, an immediate response to detected contamination is required. This includes for example, during beach surveys where operators are looking for, and aim to recover, radioactive particles such as fuel fragments. Due to the dynamic environment in which the survey is undertaken, it is essential that a radioactive particle is removed promptly after detection. In these cases, the system can be set up to generate an alarm when peaks in activity are detected, facilitating an immediate response. For a standard survey, radiological and GPS data is transferred to a database where it is processed, and quality checked. The data is then transferred to an ArcGIS software package for further processing and generation of (visual) output data (Nuvia 2018). This can include, for example, radiation distribution (heat) maps and count rate

distribution graphs that support the identification of any areas of concern/ interest. The data can also be used to inform decisions regarding the extent of remediation required at a site, or whether to release a site from regulatory control.



Source: (Personal Photographs)

Figure 2.3 – Nuvia Groundhog System in Uncollimated (A) and Collimated (B) Configurations

The Groundhog System ‘Family’ – An Overview

There are multiple systems available that are capable of completing real-time gamma radiation surveys, with each measurement/ data point plotted with centimetre accuracy via accompanying global positioning data. At the time of writing, commercially available systems include Aurora’s ‘RadSurvey’, Wood’s ‘ORION ScanPlot’ and Nuvia’s ‘Groundhog’. All comprise rugged, portable detectors with mapping GPS systems; the latter two also offering various configurations (e.g. hand-held, trolley and vehicle-mounted systems) and gamma spectrometric capability (Aurora 2020, Kerr, 2016, Nuvia 2015).

Nuvia’s Groundhog series in particular offers a variety of systems and configurations that can be selected based on the contaminants of concern, scale/ location of the study, and purpose of the study. All Groundhog systems have the same core features including gamma spectrometric

capability, automatic recording of high density survey measurements, use of mapping-grade GPS systems, high quality data outputs and lightweight robust carbon fibre casings (Nuvia 2015). An overview of the unique features Groundhog systems available are summarised in Table 2.2.

Table 2.2 – Overview of Groundhog Systems Available for Carrying out Radiation Surveys and their Applications

System	Detector Type	Method(s) of Deployment	Target Radionuclides	Applications
Fusion	76 x 76 mm NaI Crystal	Manual deployment, towed on a (collimated) trolley, vehicle mounted.	Cs-137, Ra-226, Co-60	Land characterisation.
Insight	125 x 1.6 mm NaI Crystal (FIDLER* Probe)	Manual deployment.	Am-241, Pu-239	Land characterisation.
Evolution 2	76 x 400 mm NaI Crystal	Vehicle mounted.	Cs-137, Ra-226, Co-60	Particle detection – a bank of 5 detectors supports the surveying of a 2 m strip for each pass along the site.
Synergy	Five NaI Detectors Plus Eight Insight (FIDLER*) Probes	Vehicle mounted	Cs-137, Ra-226, Co-60, Am-241, Pu-239	Particle detection – particularly in challenging and dynamic environments such as beaches. The real time particle detection and alarm supports immediate particle recovery.

*FIDLER = Field Instrument for the Detection of Low-Energy Radiation

Source: Davies (2017) and Nuvia (2015)

Due to the size of the proposed sites to be investigated as part of this study and the nature of the radiation at the selected archaeological sites, Groundhog ‘Fusion’ will be used (Figure 2.4). Due to the larger NaI crystal size within the system, the Groundhog Fusion system is capable of achieving good detection limits. Further, the simplicity of the system and flexibility to deploy in various configurations (including hand-held, vehicle mounted and collimated) make it ideally suited to testing gamma radiation survey methods in this novel application.



Source: Davies (2017)

Figure 2.4 – Examples of some of the more common Groundhog configurations. The Fusion System (front) will be deployed as part of this study.

Radiation Detection/ Quantification

The Groundhog Fusion system uses a 76 x 76 mm NaI crystal detector for capturing gamma photons (Davies 2011). This is supported by photomultiplier tube and multi-channel analyser enabling the identification of the specific isotopes responsible for the detected radiation (Ortec 2015). It allows operators to attribute measured count rates to naturally occurring isotopes in the soil or the presence of anthropogenic radioactive contamination. The carbon fibre casing holding this equipment is very thin, minimising loss of lower energy gamma signals (Davies 2011, Nuvia 2018). A collimator can be fitted to the system to ensure the detectors are sensitive to radiation from one particular direction; i.e., the ground directly beneath it.

The system is capable of completing high-density surveys. Operators will systematically walk along one metre transects at an average speed of approximately 1 metre per second resulting in a data resolution of one reading per square metre and a typical total of 15,000 readings per person per day (Davies 2017). However, greater densities can be achieved by traversing the site at a slower speed and along narrower transects. In all configurations, the detector unit is typically held approximately 20 cm above the ground surface.

Throughout the survey, spectral data are continuously collected. The system is configured to measure multiple regions of interest and therefore energy ranges. Fifteen regions are typically set

up, and can include for example, cobalt-60 (Co-60) (1090 – 1400 keV) or U-238 (by Bi-214) (1600 – 1900 keV) (Davies 2011). In applying this method, it is possible to analyse the ratios between windows and therefore isotopes of interest – for example, potassium-uranium-thorium analysis.

Global Positioning System

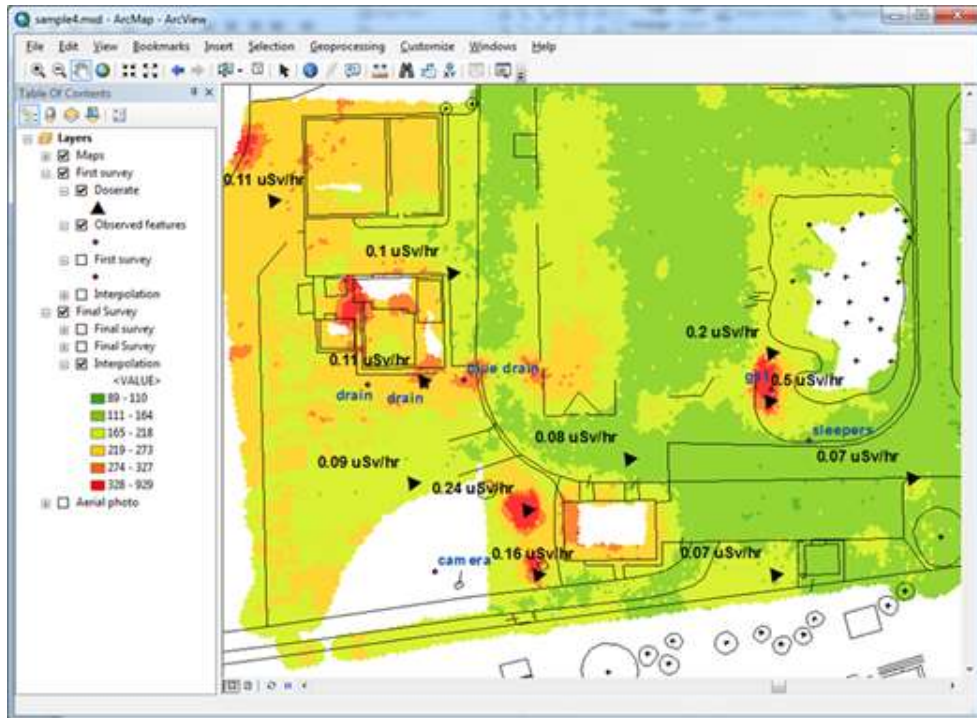
A GPS/ GLONASS system, capable of achieving centimetre accuracy for land surveys is also deployed as part of the Groundhog system, supporting accurate positioning of each radiation measurement.

Data Collection and Processing

Radiation and GPS data is continuously collected, with a typical data-time interval of 0.2 – 1 seconds via a proprietary data logger; a hand-held UMPC. At the end of each surveying session, the data is transferred to a desktop processing PC where several data management activities are performed. This includes cross referencing GPS data against local base station measurements, conversion to the required format and checks on the quality and completeness of the GPS and radiation data (Nuvia 2018).

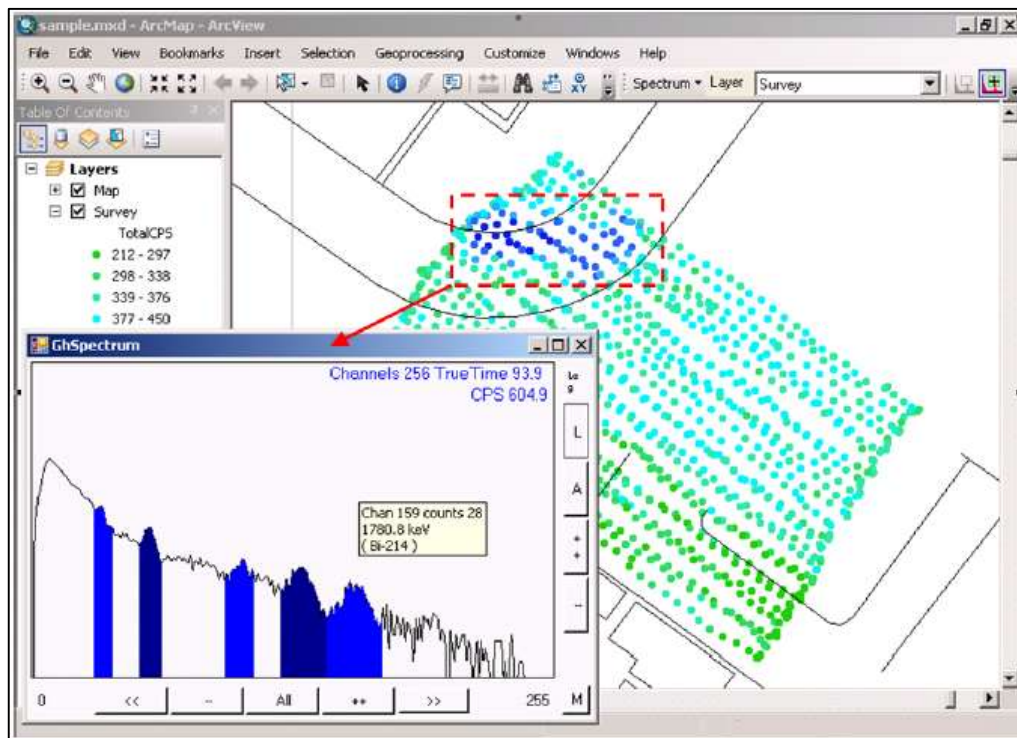
Once the major processing is complete, approved/ accepted data are imported into a standard ArcGIS (version 10.1) software programme, supported by bespoke tools, to produce a variety of visual outputs. This includes high-resolution radiation distribution maps representing radiation levels across the surveyed area (Figure 2.5) and count rate distribution graphs which show the overall profile of the survey and spectral data (Figure 2.6). The count rate distribution graphs also support the identification of background radiation levels at the site. Resolution of the contour maps, as shown in Figure 2.5, is selected during data interpolation. A typical cell size/ resolution set for the map is 0.25 m. However, the settings used to display the data can be altered to help bring out anomalies.

Further detail on the data processing can be found in Chapters 3, 4 and 5.



Source: Nuvia (2018)

Figure 2.5 – Sample Map Produced by ArcGIS Showing Dose Rate in $\mu\text{Sv/hr}$. The typical cell resolution is set at 0.25 m.



Source: Nuvia (2018)

Figure 2.6 – Measured Radioactivity (Total Gamma Counts Collected) in Counts Per Second (CPS). Inset graph focuses on spectra data for an area of interest, showing presence of Bi-214

2.3.3 Application of Gamma Radiation Surveys

Applications of gamma radiation and spectrometric surveys using systems such as Groundhog are diverse. They can complement academic, commercial and safety investigations. This ranges from the surveying of a nuclear site in preparation for delicensing through to the monitoring of shipping ports and airports as part of the UK's security infrastructure. An overview of the applications for gamma surveys is presented in Figure 2.7. With the exception of materials testing where known radioactive sources are used and detected, for example to establish the thickness of scale within an oil and gas pipeline, the aim of a gamma survey is to establish where the radioactive material is, how much material is there, the source of the radioactivity, and whether contamination migration has occurred or could occur.



Source: Personal Image

Figure 2.7 – Overview of the Typical Applications of Gamma Surveys

2.3.3.1 Site Characterisation and Identification of Radioactive Contamination

According to the International Atomic Energy Agency (IAEA), radioactive contamination may be defined as “...radioactive substances on surfaces, or within surfaces, liquids or gases (including the human body), where their presence is unintended or undesirable” (IAEA 2007). Such contamination can be attributed to naturally occurring or anthropogenic sources. Sources of the latter are numerous. They include nuclear power generation, research and development, historic manufacturing activities such as luminising works, defence, nuclear accidents and the production and use of medical isotopes (IAEA 2017). Contamination may be confined to buildings or

dispersed in terrestrial and aquatic environments through planned discharges (e.g. via stacks, drains or waste disposals) or unplanned releases (e.g. nuclear accidents or incidents).

Contamination surveys can support numerous objectives over the lifecycle of a project or event. Routine surveys can fulfil a monitoring function, providing confidence that radiological conditions remain acceptable, and that no contamination has occurred. This might occur within the confines of a laboratory environment for example. It can also be used to monitor trends over time. For example, monitoring contamination dispersal following an accidental release of radioactive material during an emergency/ abnormal event. This is exemplified in the wide-scale environmental monitoring undertaken following the Chernobyl accident in 1986 (Steinhauser *et. al.* 2014) and more recently, after the earthquake and associated tsunami that caused major damage to the Fukushima Nuclear Power Plant in March 2011 (Steinhauser *et. al.* 2014, Saito and Onda 2015).

Targeted surveys can be employed to inform the nature and extent of any remedial works required to decontaminate a site where radioactive contamination is expected. Alternatively, targeted surveys can provide confidence that residual contamination at a site is below the level of regulatory concern and is therefore suitable for release from regulatory control. In addition to land characterisation, this technique can also be applied to otherwise inaccessible areas such as pipelines or boreholes. Some examples of where Nuvia's Groundhog system has been successfully deployed to support site characterisation and delicensing activities are provided below. The first case study (highlighted in Box 2.1) explores the use of the Groundhog system in locating and quantifying accumulations of technologically enhanced naturally occurring radioactive material (TENORM) within spoil heaps at the Olen radium production facility in Belgium. This case study has been chosen as it provides a good example in the use of Groundhog in the detection of naturally occurring radionuclides.

Box 2.1 – Olen Metal Ore Processing Site: A Case Study

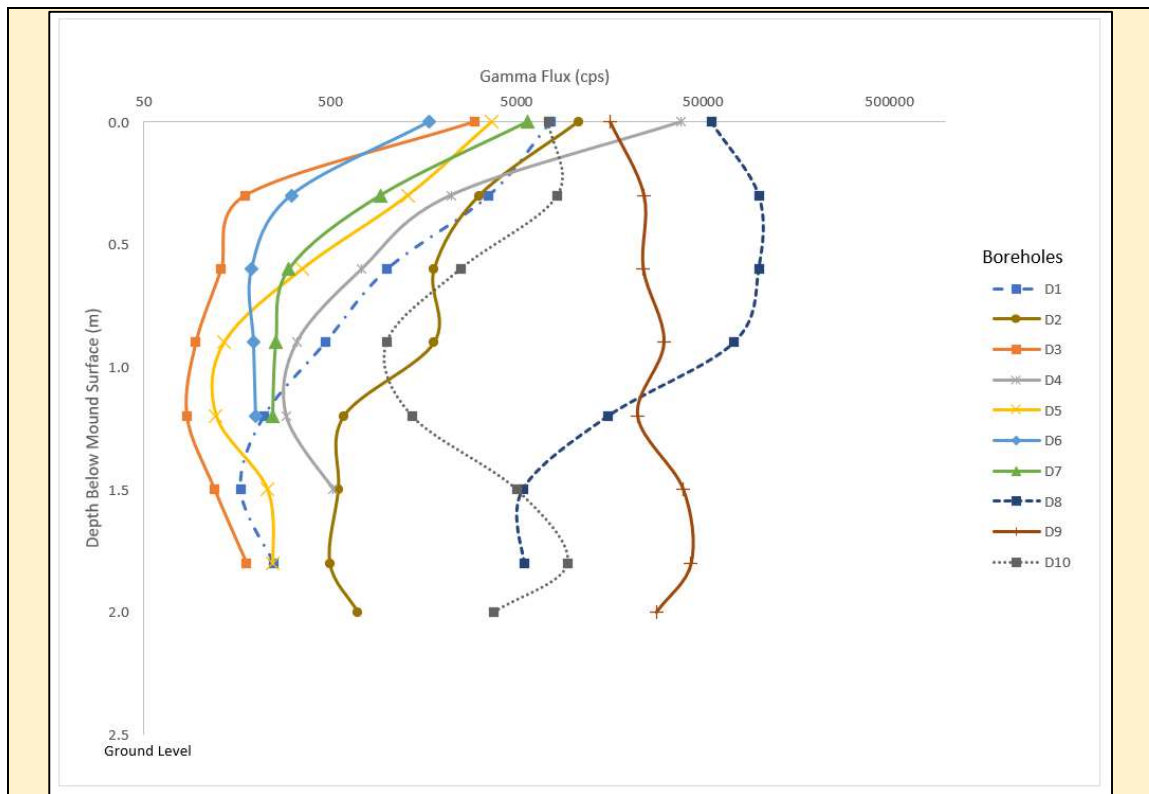
Groundhog Surveying of the Olen Ore Processing Site, Belgium – An Example of Deploying Groundhog for the Detection of Naturally Occurring Radioactive Material.

Umicore, formerly the 'Union Manière due Haut-Katanga (UMHK)', owned and operated an ore processing plant at the Olen site for nearly 40 years. The plant was responsible for the extraction and purification of various metals including cobalt and uranium (IAEA 2010, Umicore 2019). One of its primary operations was the commercial extraction of Radium-226 (Ra-226) from uranium ore (pitchblende). Indeed, it was the UMHK facility that presented Marie Curie with her first gram of the isotope for use in her experiments (Chemical Book 2021, Umicore 2019).

During normal operations, several buildings and the surrounding ground became progressively contaminated with naturally occurring radioactive material (Nuvia 2008). Following cessation of processing activities, a programme of remedial works was completed. The resultant wastes, along with legacy ore processing wastes, were disposed of in-situ in two spoil heaps: D1 and Stort 1 (Nuvia 2008, IAEA 2010).

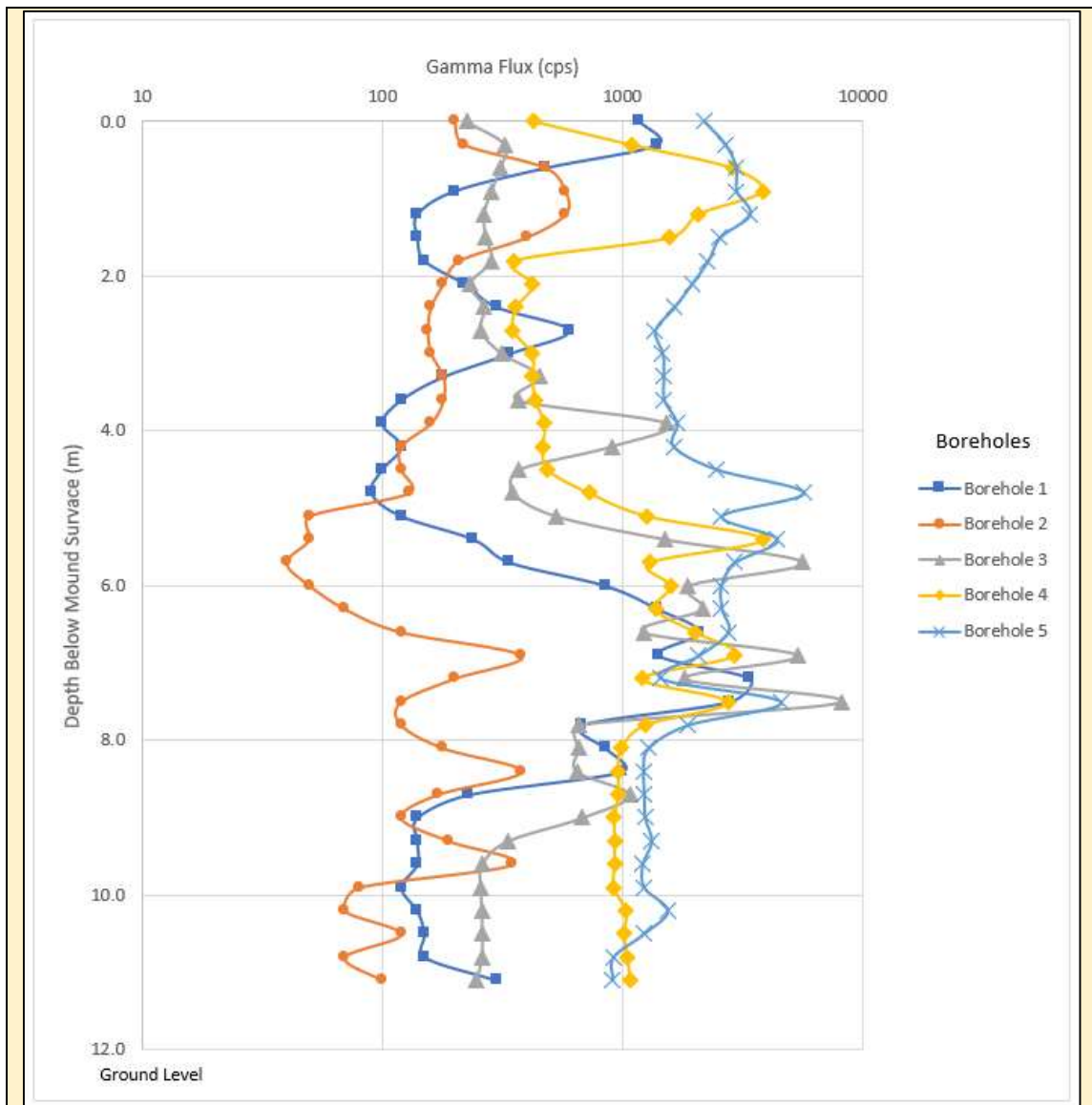
Recognising that both spoil heaps were in close proximity to the Herentals-Bocholt Canal (IAEA 2010), a programme of geotechnical and radiological characterisation was initiated in 2008 to inform a robust strategy for their long-term management (Nuvia 2008). This built on previous Groundhog surveys of Stort 1 undertaken in 2003. Nuvia's Groundhog system was deployed to support radiological characterisation. The detector unit was lowered down a series of boreholes, lined with polyvinyl chloride (PVC) tubing, set into each of the spoil heaps. The detector was lowered at a rate that facilitated collection of a radiation measurement every 0.5 m for the D1 spoil heap and 0.3 m for Stort 1 (Nuvia 2008). Groundhog surveys of the spoil heap surfaces were also undertaken.

Figure 2.8 and Figure 2.9 show the gross gamma radiation levels, presented in counts per second (cps) for the D1 and Stort 1 spoil heaps respectively. At both sites, all boreholes presented radioactivity levels above natural background (Nuvia 2008). At the D1 spoil heap, Figure 2.8 suggests that radioactivity levels reduce as the detector approaches ground level, with most radioactivity present within the top 0.5 m. It is highlighted in the Nuvia 2008 report that in borehole D8, the Groundhog detector became saturated at a count rate of 100,000 cps measured at a depth of 0.6 – 0.3 m. This led to an estimated Ra-226 concentration of ≥ 60 Bq/g (Nuvia 2008). In contrast, the maximum Ra-226 concentration measured in Stort 1 was calculated as 4.7 Bq/g (Nuvia 2008). The Stort 1 data shows a clear band of activity in all boreholes at a depth of 6 – 8 m. This is corroborated by comparing these results with a previous Groundhog survey of Stort 1 undertaken in 2003. Figure 2.10 is a radiation contour map for Stort 1 generated during the 2003 survey which also shows a clear band of elevated radioactivity approximately half way down the spoil heap.



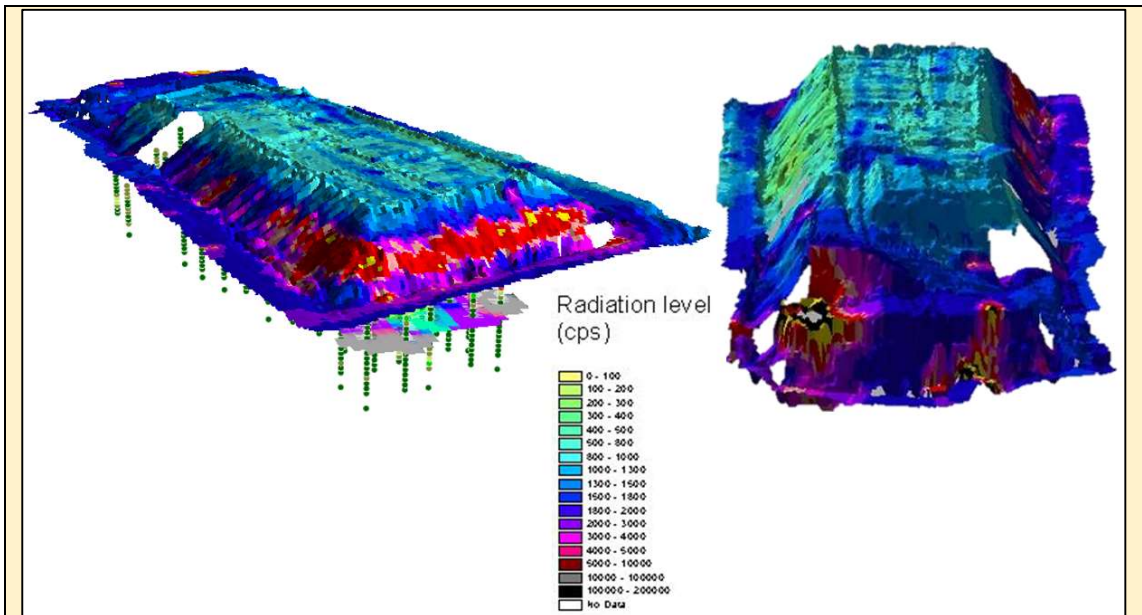
Source: Graph generated using raw data from Nuvia (2008)

Figure 2.8 – Gamma Flux (cps) Profiles for the D1 Spoil Heap at the Olen Metal Ore Processing Site



Source: Graph generated using raw data from Nuvia (2008)

Figure 2.9 – Gamma Flux (cps) Profiles for the Stort 1 Spoil Heap at the Olen Metal Ore Processing Site



Source: Beddow (2007)

Figure 2.10 – Radiation Contour Map of Stort 1, Showing Gross Gamma Flux in Counts Per Second. These images were generated as part of an earlier Groundhog Survey undertaken in 2003.

The data from both the 2003 and 2008 Groundhog surveys were compared against data from the radiochemical analysis of samples collected during borehole excavation. This comparison demonstrated a moderate to good correlation, verifying the validity of the Groundhog data.

This case study demonstrates the efficacy of the Groundhog system in identifying and measuring concentrations of naturally occurring radioactive material and the value of visual outputs. It is however acknowledged that the radioactive material present here has been technologically enhanced. This has led to concentrations of naturally occurring isotopes such as Ra-226 greater than would be found following natural processes as explored in Section 2.4.

2.3.3.2 Geological Surveys

It is recognised that gamma ray surveying has multiple Earth Science applications, such as gaining a better understanding of the thermal and geological histories of the Earth. For example, in a study by Chiozzi *et. al.* (2000), trials were undertaken to establish the effectiveness of gamma spectrometric techniques to measure the relative concentrations of primordial heat generating isotopes of potassium, uranium and thorium in volcanic and sedimentary rock samples. The study compared the efficiency and effectiveness of a lower resolution NaI detector against the higher resolution HPGe detector. The study concluded that the portable NaI detector would be a valuable tool in geophysical applications (Chiozzi *et. al.* 2000). In particular, noting that the

system was effective at determining the concentrations of heat producing elements in rocks and soils (Chiozzi *et. al.* 2000).

In a later study by Kozhevnikov, *et. al.* (2018) a portable gamma ray spectrometry system was used in conjunction with other geophysical survey methods, including magnetic and resistance surveys, over a period of several years to study the location of a suspected ancient iron smelting site and subsequently inform excavations in the area. Kozhevnikov's study concluded that whilst the gamma ray survey was not directly linked to the search for and study of archaeometallurgical targets, the gamma survey data were valuable in establishing the geological context of the area. For example, it was possible to establish areas of elevated radioactivity created by accumulations of sediment and debris from the Primorsky Range which is predominantly granitic in nature (Kozhevnikov, *et. al.* 2018).

Of increasing interest is the ability to use remote gamma ray spectrometry surveys to prospect for valuable mineral resources. Such techniques have been used successfully since the mid-20th century to identify uranium deposits (IAEA 1979). Gamma radiation surveys have since been effectively deployed in the identification of other valuable mineral deposits as the techniques and technologies have been refined. This has been, in part, driven by the general desire to develop reliable and cost effective methods for identifying mineral deposits – especially in more remote areas with challenging terrain (Campos, *et. al.* 2017). Examples of the successful deployment of airborne gamma spectrometry methods for the detection of minerals can be seen in multiple studies, including those of de Quadros, *et. al.* (2002) and Tourlière, *et. al.* (2003).

In the study by de Quadros, *et. al.* (2002) an airborne gamma ray survey was undertaken to generate a series of contour maps revealing the relationship between potassium, uranium and thorium concentrations. This was done with the aim of identifying areas characterised by elevated concentrations of K-40, which in the area of interest, are indicative of hydrothermal activity and valuable lode gold deposits (i.e. veins of gold embedded in rock fissures). The maps were able to identify medium to high favourable target areas for exploring gold deposits (de Quadros *et. al.* 2002). The data were verified by comparing the generated maps with known lode gold deposits in the (anonymised) region and potassium concentrations from other processing methods.

In contrast to the de Quadros study, Tourlière, *et. al.* (2003) utilised existing radiometric data from an earlier geophysical survey to identify areas of K-40 depletion within the granite dominated Armorican Massif in northwest France. The aim here was to identify areas with a high probability of containing elevated concentrations of kaolinite; a valuable mineral resource. Kaolinite is formed when potash feldspar is exposed to high water through-flow (either precipitation or hydrothermal water sources) which is further enhanced by the presence of rock fractures that promote water movement (Tourlière, *et. al.* 2003). Potassium, which is a significant component of potash feldspar ($4\text{KAlSi}_3\text{O}_8$) is soluble in water and therefore highly mobile (Bezuidenhout 2012). Due to the conditions required for kaolinite formation, potassium (including its radioactive isotope K-40) consequentially becomes depleted in these areas. The authors therefore believed that kaolinite identification may be possible through completion of a gamma survey. The survey was completed using an Exploranium GR820 system (which utilises a NaI crystal detector). Resultant data highlighted 24 areas with significant potassium depletion. When overlain with the locations of geological fault intersections, nine high priority areas were identified. Fifteen of the 24 areas were physically inspected to confirm the presence of kaolinite. When focussing on potassium concentrations at a local scale, a success rate for identifying kaolinite of 54% was recorded (Tourlière, *et. al.* 2003). This increased to 64% for high priority areas (Tourlière, *et. al.* 2003). Although still statistically significant, a much lower and more representative average success rate of 30% was recorded on a regional level (Tourlière, *et. al.* 2003).

In comparing the two studies described above, it is valuable to note that anomalies of interest are not limited to areas of elevated radioactivity. Rather, localised areas of activity *depletion* could also indicate the presence of a potential target. This is an important consideration when reviewing data generated as part of this research project.

A number of limitations for the gamma surveying technique were identified by Tourlière, *et. al.* (2003). These included the risk of shielding from overburden and the need to carefully consider impact of variations in flying altitude, speed and survey grid size on data quality. The shielding effect of overburden in this research project is an important consideration, likely limiting suitable target sites to those with suspected targets relatively close (<1 metre) to the surface. The study also noted that the technique was only capable of indicating areas likely to host kaolinite and not the volume of kaolinite – valuable information for miners (Tourlière, *et. al.* 2003). It was however

concluded that the combination of gamma survey data and fault intersection locations is an environmentally sound technique for identifying high priority zones that warrant intrusive investigation. This again highlights the benefits of applying complementary techniques to aid site characterisation.

2.3.3.3 Archaeological Surveys

A more novel application of portable gamma radiation/ spectrometry surveying is the mapping of buried artefacts of archaeological interest. The technique follows a similar strategy to traditional geophysical methods, insofar as the aim is to detect/ measure a contrast in the (radiological) properties of the target and surrounding substrate. This less-well established application, and the focus of this thesis, is considered in more detail in Section 2.4.

2.4 Use of Gamma Radiation Surveys in an Archaeological Context

An extensive review of the available literature suggests that only a very limited number of studies have been undertaken where gamma-ray surveying methods have been used in archaeological investigations. Consequently, the efficacy of gamma radiation surveying in this context is not well understood. Numerous variables, such as the impact of geology and target type on the technique's effectiveness, remain largely unexplored. This results in considerable uncertainty regarding the reliability of this method for such applications.

In the few studies identified, the objective has been to identify contrasts in radioactivity concentrations in the natural background geology of the area and potential features of interest. All cases reviewed as part of this literature review employed a similar methodology. A static counting system is used to take gamma radiation readings for a pre-determined period of time along defined survey points (e.g. transects or a grid), with data recorded manually or automatically (electronically). The data has then been processed to generate a visual output, such as a matrix or contour map. These visualisations were used to identify any contrasts in radioactivity that could indicate the presence of a buried feature of interest.

This section begins by discussing the importance of existing non-intrusive techniques in archaeological prospection and the value of applying complementary geophysical techniques at a

site. The section continues by exploring the potential contribution of gamma radiation surveying to this context. It provides a review of the published literature, exploring the work undertaken so far in establishing the practical applications of applying gamma radiation surveying methods in this more novel scenario. In some of the studies reviewed, application of radiation surveys worked well, successfully revealing the location of buried features. In others, no difference was discerned between known buried features and the natural background radioactivity. This has provided a valuable insight into the challenges in successfully applying the technique, the survey methods that have worked well and where there may be shortfalls. This chapter therefore concludes with a discussion on the advantages and limitations of the survey techniques deployed, the shortfalls identified and in consequence, the technical challenges and uncertainties to be investigated as part of this thesis.

2.4.1 Existing Non-Intrusive Techniques in Archaeological Prospection

Intrusive investigation is an essential part of identifying, recording, retrieving and interpreting buried archaeological artefacts and other environmental evidence (Drewett 2011). It also facilitates analysis of the finds and their context in the surrounding environment (Historic England 2018). However, it is acknowledged that excavations can be disruptive (particularly to landowners), resource intensive (including cost materials and labour) and time consuming (Barker 1993). Intrusive surveys are also unrepeatable and destructive (Drewett 2011, Perrin, *et. al.* 2014). It is therefore necessary to conduct excavations meticulously to ensure all data is adequately recorded and processed – particularly when an object is moved from its resting position (Perrin, *et. al.* 2014). Excavations in culturally sensitive or protected areas must also be managed with sufficient care and attention (Barker 1993). Obtaining the necessary permissions can also create delays to the start of a project.

To maximise the value of each excavation, optimised siting is of critical importance; ideally aiming to find multiple features or artefacts in a single trench (Barker 1993). The completion of a non-intrusive geophysical survey can generate valuable information that can help identify an optimised location for an excavation that will yield the most data. This is particularly useful for ‘commercial’ or ‘rescue’ archaeological investigations where there is pressure to complete a site survey (normally as part of an environmental impact assessment under the Town and Country Planning (Environmental Impact Assessment) Act 2017) within limited time and financial budgets (Gaffney

et. al. 2002). Non-intrusive techniques that can support effective targeting of excavations are therefore valuable (Gaffney *et. al.* 2002).

The application of non-intrusive investigation techniques, using dedicated geophysical methods, for the prospection of archaeological features dates back to 1938 (Turk *et. al.* 2011, Gaffney and Gater 2003). A resistance survey undertaken over a defined area near a Parish Church in Williamsburg Virginia in the US was able to detect an anomaly. However, subsequent excavation yielded no artefacts or archaeological features (Turk *et. al.* 2011). Greater development and successful application of geophysical techniques began in the 1940s with the successful completion of a resistance survey at a monument complex in Dorchester, UK (David and Payne 1997, Turk *et. al.* 2011). The range and capability of geophysical techniques evolved over the coming decades, most notably in the 1990s with the development of computerised systems capable of generating and recording large amounts of data digitally, and in a short period of time (Turk *et. al.* 2011). The more common geophysical surveying techniques for archaeological prospection can be divided into the following groups:

- Magnetic
- Electrical
- Electromagnetic
- Ground penetrating radar

Each of these overarching methods/ technologies measures a different physical property that is either naturally occurring (a ‘passive’ technique) or artificially induced (an ‘active’ technique). Examples of active techniques include magnetic susceptibility, whereby an electromagnetic field is induced in the soil, and electrical resistivity where the electrical resistance of a substrate is measured following active application of a DC electrical current (Milsom and Eriksen 2011). In contrast, a magnetometer survey is a passive technique which measures the changes of magnetic flux to the Earth’s magnetic field.

In each case, the effectiveness of the chosen technique relies on the ability to measure clear differences in the physical properties of potential targets and the surrounding substrate (Gaffney and Gater 2011, Milsom and Eriksen 2011, Ruffell and McKinley 2008). In consequence, there is

no single technology that can be ubiquitously applied to all sites (Gaffney and Gaffney 2010, Gaffney *et. al.* 2002, Milsom and Eriksen 2011). Rather, it is essential to consider the physical and chemical properties of the suspected target and surrounding substrate, target size (Ruffell and McKinley 2008), and amount of overburden when identifying the optimal strategy. This is due to the varying ability of each survey method to differentiate between certain materials and the background substrate. For example, magnetic surveys are less effective at identifying smaller features and structures made from non-fired brick (Gaffney and Gater 2003). This is further explored by Schmidt *et. al.* (2015) who offer a theoretical scenario for the demonstration for the selection of ‘good’, ‘better’ and ‘best’ geophysical techniques. In the proposed scenario, the aim is to confirm the location of local marble blocks buried in soil from the same parent material. Schmidt, *et. al.* 2015 proposes that magnetic techniques would be less effective due to the limited amount of contrast achievable from materials from the same/ similar parent rock. Resistivity techniques may offer better contrasts due to the increased resistance experienced by the marble blocks which will retain less moisture. The ‘best’ option in this scenario is considered to be GPR which will be capable of measuring the contrast between the solid blocks and less dense soil (Schmidt, *et. al.* 2018). Building on this, Table 2.3 provides an overview of suitable targets for the more common geophysical techniques, their known vulnerabilities and suitable target types.

The targeted selection of a single geophysical technique based on the suspected target type and technology limitations (as indicated in Table 2.3), is a justifiable and cost effective (Ruffell and McKinley 2008) strategy as it avoids collection of data that cannot or will not be used as part of the study. It is also recognised that application of multiple survey techniques is not always viable. This is especially relevant for commercial projects where mobilisation, fieldwork, data interpretation and resultant reports must be completed within limited budgetary and time constraints in the context of a larger inter-disciplinary project (Gaffney *et. al.* 2002).

It is however recognised that application of a (limited) range of contrasting techniques could offer numerous benefits; particularly if little (if anything) is known about the potential target. For example, assessment of datasets reflecting different properties of the same site could minimise the risk of identifying ‘false positives’ (wrongly concluding that an anomaly is a feature/ target of interest) or ‘false negatives’ (wrongly concluding that there are no features of interest). If multiple survey types identify an anomaly in the same area, the operator can be more confident

that there is a feature that warrants intrusive investigation. Milsom and Eriksen (2011) further expand on this, noting that the properties of the anomaly (strength of signal, size, shape, etc.) can be influenced by various factors such as the size of the target, the amount of overburden or surface roughness. As a result, two objects with distinct physical characteristics could generate similar anomalies, leading to a degree of ambiguity in the interpretation (Milsom and Eriksen 2011). This is particularly a risk where there is no extant knowledge of the site that could be used to inform the interpretation. The ability to compare the results of complementary survey techniques that provide different information, and therefore different insights into below ground features can help address this challenge (Kvamme 2006). Finally, appropriate selection of contrasting survey techniques can minimise the risk of the technologies used being susceptible to the same types of interference (such as from metallic objects, power lines or high water tables) that could affect data integrity (Gaffney and Gater 2011, Milsom and Eriksen 2011, Sarris, *et. al.* 2018). For example, high moisture content in soils can generate misleading signals when using electrical resistivity techniques, whereas magnetometry techniques are particularly susceptible to the presence of metallic objects such as buried pipelines (Gaffney, *et. al.* 2002, Piro, *et. al.* 2000, Schmidt, *et. al.* 2015). For these reasons, having a range of techniques that measure different physical properties and have different sensitivities is highly valuable and maximises the chance of deploying a technique that will yield positive results.

These considerations are well acknowledged in published literature as exemplified in studies such as those by Trogu, *et. al.* (2014), Zheng, *et. al.* (2013), Creighton and Fry (2016) and Halgedahl, *et. al.* (2009). In the Trogu *et. al.* (2013) study, a mixture of geophysical techniques was applied to locate a buried Roman aqueduct located in Sardinia, Italy. The structure consisted of limestone blocks and fired clay brick. The aqueduct was fully accessible and known to be approximately 10 metres underground. Due to the amount of overburden, more traditional techniques such as ground penetrating radar, magnetometry and electrical resistivity methods were discounted in favour of those techniques capable of reaching the necessary depths (Trogu, *et. al.* 2014). This included for example, electrical tomography, time-domain electromagnetic sounding and very low frequency sounding. It was acknowledged by the authors that the prior knowledge of the location of the aqueduct aided interpretation. Indeed, individual survey results alone may have been insufficient to say with confidence that the identified anomalies were attributable to the aqueduct (Trogu, *et. al.* 2014). However, it was also recognised that the comparison of the data from the

three different surveying techniques helped improve confidence in geophysical data interpretation (Trogu, *et. al.* 2014).

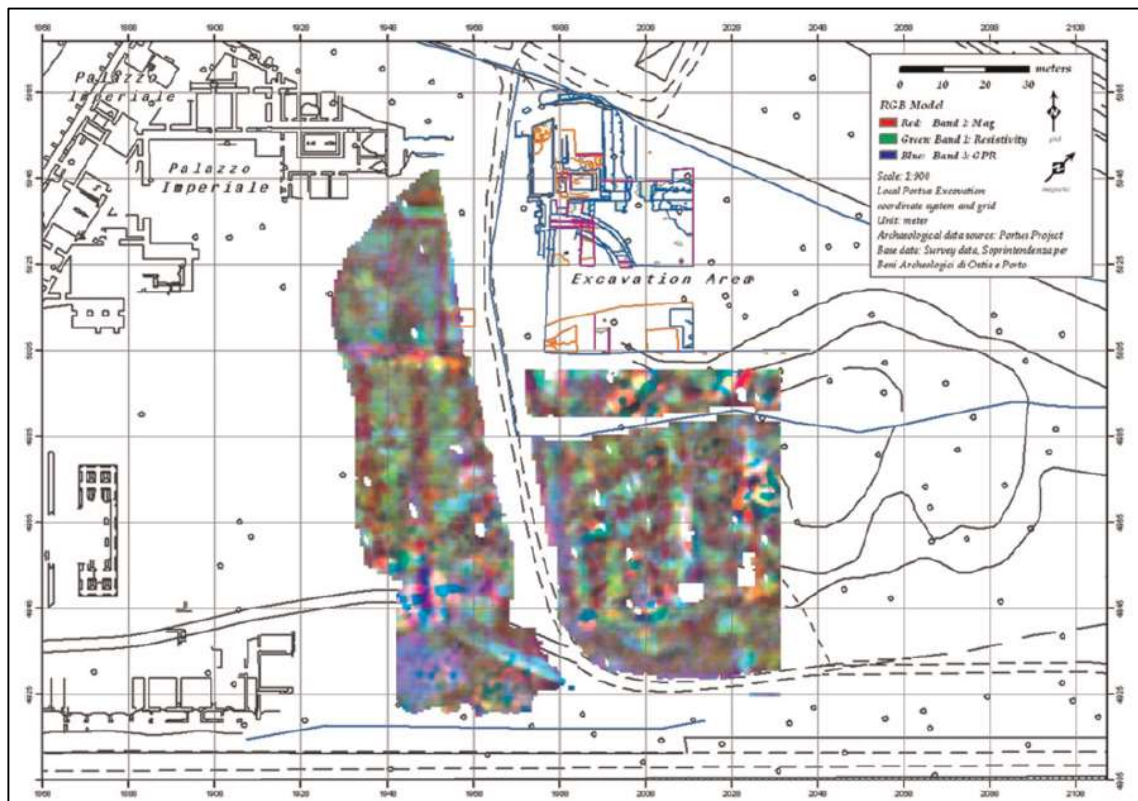
The study by Zheng, *et. al.* (2013 page 167) acknowledged that different geophysical techniques “play different roles on different scales”. Again, multiple geophysical techniques were applied. The techniques were selected by accounting for the varying properties of features expected within the survey area of the Jinsha archaeological site. High-density resistivity surveys were applied on a macroscale and used in the characterisation of a paleochannel (buried/ infilled inactive river or stream). In contrast, induced polarisation and multi-frequency electromagnetic techniques were used successfully to locate a number of bronze artefacts that were small and thin in nature resulting in weak anomalies (Zheng, *et. al.* 2013) that might have otherwise been missed if a single survey method had been deployed.

As part of the Silchester Mapping Project, the output from multiple geophysical surveys was successfully combined with alternative data sources to aid interpretation and gain a comprehensive understanding of the site (Creighton and Fry 2016). Supporting data sources included records from earlier excavations, field walking, aerial photography and Light Detection and Ranging (LiDAR) surveys (Creighton and Fry 2016).

Halgedahl, *et. al.* (2009) used the data from multiple non-intrusive and intrusive survey techniques to aid characterisation of the Upper Wheeler Formation in West-Central Utah. Data from gamma-ray spectrometry and magnetic susceptibility surveys in combination with sedimentological/ carbonate analysis of samples was used to characterise ancient depositional environments and whether this could be linked to exceptional preservation of fossils in the area (Halgedahl, *et. al.* 2009). The data showed a strong correlation between the gamma-ray spectrometry and magnetometry data; both the radioactivity and magnetic susceptibility decreased linearly with increasing calcium carbonate concentrations (Halgedahl, *et. al.* 2009). A ‘hot zone’ defined by both a rapid increase in gamma activity and magnetic susceptibility (aligning with a depletion of calcium carbonate) correlated with the area identified as being the location of very well preserved soft-bodied fossils (Halgedahl, *et. al.* 2009). The findings of the study by Halgedahl, *et. al.* 2009 are promising, and supports the hypothesis that it might be possible to use gamma radiation survey methods to support identification of fossil sites.

Multiple studies have further shown the effectiveness of multiple geophysical techniques on resultant data quality. For example, Columbero, *et. al.* 2020 applied a mixture of ground penetrating radar and magnetometry survey techniques at an archaeological site in Locri Epizephyrri in southern Italy to improve data quality. The authors concluded that the ability to compare the two data sets improved the likelihood of finding “features of significance”. This was clearly demonstrated on two different occasions. Firstly, the data from the initial magnetometry survey showed a number of moderately well-defined linear anomalies as well as two very clear anomalies. The subsequent ground penetrating radar images highlighted the linear features far more clearly. However, the circular anomalies in the magnetometry data were not reflected in the ground penetrating radar data. Later excavations confirmed that the linear anomalies could be attributable to archaeological features (Columbero *et. al.* 2020). In contrast, excavations of the circular magnetometry anomalies did not yield any archaeological features (Columbero *et. al.* 2020). Interestingly, wide sandstone blocks uncovered through excavation were not present as anomalies in any of the geophysical data (Columbero *et. al.* 2020), highlighting the importance of selecting the optimal techniques. This finding supports an observation by Schmidt, *et. al.* (2015); that the output of a geophysical survey cannot be used as ‘negative data’. I.e., it is not possible to conclude with confidence that there are no archaeological features of interest due to an absence of anomalies within the data.

Keay, *et. al.* (2009) further supports the notion that higher quality results can be obtained by generating and integrating data using a range of different geophysical techniques. In a survey of a Roman Port (Portus) on the Tyrrhenian coast, multiple geophysical surveying techniques were deployed, including magnetometry, microtopographic, resistivity tomography and ground penetrating radar (Keay *et. al.* 2009). Each technique enhanced the archaeological understanding of the area; from characterising soil overburden to improved delineation of buried features within the area such as ‘moles’ and buildings (Keay, *et. al.* 2009). The visual output from the integration of the different datasets is presented in Figure 2.11 as it provides an excellent example of the value of data integration. The authors found that applying the data in different layers that could be added and removed as required supported the identification of more subtle features that may have otherwise been overlooked (Keay, *et. al.* 2009).



Source: Keay, et. al. (2009)

Figure 2.11 – Red-green-blue composite generated by Keay, et. al. (2009) combining the geophysical responses from the multiple survey methods used. This image has supported identification of more subtle features that might otherwise have been missed.

The results from these and similar studies support the use of a ‘toolbox’ of non-intrusive surveying techniques for the characterisation of archaeological sites. Based on the findings from this literature review, gamma-surveying techniques could be an additional complementary tool that could contribute to the accuracy and efficacy of non-intrusive surveys undertaken at sites of archaeological interest. As discussed in Section 2.4.3, a limited number of studies has been undertaken to explore the validity of such an approach. A review of the available literature highlighted a number of data gaps and uncertainties that have been explored as part of this research project and are addressed in subsequent chapters.

Table 2.3 – Overview of Viable Target Types and Areas of Susceptibility for the Common Geophysical Survey Methods

Geophysical Method	Target Type							Areas of Susceptibility
	Roads	Building Structures / Walls	Disturbed Soil	Occupational Debris	Ditches/ Trenches/ Moats	Kilns/ Ovens/ Hearths	Graves	
Electrical Resistivity	✓	✓	✓		✓		✓	<ul style="list-style-type: none"> • Extreme soil moisture conditions can give misleading signals – particularly in very dry or waterlogged soils. • Requires contact with ground surface. • Less effective in highly vegetated areas – again, affects water moisture content. • Detectors can be affected by extreme changes to climatic conditions. • Detectors can also be affected by overhead or buried electricity lines, electrified railway lines and other buried cables. • Equipment can be large and awkward, making it more challenging to survey larger areas.
Magnetometry		✓		✓		✓		<ul style="list-style-type: none"> • Can be affected by metallic infrastructure such as pipelines, cables, buried tanks and nearby pylons, therefore less effective in urban environments. • Less effective for smaller targets. • Less effective for detecting non-fired brick. • Results can be skewed by the presence of iron-rich rocks.
Magnetic Susceptibility	✓	✓	✓				✓	<ul style="list-style-type: none"> • As per magnetometry. • Limited to very shallow archaeology.
Ground Penetrating Radar	✓	✓					✓	<ul style="list-style-type: none"> • Signal can be attenuated by clay-rich soils. • Requires good contact with ground surface. • Medium mobility/ flexibility of instrumentation.

Source: Table adapted from Turk *et. al.* (2011) with additional input from Sarris, *et. al.* (2018), Ruffell and McKinley (2008) & Gaffney and Gater (2003)

2.4.2 Gamma Radiation Surveying of Archaeological Sites

Gamma radiation and spectrometry techniques have, to a very limited extent, been used to successfully locate the position of fully or partially buried historic man-made structures. Indeed, at the time of writing their 2006 paper on the application of gamma ray surveys for mapping sub-surface structures, Ruffell, *et. al.* (2006) noted that only two published papers looked at gamma ray surveying techniques for locating buried buildings or archaeological remains. As we will see later in this section, this number has not increased significantly, highlighting the need for further research.

The first paper referred to by Ruffell, *et. al.* (2006) details an earlier study, conducted by Ruffell and Wilson in 1998, of the efficacy of using gamma ray survey data to identify subterranean features. Interestingly, this project was undertaken at a similar time to the study undertaken by Jones and Chure (1998) investigating the feasibility of using gamma ray survey techniques to locate fossil remains. The Ruffell and Wilson (1998) paper reviews a number of site surveys, assumed to have been completed by the authors, undertaken over the previous five years.

It is understood that at each of the survey locations presented in the 1998 paper, a common survey method was applied, whereby a Scintrex GIS-5 portable gamma-ray detector was used to take total count measurements along pre-defined transects at five different locations. Resultant data was verified using data from subsequent surveys using an Exploranium GR-256 spectrometer and Scintrex GS-256 detector. Ruffell and Wilson (1998) specified that typically, five measurements were taken at each point along the transect (count times were not specified by the authors). The maximum and minimum values were rejected and the remaining 3 averaged to give a single total count for each sample location. The radiation surveys were effectively used as a technique for identifying variations in the chemical/ geological composition of identified sites of interest, rather than looking for buried man-made features Ruffell and Wilson (1998). Most notably, the surveys were used to identify shifts between sand, till and alluvium deposits.

Each of the case studies covered in the 1998 Ruffell and Wilson review tested varying techniques for conducting surveys and presenting data to improve the quality of the final data set. Variations in survey techniques included repeating a transect survey but reducing the distance between

sampling points to increase data resolution and repeating a transect survey using an Exploranium GR-256 portable gamma ray spectrometer. The latter was used to separate out the thorium, uranium and potassium signals with the aim of identifying the radionuclides responsible for the gamma signals recorded (Ruffell and Wilson 1998). Both the higher resolution data (total counts every 16 cm) and segregated spectrum data resulted in improved data quality. The high resolution data supported identification of transitions from windblown sand to storm beach (*ibid*). The individual spectrum data revealed the increasing abundance of potassium at the expense of uranium and thorium concentrations within the sand and gravel (Ruffell and Wilson 1998). This was attributed to increased potassium concentrations in the sand deposits relative to the relatively potassium-depleted clays.

It is recognised that the Groundhog system used in this thesis can be configured to test both of these variables. Typically, Groundhog is deployed along 1 metre transects which are traversed at a speed of 1 metre per second, supporting the collection of radiological and GPS data every square metre. However, by reducing the space between transects (for example, to 0.5 m), slowing the walking speed or repeating the site survey, it is possible to increase data resolution. The Groundhog system is also capable of generating total (gross) gamma radiation measurements as well as full spectrum data which can be used for more detailed assessment. In consequence, it is proposed that this thesis builds on the work undertaken by Ruffell and Wilson (1998) by deploying the Groundhog system in a variety of configurations. The impact of collimated vs uncollimated surveys, sample resolution and the use of spectral data will also be explored.

In addition to varying surveying techniques, the case studies in the Ruffell and Wilson (1998) study also presented the survey data in a range of formats. This included line graphs, manual plotting of radiological data/drawing of contour lines and computer generated spectral gamma ray maps. All forms of graphic representation successfully identified variations in radioactivity along transects. However, the value of each format in identifying buried features varied significantly. For example, areas of elevated activity identified in the hand-drawn contour map were eventually associated with “thick clay beds or trenches, often with sewage pipes” (*ibid*). The presence of the clay sewage pipes was not discerned from the contour map, but rather following excavation of the area. In contrast, the digital maps generated from total count data taken from a Lead Mine in Northern Ireland clearly shows the position and shape of a mineralised vein (Ruffell and Wilson

1998). The computer generated spectral gamma ray maps therefore appear to be more valuable in delineating buried features.

The software used to support the Groundhog system is also capable of generating a variety of data outputs similar to those generated by Ruffell and Wilson. For example, it is possible to generate graphs highlighting regions of interest, gamma radiation spectra and count rate distribution. In addition, maps of measurement positions (to centimetre accuracy), and 'gamma radiation distribution (heat) maps' showing surface count rate distribution can also be generated. The latter is most commonly used in a nuclear industry context as this is the easiest way to identify the nature and extent of a contamination source or event for further investigation. It is proposed that this project focusses on using the gamma radiation distribution maps generated by the GIS software in an attempt to locate buried features. However, it is recognised that other data sets, including count rate distribution graphs and spectral data will be valuable in establishing background radiation levels and insight into which radionuclides are responsible for any elevations in radioactivity observed.

The second paper referenced by Ruffell *et. al.* 2006 was published by Moussa in 2001. Unlike the Ruffell and Wilson 1998 study which looked at finding contrasts in the (radio)chemical composition of different sediment deposits, Moussa (2001) focusses on using gamma radiation surveys to delineate a building of potential archaeological interest.

Moussa's 2001 survey was conducted to test the theory that the radionuclide content of the building's fired clay bricks would be sufficiently different from the surrounding sandy sediment such that a contrast would be visible in the radiation data. A Scintrex GAD-6 portable gamma spectrometer was used to take measurements across a grid with 0.5 metre spacings. It is not clear what count times were used at each location. It is also not stated if a single measurement at each spacing was taken, or if multiple measurements were taken and averaged, as observed in the Ruffell and Wilson (1998) study. Further, it is not clear to what extent the building's remains were covered by overburden, or if it had been fully or partially excavated at the time of surveying. A photograph in Moussa's 2001 paper shows the survey area with the topsoil removed, but it is not clear if excavation was completed before or after the gamma radiation surveys. It is acknowledged that this variable will impact on the viability of the technique at other sites and

therefore needs to be explored. Several contour maps were generated following the survey; total counts per second (cps), total potassium (%), total uranium equivalent (ppm) and total thorium equivalent (ppm). The total uranium and thorium equivalent maps did not effectively distinguish between the building remains and surrounding sediment (Moussa 2001). However, the total potassium and total count rate contour maps clearly delineated the building structure (Moussa 2001).

The findings from Moussa's study suggests that gamma radiation surveying and supporting spectrometry may be another tool to define the boundaries of archaeological features. However, it is highlighted that in this study that the feature of interest may have already been fully or partially excavated at the time of the survey. In consequence, this technique may be less successful in a scenario where a feature is buried. In this scenario, the soil will attenuate gamma radiation from a target, thereby reducing the contrast observed between the target and natural background activity.

In the later paper published by Ruffell *et. al.* (2006) the author built on the earlier studies of Moussa (2001) and Ruffell and Wilson (1998). This was achieved by applying a refined gamma survey and data processing methodology to successfully identify the location of a buried pipe and the partially buried foundations of a house. A Scintrex GIS-5 portable detector was used to take measurements every 25 cm across a grid, set out over the study area. As per the Ruffell and Wilson 1998 study, five measurements were taken at each location, with the maximum and minimum values discarded and the remaining three averaged. In previous studies referenced by Ruffell *et. al.* (2006), total count and individual element data were used in a variety of formats, the most valuable appearing to be contour maps and computer generated images. In this study, changes in Th/U and Th/K ratios were established for the survey area (Ruffell *et. al.* 2006). A 'thin plate spline' method of data interpolation was used to generate greyscale maps of the ratio variations (Ruffell *et. al.* 2006). These highlighted the ability of the measured ratios to define surface substructures more clearly than total count or individual isotope data alone (Ruffell *et. al.* 2006). The study recognised the potential value of this technique for archaeological, geotechnical and forensic applications, noting the requirement for further work. In particular, the requirement to apply these techniques to other geologies such as clay-rich ground. The authors also recommend that the techniques described in the paper should be used in conjunction with other

geophysical techniques as “important information may be held in each data set” (Ruffell, *et. al.* 2006). This conclusion supports the aim of this study to include gamma radiation surveying as a complementary tool that can be used to support more traditional geophysical techniques.

Two studies identified during this literature review have subsequently supported the use of gamma radiation surveys, specifically looking at the relationships between concentrations of naturally occurring uranium, thorium and potassium within the soil and potential features of interest. This includes the use of Th/U and Th/K ratios for locating buried archaeological features. In one study, measurements of Th/U and Th/K ratios across a site were used in an attempt to identify archaeological features at an excavation site in north-west Spain. The study team, led by Sanjurjo-Sanchez, *et. al.* (2017) used a portable gamma spectrometer to survey a known archaeological site containing multiple settlements from early Roman through to Late Medieval periods. The site was situated in an area rich in ultramafic rock, alluvial deposits and some granite Sanjurjo-Sanchez, *et. al.* (2017). As per the 2006 Ruffell *et. al.* study, total counts, direct measurements and Th/U and Th/K ratios were measured. The findings supported the earlier case studies by Ruffell *et. al.*, insofar as the Th/U and Th/K ratio data yielded the clearest results. However, the difference between the buried features and surrounding geology was not as well differentiated as expected. This was attributed to the unusually low levels of naturally occurring radioactive material and the use of local materials in the construction of the buried features. This further supports the need for additional work in this area, potentially using alternative survey methods to generate accurate radiation profiles of the site.

In a second study, undertaken on the west bank of the River Nile near Aswan Egypt, a bismuth germanate oxide gamma ray spectrometer was successfully deployed to locate a buried granitic monument to King Pepi I (Aziz, *et. al.* 2018). A 200 square metre area was covered, with the detector systematically traversed across a network of 0.5 m wide transects, resulting in the capture of 861 measurements (Aziz, *et. al.* 2018). The detector was positioned at each station for count time of 3 minutes. Computer generated heat maps were generated for each radionuclide of interest. Uranium and Thorium concentrations were presented in ppm and potassium in percent. Total dose rate was displayed in $\mu\text{R/hr}$. The maps presented in the Aziz paper appear to show an inverse relationship between potassium and U/Th concentrations, but no clear delineation of buried features. The authors were, however, able to use the data to narrow their investigation to

the eastern half of the grid. To better draw out any possible anomalies, a principal component analysis (PCA) was undertaken on the data including concentrations of individual radionuclides, ratios between different radionuclides and total dose rates. According to Aziz, *et. al.* (2018), this technique can be used to reduce the amount of ‘noise’ in the data as well as highlight any correlations between the different variables. This in turn supports differentiation of the distribution of radiation sources (Aziz, *et. al.* 2018). The PCA results clearly defined the boundaries of two confined areas of elevated radioactivity. The exact positions of these anomalies were re-established in the field and excavated. The location hosting the radiological anomaly with a better defined rectangular shape and dimensions revealed the buried monument (Aziz, *et. al.* 2018). The second, less well defined anomaly revealed the location of a second, smaller granitic block from a doorway.

A further two studies testing the viability of gamma radiation surveys in an archaeological context have also been found as part of this literature review.

A 2018 paper produced by Kozhevnikov, *et. al.* presents data from previously unpublished and Russian language-only archaeological investigations in the Barun-Khal valley in Siberia. The investigations undertaken between 1997 and 2005 used various techniques including magnetometry, resistivity, gradiometry and excavation to gain a better understanding of the archaeometallurgical history of the area (Kozhevnikov *et. al.* 2018). In particular, establishing the extent of the archaeometallurgical sites and their structure rather than locating specific buried features. The studies built on earlier data which suggested that iron production took place in the region between 361 to 168 cal BC (2σ) to 5 – 210 cal AD (2σ) (Kozhevnikov *et. al.* 2018).

The ‘traditional’ geophysical surveys undertaken in the Barun-Khal valley yielded valuable data on the structures of the metal generating sites and features of interest. To support this data, a gamma ray survey was also completed. An SRP-68 gamma ray scintillometer was used to capture radiation readings of 9 – 25 $\mu\text{R/hr}$ across a 64 m² grid at one of the previously identified metal production sites (Kozhevnikov *et. al.* 2018). No further detail on the survey method was provided. The radiometric survey was undertaken to ascertain the value of gamma surveys in an archaeological context. It was initially concluded by the authors that the data added no value. However, it was later recognised that the gamma surveys generated a useful insight into the

geoarchaeological context of the site (Kozhevnikov *et. al.* 2018). For example, it was recognised that elevated radiation readings could be attributed to deposits of radionuclides liberated and transported by stream from the granite massif of the Primorsky Range (Kozhevnikov *et. al.* 2018). The radiological survey also highlighted a sharp change in radioactivity readings in one area which was found to rapidly transition from granitic deposits to a 'soil-vegetative' cover (Kozhevnikov *et. al.* 2018). The authors attributed this change to a rapid shift in the climatic, hydrological or other regime in the area, leading to a cessation in granitic deposits which enabled the establishment of vegetation cover (Kozhevnikov *et. al.* 2018). In this study, the authors recommended an expansion of the radiological surveys to accrue further insight into the geoarchaeology of the region. The ease of implementation, low cost and clear visual data output were recognised as benefits of the technique.

A more novel application of gamma spectrometry in an archaeological context was tested by Williams-Thorpe, *et. al.* (2000). The authors used portable gamma ray spectrometer (PGRS) (an Exploranium GPS-21 in combination with spectrometer console model GR-256) to quantify the potassium, uranium and thorium content of the marble and granitoid columns of a Roman Temple situated in Windsor Great Park, UK (Williams-Thorpe, *et. al.* 2000). The objective was to establish the provenance of the granite used to build the temple which originated from the ancient city of Leptis Magna in Libya. The proportions of potassium, uranium and thorium within the Leptis Magna columns were compared against those found within granite samples taken from six quarries identified as being the potential source of the granite. The radionuclide profile of the columns most closely matched the sample taken from the Troad quarry (Williams-Thorpe, *et. al.* 2000). This was supported by the results of magnetic susceptibility measurements taken for the columns and the quarry samples (Williams-Thorpe, *et. al.* 2000). There were two columns that did not match either the radionuclide or magnetic susceptibility profiles for the Troad Quarry; instead being more closely correlated to the profiles taken for the Kozak Quarry (Williams-Thorpe, *et. al.* 2000). Both quarries are located in Turkey.

Whilst the Williams-Thorpe, *et. al.* study does not relate to the prospection of archaeological targets, the paper did provide a valuable evaluation of the shortfalls of the PGRS method; something that has not been considered in detail in the other studies focussing on archaeological prospection. Various factors that may influence the effectiveness of the technique were identified

including meteorological conditions, self-shielding, sample size, ability to differentiate between the feature of interest and background radiation, and data resolution (Williams-Thorpe, *et. al.* 2000). These aspects are discussed in further detail in Section 2.4.4 of this thesis.

2.4.2.1 Sources of Contrast in Radionuclide Concentrations between Archaeological Materials and Natural Background

For the effective use of gamma radiation surveys to detect buried archaeological features, it is essential that there is sufficient contrast between the radioactivity of the feature of interest and the natural background radiation. As observed in the study by Sanjurjo-Sanchez *et. al.* (2017), the use of local materials in the construction of the ancient buildings led to poor differentiation between the measured radioactivity of the target and surrounding substrate. This was responsible for the limited effectiveness of the technique. In contrast, the granitic monument rediscovered by Aziz *et. al.* (2018) revealed a far greater contrast between the measured activity from the artefact and surrounding local material. This was identified as being water-logged soil with halfa grass cover. As a result, more conclusive data was obtained. These studies highlight the importance of understanding the mechanisms that support accumulations of naturally occurring radioactive material and subsequently the types of target that may be more amenable to gamma surveying techniques.

The most common mechanisms supporting accumulation of naturally occurring radioactive material at sites of archaeological interest include:

- Import of ‘foreign’ materials;
- Concentration of material rich in naturally occurring radioactivity; and
- Industrial activity.

Construction materials have throughout history, been transported over significant distances to a desired location or settlement. This is observed in many iconic historical monuments such as the Welsh ‘blue stones’ of Stonehenge (Nash, *et. al.* 2020). These imported materials have the potential to be of a different geochemical composition to the local geology. In some cases; particularly for clays and granites, the radionuclide concentration can also be markedly different. Where imported materials are present in sufficient quantities, the difference in gamma signatures

should be measurable – either as areas of elevated or depleted radioactivity, depending on the material imported.

In addition to the import of materials, production of construction materials such as brick and tile using local resources can lead to the concentration of radioactive material, potentially leading to a clear gamma signal, as shown in Table 2.4. The clay component of brick is well-known for its adsorptive properties (IAEA 2003a, Gu *et. al.* 2019), attributable to the high surface area of the clay particles, negative surface charge, and ion exchange capability (Gu *et. al.* 2019). In consequence, clays are capable of accumulating notable concentrations of heavy metals or radionuclides released through the weathering of parent rock (as discussed in Section 2.2.2). The invention of fired bricks approximately 5500 years ago (Brick Architecture 2017), enabling their use in more temperate climates, further increased their ability to concentrate radioactive material. This concentration is achieved through compaction and condensing following removal of water, air and other volatile substances (Aliyev 2004, IAEA 2003). The ease with which bricks and tiles can be created has ensured that bricks and tiles are some of the most ubiquitous building materials throughout human history (Ruffell 2014, Brick Architecture 2017). This suggests that brick structures may be ideal target types for gamma surveying techniques.

Finally, activities such as mining and the processing of ores has historically been, and continues to be, a notable source of technologically enhanced naturally occurring radioactive material (IAEA 2013). Metal ores can have notable quantities of naturally occurring radionuclides associated with them, due to their tendency for accumulating in certain mineral structures. For example, copper ores are often associated with low concentrations of uranium and radium (EPA 2019). During the processing of ores, the feed material is separated into two phases; one containing the metal of interest and the other containing the host rock/ minerals and any additives used to facilitate separation during smelting (EPA 2019). For example, sand or limestone is used to aid copper extraction (EPA 2019) during thermal processing. The processing residues, including slag, tailings, aqueous effluent and concentrated sludges can therefore contain accumulated concentrations of naturally occurring radionuclides; (IAEA 2013). Today, the amount of radioactive material accumulated in these by-products can be sufficiently high as to require management as radioactive waste, if the radioactive material cannot otherwise be recovered (IAEA 2013). Historically, the slag material has had no value. It was therefore typically discarded (and

accumulated) in-situ (Rehren and Pernicka 2008), providing a valuable insight into historical metal working activities. Because slags can be difficult to differentiate from natural geological features (Rehren and Pernicka 2008), the ability to utilise gamma surveys to detect the accumulated radiation may be a useful additional tool in surveying such sites. Even if it is not possible to distinguish structural detail.

Table 2.4 – Indicative values of radionuclide concentrations within common building materials

Material	Radionuclide (Bq/kg)		
	Ra-226	Th-232	K-40
Clay brick	1 – 200	1 – 200	60 – 2000
Sand-lime brick and sandstone	6 – 50	1 – 30	5 – 700
Natural building stone	1 – 500	1 – 310	1 – 4000
Tiles (glazed and unglazed)	30 – 200	20 – 200	160 – 1410

Source: IAEA (2003a)

It can be seen that some historic activities, such as building construction and metal working, could give rise to potentially measurable changes in the concentrations of naturally occurring radionuclides relative to the surrounding geology. Furthermore, it is possible that these changes may be sufficient to enable differentiation from natural background levels. There are however, a number of limitations that have the potential to significantly impair efficacy.

2.4.3 Advantages and Limitations of Gamma Radiation Surveying in an Archaeological Context

Table 2.5 provides an overview of potential advantages and limitations of applying gamma radiation surveys, specifically using Nuvia’s Groundhog system, in an archaeological context. In general, it appears that the technique could be a valuable tool to aid identification of buried targets. However, the table highlights several limitations. Some of these are common to other traditional geophysical techniques, such as dependence on their being sufficient contrast between target and background, depth penetration and conventional hazards. Many of those identified will inform the viability of the technique in some scenarios; most notably regarding the amount of overburden, soil moisture content and local geology.

Table 2.5 – Overview of Advantages and Limitations Associated with the Application of Gamma Radiation Detection Spectrometry (Groundhog) to Archaeological Surveys

Performance Parameter		Advantages	Limitations
Technical Performance	Susceptibility to Interference	<ul style="list-style-type: none"> Not susceptible to interference from other metals, local electrical cables, etc. 	<ul style="list-style-type: none"> Sources can be readily shielded with overburden (especially greater than 50 cm). High soil water content can impact on data accuracy as this can also act as shielding.
	Range	<ul style="list-style-type: none"> Multiple deployment mechanisms are available to survey areas ranging from just tens of metres to square kilometres. 	<ul style="list-style-type: none"> None identified.
	Ability to Differentiate	<ul style="list-style-type: none"> Spectrometric capability of the chosen survey system will support identification of radionuclides of interest and review of ratios to support differentiation. 	<ul style="list-style-type: none"> If an archaeological feature is made from (very) local material, it may not be possible to differentiate from local background. If natural background radiation is high due to geology (e.g. granite), it will be more challenging to detect any feature of interest (although some depletion leading to a negative response may occur).
	Suitable Targets	<ul style="list-style-type: none"> Potentially suitable for features constructed from material naturally enriched with radionuclides (e.g. granite), or capable of adsorbing naturally occurring radionuclides from the environment (e.g. clay). Potentially suitable for the identification of trenches or pits that have been infilled with imported material with a different radiochemical composition. 	<ul style="list-style-type: none"> Less suitable for features made from organic material (wood), and stone containing low radionuclide concentrations (e.g. sandstone). It is however recognised that if these materials contain much <i>lower</i> concentrations of naturally occurring radioactive material relative to the surrounding substrate, a distinctive area of depletion may be visible in the data.
	Risk of False Positives/Negatives	<ul style="list-style-type: none"> Detector will only respond to gamma radiation. Gamma spectrometric capability supports detailed analysis of the data. A collimator can be used to ensure only gamma radiation directly beneath the detector is recorded. 	<ul style="list-style-type: none"> Surveying immediately after heavy rain can lead to artificially elevated readings due to wash out of radon, giving a 'false positive'. It is good practice to wait 2 -3 hours after heavy rain to complete a survey. It is possible that a natural feature/ change in geology could result in a false positive due

Performance Parameter		Advantages	Limitations
		<ul style="list-style-type: none"> The survey method can be modified to increase the density (resolution) of measurements collected as required – particularly for smaller targets. This can be achieved either by adjusting walking speed and transect spacing, or by conducting repeat surveys over a defined area and aggregating the data sets. This can improve the quality of the resultant radiation distribution maps by reducing the amount of interpolation undertaken. This in turn minimises the risk of false positives, or overlooking a feature of interest (false negative). 	<p>to a change in the gamma signature of the material.</p>
	Sensitivity	<ul style="list-style-type: none"> Well suited to low energy gamma radiation associated with naturally occurring radioactivity. 	<ul style="list-style-type: none"> For radionuclides such as uranium and thorium, accuracy of the results is heavily dependent on their being in secular equilibrium with their (gamma emitting) progenies. This equilibrium may be disrupted in some environmental conditions, such as leaching from heavily weathered rock.
Practicability	Robustness	<ul style="list-style-type: none"> Rugged system tried and tested in a variety of scenarios including concreted surfaces through to open fields. 	<ul style="list-style-type: none"> Not suitable for use in very heavy rain. Detector unit (specifically the NaI crystal) is susceptible to damage through exposure to excessive vibration and/ or extreme temperature swings.
	Resource Requirements	<ul style="list-style-type: none"> Minimal resource requirement – rechargeable battery pack necessary to operate detection system, GPS and data logger. Does not require coolant or other consumables. 	<ul style="list-style-type: none"> Periodic calibration of the detector using a sealed source is required.

Performance Parameter		Advantages	Limitations
	Ease of Deployment	<ul style="list-style-type: none"> • Easy to implement. The system designed to enable the operator to focus on local surroundings – to avoid trips/ falls, identify any features that may cause an anomaly or gaps in readings (e.g. unsafe ground, building). Some training is required to operate software, address alarms, etc. • For larger sites, vehicle-mounted detectors can be deployed. 	<ul style="list-style-type: none"> • GPS signal may be interrupted if surveying in close proximity to tall buildings, trees, etc. • Collimator trolley is heavy (approximately 45 kg), and difficult to deploy over rough terrain. • Due to slow walking pace required and static position of the operator’s arm whilst carrying the detector, fatigue is possible. • Operator exposed to typical conventional hazards associated with fieldwork.
	Availability	<ul style="list-style-type: none"> • The detector system itself predominantly comprises commercially available off the shelf equipment. • As part of this study, it has been discovered that the commercially available software tool Geoplot is also capable of generating high quality visual outputs (radiation distribution maps) using Groundhog data. 	<ul style="list-style-type: none"> • Currently limited to nuclear industry applications. • Proprietary processing software used with the Groundhog system is owned and operated exclusively by Nuvia Limited.
Output	Ease of Processing	<ul style="list-style-type: none"> • Processing method supports completion of quality checks and exclusion of erroneous data from the main data set. 	<ul style="list-style-type: none"> • More extensive training required to operate bespoke ArcGIS software and interpret data.
	Ease of Interpretation	<ul style="list-style-type: none"> • Radiation distribution maps are easy to interpret and can be superimposed onto site maps or other geophysics data to identify features of interest/ correlation. • The technique is well suited for combining radiological data with data other survey methods (e.g., magnetometry) to confirm support more accurate interpretations. 	<ul style="list-style-type: none"> • Identification of anomalies is subjective. The technique requires a degree of experience to determine whether an anomaly relates to a potential feature or is a natural occurrence, as recognised by other authors such as Onok, <i>et. al.</i> 2009. For example, a localised area of depletion may be attributable to the natural weathering and transport of radionuclides rather than a man-made feature.

Performance Parameter		Advantages	Limitations
			<ul style="list-style-type: none"> • Other output sources such as count rate distribution graphs require a greater level of interpretation and specialist knowledge.
	Compatibility with other Geophysics Data	<ul style="list-style-type: none"> • Combination with other geophysical data would improve quality of data interpretation. • All data can be processed/ viewed in ArcGIS & Geoplot. 	<ul style="list-style-type: none"> • None identified.

2.5 Conclusion: Gamma Radiation Surveying in the Geophysics Toolbox

The application of non-intrusive ground surveying techniques in support of archaeological prospection is well established. Such an approach generates valuable data that can aid site interpretation. It can also support the generation of optimised, well-targeted excavation plans, which in turn minimises site disruption/ damage and efficient resource use. The main geophysical methods typically applied in archaeological surveys include magnetic, electrical and ground penetrating radar.

Available literature suggests that application of contrasting geophysical techniques to a site of archaeological interest can improve data quality and data interpretation. The ability to compare multiple datasets supports discrimination of genuine anomalies of interest and those caused by natural features or modern infrastructure. In consequence, it may be concluded that access to a ‘toolbox’ of non-intrusive techniques offers a notable benefit to archaeological investigation.

The intent of this research project is to test the efficacy of a new potential tool, gamma radiation surveying, that could be added to this toolbox. The study focusses on the use of a portable system, Nuvia Groundhog. Processed data can be presented in multiple ways, the most valuable being a gamma radiation distribution map. Unlike traditional geophysical techniques which look for contrasts in the physical properties of the target and surrounding substrate, gamma surveying techniques measure changes in concentrations of naturally occurring radioactive material present. If the concentration of radioactive material in an archaeological feature is sufficiently different from the surrounding soil, it may be possible to see this contrast in the generated radiation distribution maps. Mechanisms for achieving contrasting radiation measurements include: import of foreign material, concentration of materials rich in naturally occurring radioactive material and industrial activity.

This chapter has reviewed available studies that have conducted gamma radiation surveys in support of archaeological prospection. This review yielded the following key findings:

- 1. Several studies support the hypothesis that gamma surveying techniques can support identification of buried archaeological features.** Most notably, radiation surveys undertaken by Aziz *et. al.* (2018) and Sanjurjo-Sanchez *et. al.* (2017) supported recovery of

an Egyptian granitic monument and investigations into buried Medieval structures in Ciudadela, Spain respectively.

- 2. The number of studies exploring the use of gamma survey methods in this unique context is very small.** Seven studies were identified where gamma survey techniques were used specifically to delineate buried man-made features. Of these, five were applied sites of archaeological interest. A final study focussed on the use of gamma spectrometric data to ascertain the provenance of Roman granitic columns.
- 3. All studies used a similar survey method.** Rather than using a portable system that traverses the site allowing continuous collection of data, as proposed for this research project, a static survey method was used. In each of the referenced studies, a gamma detector was placed on a defined position on a grid or transect and left for a defined counting period before being moved to the next sampling location.
- 4. Gaps in the survey methods presented were identified,** leading to some uncertainty regarding the robustness of the approaches used and resultant data. Issues highlighted included multiple studies not reporting detector count times applied (leading to uncertainty regarding the adequacy of counting periods for naturally occurring radionuclides), ambiguity regarding the amount of overburden (if any) present during the survey, limited comparison of radiation data against standard geophysical survey data, and absence of radiochemical analyses of target and substrate material to establish the cause of measured contrasts. Due to the limited number of studies available and gaps in the methodologies applied, the repeatability of these surveys is unknown.
- 5. Significantly more work is required to be able to more confidently accept the hypothesis presented in point 1.** Further targeted studies testing the efficacy and repeatability of the method are required to support the conclusion that gamma radiation surveying techniques can be used alongside existing geophysical methods, to aid archaeological prospection.

This research project seeks to reinvestigate the hypothesis discussed above, which has informed the hypothesis, aims and objectives detailed in Chapter 1. This will be achieved using technologies and techniques not previously applied in this context. For the first time, experiences from the nuclear industry will be utilised to optimise survey method design and interpretation. Additionally, fieldwork will be planned to address gaps in the existing research.

2.6 References

- Aliyev, C. (2004) NORM in Building Materials, in: IAEA (2004) Naturally Occurring Radioactive Materials (NORM IV): Proceedings of an International Conference held in Szczyrk Poland, 17 – 21 May 2004, IAEA-TECDOC-1472, International Atomic Energy Agency, Vienna
- Aliyu, A.S. and Ramli, A.T. (2015) Review: The world's high background natural radiation areas (HBNRAs) revisited – A broad overview of the dosimetric, epidemiological and radiobiological issues, *Radiation Measurements*, **73**: 51 – 59, <https://doi.org/10.1016/j.radmeas.2015.01.007>
- Aurora (2020) Aurora's RadSurvey System, www.aurorahp.co.uk/services/environmental-radiological-surveys/auroras-radsurvey-system, Date Accessed: 30th May 2020
- Aziz, A. Attia, T. McNamara, L. and Friedman, R. (2018) Application of Gamma-ray Spectrometry in Discovering the Granitic Monument of King Pepi I: A Case Study from Hierakonpolis, Aswan, Egypt, *Pure and Applied Geophysics*, Published Online 09/11/2018, DOI: 10.1007/s00024-018-2036-1
- Banerjee, K.S. Sharma, S.P. Sarangi, A.K. and Sengupta, D. (2011) Delineation of subsurface structures using resistivity, VLF and radiometric measurement around a uranium-tailings pond and its hydrogeological implication, *Physics and Chemistry of the Earth*, **36**: 1345 – 1352, <https://doi.org/10.1016/j.pce.2011.03.008>
- Barker, P. (1993) (Third Edition) Techniques of Archaeological Excavation, Routledge, Taylor and Francis Group, Oxfordshire UK.
- Beddow, H. (2007) Managing NORM Liabilities, Presentation (UNPUBLISHED) generated on behalf of NUKEM Ltd. (now Nuvia Ltd.), created June 2007
- Bezuidenhout, J. (2015) In-situ gamma ray measurements of radionuclides at a disused phosphate mine on the west coast of South Africa, *Journal of Environmental Radioactivity*, **150**: 1 – 8
- Brick Architecture (2017) The History of Bricks and Brickmaking, <https://brickarchitecture.com/about-brick/why-brick/the-history-of-bricks-brickmaking>, BrickArchitecture Online Service operated by the BK Group, Page Created: 2017, Date Accessed: 22nd November 2019
- Burns, P.C. (1999) The Crystal Chemistry of Uranium in Burns, P.C. and Finch, R. (1999) Uranium: Mineralogy, Geochemistry and the Environment, Reviews in Mineralogy, Volume 38, Mineralogical Society of America, pp: 23 – 90
- Campos, L.D. de Souza, S.M. de Sordi, D.A. Tavares, F.M. Klein, E.L. and de Santos Lopes, E.C. (2017) Predictive Mapping of Prospectivity in the Gurupi Orogenic Gold Belt, North-Northeast Brazil: An example of District Scale System Approach to Exploration Targeting, *Natural Resources Research* **26**(4): 509 – 536, DOI: 10.1007/s11053-016-9320-5

Chemical Book (2021) CAS Database List: Radium: Radium Properties, www.chemicalbook.com/ChemicalProductProperty_EN_CB2900292.htm, Chemical Book Chemical Service Platform, Accessed 13/11/2021

Chiozzi, P. De Felice, P. Fazio, A. Pasquale, V. and Verdoya, M. (2000) Laboratory Application of NaI gamma-ray spectrometry to studies of natural radioactivity in geophysics, *Applied Radiation and Isotopes*, **53**: 127 – 132, DOI: 10.1016/s0969-8043(00)00123-8

Chiozzi, P. Pasquale, V. Verdoya, M. and De Felice, P. (2000a) Practical applicability of field gamma scintillation spectrometry in geophysical surveys, *Applied Radiation and Isotopes*, **53**: 215 – 220, DOI: 10.1016/s0969-8043(00)00123-8

CNDNI (2009) European Radiation Survey and Site Execution Manual (EURSSEM), Final Report, Published June 2009 by the Coordination Network on Decommissioning of Nuclear Installations (CNDNI) on behalf of the European Commission

Creighton, J. and Fry, R. (2016) Silchester: Changing Visions of a Roman Town. Integrating Geophysics and Archaeology: The Results of the Silchester Mapping Project 2005 – 2010, Society for the Promotion of Roman Studies, ISBN 9780907764427, Published book retrieved from <http://centaur.reading.ac.uk/62521/> on 28th December 2018

Columbero, C. Elia, D. Meirano, V. and Sambuelli, L. (2020) Magnetic and radar surveys at Locri Epizephyrii: A comparison between expectations from geophysical prospecting and actual archaeological findings, *Journal of Cultural Heritage*, **42**: 147 – 157, <https://doi.org/10.1016/j.culher.2019.06.012>

Cumberland, S.A. Douglas, G. Grice, K. and Moreau, J.W. (2016) Uranium mobility in organic matter-rich sediments: A review of geological and geochemical processes, *Earth-Science Reviews*, **159**: 160 – 185, <https://doi.org/10.1016/j.earscirev.2016.05.010>

Dobrzyński, L. Fornalski, K.W. and Feinendegen, L. E. (2015) Cancer Mortality Among People Living in Areas with Various Levels of Natural Background Radiation, *Dose Response*, **13** (3) DOI: 10.1177/1559325815592391

David, A. and Payne, A. (1997) Geophysical Surveys within the Stonehenge Landscape: A review of past endeavour and future potential, *Proceedings of the British Academy*, **92**: 73 – 113.

Davies, M. Murley, R. and Adsley, I. (2003) Development and Evolution of a Site Survey System – GROUNDHOG, The 9th International Conference on Radioactive Waste Management and Environmental Remediation. September 21 – 25 2003, Examination School, Oxford, England

Davies, M. (2011) Comparison of ‘Groundhog Fusion’ and ‘Groundhog Classic’, 10390/TR/001, Issue 1, Internal Publication, August 2011

Davies, M. (2017) So, Just What is GROUNDHOG? Lunch and Learn Presentation for Nuvia Limited, Presented 8th June 2017, UNPUBLISHED

Davies, M. (2018) Groundhog Survey of Selected Roads at Sizewell B, 72769/TR/001, Issue 1, March 2018, Nuvia Limited, Didcot, Oxfordshire (Client Issued Report)

De Quadros, T.F.P. Koppe, J.C. Strieder, A.J. and Costa, J.F.C.L. (2002) Gamma ray data processing and integration for Lode-Au deposit exploration, *Natural Resources Research*, **12** (1): 57 – 65

Drewett, P. (2011) *Field Archaeology: An Introduction*, Second Edition, Routledge Taylor and Francis Group, London and New York, pp: 1 – 173, ISBN: 978-0-203-83087-1 (ebk)

EPA (2019) TENORM: Copper Mining and Production Wastes, www.epa.gov/radiation/tenorm-copper-mining-and-production-wastes, United States Environmental Protection Agency, Accessed on 02/01/2020, last updated on 08/07/2019.

European Commission (1999) Radiological Protection 112: Radiological Protection Principles Concerning the Natural Radioactivity of Building Materials, Director General: Environment, Nuclear Safety and Environmental Protection

Fayek, M. and Kyser, T.K. (1999) Stable Isotope Geochemistry of Uranium Deposits *in* Burns, P.C. and Finch, R. (1999) Uranium: Mineralogy, Geochemistry and the Environment, Reviews in Mineralogy, Volume 38, Mineralogical Society of America, pp: 181 – 220

Finch, R. and Murakami, T. (1999) Systematics and Paragenesis of Uranium Minerals *in* Burns, P.C. and Finch, R. (1999) Uranium: Mineralogy, Geochemistry and the Environment, Reviews in Mineralogy, Volume 38, Mineralogical Society of America, pp: 91 – 180

Flakus, F.N. (1981) Detecting and measuring ionizing radiation – a short history, IAEA Bulletin Volume 23, No. 4, International Atomic Energy Agency, Vienna

Gaffney, C. and Gaffney, V. (2010) Chapter 10 – Through an Imperfect Filter: Geophysical Techniques and the Management of Archaeological Heritage, *in*: Cowley, D.C. (2010) (Editor) Remote Sensing for Archaeological Heritage Management, EAC Occasional Paper No. 5, *Europae Archaeologiae Consilium*, pp 117 – 127

Gaffney, C. and Gater, J. (2003) *Revealing the Buried Past: Geophysics for Archaeologists*, Tempus Publishing Ltd, UK.

Gaffney, C. and Gater, J. (2011) *Revealing the Buried Past: Geophysics for Archaeologists*, Tempus Publishing Ltd, UK.

Gaffney, C. Gater, J. and Ovenden, S. (2002) *The Use of Geophysical Techniques in Archaeological Evaluations*, Paper No. 6, Institute of Field Archaeologies, University of Reading, UK, ISBN: 0948393163

Gaffney, C. and Gater, J. (2003) *Revealing the Buried Past: Geophysics for Archaeologists*, Tempus Publishing Ltd., UK, ISBN: 0752425560

Grimstead, D.N. Clark, A.E. and Rezac, A. (2017) Uranium and Vanadium Concentrations as a Trace Element Method for Identifying Diagenetically Altered Bone in the Inorganic Phase, Journal of Archaeological Method and Theory, published online on 18th September 2017, DOI: 10.1007/s10816-017-9353-z

Halgedahl, S.L. Jarrard, R.D. Brett, C.E. and Allison, P.A. (2009) Geophysical and Geological Signatures of Relative Sea Level Change in the Upper Wheeler Formation, Drum Mountains, West-Central Utah: A Perspective into Exceptional Preservation of Fossils, Palaeogeography, Palaeoclimatology, Palaeoecology, **277**: 34 – 56, DOI: 10.1016/j.palaeo.2009.02.011

Hazen, R.M. Ewing, R.C. and Sverjensky, D.A. (2009) Evolution of Uranium and Thorium Minerals, American Mineralogist, **94**: 1293 – 1311

Historic England (2018) Archaeology Recording Manual, www.historicengland.org.uk/content/docs/research/historic-england-archaeological-recording-manual-2018, Last Updated: 2018, Accessed on 04/11/2021

Holiday, D.A. (1948) Radiation Measuring Instruments: Their Selection and Use, Industrial Hygiene Newsletter, **8** (8): 10 – 13

IAEA (1979) Gamma Ray Surveys in Uranium Exploration. Technical Report Series No. 186, International Atomic Energy Agency, Vienna

IAEA (2003) Guidelines for radioelement mapping using gamma ray spectrometry data. IAEA-TECDOC-1363, International Atomic Energy Agency, Vienna

IAEA (2003a) Extent of Environmental Contamination by Naturally Occurring Radioactive Material (NORM) and Technological Options for Mitigation, Technical Report Series No. 419, International Atomic Energy Agency, Vienna

IAEA (2007) IAEA Safety Glossary: Terminology used in Nuclear Safety and Radiation Protection, 2007 Edition, International Atomic Energy Agency, Vienna

IAEA (2010) Olen: Dumpsites of a Former Radium Extraction Facility (Olen – Belgium), Environmental Modelling for Radiation Safety (EMRAS) Working Group 2 – Reference Approaches to Modelling for Management and Remediation at NORM and Legacy Sites, <https://www-ns.iaea.org/downloads/rw/projects/emras/emras-two/first-technical-meeting/second-working-group-meeting/working-group-presentations/workgroup2-presentations/factsheet-olen.pdf>, Created: January 2010, Accessed: November 2021

IAEA (2012) Safety Report Series No. 67 – Monitoring for Compliance with Exemption and Clearance Levels, Published January 2012, International Atomic Energy Agency, Vienna

IAEA (2013) Management of NORM Residues, IAEA-TECDOC-1712, International Atomic Energy Agency, Vienna

IAEA (2014) Radiation Protection and Safety of Radiation Sources: International Basic Safety Standards, General Safety Requirement Part 3, No. GSR Part 3, Published July 2014, International Atomic Energy Agency, Vienna

IAEA (2017) Making Sense of Radiation Safety: Protecting people and the environment, Brochure No. 16-3438, Division of Radiation, Transport and Waste Safety, Department of Nuclear Safety and Security, International Atomic Energy Agency, <https://www-ns.iaea.org/downloads/rw/about-radiation-safety.pdf>, Published 2017, Accessed on 17th October 2019

IAEA (2018) URAM-2018: Five Years On, Tanzania's Progress in Uranium Exploration, IAEA Bulletin – IAEA Office of Public Information and Communication, <https://www.iaea.org/newscenter/news/uram-2018-five-years-on-tanzanias-progress-in-uranium-exploration>, Last Updated: 25th January 2019, Accessed: 16th April 2022.

IAEA (2019) Radiation in Everyday Life, International Atomic Energy Agency, Accessed on 17th October 2019, <https://www.iaea.org/Publications/Factsheets/English/radlife>

Keay, S. Earl, G. Hay, S. Kay, S. Ogden, J. and Strutt, K.D. (2009) The Role of Integrated Geophysical Survey Methods in the Assessment of Archaeological Landscapes: The Case of Portus, *Archaeological Prospection*, **16**: 154 – 166, DOI: 10.1002/arp.358

Kerr, D. (2016) Driving innovation on projects: radioactive land remediation, www.woodplc.com/news/2016/driving-innovation-on-projects-radioactive-land-remediation, Page Published on 1st June 2016, Page Accessed on 30th May 2020

Kozhevnikov, N.O. Kharinsky, A.V. and Snopkov, S.V. (2018) Geophysical prospection and archaeological excavation of ancient iron smelting sites in the Barun-Khal valley on the western shore of Lake Baikal (Olkhon region, Siberia), *Archaeological Prospection*, **2018**: 1 – 17, <https://doi.org/10.1002/arp.1727>

Kvamme, K. L. (2006) Integrating multidimensional geophysical data, *Archaeological Prospection*, **13**: 57 – 72, <https://doi.org/10.1002/arp.268>

L'Annunziata, M.F. (2012) Chapter 16 – Solid Scintillation Analysis, pp: 1021 – 1115 *in*: L'Annunziata, M.F. (2012) (Editor) Handbook of Radioactivity Analysis (Third Edition), Elsevier, <https://doi.org/10.1016/B978-0-12-384873-4.00016-5>

Landa, E.R. (2007) Chapter 3 – Form, fate and transport of radionuclides in the biosphere, pp: 211 – 237 *in* Shaw, G. (Editor) (2007) Radioactivity in the Terrestrial Environment, Elsevier Amsterdam, Boston, ISBN: 9780080438726

Larivière, D. and Guérin, N. (2010) Natural Radioactivity, pp 1 – 19 *in*: Atwood, D.A. (Editor) (2010) Radionuclides in the Environment, John Wiley and Sons, UK

Lliboutry, L. (1999) Quantitative Geophysics and Geology, Springer Praxis, UK

- Mahmood, Z.U. and Mohamed, C.A.R. (2010) Thorium, *in*: Atwood, D.A. (Editor) (2010) Radionuclides in the Environment, John Wiley and Sons, UK, pp: 247 – 255
- Milsom, J. and Eriksen, A. (2011) The Geological Field Guide Series: Field Geophysics, Fourth Edition, Wiley-Blackwell, UK pp 3 – 4
- Mindat.org (2019) Mineral Database, www.mindat.org, copyright: mindat.org/ Hudson Institute of Mineralogy 1993 – 2019, Accessed 22nd November 2019
- Mindat.org (2022) Monazite – (Ce), www.mindat.org/min-2751.html, copyright : mindat.org/Hudson Institute of Mineralogy 1993 – 2022, Accessed 27th February 2022
- Mirion Technologies (2015) Types of Ionizing Radiation, <https://www.mirion.com/learning-center/radiation-safety-basics/types-of-ionizing-radiation>, by Mirion Technologies, Last Updated: 3rd April 2015, Accessed 17th September 2020
- Mirion Technologies (2017) Gamma and X-Ray Detection (Brochure), Published 2017, Accessed 7th February 2019, <http://www.canberra.com/literature/fundamental-principles/pdf/Gamma-Xray-Detection.pdf>
- Moussa, M. (2001) Gamma-ray Spectrometry: A new tool for exploring archaeological sites; a case study from East Sinai, Egypt, *Journal of Applied Geophysics*, **48**: 137 – 142, [https://doi.org/10.1016/S0926-9851\(01\)00077-5](https://doi.org/10.1016/S0926-9851(01)00077-5)
- Nash, D. Jake, T. Ciborowski, R. Ulyyott, J. Pearson, M. Darvill, T. Greaney, S. Maniatis, G. and Whitaker, K. (2020) Origins of the Sarsen Megaliths at Stonehenge, *Science Advances*, **6** (31), DOI: 10.1126/sciadv.abc0133
- Nemeth, N. Pethô, G. and Zajzon, N. (2015) In-situ gamma ray survey for geological mapping of K-metasomatized metavolcanics at Bükkszentkerest, Bükk Mountains, Hungary, *Open Geosciences*, **7**: 318 – 331, <https://doi.org/10.1515/geo-2015-0033>
- NISDF (2017) The UK Nuclear Industry Guide to Clearance and Radiological Sentencing: Principles, Processes and Practices, Nuclear Industry Safety Directors' Forum, May 2017, https://www.nuclearinst.com/write/MediaUploads/SDF%20documents/CEWG/Clearance_and_Exemption_GPG_2.01.pdf
- NPL (2014) Good Practice Guide No. 30 – Practical Radiation Monitoring, Issue 2, National Physical Laboratory, ISSN: 1368-6550
- Nuvia (2008) Radiological and Geotechnical Characterisation of Waste Dumps at Umicore Olen, 60003/3, Issue B, December 2008: Technical Report Produced by Nuvia Limited and Issued to Umicore.
- Nuvia (2015) Land and Waste Characterisation Services: Nuclear Technology and Innovation, Corporate Brochure, Published 2015, Accessed 27th December 2018, <http://www.nuvia.co.uk/product-groundhog.asp>, Nuvia Limited

Nuvia (2017) Visio Drawing: GROUNDHOG Processing Overview, Internal Document, Created 17th July 2017

Nuvia (2018) GROUNDHOG Survey Services, Internal Publication, September 2018

Ojovan, M.I. and Lee, W.E. (2013) An Introduction to Nuclear Waste Immobilisation, Elsevier, Oxford, Available from: ProQuest eBook Central (Accessed 24th August 2019), Chapter 4 – Naturally Occurring Radionuclides

Ortec (2015) Radiation Technology – digiBASE gamma ray spectroscopy, Published 2015, https://www.peo-radiation-technology.com/wp-content/uploads/sites/4/2015/09/ort_11_digiBASE1_peo1.pdf, Accessed on 27th December 2018,

Oonk, S. Slomp, C.P and Huisman, D.J. (2009) Geochemistry as an Aid in Archaeological Prospection and Site Interpretation: Current Issues and Research Directions, Archaeological Prospection, **16**: 35 – 51, DOI: 10.1002/arp.344

Park, C. (2001) Environment: Principles and Applications, Second Edition, Routledge London and New York, ISBN: 0-415-21771-7

Perrin, K. Brown, D.H. Lange, G. Bibby, D. Carlsson, A. Degraeve, A. Kuna, M. Larsson, Y. Palsdottier, S.U. Stoll-Tucker, B. Dunning, C. Rogalla von Beiberstein, A. (2014) A Standard and Guide to Best Practice for Archaeological Archiving in Europe, EAC Guidelines 1

Peterson, J. MacDonell, M. Haroun, L. Monette, F. Hildebrand, R.D. and Taboas, A. (2007) Radiological and Chemical Fact Sheets to support Health Risk Analysis for Contaminated Areas, Prepared by Argonne National Laboratory Environmental Science Division, in collaboration with the United States Department of Energy and Chicago Operations Office, March 2007 (https://www.remm.nlm.gov/ANL_ContaminantFactSheets_All_070418.pdf)

Piro, S. Mauriello, P. and Cammarano, F. (2000) Quantitative Integration of Geophysical Methods for Archaeological Prospection, Archaeological Prospection, **7**: 203 – 213, DOI: 10.1002/1099

Podgorsak, E.B. (2005) Chapter 1: Basic Radiation Physics IN Podgorsak, E.B. (Ed) (2005) Radiation Oncology Physics: A Handbook for Teachers and Students, International Atomic Energy Agency, Vienna

Popp, S. Altdorff, D. and Dietrich, P. (2013) Assessment of shallow subsurface characterisation with non-invasive geophysical methods at the intermediate hill-slope scale, Hydrology and Earth System Sciences, **17**: 1297 – 1307, <https://doi.org/10.519/hess-17-1297-2013>

Press, F. and Siever, R. (2002) Understanding Earth (Third Edition), W.H. Freeman and Company, New York

Purnell, M.A. Donoghue, P.J.C. Gabbott, S.E. McNamara, M.E. Murdock, D.J.E. and Sansom, R. S. (2018) Experimental analysis of soft-tissue fossilization: opening the black box, Palaeontology **61** (3): 317 – 323, doi: <https://doi.org/10.1111/pala.1263>

Putiška, R. Kušnirak, D. Dostál, I. Lačný, A. Moješ, A. Hók, J. Pasteka, R. Krajňák, M. Bosansky, M. (2014) Integrated Geophysical and Geological Investigations of Karst Structures in Komberek, Slovakia, Journal of Cave and Karst Studies, the National Speleological Society bulletin **76** (3): 155 – 163

Rawlins, B.G. McGrath, S.P. Scheib, A.J. Breward, N. Cave, M. Lister, T.R. Ingham, M. Gowing, C. and Carter, S. (2012) The Advanced Soil Geochemical Atlas of England and Wales, British Geological Survey, Keyworth, www.bgs.ac.uk/gbase/advsoilatlasEW.html, Last updated: 2012, Accessed on: 18th November 2018

Rehren, T. and Pernicka, E. (2008) Coins, artefacts and isotopes – archaeometallurgy and archaeometry, Archaeometry, **50**: 232 – 248, <https://doi.org/10.1111/j.1475-4754.2008.00389.x>

Reinhardt, N. and Herrmann, L. (2019) Review Article – Gamma-ray spectrometry as a versatile tool in soil science: A Critical Review, Journal of Plant Nutrition and Soil Science, **182**: 9 – 27, <https://doi.org/10.1002/jpln.201700447>

Ruffell, A. and Wilson, J. (1998) Near-Surface Investigation of Ground Chemistry using Radiometric Measurements and Spectral Gamma Ray Data, Archaeological Prospection, **5**: 203 – 215

Ruffell, A. McKinley, J. Lloyd, C.D. and Graham, C.J. (2006) Th/K and Th/U Ratios from Spectra Gamma-Ray Surveys Improve the Mapped Definition of Subsurface Structures, Journal of Environmental and Engineering Geophysics, **11** (1): 53 – 61, DOI: 10.2113/jEEG11.1.53

Ruffell, A. and McKinley, J. (2008) Geoforensics, Wiley, Blackwell, New Jersey USA.

Ruffell, A. (2014) A Search Methodology for Objects Below and Behind Brick and Concrete, Forensic Science International, Published Online: <http://dx.doi.org/10.1016/j.forsciint.2013.12.036>

Saito, K. and Onda, Y. (2015) Outline of the National Mapping Projects Implemented after the Fukushima Accident, Journal of Environmental Radioactivity, **139**: 240 – 249, <https://doi.org/10.1016/j.jenvrad.2014.10.009>

Sanjurjo-Sanchez, J. Chamorro, C.A. Alves, C. Sanchez-Pando, J.C. Blanco-Rotea, R. and Costa-Garcia, J.M. (2017) Using In-Situ Gamma Ray Spectrometry (GRS) Exploration of Buried Archaeological Structures: A case study from north-west Spain, Journal of Cultural Heritage, Published Online, <https://doi.org/10.1016/j.culher.2018.05.004>

Sarris, A. Kalayci, T. Moffat, I. and Manataki, M. (2018) An introduction into geophysical and geochemical methods in: Siart, C. Forbriger, M. and Bubenzer, O. (Eds) (2018) Digital Geoarchaeology: New Techniques for Interdisciplinary Human-Environmental Research, pp: 215 – 236, Springer International Publishing, DOI 10.1007/978-3-319-25316-9_14

Schmidt, A. R. Linford, P. Linford, N. David, A. Gaffney, C.F. Sarris, A. and Fassbinder, J. (2015) EAC Guidelines for the use of Geophysics in Archaeology: Questions to Ask and Points to Consider, EAC

Guidelines 2, Namur, Belgium: Europae Archaeologiae Consilium (EAC), Association Internationale san But Lucratif (AISBL), ISBN: 978-963-9911-73-4, 135p

SDF (2017) The UK Nuclear Industry Guide to Clearance and Radiological Sentencing: Principles, Processes and Practices, , Last Updated May 2017, Accessed on 15th May 2020, https://www.nuclearinst.com/write/MediaUploads/SDF%20documents/CEWG/Clearance_and_Exemption_GPG_2.01.pdf, Nuclear Industry Safety Directors' Forum (SDF)
Shaw, G. (2007) Chapter 1 – Introduction, pp: 1 – 17 in Shaw, G. (Editor) (2007) Radioactivity in the Terrestrial Environment, Elsevier Amsterdam, Boston, ISBN: 9780080438726

Simon, F.G. Biermann, V. and Peplinski, B. (2008) Uranium Removal from Groundwater using Hydroxyapatite, *Applied Geochemistry*, **23**: 2137 – 2145, <https://doi.org/10.1016/j.apgeochem.2008.04.025>

Smidt, S. and Warriner, G. (2019) Alpha, beta and gamma radiation. Open University Online Course: The Science of Nuclear Energy, Week 1 – Into the Atom, <https://www.open.edu/openlearn/ocw/mod/oucontent/view.php?id=26801§ion=2.2>, Last Updated 20/12/2019, Accessed 12/09/2021

Smith, H.A. and Lucas, M. (1991) Chapter 3 – Gamma Ray Detectors in Reilly, D. Ensslin, N. Smith, H.A. and Kreiner, S. (Editors) (1991) Passive Non-destructive Assay of Nuclear Materials, NUREG/CR-5550/LA-UR-90-732, Published March 1991

Smith, C. (2001) Environmental Physics, London: Routledge, UK, pp:205 – 240

Steinberg, E.P and Rasmussen, J.O. (2021) Radioactivity, Encyclopaedia Britannica, <https://www.britannica.com/science/radioactivity>, Last Updated 18/01/2021, Accessed 12/09/2021

Steinhauser, G. Brandl, A. and Johnson, T.E. (2014) Comparison of the Chernobyl and Fukushima nuclear accidents: A review of the environmental impacts, *Science of the Total Environment*, **470-471**: 800 – 817, <https://doi.org/10.1016/j.scitotenv.2013.10.029>

Thermo Scientific (2007) G5 “FIDLER” Scintillation Probe, Product Specification Sheet, Published 2007, Accessed on 28th December 2018, http://www.thermo.com.cn/Resources/200802/productPDF_19631.pdf, Thermo Scientific

Thorne, M. (2003) Background radiation: natural and man-made, *Journal of Radiation Protection*, **23**: 29 – 42, DOI: 10.1088/0952-4746/23/1/302

Tourlière, B. Perrin, J. Le Berre, P. Pasquet, J.F. (2003) Use of airborne gamma-ray spectrometry for kaolin exploration, *Journal of Applied Geophysics*, **53**: 91 – 102, [https://doi.org/10.1016/S0926-9851\(03\)00040-5](https://doi.org/10.1016/S0926-9851(03)00040-5)

Trogu, A. Ranieri, G. Calcina, S. Piroddi, L. (2014) The Ancient Roman Aqueduct of Karales (Cagliari, Sardinia, Italy): Applicability of Geophysics Methods to Finding the Underground Remains, *Archaeological Prospection*, **21**: 157 – 168, <https://doi.org/10.1002/arp.1471>

Turk, A.S. Hocaoglu, K.A. and Vertiy, A.A. (2011) *Subsurface Sensing*, John Wiley and Sons, UK.

Umicore (2019) *Staying the Course – Integrated Annual Report 2019*, Umicore Materials Technology and Recycling Group, https://www.umicore.com/storage/annualreport_2019/2020-03-30-umicore-ar19-en-interactive.pdf, Published March 2020, Accessed November 2021.

UNSCEAR (2000) *Sources and Effects of Ionizing Radiation*, UNSCEAR 2000 Report to the General Assembly with Scientific Annexes, Annex B Volume 1: Sources, United Nations Scientific Committee on the Effects of Atomic Radiation (UNSCEAR), United Nations New York, 92-1-142238-8

UNSCEAR (2008) *Sources and Effects of Ionizing Radiation, Volume I: Sources – Report to the General Assembly, Scientific Annexes A and B*, United Nations Scientific Committee on the Effects of Atomic Radiation (UNSCEAR), United Nations New York, ISBN: 978-92-1-142274-0

USNRC (2009) *Multi-Agency Radiation Survey and Assessment of Materials and Equipment Manual (MARSAME) (NUREG-1575), 'Supplement 1'*, Office of Nuclear Regulatory Research, US Nuclear Regulatory Commission (USNRC), Washington DC, January 2009

Vandenhove, H. and Hurtgen, C. (2010) *Uranium*, *in*: Atwood, D.A. (Editor) (2010) *Radionuclides in the Environment*, John Wiley and Sons, UK, pp: 261 – 273

USGS (2013) *Open File Report 2005-1413*, <http://pubs.usgs.gov/of/2005/1413/maps.htm>, United States Geological Survey (USGS), Last updated: 12/01/2013, Accessed: 08/04/2022

Williams-Thorpe, O. Webb, P.C. and Thorpe, R.S. (2000) *Non-destructive portable gamma ray spectrometry used in provenancing Roman granitoid columns from Leptis Magna North Africa*, *Archaeometry*, **42** (1): 77 – 99, <https://doi.org/10.1111/j.1475-4754.2000.tb00867.x>

Zheng, W. Li, X. Lam, N. Wang, X. Liu, S. Yu, X. Sun, Z. Yao, J. (2013) *Applications of Integrated Geophysical Method in Archaeological Surveys of the Ancient Shu Ruins*, *Journal of Archaeological Science*, **40**: 166 – 175, <https://doi.org/10.1016/j.jas.2012.08.022>



CHAPTER 3

Research Project Methodology

3 RESEARCH PROJECT METHODOLOGY

3.1 Introduction

Due to the necessary brevity of the methodology sections within the papers that form Chapters 4 – 6 of this thesis, a more detailed, dedicated methodology section is provided here. This addresses the ‘What, Why, How, Where and When’ aspects of the methodological approaches applied. Background information on the principles of naturally occurring radioactivity and the rationale for utilising only gamma radiation survey methods are not considered here. These aspects are presented in Chapter 2 (Sections 2.2 and 2.3) of this thesis. Challenges and constraints experienced with the chosen methodologies, as well as successes and opportunities for improvement, are presented.

This chapter starts by reflecting on the original research question and objectives to provide the context for the subsequent sections.

Section 3.3 details the data collection methods used – what equipment was used, why these systems were selected and how they were deployed. It emphasises the need to apply an iterative process to methodology development as more information became available, to ensure that data of the right type, quantity and quality was collected. The associated benefits and limitations of the data collection methods used are also addressed. The chapter then proceeds, in Section 3.4, to present the rationale behind the selection of the sites targeted for surveying. Challenges faced during this stage of work and mitigation measures applied to overcome these challenges are set out.

The data processing and analysis methods are presented in Section 3.5. Again, the benefits and limitations of the methods used are discussed.

Concluding comments are presented in Section 3.6. This sets out key reflections on the overall effectiveness of the methods used, and recommendations for improvement for future projects.

3.2 Addressing the Research Problem

The aim of this research project is to test the following hypothesis:

“Some past human activities have created measurable differences in concentrations of naturally occurring gamma radiation emitting radionuclides, enabling detection of buried structures and objects of archaeological interest using portable gamma radiation surveying methods”.

The methodology developed to test this hypothesis, and address the associated research aim and underpinning objectives, was designed to generate data that would enhance our understanding of the feasibility of portable gamma survey methods for archaeological prospection, and its role in the toolbox of existing geophysical survey methods. The broad approaches applied recognise the lack of research undertaken in this field to date, and therefore the scarcity of extant data, upon which to develop more refined methods.

As discussed in Chapter 2, a review of the available literature confirmed that targets containing higher concentrations of naturally occurring radionuclides (NORs), when buried in substrate with naturally low concentrations of radioactivity, can produce positive anomalies in the gamma radiation data. One of the more compelling examples comes from Aziz *et. al.* (2018), where a granite block - rich in NOR-bearing minerals such as uraninite (Zekun 2021) – which was buried in alluvial deposits, produced a distinct positive anomaly in K, Th and U distribution maps. Another relevant example is from a study by Ruffell, *et. al.* (2006). Here, a modern sewage outfall pipe buried in sandy soil produced a strong positive anomaly in total count, K, U and Th distribution maps (*ibid*). The pipe, predominantly of concrete construction, exhibited elevated NOR concentrations; likely due to the use of additives such as fly ash in the production of the cement (IAEA 2003).

Whilst no instances of the inverse scenario to the examples provided above were found in the published literature, it is reasonable to hypothesise that a feature with naturally low radioactivity concentrations, when buried in a substrate with elevated NOR levels, would produce a distinct negative anomaly in the gamma radiation data.

Figure 3.1 provides an illustration of the relationship between naturally occurring radioactivity in buried targets, the surrounding substrate and the type of anomaly (strong positive to strong negative) this would create in mapped gamma radiation data. The figure shows the approximate positions of targets that produced positive anomalies in gamma radiation survey data, as reported in studies published by Aziz *et. al.* (2018) and Ruffell, *et. al.* (2006). The hypothesised location of a low-radioactivity containing feature buried in substrate with elevated NOR concentrations is also presented. This simplified representation provides a conceptual framework for understanding these interactions.

As this research progresses, it is anticipated that additional data will improve our understanding of the relationships of different target types in various substrates and the types of anomaly produced. This additional insight should enable further development of this figure and the addition of more detailed regions (i.e., which conditions are most likely to yield strong positive or negative anomalies).

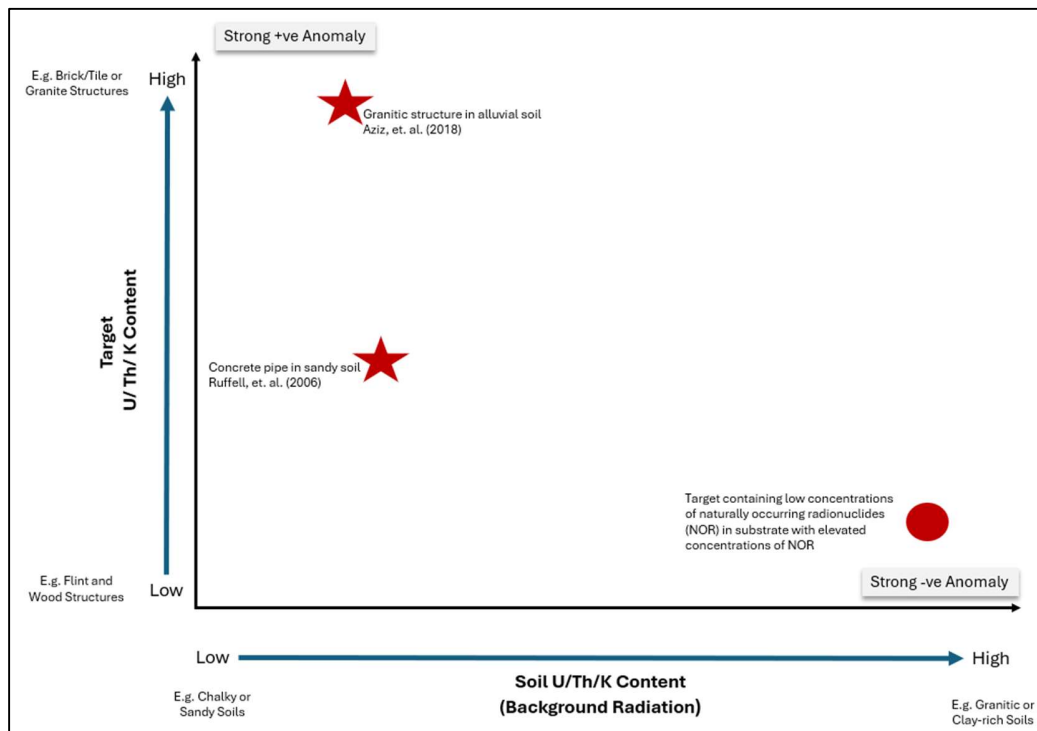


Figure 3.1 – Relationship between naturally occurring radioactivity in buried targets, the surrounding substrate and the type of anomaly generated in mapped gamma radiation data. Approximate positions of targets from published studies that produced positive anomalies are plotted, along with the hypothesised position of a scenario expected to produce a negative anomaly.

3.3 Data Collection Method – What, Why and How?

3.3.1 Data Requirements and Management (What and Why)

The ability to address the research question was dependent on the collection of quantitative and qualitative data of the right type, quantity and quality. To obtain this data, a combination of desktop study, fieldwork and laboratory analysis was undertaken. Table 3.1 provides a breakdown of the types of data required, methods of collection, desired outcome and key challenges/ limitations identified that could impact on data collection and quality. By setting out data requirements in this way, it was possible to develop a baseline research plan that could be readily revised as more information became available. Importantly, it also provided early insight into potential challenges that could impact on the ability to either undertake the research or obtain meaningful data. It therefore also enabled early identification of mitigation measures to overcome these challenges.

Setting out data requirements and expected outputs as per Table 3.1 also highlighted the various formats in which data would be collected and would require management. For example, key findings from the review of existing literature were recorded in notebooks; these were fully referenced to facilitate compilation of the literature review. Quantitative data, comprising radiological and GPS data, collected during field surveys was automatically recorded by the UMPC which is an integral part of the Groundhog system. On return to the office, the data was downloaded onto a secure desktop PC in a dedicated folder clearly labelled with the project name and date. The data was stored securely on a network with access restricted to a small number of individuals. Qualitative data from fieldwork activities, including photographs, maps and field notes were recorded in a formal field notebook. Quantitative data from lab work, including radiation measurements from mammal fossils and pXRF analysis of archaeological and environmental samples were captured in online databases and the field notebook. Electronic copies of data sets and field notebook pages were regularly backed up on an external hard drive.

Table 3.1 – Overview of the Proposed Strategy for Collecting the Data Required to Address the Research Question

Desired Outcome	Required Data	Method of Collection	Outputs	Potential Challenges / Limitations	Mitigation Measures
Understanding of similar work undertaken, gaps in the methods used/ information available and areas for improvement.	Existing Research	Desktop study	Literature review – qualitative assessment. Updated research strategy – more concise aims and objectives.	<ul style="list-style-type: none"> • Limited number of similar studies undertaken. • Previous studies focus on use of static gamma radiation survey methods. 	<ul style="list-style-type: none"> • Identify limitation in extant research to help identify areas for investigation. • Draw on nuclear industry experience.
Improved methods for data collection following experiential learning.	Appraisal/ Lessons Learned	Critical review of work undertaken	Revised methodologies for future fieldwork.	<ul style="list-style-type: none"> • Initial fieldwork reliant on well-established methods used in nuclear industry applications. • Availability of equipment limits range of trials that can be undertaken. 	<ul style="list-style-type: none"> • Early planning of fieldwork in expected 'quiet periods'. • Pre-booking of equipment.

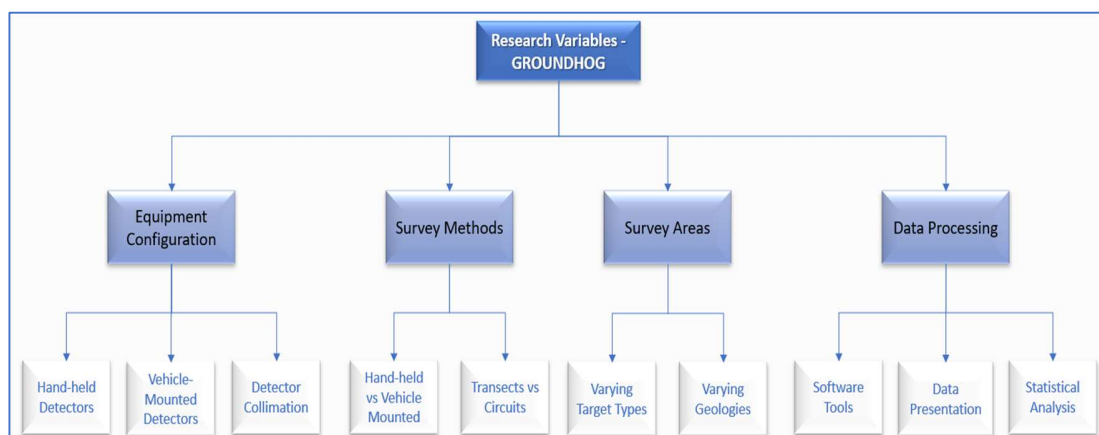
Desired Outcome	Required Data	Method of Collection	Outputs	Potential Challenges / Limitations	Mitigation Measures
<p>Measured intensity of gamma radioactivity present in targets and substrate for processing and interpretation (including statistical analysis).</p>	<p>Radiation Data GPS Data</p>	<p>Field surveys using a portable gamma surveying system (Groundhog), which uses a scintillation-type detector, spectrometer and GPS system.</p>	<p>High-density radiation intensity measurements (counts per second); at least one measurement per square metre.</p> <p>GPS coordinates</p> <p>Date/ Time information</p> <p>Speed (important to confirm that detector(s) were traversed at a speed of ~1m/s)</p>	<ul style="list-style-type: none"> • Data not representative of true conditions due to shielding (e.g. from overburden, interstitial water). • Insufficient data collected – area covered too small, measurements too widely spaced, failure to target buried features, missing data points. • Higher quality data more likely in drier, summer months – limits the period suitable for completing fieldwork. • Difficulty accessing suitable sites – either unable to gain necessary permissions or physical limitations. • Uncertainty regarding anomaly identification; i.e. whether it is attributable to a natural variation, artefact of the survey method, or target of potential interest. 	<ul style="list-style-type: none"> • Surveys targeted for summer months. • Minimum of one measurement per square metre to be collected. • Early engagement with site owners. • Target sites already subject to geophysical survey to enable comparison of the gamma radiation data with existing data sets.

Desired Outcome	Required Data	Method of Collection	Outputs	Potential Challenges / Limitations	Mitigation Measures
Visualisation of radiation data to identify any differences in the radiological characteristics of targets and substrates.	Radiation Data, GPS Coordinates	Compiled and quality check data collected during fieldwork exercises. Processing using proprietary software tools.	Radiation heat maps – provide a clear indication of any anomalies present and facilitates direct comparison with traditional geophysics data. Count rate distribution graphs.	<ul style="list-style-type: none"> Any variations are too subtle to be clearly delineated or are hidden in background noise. Timely access to software tools. 	<ul style="list-style-type: none"> Planning work during quieter periods. Explore alternative data processing methods.
Identification of radionuclides responsible for any anomalies observed.	Spectrometric Data	Field surveys using Groundhog using its integrated spectrometric capability.	Identification of specific radionuclides present within area surveyed, focussing on anomalies indicative of a target being present.	<ul style="list-style-type: none"> Measured activity will be limited to small variations in concentrations of U, Th and K isotopes limiting value of this data. Site accessibility. 	<ul style="list-style-type: none"> Use of pXRF data from archaeological and environmental samples to aid interpretation.
Insight into the radiological characteristics of targets and substrate to help determine the cause of observed anomalies	Radiation Data	Ex-situ High Resolution Gamma Spectrometry (HRGS) analysis of collected samples (i.e. in a laboratory setting).	Radionuclide composition of analysed samples – concentrations presented in Bq/g	<ul style="list-style-type: none"> Ability to collect representative samples of target material from buried features. HRGS system not available. 	<ul style="list-style-type: none"> Sampling of material in close proximity to survey area. Use of alternative analytical methods – pXRF.

3.3.2 Data Collection in the Field – An Iterative Process (How)

The principal method for collecting data capable of addressing the research question was the deployment of the portable gamma radiation surveying system Groundhog. This system has a long operational history within the nuclear industry, with analogous systems now also commercially available. However, its application in the fields of archaeological prospection is novel.

To fully test the effectiveness of the Groundhog system in addressing the research problem, the impact of multiple variables on data quality was explored, as summarised in Figure 3.2. To help understand any variations observed in radioactivity concentrations within targets and surrounding substrate, laboratory analysis of environmental and archaeological samples was also undertaken. This is explored further in Section 3.3.3.



Source: Personal Image

Figure 3.2 – Overview of research variables explored when deploying the portable gamma radiation surveying system Groundhog

As discussed in Chapter 2, the amount of published literature on the application of gamma radiation survey methods for archaeological prospection is limited. Despite extensive desktop studies, no information on the use of portable survey methods was found in the published literature. In consequence, no baseline was available on which to build a robust survey strategy for this novel application. Rather, an iterative approach was applied. The initial plan for the preliminary survey was based on well-established methods deployed for traditional ‘nuclear’ applications. Following implementation and data processing, the methodology was reviewed and

opportunities for improvement identified. These lessons learned were applied in subsequent fieldwork expeditions, with the aim of improving the overall methodology for this application.

Preparatory Checks

All Groundhog detector units are subject to annual calibration to ensure that the detector is performing as expected, and is in good working order. Calibration involves checking that the 662 keV photopeak associated with a known Cs-137 source is centred over a specific channel (data bin); in this case, channel 250. If this deviates by ± 5 channels, minor adjustments can be made to recentre. Otherwise, a greater level of correction work is required. The calibration checks also provide confidence that the detector's efficiency (ratio of light pulses generated by the NaI crystal relative to the number of gamma rays emitted by the check source) and energy resolution (the detector's ability to differentiate between energy peaks in a spectrum) are within acceptable pre-defined limits. Annual calibration is undertaken by a suitably qualified and experienced practitioner in accordance with well-established procedures and method statements. These were developed by Nuvia as the owner and operator of the system. This therefore does not fall within the scope of this study. However, it is noted that a check was undertaken to confirm that an up to date calibration certificate was issued for the detectors being used for each planned survey confirming operability, with the certificate number noted for future reference.

Before the detectors were taken out into the field, multiple pre-use checks were undertaken. A visual inspection of the detectors and supporting equipment was conducted. This included checking that the detector case, connection ports and handle socket were in good condition and not loose. It was also necessary to ensure that battery packs were fully charged, and that the necessary data and power cables were present and in good condition. A function check of the detector unit was also completed. This was undertaken using a known Cs-137 source and the onboard proprietary software, which is used to control the system and log the radiation and positional data. The Cs-137 source was placed next to the detector, and the onboard software launched and placed into calibration mode. Once the system confirmed that calibration was completed successfully, the detector was ready for use in the field.

These confirmatory checks are key to ensuring the collection of accurate/ representative data. In consequence, the same approach was applied for all fieldwork undertaken. The importance of

conducting such checks was highlighted during the final Silchester survey, when one of the three detectors failed the pre-use operability check on the morning of the survey. The faulty detector was withdrawn from service for repair, and replaced with an alternative unit.

Site Set-Up

For each site survey planned, the specific areas to be surveyed were determined well in advance. The aim was to identify areas containing a variety of target types that could challenge the Groundhog system. This in turn would provide insight into what types of feature might be capable of generating measurable contrasts in gamma radiation relative to background values, and thus help address the research question. It was also important to identify areas that could be realistically surveyed within the limited timeframes available; approximately 0.5 – 1ha/day for hand-held surveys and up to 4 ha/day for vehicle-mounted surveys. Identifying specific locations for surveying also supported the development of robust and defensible strategies when applying for the necessary permissions to access the survey sites. This was particularly important when planning for vehicle surveys which have the potential to be more disruptive; particularly in agricultural or potentially culturally sensitive areas.

For each survey planned, targets were selected by interrogating extant geophysical datasets (from fluxgate gradiometry, caesium magnetometry and Frequency-Domain Electromagnetic (FDEM) surveys) that revealed anomalies of interest. Geographic information system software (ArcGIS) was used to map out suitably sized survey areas over selected targets. Coordinates corresponding with the four corners of the survey boundary were also recorded for each survey area using the software. The coordinates were loaded into a portable RTK-GNSS system, facilitating the demarcation of the survey areas in the field, using marking poles.

On arrival at each site, a brief walk-round was undertaken to identify any hazards or obstacles that could impact on safety or accessibility of the survey area. This was particularly important for hand-held surveys where uneven ground or long grass could present trip hazards to be mindful of when traversing a site, or accessibility issues for the heavy collimator trolley. A final functional check is then undertaken of the Groundhog equipment to ensure the GPS and detector units are fully operational.

Site Surveying

The pilot and preliminary investigations, undertaken at Bisham (Berkshire) and Silchester Roman town (Hampshire) respectively, were completed using the Groundhog system in a hand-held configuration. This conveyed multiple benefits including:

- The hand-held configuration is simple to set up and operate, utilising only a single detector.
- The simpler configuration provided a valuable opportunity to become familiar with the equipment; how it operates in the field, understanding the information presented on the display screen and how to manage error messages or alarms without having to control a vehicle.
- A hand-held system is easier to transport between different survey areas; there is no requirement to dismantle a vehicle mounting frame. This therefore provided flexibility to move between multiple survey sites efficiently – particularly valuable at the Silchester site.
- This approach provided an early opportunity to test the impact of detector collimation (shielding) on data quality (Silchester only), as it was expected to have a significant impact on how future surveys would be undertaken.
- The technique provided a ‘worst-case’ for the total area that could be surveyed in a 1 to 2 day period, again recognising that surveys had not been undertaken in a non-nuclear context before, supporting the planning of future surveys.

For the pilot and preliminary surveys, guide ropes with 1 metre markings were run along the top and bottom of each survey area, as guided by the four marker poles. The Groundhog system was connected and the onboard software activated to bring up the operating screen (Figure 3.3). The detector unit was carried consistently in the right hand, supporting equal spacing of measurements. The detector unit is carried with the arm resting against the body, ensuring the face of the detector remains at a consistent height of ~20 cm above the ground surface.

Starting in the bottom left corner of the survey area, the detector is systematically traversed along 1 metre transects as shown in Figure 3.4. To support the collection of radiation measurements at a frequency of 1 measurement per square metre, an approximate walking speed of 1 m/s was maintained. This was monitored periodically by referring to the operating screen on the UMPC which shows current speed. As a further control, the software alarms should this speed be

exceeded. Siting poles were moved along the guide ropes as the survey progressed to ensure the detector remained on target.

All GPS and radiological data was automatically logged by the onboard software. Additional photographs and notes were taken over the course of the survey period to support findings.

For collimated surveys, the detector was positioned in a lead sleeve approximately 5 cm thick, comprising a coiled lead sheet. Due to its ~45 kg weight, the sleeve is set on a trolley to which the GPS is also fixed (Figure 3.5). The lead shielding reduces the amount of background 'noise' picked up by the detector, by ensuring that only gamma radiation directly beneath the detector reaches the NaI crystal. As for the hand-carried detector, the trolley was drawn along the 1 m transects, using the siting poles as a guide.

Two of the four survey areas targeted during the Silchester preliminary study were subject to both collimated and uncollimated survey methods. Approximately 50% of each area was surveyed with the collimator trolley, and the remaining 50% without. This supported a direct comparison of the two data sets and the impact the collimator has on data quality.

As discussed in subsequent chapters, data from the preliminary study at Silchester suggested that 1 m transect spacings could be sub-optimal in an archaeological context. Contributing factors included the limited size of the targets and the challenge of looking for small variations in the intensities/ concentrations of naturally occurring radionuclides. The latter being a significant deviation from the traditional operating conditions in which Groundhog is deployed; i.e. looking for anthropogenic radionuclides against a background of naturally occurring radioactivity. It was acknowledged that the fidelity of the visual outputs was impacted by the data interpolation process; a necessary step in generating continuous data sets and visual outputs from sampled data points (ESRI 2024). For example, some small anomalies in one survey area that were originally appeared to align with known archaeological features were later attributed to artefacts created by the interpolation process. In other instances, it was felt that smaller or less distinct features were either not detected due to inadequate sampling or otherwise lost during data interpolation.

To address this challenge, the use of 0.5 m transects in a grid pattern was trialled, as shown in Figure 3.6. The same walking speed of ~ 1 m/s would be maintained. It was assumed that this approach would improve the quality of visualisations by significantly increasing the density of measurements taken and reducing the risk of interpolation errors. Unfortunately, application of this method did not improve data quality. Indeed, a reduction in quality was observed due to an increased amount of ‘noise’ in the output images, making it more challenging to identify any anomalies in the data. In consequence, this data was not included in the associated published paper (Chapter 5). A second attempt at the 0.5 m spacing was made within a very small area within the East Heselton site in Yorkshire was planned. However, this was not possible due to time constraints. It is acknowledged that this is something that should be explored further as part of future research.

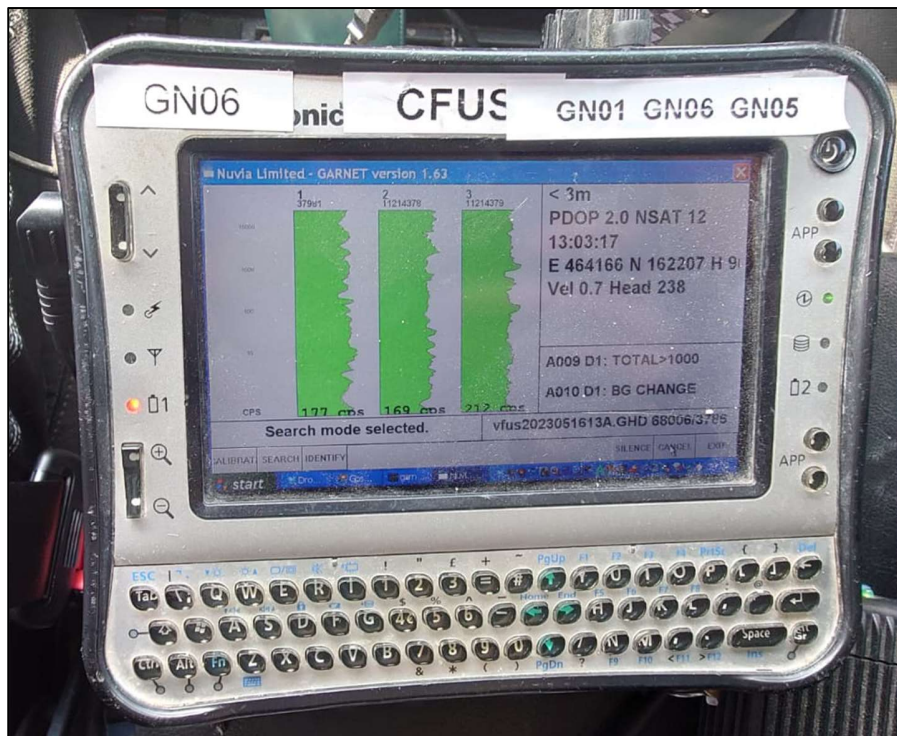
Subsequent fieldwork instead focussed on the use of a vehicle-mounted Groundhog system. This approach facilitated the simultaneous deployment of three detector units. The detectors are fitted to the front of the vehicle using a dedicated mounting frame (Figure 3.7). The detectors and GPS unit are connected to a UMPC which sits in the cabin of the vehicle; a Land Rover Defender. The use of this system effectively increased the number of data points that could be collected in a day from thousands to tens of thousands.

Due to the size and turning circle of the vehicle, it is not possible to complete a survey in simple transects as per handheld surveys. Instead, two potential methods are available. The first involves driving along transects over the main survey area, and at each end, driving in a circle to form a ‘lightbulb’ shape thereby allowing the vehicle to return to the transects. The second method is to drive around the perimeter of the survey area, which is delineated as per the handheld surveys. For each lap, the vehicle moves slightly inwards, forming a spiral. To ensure that the vehicle traversed each site at a constant speed of ~ 1 m/s, it was put into first gear in low range (low transfer case setting). This avoided the need to apply any acceleration, thereby supporting a more constant speed.

For both the subsequent Silchester and East Heselton surveys, the second method; driving in a spiral, was chosen (Figure 3.8). This method made it easier to slightly overlap each pass, making sure a high measurement density was maintained. This was considered particularly important

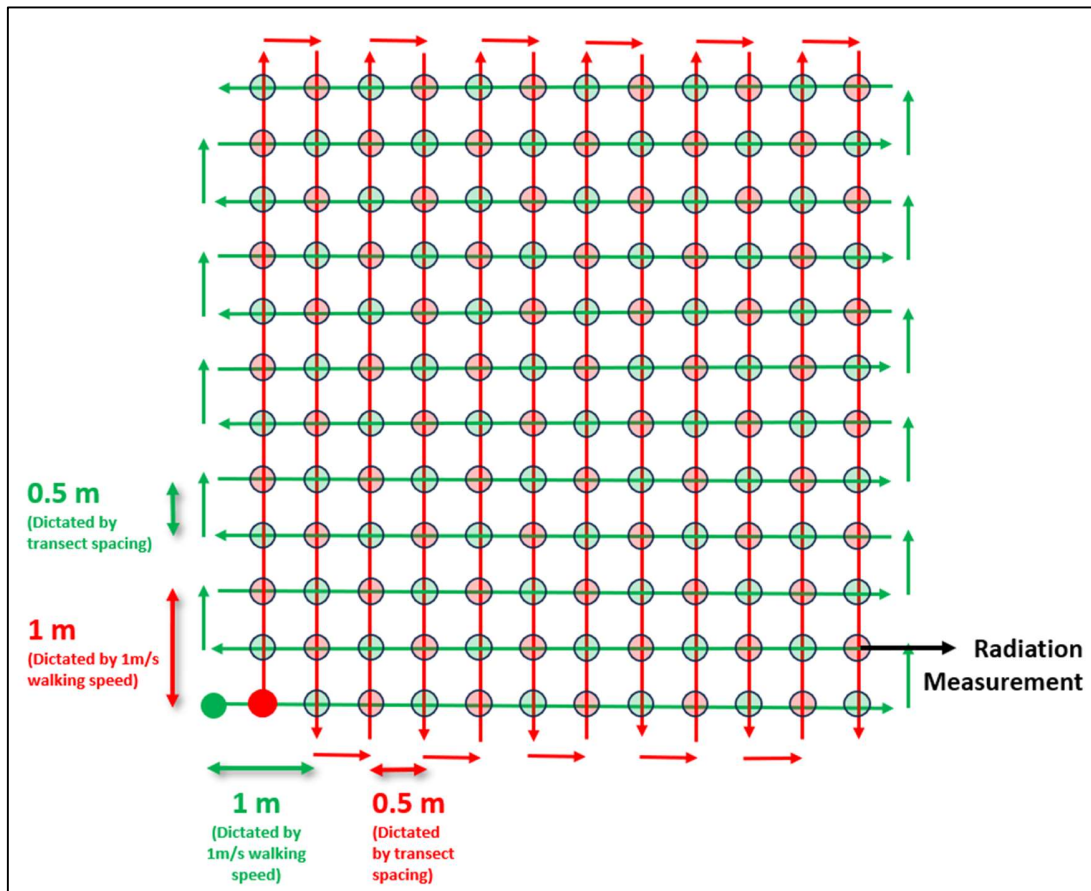
following the lessons learned from the preliminary survey. From a practical perspective, this method was found to be easier in this context, as it was possible to follow the tyre marks from the previous pass. This is less significant in traditional nuclear contexts where more industrial environments are surveyed and man-made radionuclides are sought. In consequence, achieving the maximum possible measurement density is less important.

At the end of each survey period, equipment was demobilised and packed away. Siting poles were removed from site. On return to the Harwell office, data collected on the UMPC was transferred to the dedicated office computer in preparation for processing.



Source: Personal Photograph

Figure 3.3 – Operational view of the Groundhog UMPC. The radiation measurements (green bars), coordinates, velocity and alarm notices can be seen. Note: It is possible to see data being recorded for three detector units in this example. This photo was taken during a vehicle based survey at Silchester.



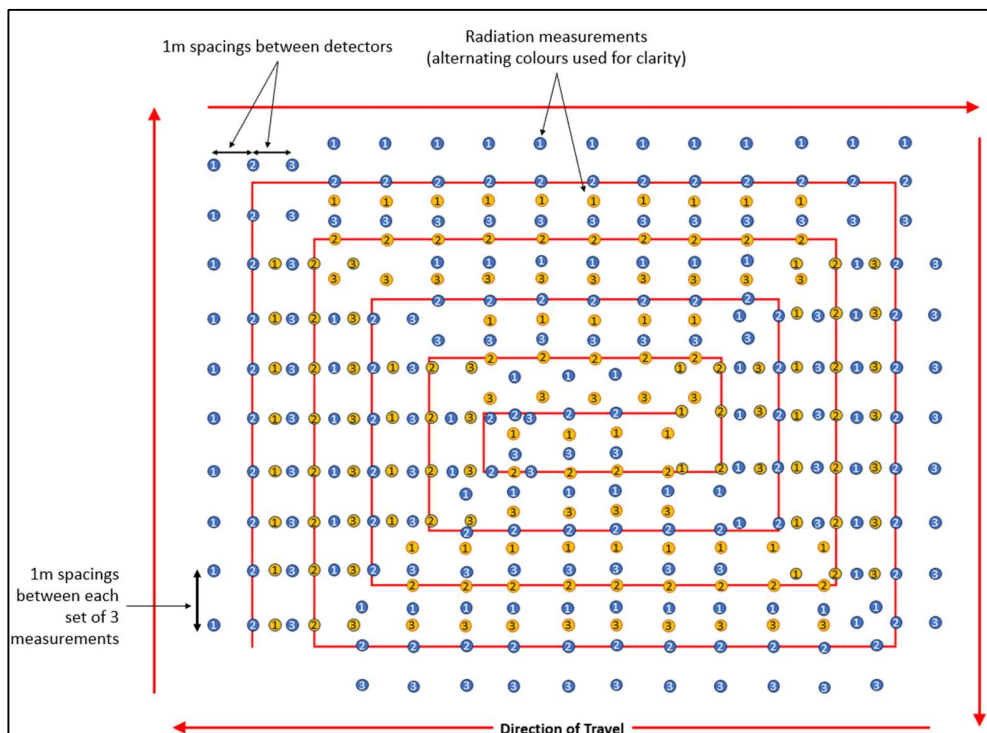
Source: Personal Image

Figure 3.6 – 0.5 metre transect survey pattern trialed at the second Groundhog survey undertaken at Silchester during the follow-up study at the site. This figure highlights the significant impact utilising a 0.5 m grid has on measurement density, when compared to 1 m transects.



Source: Personal Photos

Figure 3.7 – Left: View of the Groundhog in its vehicle-mounted configuration. Right: Fitting the mounting frame



Source: Personal Image

Figure 3.8 – Planned route of the Groundhog vehicle in a spiral pattern. The alternating colours for each pass demonstrates how an overlap is achieved.

3.3.3 Sampling and Analysis of Soil and Target Samples (How)

To aid interpretation of the Groundhog data collected across the Silchester, Bisham and East Heselton sites, various material samples recovered from Silchester were subject to pXRF analysis. The primary aim of this analysis was to confirm the presence of any variations in the concentrations of naturally occurring radionuclides, specifically potassium, uranium and thorium, across the different material types found at the Silchester site. This in turn, would help validate the findings from the Groundhog surveys. Samples of soil, gravel, flint and tile were collected for analysis.

Samples from Silchester were selected for analysis due to the pronounced contrasts observed in gamma radiation measurements between archaeological targets and surrounding soil as observed within the Groundhog data. Due to time constraints and a desire to minimise disruption to the site, recognising its status as an active agricultural area, existing materials and soils collected from previous excavations undertaken by the University of Reading and surface finds from other site visits were used. The limitations of this approach were acknowledged and are captured in Section 3.2.4 below.

Soils were fully dried prior to analysis to minimise the risk of x-ray attenuation or scattering from soil moisture. Soil residues were removed from the surface of the gravel, flint and tile samples to ensure the resultant data was reflective of the material of interest. Three sub-samples of the soil, gravel and flint were taken and placed into sample capsules to a minimum sample depth of 150 mm. This ensured that an 'infinite thickness' was achieved, and ensured full containment of the primary and secondary x-rays within the sample. The capsules used a mylar film base as this incurs only negligible attenuation effects for most contaminant x-ray lines. The capsules were analysed with the pXRF secured in a benchtop test stand, and connected to a desktop computer. This offered multiple benefits including greater precision for analysing smaller samples, direct transfer of analytical data to the computer minimising the risk of data loss or transposing errors, and remote operation thereby maximising operator distance from the x-ray source. The same method was applied to the gravel and flint samples that were placed on mylar film within the test stand.

It was not possible to place the tile in the test stand due to its size. Instead, the sample was analysed with the pXRF in a freehand configuration, but was still connected to the desktop computer. The tile was analysed in two separate locations – on its external surface which was exposed to soil contamination and weathering over time, and its internal surface which is more representative of the bulk material.

All samples were analysed using a Thermo Scientific Niton XL3-700 portable XRF analyser for a period of 120 seconds. The 'All Test Geo' calibration setting was applied, as this provided data for the widest suite of elements, including those of interest to this study – potassium, uranium and thorium. The results, which were recorded in parts per million (ppm) (uranium and thorium) and percentage (potassium) were averaged across the sub-samples for each material.

To increase the amount of data available for interpretation, it was possible to obtain pXRF data for soils collected from boreholes within the East Heselton survey area. The samples were collected and analysed by Philippe De Smedt and Jeroen Verhegge (University of Ghent) with whom I engaged when undertaking the Groundhog survey at East Heselton.

3.3.4 Benefits and Limitations of the Chosen Survey Methodologies

Field Methods

The application of Groundhog in the multiple configurations discussed in this chapter offered a robust approach to explore the efficacy of portable gamma survey methods in this unique context. The Groundhog system itself comprises rugged, reliable and well-established technologies that can be easily deployed in rural through to industrialised sites. Both hand-held and vehicle mounted configurations facilitated the collection of large data sets within the limited timeframes available. This extensive dataset not only helped address the original research aim and objectives, but also provides a valuable baseline upon which further research projects can be developed.

The Groundhog system provided excellent flexibility to apply multiple survey configurations, with the aim of identifying which method yields the best data for archaeological applications. It was also possible to refine the survey methods used, as required, drawing on lessons learned from previous studies.

The methods used however, were not without their challenges. It is recognised that each area surveyed is dynamic, with site conditions changing over even short periods of time. This is particularly relevant when considering variables outside of the control of the project, such as groundwater concentrations (which may attenuate gamma radiation), the timing of recent rainfall which may cause radon washout (and therefore possible peaks in measured activity concentrations) and amount of vegetation cover which may interact with the low levels of radioactivity. Due to time and resource constraints, it was not possible to conduct repeat surveys as well as trialling the multiple configurations available. It is recognised that in an ideal situation, multiple target sites would be surveyed using exactly the same Groundhog configuration. In addition, a single site would be repeatedly surveyed using multiple Groundhog configurations. This would facilitate a more effective comparison of datasets, and thoroughly test the efficacy of each survey method. For the purpose of this research project, a compromise was reached whereby analogous target types were surveyed using the same method, and a limited number of survey areas were subject to multiple survey methods.

It was found that the data from each period of fieldwork raised as many questions as it answered. In consequence, multiple recommendations for further work have been made as discussed in Chapter 7.

Laboratory Methods

As noted in the previous section, materials collected from previous excavations undertaken by the University of Reading and other site visits to Silchester were used for pXRF analysis. Unfortunately this meant that materials not directly connected to the areas subject to gamma radiation surveying were used. The limitations of this approach are understood. These extend to the possible variability in the soil composition across the Silchester site, and the potentially diverse sources (and therefore composition) of the gravel and flint present in the roads compared to that found elsewhere on site. However, it was felt that the samples collected served as sufficient analogues to provide valuable insights into the composition of the different material types, thereby aiding the interpretation of the gamma radiation data.

As part of future work, the intent would be to collect soil samples (and possibly archaeological samples if possible) at the same time as conducting Groundhog surveys to improve the fidelity of the pXRF results to the gamma radiation survey data.

3.4 Data Collection Method – Where and When?

3.4.1 An Ideal Test Site – Silchester Roman Town, Hampshire

The Roman town of Silchester was quickly identified as an optimal site for testing the hypothesis revisited at the start of this chapter. Of particular relevance is the broad range of target types and sizes present at Silchester and its peripheral locations. Features associated with urban dwelling (such as road networks and buildings of varying sizes), industrial activities (for example, kilns), burial sites and other common archaeological features such as defensive ditches can be found. Some features, such as some ditches can be attributable to earlier Iron Age settlements, further adding to the diversity of the target types available. The presence of these targets is underpinned by a substantial body of high quality survey data which is available in the published literature. Data sets, dating back to the Victorian period to present day, have been generated through extensive programmes of intrusive site investigations and non-intrusive geophysical surveys. The availability of these data sets supported the selection of a broad range of target types that could be tested with the Groundhog system. Further, it enabled comparison of the visual outputs from the gamma radiation surveys against those generated by well-established geophysical methods.

It was also felt that the target types and geology present at Silchester were broadly representative of other sites of archaeological interest across the UK. In consequence, it would be possible to more accurately determine whether gamma survey methods could add value to archaeological surveys beyond Silchester. For example, if a site with known granitic features was targeted for the preliminary investigation, it is possible that a radiation survey would be more likely to yield a positive result due to the higher concentrations of naturally occurring radioactivity present in granite. This in turn, would give an unrealistic expectation of the efficacy of the technique at other archaeological sites where contrasts between the target and surrounding substrate are less distinct.

Silchester also conveyed multiple benefits from a more practical perspective. The site is situated in relatively close proximity to Nuvia's Harwell office, where the Groundhog system was kept. The site could also be easily accessed by Groundhog in both its hand-held and vehicle mounted configurations, providing full flexibility to trial different survey methods. Finally, the University of Reading has a long and positive relationship with the Silchester site, having hosted multiple summer schools there. Gaining the necessary permissions to access and survey the site was therefore expected to be less challenging than for other, less well studied sites.

Surveys undertaken at Silchester were completed during the summer months as far as possible. This maximised the chances of being able to conduct surveys in drier weather, and therefore increase the likelihood of achieving positive results. However, an equipment malfunction during the August 2022 Silchester survey necessitated the re-survey of the eastern side of the targeted study area some months later. The re-survey work was undertaken in May 2023 following a higher than average period of rainfall, providing an unplanned opportunity to briefly explore the impact of increased groundwater conditions.

3.4.2 Looking Further Afield – Bisham, Berkshire and East Heselton

The Bisham site served as the pilot study location for this research project. At the time, the site was less well explored and included three potential targets of interest: a chalk pit, an Iron Age grave site, and what is believed to be a historic field boundary. The primary objective of the Bisham survey was to provide a training opportunity – to practice using the equipment, evaluate the effectiveness the typical Groundhog survey method in an archaeological context, and develop data processing skills. As such, there was no initial expectation that the data generated would contribute to the research findings, which is why the Bisham survey results are not presented until Chapter 6.

The Bisham survey was beneficial, providing a valuable opportunity to become familiar with the Groundhog equipment and offering a simple site to trial survey and data processing methods before conducting the first formal survey at Silchester. Whilst the gamma radiation distribution map produced at Bisham did not delineate the chalk pit or grave site, it did highlight what

appeared to be a historic field boundary. However, the significance of this observation was not initially recognised.

Following the pilot study, attention immediately shifted to the Silchester site, and the Bisham data was set aside. As the Silchester surveys progressed, a recurring pattern emerged: Groundhog's ability to detect historic field boundaries that did not always present physical (visible) or geophysical evidence. This discovery prompted a re-examination of the Bisham data, where a similar boundary had initially been identified. Ultimately, the Bisham data provided valuable additional insights that reinforced the findings and supported the consolidated study presented in Chapter 6.

The archaeological site at East Heselton offered another excellent test site for the Groundhog system. As for Silchester, this site has been subject to extensive archaeological research and is therefore very well understood. Again, large amounts of data for this site are available in the published literature, accessible through the Landscape Research Centre (LRC 2024).

Due to the scale of the site, only one archaeological feature was targeted; a Roman ladder settlement. This type of feature is analogous to some of urban structures surveyed at Silchester, and therefore provided a valuable opportunity to explore the impact of a different geological context when looking for targets of a similar type.

As per previous studies, data from the Groundhog surveys at East Heselton were compared against previous geophysical surveys of the same area. These earlier surveys used electrical conductivity and electrical susceptibility methods. This provided an opportunity to compare the visual outputs from the Groundhog survey against a different type of geophysical data, noting that surveys undertaken at Silchester are dominated by magnetic methods.

Finally, the field work undertaken at this site afforded a valuable opportunity to engage with other organisations, including the Universities of Glasgow and Ghent, who are exploring the potential value of knowledge and data sharing between the disciplines of precision agriculture and archaeology. The work undertaken recognises that both disciplines utilise broadly similar types of data, albeit with different requirements regarding scale, precision and output formats. As well as

undertaking the fieldwork necessary to address the requirements of this research project, some preliminary work was undertaken to explore the role of portable gamma survey methods in this application. This presents another exciting avenue of research to explore, following on from the work undertaken for this project.

3.4.3 Challenges Faced and Mitigations

Over the course of this research project, several key challenges associated with fieldwork were faced. These were principally attributable to seasonal restrictions, resource availability and the Covid-19 pandemic.

As alluded to previously, the ability to conduct fieldwork was limited to the summer months. This maximised the chances of collecting good quality data by avoiding gamma radiation attenuation from groundwater and misleadingly high radiation measurements from radon washout. This was managed as far as possible by looking at historic weather data and monitoring current weather forecasts to select optimal dates for conducting surveys. If rain was forecast, surveys were rescheduled. It is noted that this aspect was identified as a limitation for this research project as there was a drive to collect the highest quality data possible. However, it is recognised that conducting surveys in conditions where groundwater concentrations are higher will be an important element to future research, where the impact of groundwater on data quality is explored in more detail than achieved here.

The Groundhog system is extensively used to support various characterisation projects; both within a nuclear industry context and other scenarios where radioactive contamination is suspected. In consequence, the equipment is regularly deployed on commercial projects. This is similarly the case for the software and supporting IT infrastructure used to process the raw data. The use of Groundhog for research purposes therefore had to be scheduled around commercial demands. This was mitigated as far as possible by booking time slots at the earliest opportunity, and seeking periods of down time between contracts.

The final major challenge faced was the Covid-19 pandemic. This major event prevented any fieldwork from being undertaken for nearly 2 years. This was managed by using this period to

focus more on desktop study and the development of a more extensive literature review; something considered beneficial, recognising the multi-disciplinary nature of this work.

3.5 Data Analysis Methods (Why and How)

This chapter provides an overview of the methods used to process the data collected during each of the surveys undertaken.

3.5.1 Data Preparation and Processing

All data was subject to the same level of preparation and processing to support the subsequent generation of visual outputs that could be used to identify what, if any, archaeological features could be identified. In each case, the following key steps were followed:

- Step 1 – Import data into a Microsoft Access (v. 16.0.14131.20278) database
 - Data downloaded from the UMPC, including .GHD files (GPS data) and .GHC files (radiation data) is imported into a pre-existing Microsoft Access template which contains macros that automatically converts the data into a standardised form (database file) that can be readily accessed by other software packages. The file is saved in a dedicated project folder on the standalone desktop PC.
- Step 2 – Import data into ArcGIS
 - Data is imported into the ArcGIS software tool to give early insight into to the completeness of the data. The version of ArcGIS (version 10.1) used contains bespoke add-ins developed by Nuvia specifically for the processing of radiological data.
- Step 3 – Differential processing of positional data
 - Positional data is subject to differential processing using the GrafNav software tool (version 8.3). Both the .GHD files recorded during the site survey and RINEX data from the nearest identified base station are uploaded and processed using the pedestrian profile.
 - A separate word file is generated, capturing the name of the base station used, whether all of the files were correctly converted, and the quality of the GPS data (including the output graph from GrafNav and estimated position accuracy). If there had been any issues with data quality, this would also have been captured here.

- The processed data is exported as a .GHE file (ensuring that the settings are changed from static to kinematic).
- Step 4 – Update ArcGIS file with corrected positional data
 - The .GHE file is uploaded into the Access database. This data can now be either imported back into ArcGIS as a new layer, or saved as a .dbf file that can be used to extract relevant data for import into Geoplot.
- Step 5 – Generate visual outputs in ArcGIS and Geoplot.
 - Data from the Microsoft Access file can be automatically imported into Nuvia’s bespoke version of ArcGIS in preparation for processing to generate the required visualisations.
 - To process data in Geoplot, the data to be plotted must be saved as comma separated values (header rows removed) in preparation for import and processing.
 - The types of processing undertaken is presented in Section 3.4.2 below.

3.5.2 Data Analysis and Interpretation

Radiation Data Analysis/ Interpretation

Data generated during the preliminary investigation at Silchester was processed using ArcGIS only. This was the most logical approach at the time, as it is the well-established method with which commercial Groundhog data is processed. Data from subsequent surveys was processed using Geoplot as this was found to be a more effective tool in this [archaeological] context. It is an intuitive tool that facilitated the application of various filters, interpolations and colour palettes that helped to draw out anomalies. Further, by using commercially available software rather than ArcGIS and its bespoke tools, it was possible to demonstrate that the results observed could be replicated by others, using the raw data accessible in Appendix 1.

When using ArcGIS for generating visualisations, a map of the site is imported, over which the radiation data can be superimposed. The radiation data are initially presented as individual points on the map, making it difficult to identify any anomalies present. This is resolved by interpolating the total gamma activity data by applying an inverse distance weighting technique with a grid size of 0.5 m and effective range of 1.5 m. This has the effect of creating a continuous, smooth image of the survey data which is easier to interpret. In this context, we are looking for subtle variations in naturally occurring radioactivity distributed across each site. To help achieve

this, different colour ramps were applied to identify the most effective ones for highlighting any anomalies of interest. The bespoke tools created by Nuvia for use within ArcGIS also supported interrogation of the spectral data which confirmed that the radiation measurements could be attributed to naturally occurring primordial radionuclides. Finally, the bespoke tools were used to generate count rate distribution graphs which helped determine whether data were normally distributed across each of the survey areas.

The efficacy of Geoplot (version 4) was first trialled using simplified spreadsheets containing only GPS data and total counts data for a survey area. These spreadsheets were saved as comma separated value files to ensure compatibility. Combinations of GPS Gap Filling, Interpolation and Filters were applied to the data to establish how best to present the data. The aim was to create the best quality image possible without deviating too far from the original data in order to maintain fidelity to the true conditions of the site. The most successful combinations were identified as follows:

- GPS Gap Fill only
- GPS Gap Fill + Wallis Filter (x/y radius = 3, uniform weighting, desired SD – 2, desired limit = 1)
- GPS Gap Fill + Median Filter (x/y radius = 2, block = off)
- GPS Gap Fill + Low Pass Filter (x/y radius = 2, weighting = gaussian, block = off)
- GPS Gap Fill + High Pass Filter (x/y radius = 10, uniform weighting, block = on)

It was found that the combination of 'GPS Gap Fill + Wallis Filter' was the optimal method for processing the data. It created a smooth dataset capable of drawing out anomalies without excessive deviation from the raw data. This method was therefore applied to all subsequent processing activities. To demonstrate how anomalies found in the gamma radiation data aligned with anomalies found in the existing geophysical data for a site, processed images generated in Geoplot were exported as '.grd' files. These were imported into ArcGIS and added as a semi-transparent layer over existing fluxgate gradiometer and caesium magnetometer data. Count rate distribution graphs were generated in Excel, which also facilitated the application of normal distribution curves to aid data interpretation.

The use of Geoplot also facilitated the analysis of data sets for individual radionuclides. This helped establish what, if any, impact certain radionuclides were having on the results observed. Key naturally occurring radionuclides of interest were: K-40, U-238, Th-232. Energy windows that aggregated measurements falling below the caesium-137 energy range ('Below Window') and above it ('Above Window') were also analysed. Whilst this was a useful exercise, it was found that total count data was capable of generating consistently high quality images, and was the target of analysis for the data collected from the Bisham and East Heselton sites. However, as noted in Chapter 7, the ability to compare the visualisations generated using total count data against visualisations from other regions of interest yields significant additional interpretive value.

Statistical Analysis

Count rate distribution graphs were created for all data sets to aid interpretation of the gamma radiation distribution maps.

Further statistical analysis was undertaken to support interpretation of the August 2022 and May 2023 data sets collected at the Silchester site. This included a two-tailed t-test to determine whether the two data sets were significantly different. Attempts were also made to normalise these two datasets to allow them to be combined to form a single dataset for that area.

Normalisation methods applied included:

- Normalising the pre-combined August 2022 and May 2023 datasets using the formula 'x normalised = (x – x minimum)/ range of x'.
- Dividing all measurements by the maximum recorded value from the combined dataset.
- Normalising by subtracting the median value from all measurements
- Normalising by dividing all measurements by the mean value for the May '23 data.
- Normalising by establishing the median values for the August '22 and May '23 data, establishing the mean of those two values and dividing all measurements by the 'mean of the two means'
- Normalising by dividing all measurements by the mean value for the August '22 data.

Unfortunately, none of these methods worked to support combination of the two datasets. In consequence, a decision was made to present them separately. This is explored in more detail in Chapter 5 of this thesis.

3.5.3 Benefits and Limitations of the Methods Used

Use of the bespoke version of ArcGIS developed by Nuvia Limited is, in principle, the optimal method for analysing data generated through Groundhog surveys and generating the radiation distribution maps. The software tools were created specifically for analysing data generated by the Groundhog system. The software is capable of detailed interrogation of the data including conducting spectral analysis of areas of interest. However, it was found that many of the features offered by this bespoke version of ArcGIS were less useful when the intent is to identify very small variations in naturally occurring radioactivity and whether these align with any known or suspected archaeological features. This might be expected, recognising that this system was principally designed for detecting distinctive man-made radionuclides. Further, due to the commercial demands on this software impacting on its availability for this research, Geoplot rapidly became a highly viable alternative.

Geoplot (Geoscan Research) was capable of generating high quality gamma radiation distribution maps that drew out anomalies of interest. The ability to apply GPS gap fill and filters facilitated enhancement of these images without deviating significantly from the original data. Further, Geoplot was capable of generating image files that could be imported into a standard version of ArcGIS Pro, allowing overlaying of gamma radiation heat maps on geophysical data. This could be used to demonstrate alignment of anomalies in the geophysical and gamma radiation data sets.

3.6 Conclusions

This chapter has outlined the methodologies employed for survey site selection, portable gamma radiation surveys, sample analysis and data processing. Through application of an iterative approach, these methodologies were reviewed and refined, acknowledging the novelty of this research and absence of existing guidance in deploying portable gamma survey methods in archaeological contexts.

The methods applied were robust, generating reliable and representative data sets capable of addressing the research question posed. Particularly noteworthy were the discoveries regarding the effectiveness of both the hand-held and vehicle mounted Groundhog systems, demonstrating scalability, and the ability to use Geoplot software for data processing, improving accessibility to gamma radiation survey methods within the archaeological community.

It is however recognised that this research is still in its infancy. There are therefore multiple opportunities to improve and expand on the methods applied within this research project. Further investigation into the efficacy of 0.5 m transect spacings for handheld gamma radiation surveys, broader testing of the Groundhog system across a wider range of climatic and geological conditions, exploration of alternative detector types, and the collection and analysis of environmental and archaeological samples from the same location and time as gamma radiation surveys are all avenues for improvement.

The following chapter presents the results from the preliminary investigation undertaken at Silchester Roman town. This early study used Groundhog in a hand-held configuration. Subsequent chapters will detail the refinement of these methods, demonstrating their scalability, resilience and overall efficacy in archaeological prospection.

3.7 References

Aziz, A. Attia, T. McNamara, L. and Friedman, R. (2018) Application of Gamma-ray Spectrometry in Discovering the Granitic Monument of King Pepi I: A Case Study from Hierakonpolis, Aswan, Egypt, Pure and Applied Geophysics, Published Online 09/11/2018

ESRI (2024) ArcGIS PRO – An overview of the Interpolation toolset, <https://pro.arcgis.com/en/pro-app/latest/tool-reference/spatial-analyst/an-overview-of-the-interpolation-tools.htm>, Accessed: 15/11/2024.

IAEA (2003a) Extent of Environmental Contamination by Naturally Occurring Radioactive Material (NORM) and Technological Options for Mitigation, Technical Report Series No. 419, International Atomic Energy Agency, Vienna

LRC (2024) East Heselton, www.landscaperesearchcentre.org/html/east_heselton.html, Landscape Research Centre (LRC), Accessed 06/01/2024

Ruffell, A. McKinley, J. Lloyd, C.D. and Graham, C.J. (2006) Th/K and Th/U Ratios from Spectra Gamma-Ray Surveys Improve the Mapped Definition of Subsurface Structures, Journal of Environmental and Engineering Geophysics, **11** (1): 53 – 61

Zekun, L. (2021) Metallogenic characteristics and genesis of granite type uranium ore bodies in South China, 7th International Conference on Energy Materials and Environmental Engineering 2021 (ICEMEE21), Article No: 02068, DOI: <https://doi.org/10.1051/e3sconf/202126102068>



CHAPTER 4

Portable Gamma Ray
Spectrometry for
Archaeological Prospection: A
Preliminary Investigation at
Silchester Roman Town

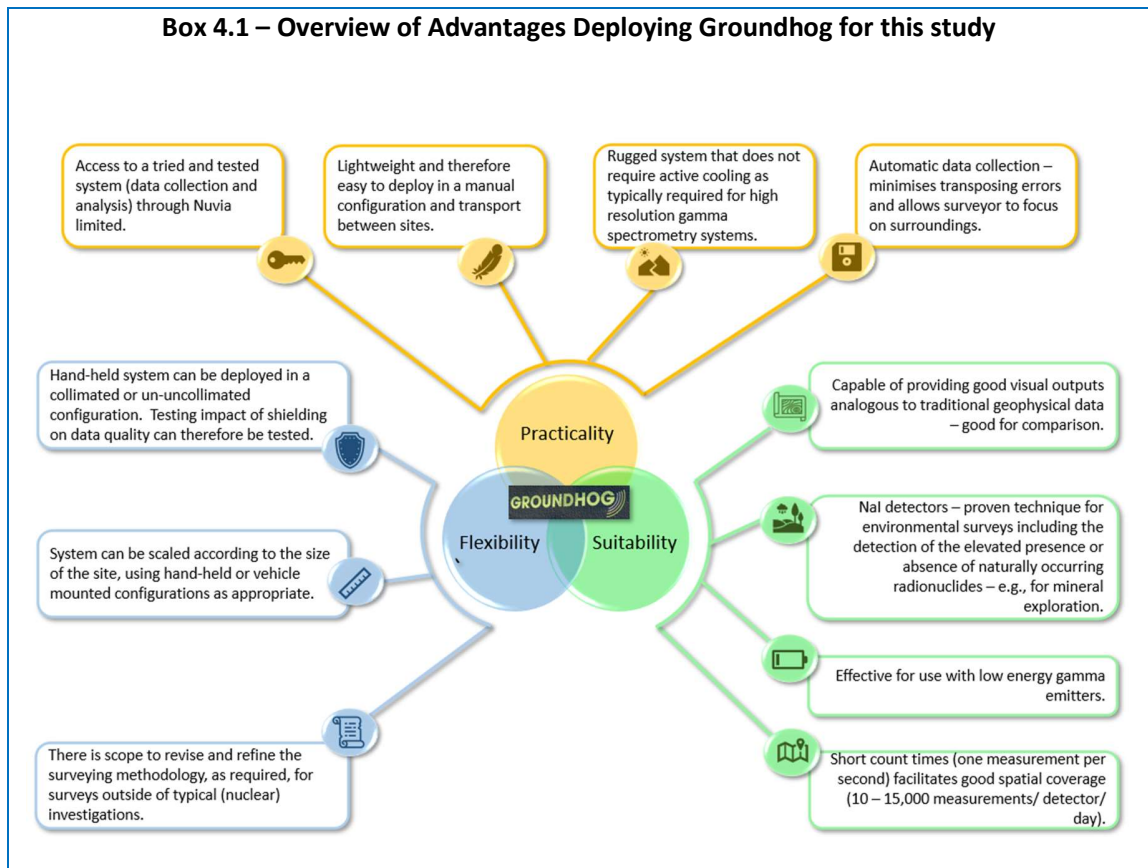
4 PORTABLE GAMMA RAY SPECTROMETRY FOR ARCHAEOLOGICAL PROSPECTION: A PRELIMINARY INVESTIGATION AT SILCHESTER ROMAN TOWN

4.1 Introduction to Paper (as published in *Archaeological Prospection*, Vol 29(3))

This paper forms Chapter 4 of this thesis. It was published in *Archaeological Prospection* in March 2022 and presents the findings from a preliminary study to evaluate the efficacy of portable gamma ray surveying techniques for archaeological prospection. Silchester Roman town was selected for this study due to the quality and extent of existing archaeological data available, providing a robust dataset against which the radiation data could be compared, and any radiation anomalies identified subsequently verified. Further, Silchester provides a diverse range of target types to survey; the selection of which was aided by the extant fluxgate gradiometer and caesium magnetometer data. This provided a valuable opportunity to establish which, if any, target types could be 'seen' using this method.

The paper presents the findings from multiple gamma radiation surveys over several different targets; a cross section of roads in an 'urban area', cremations and inhumations, the temenos wall of a temple and kilns in an industrial area. Surveys were undertaken using the portable gamma radiation surveying system, Groundhog, as presented in Chapters 1 and 2 of this thesis. Groundhog was developed for use in the nuclear industry. It is therefore designed for confirming the presence or absence anthropogenic radionuclide accumulations that are typically present at higher intensities, rather than looking for slight variations in natural background radiation. However, due to its availability, ability to achieve higher resolution/ quality data (i.e., improved ability to differentiate between different source radionuclides) through data aggregation and ability to generate visual outputs analogous to traditional geophysical images, Groundhog was identified as an ideal candidate system. Other features of Groundhog that make this particularly well-suited to this application are summarised in the call out box (Box 4.1) below.

Box 4.1 – Overview of Advantages Deploying Groundhog for this study



Methodology Rationale

For this preliminary investigation, a decision was made to deploy Groundhog in a hand-held configuration, traversing each survey area along 1 m transects. The transect spacing combined with an approximate walking speed of 1 m/s follows the well-established methodology used in commercial applications. It enables the collection of one radiation measurement every square metre, generating sufficiently high-density data for later processing to generate higher resolution data.

Due to the novel application of Groundhog in this context and the exploratory nature of this study, it was considered prudent to follow an extant, tried and tested methodology that is known to achieve an optimal balance between generating a high-density data set and making efficient/ timely progress across each survey area. Further, a pilot study undertaken at a different site (Bisham) confirmed the suitability of the method.

Deploying Groundhog in a hand-held configuration provided the flexibility to deploy the system in both a collimated (shielded) and un-collimated (un-shielded) configuration, evaluating the impact of collimation on data quality. As the aim of the study is to measure subtle changes in naturally occurring background radioactivity, it was anticipated that collimation would improve data quality. However, as shown in this paper, this was not the case.

From a practical perspective, using a hand-held system facilitated easy transport to each survey area, recognising that the sites were distributed from 100s of metres to over three kilometres apart.

Journal Rationale

The journal *Archaeological Prospection* was selected for publication as its aims and scope closely align with the research aim of this project. Of particular relevance is the journal's aim to "disseminate information about new (or newly applied) prospecting techniques" and that "Reports and evaluations of new techniques will be welcomed" (Wiley Online Library 2023). A broader aim is to inform the scientific community about the range of methods available to study the near-surface environment (Wiley Online Library) was also considered relevant.

4.2 Confirmation of Candidate Contribution

Victoria Robinson: Conceptualisation, literature review, methodology development, data collection, data analysis, writing – original draft, incorporation of peer reviewer comments.

Robert Clark: Preparation of Groundhog equipment, supporting data processing, supported creation of Groundhog visualisations, writing – review.

Dr Stuart Black: Conceptualisation, supporting data analysis, writing – review and editing.

Dr Robert Fry: Conceptualisation, permissions for access to Silchester, fieldwork setup, supporting data analysis, writing – review and editing.

Dr Helen Beddow: Conceptualisation, writing – review and editing.

4.3 Published Paper

4.3.1 Keywords

Archaeological Survey, Natural Radioactivity, Gamma Spectrometry, Gamma Ray Surveying, NUVIA Groundhog®, Silchester, Radioactive Isotopes, Roman Town, Integrated Techniques

4.3.2 Abstract

Several studies have suggested the potential value in applying gamma radiation surveys to support identification of buried archaeological features. However, the number of previous studies is very small, and have yielded mixed results. The true efficacy of the technique is therefore unclear.

Here, we report on an alternative survey method that uses Groundhog®; a portable gamma radiation system with spectrometric capability, to achieve high spatial density monitoring of archaeological sites. The system, which is used extensively in the nuclear industry, was used to carry out preliminary surveys at four different locations within the Silchester Roman Town. Targeting a site for which an extensive amount of archaeological data is available facilitated testing of the method on a range of known target types. Surveys were carried out along one metre transects at an approximate walking speed of one metre per second, resulting in the capture of one radiation measurement per square metre. Total gamma radiation, recorded in counts per second, were presented in the form of surface radiation (contour) maps and compared against existing fluxgate gradiometer and caesium magnetometer data. Total gamma counting consists of counting gamma-rays, without energy discrimination, that are spontaneously emitted by the material under investigation. The obtained counts represent the total, or gross, gamma contribution from all radionuclides, both natural background series and anthropogenic. Radiation anomalies were identified in two of the four survey sites. These anomalies correlated with anomalies present in the fluxgate gradiometer and caesium magnetometer data and can be attributed to a Temenos wall bounding the temple complex and an infilled clay pit.

Early results suggest that this may be a complementary technique to existing geophysical methods to aid characterisation of archaeological sites. However, it is believed that data quality could be

significantly improved by further increasing spatial resolution. This will be explored as part of future field work.

4.3.3 Introduction

The use of non-intrusive survey techniques for the prospection of archaeological targets is well established (Cardarelli and De Filippo 2009, Columbero, *et. al.* 2020, Dick *et. al.* 2015 and Gaffney & Gaffney 2010). They provide an opportunity to undertake timely, resource effective, non-destructive (and therefore repeatable) data gathering exercises at sites of potential archaeological interest (Barker 1993). The resultant data can be used to plan targeted intrusive investigations that are more likely to yield finds, minimise environmental disturbance and minimise potential harm to culturally sensitive or protected areas (Barker 1993).

The most commonly used geophysical surveying techniques can be grouped into three overarching categories – ‘magnetic’, ‘electrical’ and ‘ground penetrating radar’. It is recognised that there is no single technique within these groups that can be ubiquitously applied to all scenarios (Gaffney & Gaffney 2010). Rather, consideration must be given to the physical and chemical properties of the suspected target (Gaffney and Gater 2003) and surrounding substrate, target size (Ruffell and McKinley 2008) and likely level of overburden. Consideration must be given to nearby infrastructure (such as pipelines, metal fences and cars) which may generate misleading results (Schmidt, *et. al.* 2015). By accounting for these variables, it is possible to improve the quality of the data. Targeted selection of the optimal geophysical technique will therefore increase the likelihood of measuring sufficient contrast between the target and surrounding material, minimise the risk of interference from other infrastructure and minimise the risk of false positive and negative results (Milsom and Eriksen 2011).

Survey data quality can be further improved by utilising contrasting techniques at the same site. Whilst more costly and time consuming (Ruffell and McKinley 2008), such a strategy can minimise the risk of false positives. If contrasting techniques both identify an anomaly in a specific area, it is more likely to be a feature of interest. Comparing the two data sets may highlight less distinctive anomalies that could have otherwise been overlooked. The value of using multiple surveying techniques has been exemplified in multiple studies including those by Creighton and Fry (2016), Halgedahl, *et. al.* (2009), Putiska, *et. al.* (2014), Trogu, *et. al.* (2014) and Zheng *et. al.* (2013).

A New Geophysical Tool

When considering these studies, it may be valuable to think of the available geophysical techniques as tools within a toolbox that can be selected and combined to achieve an optimised solution for archaeological surveys. An alternative non-intrusive survey technique that may offer a valuable contribution to the ‘geophysics toolbox’ is gamma radiation surveying. The completion of radiation surveys using non-intrusive techniques is already well established in the nuclear industry (IAEA 1998). They are typically used to identify and characterise anthropogenic contamination in support of reassurance surveys and remediation planning (IAEA 1998). Rugged, portable systems can be readily deployed; principally for site characterisation and hotspot detection (Davies, *et. al.* 2011). Gamma spectrometry techniques have been successfully deployed in multiple geological applications. For example: soil structure characterisation or identification of features of interest such as karst structures (Reinhardt and Hermann 2019, Putiska, *et. al.* 2014). Its use in the field of archaeological prospection is, in contrast, significantly less-well established. Only a limited number of studies are currently available in the published literature. The specific techniques applied in this study have not, to the authors’ knowledge, been applied in an archaeological context before. This is explored in more detail below.

The application of gamma spectrometry in the context of archaeological prospection works on the principle that the compositions of primordial radionuclides, and in particular, K-40, U-238 and Th-232 within archaeological features are measurably different to that in the surrounding substrate (Moussa 2001, Sanjurjo-Sanchez, *et. al.* 2017). This contrast may be attributable to one or more factors including:

- Import of material – Construction materials have throughout history, been transported over significant distances to a desired location or settlement as exemplified by the Welsh ‘blue stones’ of Stonehenge (Nash, *et. al.* 2020) and Dorset-provenanced Purbeck Marbles of Westminster Abbey (Westminster Abbey 2020). These imported materials will have a different geochemical composition to the local geology. In some cases; particularly for clays and granites, the radionuclide concentration will be markedly different. Where imported materials are present in sufficient quantities, the difference in gamma signatures should be measurable. This is particularly relevant for construction materials such as clay-fired bricks

which are known to concentrate radionuclides during the brick making and firing process (Aliyev 2004, IAEA 2003).

- Concentration of materials rich in naturally occurring radioactivity – Many historic and ancient structures; from basic houses to places of worship and monuments, used building materials rich in naturally occurring radionuclides. This includes for example clay bricks which can contain significant concentrations of Ra-226, Th-232 and K-40 (1 – 200 Bq/kg Ra and Th, and 60 – 2000 Bq/kg K-40) (IAEA 2003) and granite which in the UK, can contain 2 – 770 Bq/kg of U-238 and 2 – 280 Bq/kg Th-232 (IAEA 2005). When present in the volumes required for construction, a cumulative effect may be achieved whereby it may be possible to discern a measurable contrast in radioactivity when compared to surrounding areas.
- Industrial activities – Activities such as mining and the processing of ores has been, and continues to be, a notable source of technologically enhanced naturally occurring material (IAEA 2013). In consequence, historic industrial areas have the potential to generate a measurable contrast to natural background radiation levels.

Extending the application of gamma radiation surveying to an archaeological context could offer several benefits including: lack of susceptibility to interference from modern structures such as fences, pipelines and cables; ability to be deployed on foot (Figure 4.1 a, b) or vehicle mounted (Figure 4.1c) as required; ease of deployment and compatibility of output data with traditional geophysical outputs. Further, when deploying a monitoring system with spectrometric capability, specific radionuclides responsible for generating the measured radiation can be identified. By comparing the isotopic composition of an anomaly against the background radiation, it may be possible to identify two distinct material types. This would support a more robust conclusion that the anomaly can be attributable to an archaeological deposit rather than a naturally occurring variation. It is noted that a difference in isotopic composition would only occur where non-local materials are present in the archaeological deposit. For example, if a brick wall was built using local clays, an area of increased radioactivity might be found due to the concentration of the naturally occurring radioactive material. However, the isotopic composition would be comparable to the local source material. If the bricks were imported from elsewhere, a different isotopic fingerprint may be observed.



Source: Personal Photo

Figure 4.1 – NUVIA Groundhog[®] system in Uncollimated (a), collimated (b) and vehicle mounted (c) configurations. Sources: Personal photographs, NUVIA (2021)

Some studies have suggested that gamma radiation data can provide valuable insight into the geoarchaeological context of a site. For example, Kozhevnikov, *et. al.* (2018) highlighted the value of collecting gamma ray measurements alongside traditional geophysical data during the survey of ancient iron smelting sites in Siberia. In this study, radiation data supported the identification of a rapid change in climatic and/or hydrogeological conditions at the site. This led to a cessation of

granitic deposits from the nearby Primorsky Range (Kozhevnikov, *et. al.* 2018). This change enabled soil accumulation and vegetation growth over the granitic material which, due to attenuation by the soil, was characterised by a notable reduction in radioactivity (Kozhevnikov, *et. al.* 2018). In a separate study, preliminary findings from Bezuidenhout (2012) suggest that historic human activity at a site may be characterised by a depletion in potassium concentrations. Bezuidenhout's 2012 study suggests that human activities can enhance the rate of topsoil erosion and expose lower soil layers which then begin to weather resulting in the potassium depletion observed.

Previous Applications of Gamma Spectrometry in Archaeology

The use of the radioactive properties of naturally occurring radionuclides in archaeology dates back to the 1940s and the evolution of radiocarbon dating (Kern 2020). The technique, which measures residual Carbon-14 concentrations in artefacts of typically organic origin, is used to estimate the target's age. The technique has since expanded. An increased number of radionuclides, most commonly uranium, can be measured in a similar way to establish the age of a broader range of materials including those of geological origin (Peppe 2013).

The application of gamma spectrometry in the field of archaeological prospection is more novel, having only been demonstrated in a small number of studies, including those by Ruffell and Wilson (1998), Moussa (2001), Ruffell, *et. al.* (2006), Sanjurjo-Sanchez, *et. al.* (2017), Aziz, *et. al.* (2018) and Kozhevnikov, *et. al.* (2018). In each case, static detection systems were used to survey a pre-defined area with the aim of detecting buried features of interest. Some of these studies, including those by Aziz, *et. al.* (2018) and Moussa (2001) yielded positive results. In these two examples, the processed data were successfully used to delineate the position of archaeological features of interest; a granitic Egyptian monument and the foundations of a building respectively.

Whilst these preliminary studies suggest that the use of static gamma spectrometry systems may be a viable technique, it is recognised that this can be time consuming. When surveying for naturally occurring radioactivity, count times of up to 6 minutes per sample can be required in areas depleted in naturally occurring radionuclides to achieve the required measurement precision and data quality (IAEA 2003, USNRC 2009). Such an approach, however, will limit the amount of data that can be collected in the available time period.

This study therefore proposes and tests an alternative strategy that utilises a portable gamma radiation detection system with spectrometric capability to achieve high spatial density monitoring of archaeological sites. The proposed strategy of collecting a high number of low data resolution (i.e. low ability to distinguish between gamma rays with similar energies) measurements has been used to good effect in the nuclear industry (Davies, *et. al.* 2011). Available literature however, suggests that such an approach has not previously been applied in an archaeological context. The system used in this study, known as Groundhog[®], is developed and owned by NUVA Limited. It is extensively used for radiation surveys of land, buildings, and other infrastructure. Groundhog[®] is a portable system principally comprising a sodium iodide (NaI) based scintillation detection system with spectrometric capability, survey grade GPS system and data logger that can be operated in either an uncollimated or collimated configuration (Figure 4.1a, b). It is capable of continuously recording radiation measurements, at one measurement per second, and global positioning data on an ultra-mobile PC (UMPC). Data is processed to generate multiple visual outputs, including radiation contour maps, spectral distribution graphs and sample maps.

The Groundhog[®] system can be adapted to accommodate a single hand-carried sodium iodide (NaI) detector through to a bank of detectors mounted on a vehicle. It is possible then, for a single person to survey tens to multiple thousands of square metres in a day. In consequence, the methodology proposed in this study supports the collection of much larger, high density data sets over a greater geographical area than has previously been achieved for gamma surveying techniques applied in an archaeological context. This should in turn, improve the quality and spatial resolution of output data available. Further, the visual outputs generated as a result of these surveys can be easily compared with existing geophysical survey data for the same area, as exemplified later in Figures 4.4, 4.6, 4.7 and 4.8. This will make it easier to test the effectiveness of gamma radiation surveying in this unique context.

The overall aim of this investigation is to further explore the effectiveness of radiation surveys in the detection of potential archaeological features of interest and whether it could contribute to the existing range of geophysical surveying techniques available. This will be achieved by building on the findings of previous studies and surveying new sites using the Groundhog[®] system at sites

of known archaeological interest. An initial survey using Groundhog® has been completed at a well-known archaeological site that has been extensively surveyed using standard geophysical techniques.

4.3.4 Study Site and Existing Data

This initial study was completed at the site of the Roman town of Silchester (Callewa Atrebatum), which is situated approximately two kilometres to the west of the current day village of Silchester, within the UK. Silchester and the surrounding area sits on a bedrock of London Clay Formation (sandy sedimentary bedrock) which is overlain by the Silchester Gravel Member (sand and gravel of alluvial origin) (BGS 2019).

The site has a long history of settlement, with archaeological evidence confirming that Silchester has been occupied since the Iron Age (Creighton and Fry 2016, Fulford, *et. al.* 2006). It evolved into an expansive Roman town covering approximately 0.4 km² (EDINA DIGIMAP 2019) with various distinguishing features including an amphitheatre and town structure that utilised a grid structure comprising discrete blocks or ‘insulae’ (Creighton and Fry 2016). Occupation continued until its deliberate abandonment in the 6th/ 7th centuries (Fulford, *et. al.* 2006).

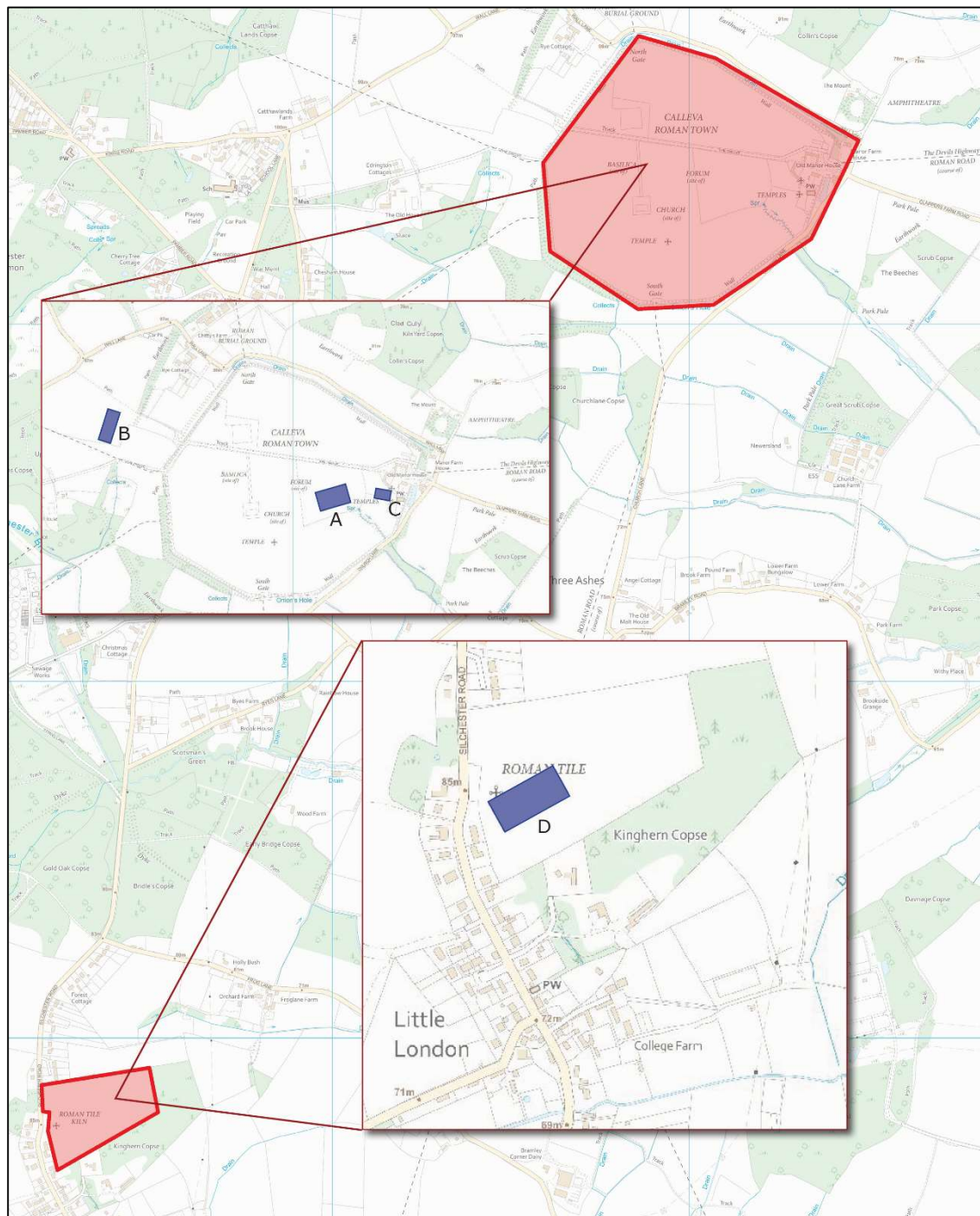
The Silchester site was selected due to the excellent breadth and depth of existing archaeological data available. This derives from extensive programmes of fieldwork and research that have been completed since the early 18th Century and continues to this day. Much of this data has been compiled and is accessible through open sources such as the Britannia Monograph Series (SPRS 2020) and the Archaeological Data Service (ADS 2021). The history of investigation at Silchester is detailed in Creighton and Fry (2016).

The study targeted four specific areas linked to Silchester Roman Town. These sites were selected as they offered a range of contrasting features/ targets and material types, as indicated by previous excavations and geophysical surveys. Each site therefore offered a slightly different condition for the Groundhog® system to test and an opportunity to obtain a range of data across the site. This strategy was adopted with the aim of providing an early indication of efficacy and whether this technique could be pursued in support of archaeological prospection. The targeted survey areas were situated within the following areas:

- Site A – Urban Area (Insula XXXIV)
- Site B – Inhumation/ Cremation Area (Close to the West Gate)
- Site C – Temple Area (Insula XXX)
- Site D – Industrial (Kiln) Area (Little London)

Descriptions for each site can be found in Supplementary Table S4.1 (Section 4.7), with a map showing their location in Figure 4.2.

Chapter 4 – Portable gamma ray spectrometry for archaeological prospection: A preliminary investigation at Silchester Roman Town



Source: Source: Adapted from: EDINA DIGIMAP (2019)

Figure 4.2 – Survey Locations (a, Urban Area; b, Cremation/ Inhumation Site; c, Temple Area, d, Kiln Area) in the context of the site of the Roman town of Calleva Atrebatum (Silchester).

Source: Adapted from: EDINA DIGIMAP (2019)

4.3.5 Methodology

Surveys were undertaken over two days in July 2019, using NUVIA's Groundhog Fusion® system. A manually operated single detector. The detector unit was deployed in both an uncollimated and collimated configuration. As shown in Table S4.1 (Section 4.7 – Supplementary Data), Sites A and D were subject to both collimated and uncollimated surveys within the same defined survey area. This approach was applied to test whether use of a collimator, which ensures the detector only captures radiation from the ground directly beneath it, improves data quality. Particularly when surveying areas likely to yield poor contrasts relative to background levels. The remaining two sites (Sites B and C) were surveyed in an uncollimated configuration only.

Nuvia's Groundhog probes are subject to annual calibration to ensure they are performing as expected and fit for use, limiting the potential for systematic errors. Calibration is completed in accordance with internal procedures HPP357 (Davies 2015) and HPI4214 (Clark 2017). These procedures are based on the National Physics Laboratory's Good Practice Guide 14 (Lee and Burgess 1999). The calibration process measured the detector's responses against background radiation and a 6 kBq Cs-137 check source for a period of 600 seconds each. This confirmed that the detector was operating reliably and within acceptable ranges. The response curve for Cs-137 can be found in Supplementary Figure S4.1 (Section 4.7).

Before the Groundhog® system was deployed on site, a number of preparatory equipment checks were undertaken at the Harwell office in accordance with NUVIA Method Statement 72736/MS/001 (Beddow 2019). Key activities included:

- Ensuring equipment portable appliance test (PAT) labels were present and correct and that dates would not be exceeded in the planned survey period.
- Physical inspection of equipment and cables are in good condition and that batteries are fully charged.
- Functional checks of the individual components of the Groundhog® system to ensure the receiver and detector were operating correctly and that the UMPC was recording the resultant data:

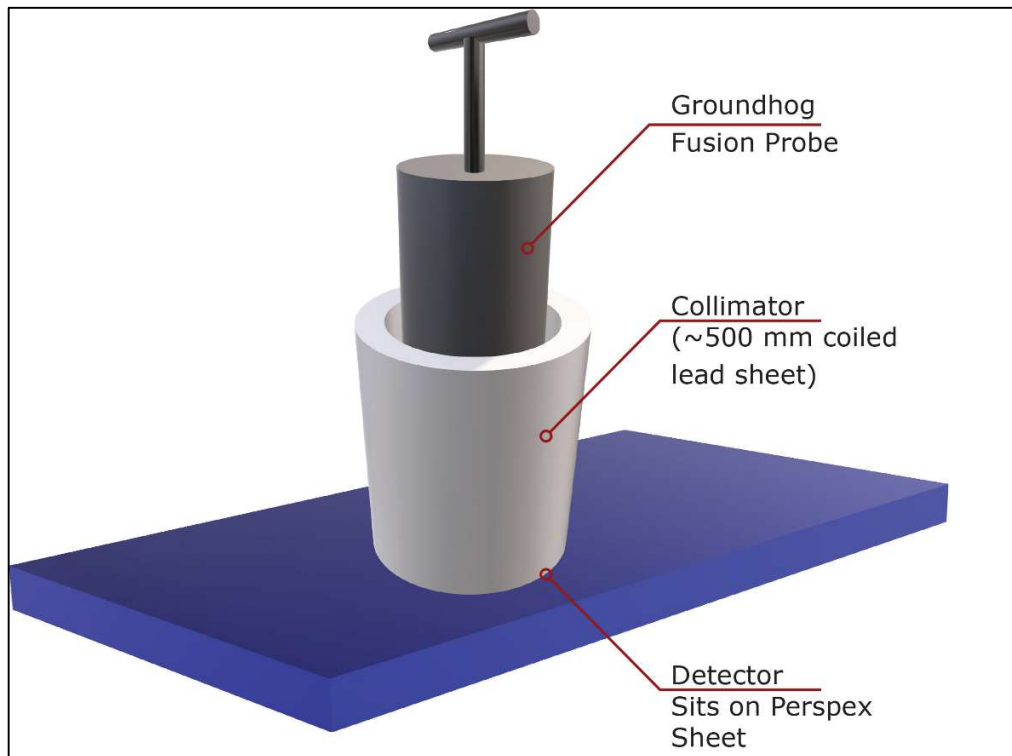
- The UMPC was tested by running the bespoke software and checking that it was operating correctly. Subsequent equipment checks could not be completed until the software was running.
- The radiation detector was subject to a test to ensure the detector was operating correctly. This was achieved by placing a 10 kBq Cs-137 check source approximately 5 cm from the base of the detector unit. This provides confirmation that the detector is working and that the spectrometer is correctly identifying the 662 keV Cs-137 peak.
- The GPS unit was tested outside to confirm that a suitable number of satellites were available and that there was a sufficiently strong signal.

Once at the site, a brief walk-down of each survey area was undertaken. This allowed familiarisation with the site topography and to identification of any features that may limit accessibility – particularly for the collimator trolley. No significant issues were initially identified.

The pre-determined survey areas were delineated using a Leica GS16 GNSS unit. Guide ropes with 1 m transect markers were run across the long edges of the survey area to aid positioning of siting poles used during the survey.

Uncollimated surveys were conducted using the UMPC and the detector/ probe was carried next to the body, arm fully extended to ensure a consistent height of approximately 20 cm between the ground and the detector. The 1 m transects were traversed at an approximate walking speed of 1 m s⁻¹ using the siting poles to ensure the detector remained on target. The UMPC was regularly monitored to ensure a 1 m s⁻¹ walking pace was maintained as far as practicable. For the collimated surveys, a dedicated collimator trolley was used (Figure 4.1b). The collimator comprises a 4.5 cm thick cylinder made from a coiled lead sheet. It has an aperture of ~18 cm, allowing the Fusion probe to slot inside without excessive movement (Figure 4.3). The base of the probe rests on a thin Perspex sheet set into, and flush with, the base of the trolley. This provides the detector with an unobscured view of the ground directly beneath it. The collimator attenuates gamma radiation from the environment, preventing it from reaching the sides of the probe. This gives the detector directional capability to ‘see’ only the radioactivity directly beneath it. By reducing the amount of background radiation captured by the detector, it becomes easier to identify more subtle changes in radioactivity levels (NPL 2014) as might be expected in this

context. The UMPC and GPS unit was also secured inside the collimator trolley. This was then pulled along 1 m transects at the same $\sim 1 \text{ m s}^{-1}$ speed used during the uncollimated surveys.



Source: Personal Image

Figure 4.3 – Scheme diagram showing the Groundhog® detector in its collimated configuration.
Source: Drawn by authors

For each survey area, the Groundhog® Fusion system was set to take one radiation recording per second. This combined with an approximate surveying speed of 1 m s^{-1} facilitated the capture of radiation measurement for each square metre of the survey area. The survey speed is monitored by the Groundhog® system. A visual display on the UMPC which can be monitored by the operator. In addition, an audible alarm will alert the operator if the 1 m s^{-1} speed is exceeded. The regions of interest for this study are those associated with isotopes of potassium, uranium and thorium and their decay products ('daughters').

The captured GPS and radiation data was transferred from the UMPC to a desktop computer for processing. Microsoft Access (v. 16.0.14131.20278) was used to compile the data. Post-processing of the GPS data was undertaken in GrafNav (v. 8.3), supporting improved GPS positioning accuracy. This was supported through the import of time and date matched data from

the Farnborough OS Reference Station (FARB). It was also possible to conduct checks on the completeness of the data. This exercise confirmed that all GPS files were successfully imported and converted to the required format (GNSS to GPB). GPS data quality was excellent across all survey sites, with a general accuracy of <2 cm. Post-processed data was imported to a new project file in ArcGIS (v10.1) as a new layer.

The Groundhog® system recorded both total gamma activity across all energies (expressed as counts per second (cps)) and spectral data (recorded in kilo electron volts (keV)). Both data sets were imported into ArcGIS to facilitate data interrogation and surface radiation mapping. The surface radiation (contour) maps support visualisation of the radiation data, improving the ease with which features or trends can be identified. Spectral data were analysed in ArcGIS using bespoke tool sets developed by NUVA. These are described in Davies, Clark and Adsley (2011). Review of the spectral data confirmed that the radiation measurements at each of the four sites was attributable to naturally occurring isotopes of potassium, uranium and thorium. Potassium was identified directly by the gamma radiation emissions of K-40 (1461 keV). Uranium was identified through the presence of its gamma emitting daughter Bi-214 (1765 keV) and thorium through the presence its daughter Tl-208.

Radiation contour maps were generated for each survey area using interpolated total gamma activity data. Interpolation was achieved using an inverse distance weighting technique with a grid size of 0.5 m and an effective range of 1.5 m. This approach, introduced in a paper by Duggan (1983) uses measured values, in this case total gamma radiation measurements at 1 m spacings, to estimate the gamma radiation levels in the surrounding space (Duggan 1983). It assumes that each datapoint has a local influence that reduces proportionately with distance (ESRI 2022). Whilst this approach 'hides' small gaps in data coverage, it generates continuous, smooth images of the survey area which are easier to interpret. The contour maps were displayed using a multipart graduated colour scale (green to red). To help draw out anomalies within each of the maps, the number of classes within the scale was adjusted to optimise the data divisions applied. Due to the generally low levels of radioactivity present at all sites, data divisions of 4 – 6 cps were most effective at drawing out subtle differences in activity across the sites. The only exception was for the uncollimated measurements for Site D, where data divisions of ~22 cps generated the highest quality images.

Total gamma activity data was also processed to generate count rate frequency distribution graphs for each site. This was achieved by importing the raw data (as comma separated values) from ArcGIS to Microsoft Excel (v 2106) and generating a series of histograms. These could then be used to identify the most frequently occurring count rates and therefore the natural background radiation for each site.

4.3.6 Results

As shown in Table 4.1, an average of 1.05 – 1.74 readings per square metre were recorded at each site, providing a good level of coverage by the Groundhog® system. This facilitated the collection of between 2100 and 8800 measurements per site. The sites with the greatest number of measurements collected (Sites A and D) were those where both collimated and uncollimated surveys were undertaken. The only area where notable gaps in survey data were present was Site A (Urban Area), where some areas were not accessible by collimator trolley. This was attributable to deep ruts generated by farm vehicles and an impassable bed of nettles and brambles. These were not immediately obvious during the initial site walk-round. However, it was still possible to survey the majority of the site, providing a good overview of radiological conditions.

Summary statistics for all four sites is provided in Table 4.1, confirming the total number of measurements taken at each site as well as the minimum, maximum and average total gamma recorded for each site. Further results are discussed on a site by site basis below.

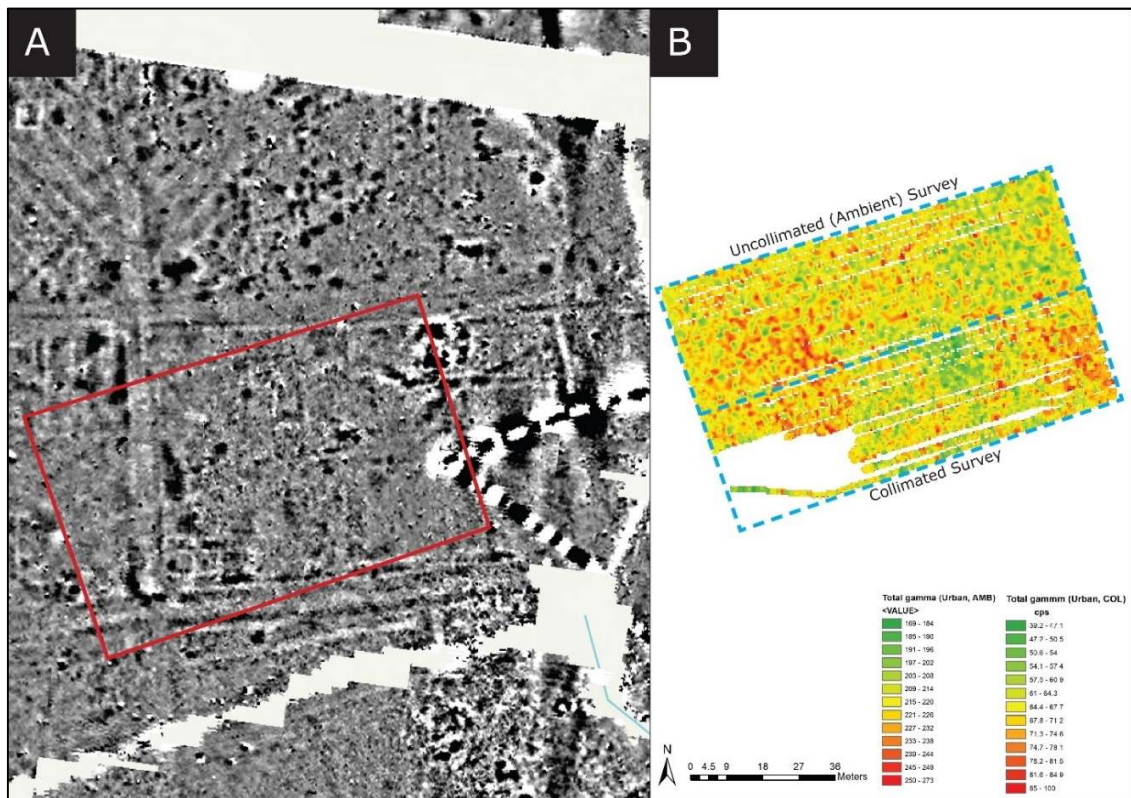
Site A – Urban Area

Both collimated and uncollimated surveys were undertaken at Site A as delineated by the blue dotted lines over the radiation contour map in Figure 4.4. It can be seen that the collimator has significantly reduced the amount of radiation reaching the detector, resulting in much lower total counts overall. The radiation data has been compared against existing fluxgate gradiometer survey data generated by the Silchester Mapping Project, Creighton and Fry (2016) (Figure 4.4a). Within Figure 4.4b, it is possible to see the area that was not fully accessible by the collimator trolley due to the thick covering of foliage and disturbed ground. The figure also shows the site to have low levels of background radioactivity. Mean count rates of 67 cps and 217 cps were recorded for the collimated and uncollimated survey areas respectively (Table 4.1).

Count rate frequency distribution graphs for the uncollimated and collimated survey areas (Figure 4.5a and Figure 4.5b respectively) confirm a normal distribution of activity. The uncollimated data (Figure 4.5b) shows that the most significant part of the frequency distribution, and therefore the background radiation for the site is between 215 – 235 cps. This is towards the lower end of the typical range of 200 – 300 cps observed in the UK (Davies, *et. al.* 2011).

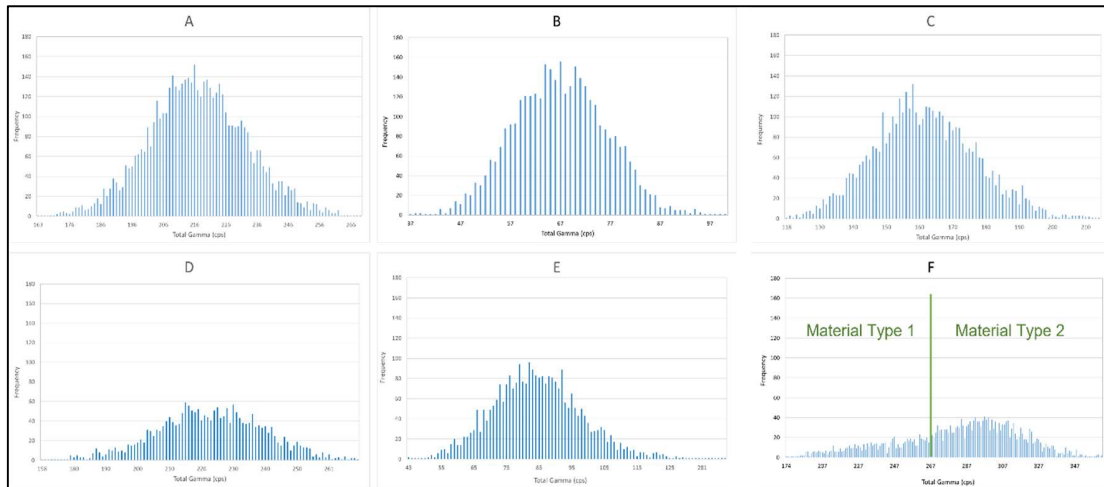
There appears to be no significant difference in data quality between the collimated and uncollimated surveys. In both instances, there are no clear anomalies present that might have been expected due to the presence of clear linear anomalies identified in the fluxgate gradiometry data. This observation is supported by the normal distribution of activity observed in Figure 4.5. Despite a long history of human occupation and disturbance at the site, the normal distribution of activity at within the survey area is not unexpected. This is due to the relatively small area surveyed, the generally homogenous distribution of trace elements (IAEA 2005), and the limited mobility of radionuclides such as thorium and uranium (in its reduced form) in soils (Mahmood and Mohamed 2010, Burns and Finch 1999).

There is an area of slightly elevated activity in the south-east corner of the survey area, as shown in Figure 4.4b. This is broadly in the same area as an anomaly, expected to be a modern feature such as a buried pipe, present in the fluxgate gradiometry data. An area of elevated activity on the west side of the radiological survey broadly aligns with the linear anomaly present in the fluxgate gradiometry data. However, this is not clearly defined and is likely attributable to normal background radiation.



Source: Fluxgate gradiometry source – Creighton and Fry (2016) plus author's primary data

Figure 4.4 – Comparison of fluxgate gradiometry data (+/- 7nT – black high to white low) (a) Against total gamma radiation data (b) Collected at the Urban Area (Site A). Both collimated and uncollimated measurements are presented. Radiation data are displayed in cps. No clear anomalies have been identified. An area of increased activity in the bottom right corner of the survey area may be attributable to a modern feature (buried pipe). An area of elevated activity to the left of the survey area broadly aligns with the cross road. However, due to its distribution, it may be a naturally occurring feature.



Source: Created from primary data

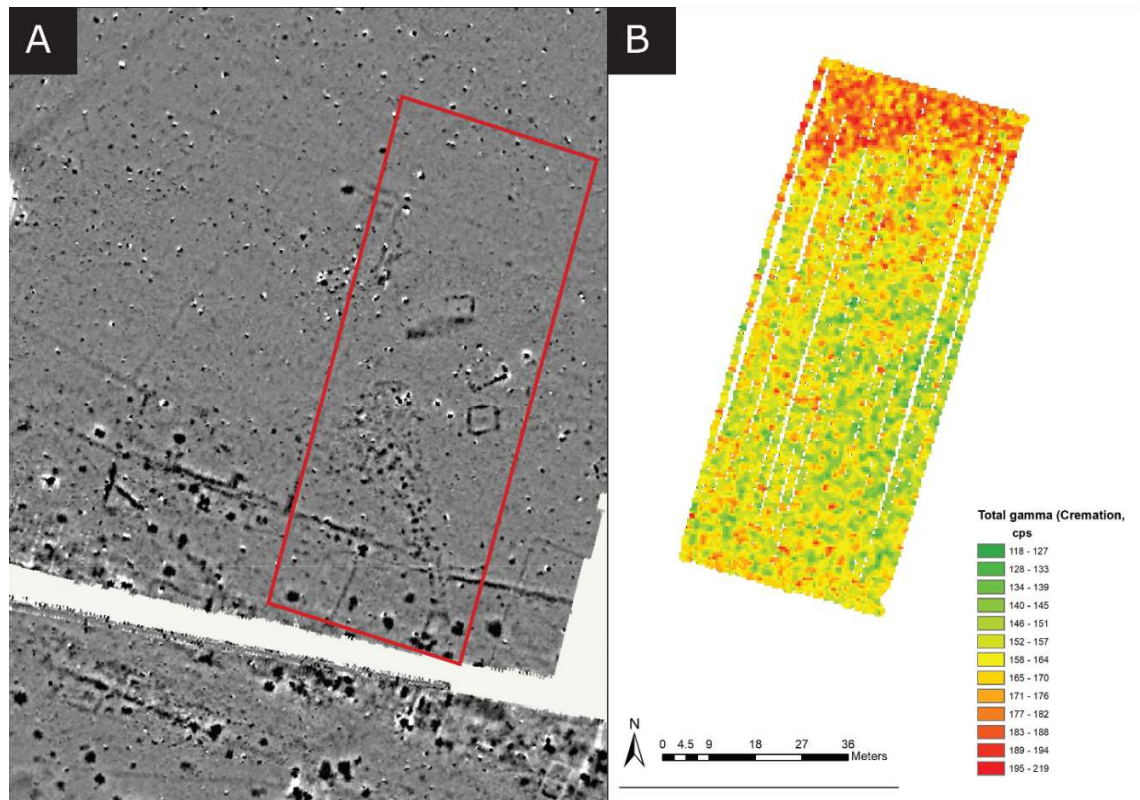
Figure 4.5 – Frequency distribution graphs for Site A (Urban Area), uncollimated (a) and collimated (b); Site B (Cremation/ Inhumation Area) uncollimated (c); Site C (Temple Area), uncollimated (d); and Site D (Kilns Area, uncollimated (e) and collimated (f). Each chart shows a normal distribution of count rates with the exception of the uncollimated data collected for the Kilns area I. This graph shows two distinctive activity distributions indicative of two different material types. This differentiation is likely attributable to the former clay pit (which has since been backfilled) in this area (Figure 4.9 and Figure 4.10).

Site B – Inhumation/ Cremation Area

Figure 4.6 presents the radiation contour map showing gamma radiation survey data for Site B. Only an uncollimated survey was undertaken for this site. As for Site A, this data is compared against existing fluxgate gradiometry data generated as part of the Silchester Mapping Project (Creighton and Fry 2016) (Figure 4.6a). This figure shows that the site contains consistently low background radioactivity across most of the site. A mean value of 161 cps was recorded, which is lower than the normal range observed for the UK. This is supported by the count rate frequency graph for this site (Figure 4.5c), which shows the highest frequency of measurements are in the 155 – 165 range. The cause of this is unclear. A contributing factor may be the soil type here. Soilscape data (MAGIC Map 2021) suggest that the soil is characterised by freely draining, slightly acid loamy soil, which is also the case for Sites A and C. In low pH conditions, radionuclides exhibit increased solubility and are therefore more readily transported from site (IAEA 2003).

An area of elevated activity is observed at the northern edge of the survey area. However, this does not correlate with any geophysical anomalies and is therefore likely naturally occurring. The lack of anomalies present in the radiation data contrasts with the fluxgate gradiometry data,

which identified multiple anomalies of interest. It does however support the data presented in the count rate frequency distribution graph (Figure 4.5c) which shows a normal distribution.



Source: Fluxgate gradiometry source – Creighton and Fry (2016) plus author's primary data

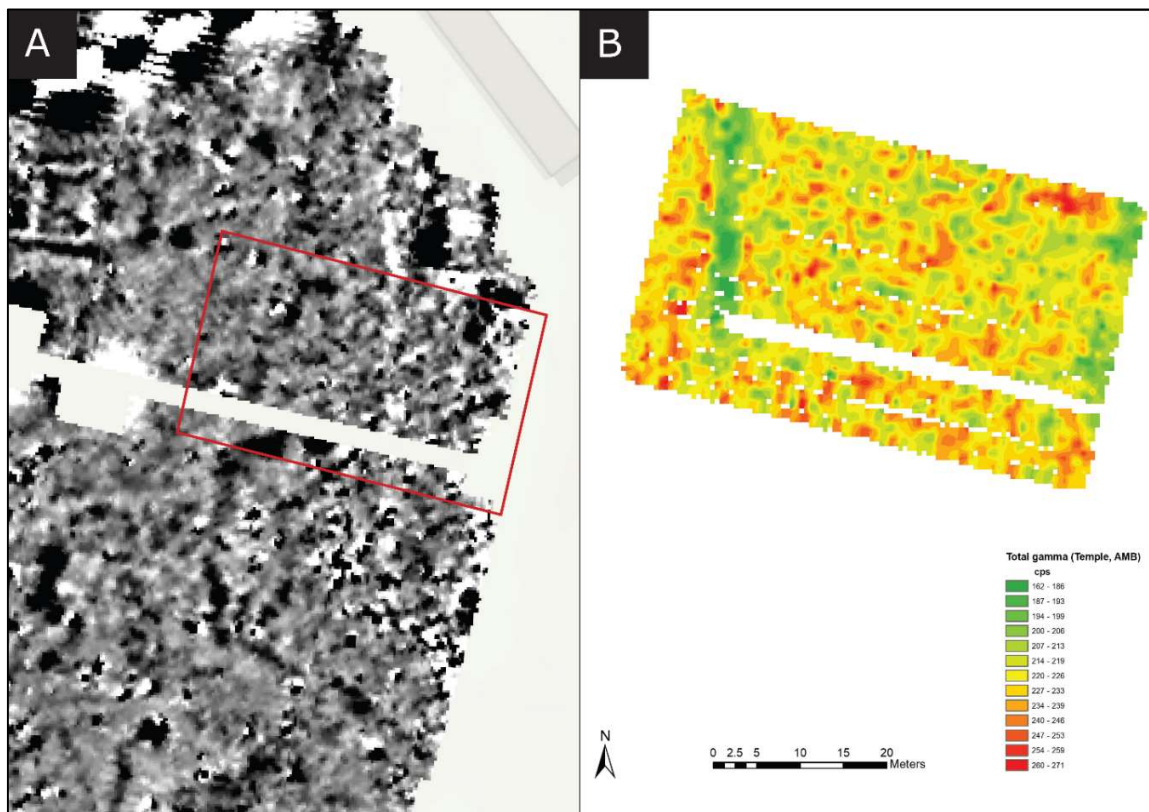
Figure 4.6 – Comparison of fluxgate gradiometry data (+/- 5nT – black high to white low) (a) Against total gamma radiation data (b) Collected at the Cremation/ Inhumation Area (Site B). Uncollimated survey data are displayed in cps. No clear anomalies are observable. The area of elevated activity at the top of the survey area is expected to be naturally occurring.

Site C – Temple Area

The gamma radiation survey data generated from an uncollimated Groundhog® survey of Site C is presented in Figure 4.7b. This is compared against the existing fluxgate gradiometry data collected as part of the Silchester Mapping Project (Creighton and Fry 2016) (Figure 4.7a). The small amount of missing radiation survey data visible within this figure is attributable to an existing field boundary fence.

Figure 4.7b shows a very clear linear anomaly in the gamma radiation data, identified as an area of depleted background radiation with a minimum reading of 161-186 cps; lower than the average of 223 cps recorded for that site. This anomaly aligns perfectly with a linear feature; a Temenos wall that bounds the temple complex, identified in previous work by Fulford, *et. al.* (2018). Although a

clear anomaly, it is not sufficient in scale to skew the count rate frequency distribution graph which shows a normal distribution for the whole site (Figure 4.5d). This figure shows the most frequent count rates are in the range of 215 – 230 cps. This is, as previously observed, consistent with the expected radiation background measurements for a site situated in south east England.



Source: Fluxgate gradiometry source – Creighton and Fry (2016) plus author's primary data
Figure 4.7 – Comparison of fluxgate gradiometry data (+/- 5nT – black high to white low) (a) Against total gamma radiation data (b) Collected at the Temple Area (Site C). Uncollimated survey data are displayed in cps. A clear linear anomaly of depleted radioactivity can be seen in the left-hand side of the survey area. This aligns with an anomaly visible in the fluxgate gradiometry data, which is known to be a Temenos wall.

Site D – Industrial/ Kiln Area

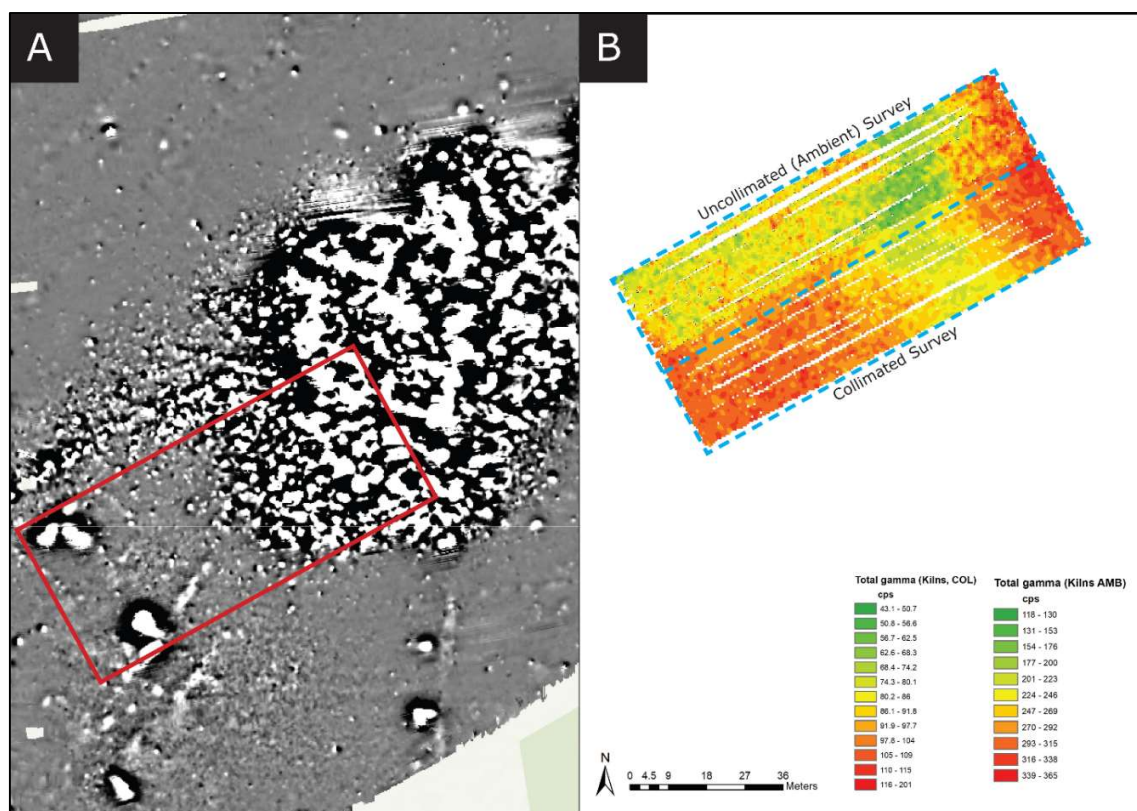
As per Site A, both collimated and uncollimated survey methods were applied at Site D. The two areas are clearly delineated in Figure 4.8. As observed for Site A, the collimator has recorded significantly lower total counts. This figure presents the radiation contour map showing the total gamma radiation measured across Site D. This has been compared against the existing caesium magnetometry data collected as part of the Silchester Environs Project (Linford, Linford and Payne 2016) as shown in Figure 4.8a. Relative to the other survey areas, Site D appears to have higher levels of background radioactivity with an uncollimated mean of 282 cps and collimated mean of 85 cps. This is the only site to have a different soil type, with the area characterised by ‘slightly acid loamy and clayey soils with impeded drainage’ (MAGIC Map 2021). The clay component within the soil here may account for the elevated background activity observed here. Figure 4.8b reveals a clear anomaly, a large area of depleted activity, to the north-east of the survey area. A possible ‘P’ shaped anomaly can be seen towards the east of the site which is in a similar location as one of the kilns identified in the geophysics data. However, there is no significant difference between this ‘anomaly’ and background radiation, and is therefore more likely to be attributable to naturally occurring activity.

The larger and most distinctive anomaly in the north-east section of the image shows a well-defined area of lower background radiation, typically in the region of 43 – 51 cps for the collimated survey area and 177 – 200 cps for the uncollimated side. When compared with the findings of the caesium magnetometry survey for the same area, it can be seen that this area of depletion closely aligns with a well-defined anomaly present in the caesium magnetometry data. This anomaly can be attributed to an infilled modern clay pit. An Ordnance Survey map from 1912 (Ordnance Survey 1912) shown in Figure 4.9 confirms the presence and location of the pit at Site D. This figure shows where the footprint of the pit and the Groundhog® survey area overlap and has been detected. An aerial photo taken later in 1947 (Figure 4.10) shows the pit as infilled with a well-established stand of trees. This suggests the pit was infilled decades before, with an unknown material of sufficiently different composition to the surrounding material, as to be detectable through both caesium magnetometry and radiation monitoring techniques. Modern satellite images (as exemplified in Figure 4.10b) show that these trees are no longer present, and hence an unimpeded Groundhog® survey of the area was possible. The satellite image reveals visible patterns/ colour variations in the grass cover, further suggesting the pit was backfilled with

imported material and/ or different soil types. The count rate frequency distribution graphs for the uncollimated and collimated survey data are presented in Figure 4.5e and Figure 4.5f respectively. Review of the uncollimated data (Figure 4.5e) shows a normal distribution and that the most common count rates are in the region of 287 – 307 cps. As for other survey areas discussed here, this is consistent with the natural background radiation for this region. It is however noted that there is a second distinctive count rate distribution on the left hand side of Figure 4.5f, suggesting the presence of a second soil type or other infill material at the site.

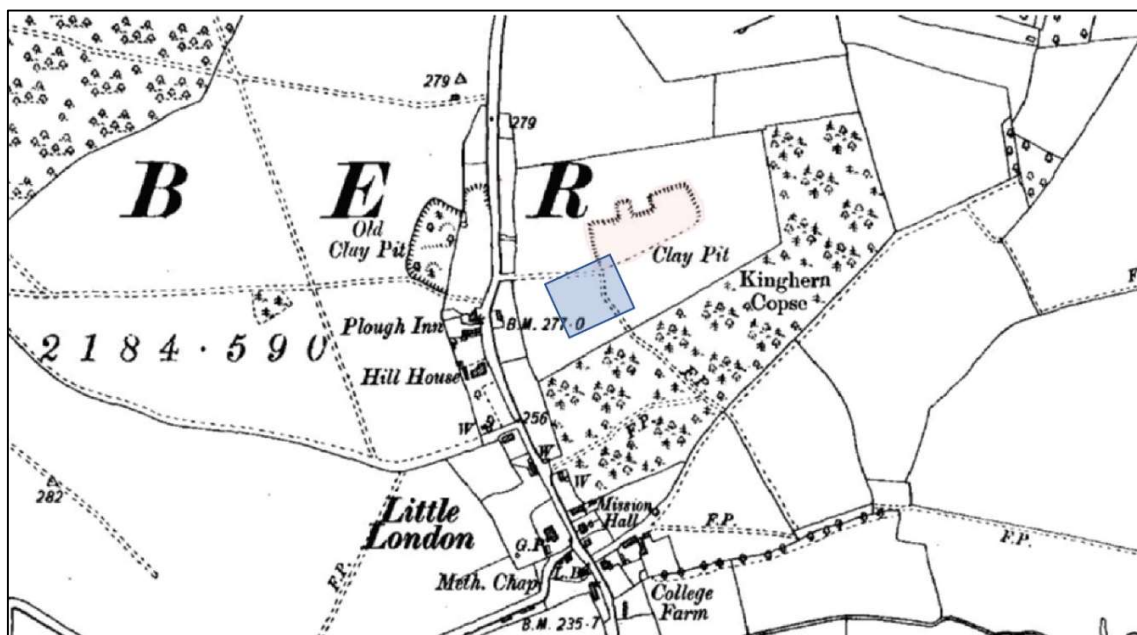
Table 4.1 – Summary survey statistics for Sites A – D, showing the minimum, maximum and average total gamma (counts per second) and total number of measurements taken.

Parameter	Site					
	Site A (Urban) Uncollimated	Site A (Urban) Collimated	Site B (Inhumation/ Cremation)	Site C (Temple)	Site D (Kiln) Uncollimated	Site D (Kiln) Collimated
No. Measurements	5255	3470	4189	2136	2678	2848
Average No. Measurements per m ²	1.31	1.74	1.05	1.42	1.07	1.42
Minimum Total γ (cps)	163	37	118	158	174	43
Maximum Total γ (cps)	274	102	220	274	367	334
Mean Total γ (cps)	217	67	161	223	282	85
Standard Deviation	15.61	9.30	15.24	16.82	34.25	18.16



Source : Caesium magnetometry source – Linford et. al. (2016) plus author's primary data

Figure 4.8 – Comparison of caesium magnetometry data (+/- 7nT – black high to white low) (a) Against total gamma radiation data (b) Collected at the Kiln Area (Site D). Both collimated and uncollimated survey data are presented and displayed in cps. An area of depleted radioactivity in the upper half of the Groundhog® survey area aligns with the clear anomaly present in the geophysics data. A 'P'-shaped anomaly in the bottom left corner of the survey area broadly aligns with one of the kilns, but is assumed to be naturally occurring.



Source: Adapted from Ordnance Survey (1912)

Figure 4.9 – Ordnance Survey map from 1912 showing where the kiln survey area (blue square) overlaps the site of a disused modern claypit (shaded light red).



Sources: Adapted images from *Historic England* (2020), *EDINA* (2018) and *Linford et. al.* (2016).

Figure 4.10 – (a) 1947 aerial photo showing the sight of the Little London claypit (circled in red) infilled and covered with a well-established tree stand, (b) Modern satellite image of the same site showing absence of the tree stand and revealing a distinct discolouration of the grass covering the former claypit (circled in red), (c) Modern satellite image overlaid with Caesium Magnetometer data revealing the Roman kilns, modern clay pit (circled in red) and the area subject to Groundhog survey (red square).

4.3.7 Discussion

The sites selected for gamma radiation surveying offered four unique conditions for the Groundhog® system to test. The data has shown varying levels of success for the efficacy of this technique for the prospection of potential archaeological features of interest.

Site B (Inhumation/ Cremation Area) appears to offer the least suitable conditions for this technique in its current configuration, with no radiological anomalies detected. The lack of contrast between the interred remains and surrounding substrate may be attributable to insufficient accumulation of naturally occurring radionuclides through the cremation process, or through insufficient accumulation of radioisotopes such as U-238 through the diagenesis of bone as explored in studies such as those by Millard and Hedges (1995), Pike, Hedges and van Calsteren (2002), Farmer, Kathren and Christensen (2008), Cid, *et. al.* (2014), and Grimstead, Clark and Rezac (2017). Even if some accumulation had occurred, it is unlikely to be in a sufficient concentration as to be detectable against background radiation. Finally, the spatial resolution of the surveys (one measurement per square metre) may be insufficient to delineate the small targets present at this site. This can be attributed to the interpolated values between each of the data points obscuring any subtle variations present. Re-surveying the area at a much higher spatial resolution may help overcome this challenge and will be explored during future site surveys with the Groundhog® system. Future work planned at the site will also involve the non-destructive analysis of samples of interred remains and surrounding substrate, via high resolution gamma spectrometry techniques, for detailed comparison. It is anticipated that this will provide a better insight into why no clear anomalies were originally detected.

The results from the survey of Site A (Urban Area) are unclear. When planning this site investigation, it was anticipated that of all the sites surveyed, the urban area would yield the best data (if any). This is because previous geophysical surveys and intrusive investigations have confirmed the presence of large linear structures such as roads and the remains of buildings. It was believed that the construction materials used in these structures would have a sufficiently different radioisotope composition (particularly if made from clays) as to be detectable by the Groundhog® system. However, if the construction material was sourced locally, then concentration of the construction material alone may be insufficient to generate a sufficient contrast. A similar issue was experienced in a study conducted by Sanjurjo-Sanchez *et. al* (2017).

Here, radiation surveys were unable to detect any significant differences in the ratios of naturally occurring radionuclides in the remains of Spanish settlements dating back to the late Roman/ Medieval period and surrounding soils. This was attributed to the use of local materials in construction and the unusually low concentrations of naturally occurring radioactivity in the area (Sanjurjo-Sanchez *et. al.* 2017). For this study, it is anticipated that increasing the spatial resolution of the radiation measurements will help confirm whether the area of elevated activity on the west side of the site is naturally occurring or attributable to the known feature present in that area. It may be possible to provide better definition for the area of elevated activity that broadly aligns with the buried pipe. As for Site B, the intent is to take samples from the targets and surrounding substrate for non-destructive analysis to better understand why targets, clearly visible in the fluxgate gradiometer data could not be differentiated by Groundhog®.

The results from Sites C and D (Temple and Kiln Areas respectively) are more promising. Clearly defined anomalies are visible that correlate closely with features identified within the existing fluxgate gradiometer and caesium magnetometer data. The cause of the depletion in radioactivity observed for the remains of the Temenos wall in Site C is not known. However, it is likely that the wall was built using materials with notably lower concentrations of naturally occurring radionuclides relative to the surrounding soil. Sampling and analysis of soils and any structural material retrieved from the area would help confirm this and will be considered as part of future work. The clearest anomaly associated with the Kiln Area is a significant feature that has been backfilled with imported material with a sufficiently different radioisotope composition as to generate a clear contrast in the survey data.

It is recognised that the large anomaly observed at the Kiln Area is attributable to a modern feature; an in-filled clay pit as identified in Figures 4.9 and 4.10. However, this is still a promising result. It confirms that the presence of material with a sufficiently different composition of naturally occurring radionuclides can be detected if present in a sufficient concentration, as one might expect to find with features such as building foundations, roads or stone monoliths. Whilst it was initially thought that the small 'P' shaped anomaly might have been attributed to a kiln, further interrogation of the data suggests that it is a chance occurrence attributable to the interpolation undertaken on the data. There are two measurements in this localised area in the 116 – 201 cps (collimated) range, contrasting against the lower surrounding measurements in the

4 – 86 cps range. The P shaped anomaly is therefore more likely a function of the interpolation undertaken which is capturing and exaggerating the two peak measurements. As for the other sites, re-surveying this site, targeting the known features at a much higher spatial resolution will help address this uncertainty.

4.3.8 Conclusions

This preliminary study into the efficacy of using portable radiation survey systems for archaeological prospection has been moderately successful. Although some sites have not yielded positive results, others have clearly identified anomalies that have also been detected using traditional geophysical techniques. The use of gamma radiation surveying may therefore be a useful additional technique in the 'geophysical toolbox'.

The results of this study have raised many questions regarding the cause of the observed anomalies at some sites, and why the technique was less effective in others; particularly at Site A where the best results were expected. Further work is required to obtain additional data to address these questions and generate more robust conclusions. There is therefore an intent to revisit the Silchester survey sites to test different configurations and surveying strategies. An area of focus will be increasing spatial resolution of the surveys. The method applied for this study aimed to capture one radiation measurement every square metre, as is applied within the nuclear industry. Due to the size of the targets and limited radiation contrast of targets to surrounding background radiation, this resolution is now believed to be too low. As observed for Site D (Kilns), the lower resolution can result in possibly misleading results due to level of interpolation required to smooth the data. By increasing resolution to one measurement per 0.5 m, or ideally 0.25 m, it is expected that finer interpolation can be achieved by introducing three times as many measurements, improving data quality. Such an approach is expected to draw out smaller anomalies that may currently be obscured. The collection of much larger data sets via a vehicle-mounted system is planned during future fieldwork.

Alternative methods of analysing the data will be explored. One such method proposed is the analysis of Th/K and Th/U ratios within the data. This technique has been used successfully by Ruffell, *et. al.* (2006), to more clearly define man-made subsurface structures present in gamma

radiation survey data. The ratios of Th/K and Th/U generated clearer images relative to total count or individual isotope measurements Ruffell, *et. al.* (2006).

Finally, sampling and analysis of soil and artefacts excavated from the sites will be undertaken. This will help gain a valuable insight into their radiochemical composition and possible reasons behind the varying levels of success at the different sites.

It is envisaged that the lessons learned from repeating the investigations at Silchester will support the development of an optimised surveying strategy for application at other sites of archaeological interest. This in turn will help establish the efficacy of gamma surveying as a complimentary tool within the current array of geophysical techniques.

4.3.9 References

Please see Section 4.6

4.4 Paper Impact

Specific details regarding the number of reads of this paper is not provided by Archaeological Prospection. However, the following metrics, 14th July 2024, are available for this paper via Altmetric:

- This paper has an ‘attention score’ of 18 – in the top 25% of all research outputs scored by Altmetric.
- Of 204 outputs from Archaeological Prospection tracked by Altmetric, this paper ranks at #12.
- Out of the 5 outputs of similar age from Archaeological Prospection, this paper ranked #1.

By July 2024, data obtained from Wiley confirmed that the paper had been downloaded a total of 1360 times. This was later followed by a certificate confirming that the paper was one of the most downloaded papers of 2022:



WILEY

Top Downloaded Article

Congratulations to:



Victoria Robinson

Whose paper was one of the most downloaded* during its first 12 months of publication in:

ARCHAEOLOGICAL PROSPECTION

Portable gamma ray spectrometry for archaeological prospection: A preliminary investigation at Silchester Roman Town

**Among work published in an issue between 1 January 2022 – 31 December 2022.*

This research has also experienced notable media interest, with a number of press releases published. This includes the following organisations/ institutions:

- Archaeology
 - <https://www.archaeology.org/news/10446-220407-gamma-ray-spectrometer>
- 24HTECH
 - <https://24htech.asia/gamma-ray-detector-helps-archaeologists-honey-sweetens-neuromorphic-computing-s909302.html>
- EurekAlert!
 - <https://www.eurekalert.org/news-releases/948757>
- Spectroscopy Europe
 - [Press Release – https://www.spectroscopyeurope.com/news/gamma-ray-spectrometers-can-aid-archaeological-discoveries](https://www.spectroscopyeurope.com/news/gamma-ray-spectrometers-can-aid-archaeological-discoveries)

Chapter 4 – Portable gamma ray spectrometry for archaeological prospection: A preliminary investigation at Silchester Roman Town

- [Feature Article – https://www.spectroscopyeurope.com/article/atomic-archaeology-using-portable-gamma-surveying-techniques-identify-buried-archaeological](https://www.spectroscopyeurope.com/article/atomic-archaeology-using-portable-gamma-surveying-techniques-identify-buried-archaeological)

The article published in Spectroscopy Europe was ranked number 18 in the publication's 'Top 22 Articles of 2022' as shown below.



Finally, following this paper, the paper authors were invited to participate in a podcast which can be accessed via the following link:

- <https://physicsworld.com/a/radiation-detectors-could-help-find-ancient-buildings-and-dinosaur-bones/>

4.5 Conclusions and Next Steps

This preliminary study yielded some promising results. The data from the Temple Area in particular has demonstrated that Groundhog is capable of delineating known buried features. The study has also highlighted some key areas for improvement in the survey methodology for implementation in subsequent surveys. This includes for example:

- Exploring the use of vehicle-mounted systems to increase the area that can reasonably be surveyed and number of measurements that can be collected within an acceptable time period.
- Completing Groundhog surveys over similar, if not the same targets to test the repeatability of the technique.
- Exploring the use of alternative software tools and methods for processing the Groundhog data, to see whether the quality of the visualisations can be improved.

In the next chapter, the impact of implementing these recommendations is tested. Building on the findings of the first study, a new area within Silchester's boundary walls is surveyed. Surveys are focussed on analogous target types, including road structures, ditches and a circular temple feature. New target types, including a water pipe and small buildings were also covered within the survey area. By surveying analogous targets, the repeatability of the method is tested.

Drawing on lessons learned from this preliminary study, a vehicle-mounted system is used to survey the new target types. This configuration utilises three gamma detectors concurrently, expanding the survey area with each pass thereby showcasing the technique's scalability. An alternative software tool to ArcGIS – Geoplot is used to generate the visualisations. Different methods of data processing, including the application of filters and creating visualisations using individual energy windows is explored. By testing these different methods, the potential for improving the quality of the resultant gamma radiation distribution maps is explored.

4.6 References

- ADS (2021) Archaeological Data Service, www.archaeologydataservice.ac.uk, <http://doi.org/10.17616/R3MW23>, Accessed 15/07/2021
- Aliyev, C. (2004) NORM in Building Materials, in: IAEA (2004) Naturally Occurring Radioactive Materials (NORM IV): Proceedings of an International Conference held in Szczyrk Poland, 17 – 21 May 2004, IAEA-TECDOC-1472
- Aziz, A. Attia, T. McNamara, L. and Friedman, R. (2018) Application of Gamma-ray Spectrometry in Discovering the Granitic Monument of King Pepi I: A Case Study from Hierakonpolis, Aswan, Egypt, *Pure and Applied Geophysics*, Published Online 09/11/2018, DOI: 10.1007/s00024-018-2036-1
- Barker, P. (1993) (Third Edition) *Techniques of Archaeological Excavation*, Routledge, Taylor and Francis Group, Oxfordshire UK
- Beddow (2019) Method Statement – Groundhog® Radiation Surveys of Land and Buildings using Portable and Vehicle Mounted Systems, 72736/MS/001, Issue 2, Last Updated – February 2019, Internal Report for NUVIA Limited UNPUBLISHED
- Bezuidenhout, J. (2012) Mapping of historical human activities in the Saldanha Bay Military Area, *Scientia Militaria*, **40** (2): 89 – 101
- BGS (2019) *Geology of Britain Viewer: Silchester, Hampshire*. <http://mapapps.bgs.ac.uk/geologyofbritain/home.html>, British Geological Society, Accessed 29/06/2019
- Burns, P.C. and Finch, R. (1999) *Uranium: Mineralogy, Geochemistry and the Environment*, Reviews in Mineralogy and Geochemistry, Volume 38, Mineralogical Society of America, USA
- Cardarelli, E. and De Filippo, G. (2009) Integrated geophysical methods for the characterisation of an archaeological site (Massenzio Basilica) – Roman Forum, Rome, Italy, *Journal of Applied Physics*, **68**: 508 – 521, <https://doi.org/10.1016/j.appgeo.2009.02.009>
- Cid, A.S. Anjos, R.M. Zamboni, C.B. Cardoso, R. Muniz, M. Corona, A. Valladares, D.L. Kovacs, L. Macario, K. Perea, D. Goso, C. Velasco, H. (2014) Na, K, Ca, Mg, and U-Series in fossil bone and the proposal of a radial diffusion-adsorption model of uranium uptake. *Journal of Environmental Radioactivity*, **136**: 131 – 139, <https://doi.org/10.1016/j.envrad.2014.05.018>
- Clark, R. (2017) Groundhog Fusion Calibration – Nuvia Health Physics Instruction HPI4214, Issue A, June 2017, Internal Report for NUVIA Limited UNPUBLISHED
- Columbero, C. Elia, D. Meirano, V. and Sambuelli, L. (2020) Magnetic and radar surveys at Locri Epizephyrii: A comparison between expectations from geophysical prospecting and actual archaeological findings, *Journal of Cultural Heritage*, **42**: 147 – 157, DOI: <https://doi.org/10.1016/j.culher.2019.06.012>

Creighton, J. and Fry, R. (2016) *Silchester: changing visions of a Roman town: integrating geophysics and archaeology: the results of the Silchester mapping project, 2005 – 10*, Britannia monograph series; no. 28, Society for the Promotion of Roman Studies, ISBN: 9780907764427, pp:486

Davies, M. (2015) Health Physics Procedure HPP357 – Calibration of Groundhog Detectors, Issue A, September 2015, Internal Report for NUVIA Limited UNPUBLISHED

Davies, M. (2017) Groundhog® Data Management Manual, HPM173, Issue B, Last Updated May 2017, Internal Report for NUVIA Limited UNPUBLISHED

Davies, M. Clark, R. and Adsley, I. (2011) High-Density Gamma Radiation Spectrometry Surveys of Contaminated Land, Proceedings of the 14th International Conference on Environmental Remediation and Radioactive Waste Management, September 25 – 29, Reims, France

Dick, H.C. Pringle, J.K. Sloane, B. Carver, J. Wisruewski, K.D. Haffenden, A. Porter, S. Roberts, D. and Cassidy, N.J. (2015) Detection and Characterisation of Black Death burials by multi-proxy geophysical methods, *Journal of Archaeological Science*, 59: 132 – 141, DOI: <https://doi.org/10.1016/j.jas.2015.04.010>

Duggan, F. (1983) A non-linear empirical prescription for simultaneously interpolating and smoothing contours over an irregular grid, *Computer Methods in Applied Mechanics and Engineering*, 44: 119 – 125, DOI: [https://doi.org/10.1016/0045-78\(84\)90123-3](https://doi.org/10.1016/0045-78(84)90123-3)

EDINA (2018) Aerial Photo of Kiln Area, High Resolution (25 cm) Vertical Aerial Imagery [JPEG Geospatial Data], Scale 1:500, Using EDINA Aerial Digimap Service, <https://digimap.edina.ac.uk>, Last Updated 29th October 2018, Accessed on 30th October 2020

EDINA (2019) Ordnance Survey of Silchester, Colour Raster (TIFF Geospatial Data), 1:25,000 Scale, Using EDINA Digimap Ordnance Survey Service, <https://digimap.edina.ac.uk>, Last Updated 19th February 2019, Accessed 19th August 2019

ESRI (2022) ArcGIS Pro: How inverse distance weighted interpolation works, <https://pro.arcgis.com/en/pro-app/latest/help/analysis/geostatistical-analyst/how-inverse-distance-weighted-interpolation-works.htm>, Accessed 14th January 2022

Farmer, N.C. Kathren, R.L. and Christensen, C. (2008) Radioactivity in Fossils at the Hagerman Fossil Beds National Monument, *Journal of Environmental Radioactivity*, 99: 1355 – 1359, DOI: 10.1016/j.jenvrad.2008.02.004

Fulford, M. Clarke, A. and Eckardt, H. (2006) Life and Labour in Late Roman Silchester: Excavations in Insula IX Since 1997, *Britannia Monograph Series*, Volume 22, Pp:638 (280 – 281), ISBN: 9780907764335

Fulford, M. Pankhurst, N. Wheeler, D. and Machin, S. (2017) *The Silchester Environs Project: The Roman Tilery and Industry at Little London*, Pamber 2017, The University of Reading Department of Archaeology, Pp: 9

Fulford, M. Clarke, A. Durham, E. Fry, R. Machin, S. Pankhurst, N. and Wheeler, D. (2018) Silchester Roman Town – The Baths 2018, The University of Reading, Department of Archaeology, Pp: 9

Gaffney, C. and Gaffney, V. (2010) Chapter 10 – Through an Imperfect Filter: Geophysical Techniques and the Management of Archaeological Heritage, in: Cowley, D.C. (2010) (Editor) Remote Sensing for Archaeological Heritage Management, EAC Occasional Paper No. 5, Europae Archaeologiae Consilium, pp 117 – 127

Gaffney, C. and Gater, J. (2003) Revealing the Buried Past: Geophysics for Archaeologists, Tempus Publishing Ltd, Gloucestershire UK.

Grimstead, D.N. Clark, A.E. and Rezac, A. (2017) Uranium and Vanadium Concentrations as a Trace Element Method for Identifying Diagenetically Altered Bone in the Inorganic Phase, Journal of Archaeological Method and Theory, published online on 18th September 2017, DOI: 10.1007/s10816-017-9353-z

Halgedahl, S.L. Jarrard, R.D. Brett, C.E. and Allison, P.A. (2009) Geophysical and Geological Signatures of Relative Sea Level Change in the Upper Wheeler Formation, Drum Mountains, West-Central Utah: A Perspective into Exceptional Preservation of Fossils, Palaeogeography, Palaeoclimatology, Palaeoecology, 277: 34 – 56, <https://doi.org/10.1016/j.palaeo.2009.02.011>

Historic England (2020) Aerial Photo of Kingham Copse and Environs, Little London, 1947. Photo Reference: EAW011004, www.britainfromabove.org.uk/image/EAW011004, Accessed 31st October 2020

IAEA (1998) Characterization of Radioactively Contaminated Sites for Remediation Purposes, IAEA-TECDOC-1017, International Atomic Energy Agency (IAEA), Vienna, May 1998

IAEA (2003) Extent of Environmental Contamination by Naturally Occurring Radioactive Material (NORM) and Technological Options for Mitigation, Technical Report Series No. 419, International Atomic Energy Agency, Vienna

IAEA (2005) Natural activity concentrations and fluxes as indicators for the safety assessment of radioactive waste disposal: Results of a coordinated research project, IAEA-TECDOC-1464, October 2005

IAEA (2013) Management of NORM Residues, IAEA-TECDOC-1712, International Atomic Energy Agency, Vienna

Kern, E.M. (2020) Archaeology enters the ‘atomic age’: a short history of radiocarbon, 1946 – 1960, The British Journal for the History of Science, 53 (12): 207 – 227, DOI: 10.1017/S0007087420000011

Kozhevnikov, N.O. Kharinsky, A.V. and Snopkov, S.V. (2018) Geophysical prospection and archaeological excavation of ancient iron smelting sites in the Barun-Khal valley on the western shore of Lake Baikal (Olkhon Region, Siberia), Archaeological Prospection, 2018: 1 – 17, <https://doi.org/10.1002/arp.1727>

Lee, C.J. and Burgess, P.H. (1999) Good Practice Guide 14, The Examination, Testing and Calibration of Portable Radiation Protection Instruments, National Physics Laboratory, Issue 2, First Issued – 1999, Updated – 2014

Linford, N. Linford, P. and Payne, A. (2016) Silchester Environs Project, Little London Roman Tiler, Pamper, Hampshire, Report on geophysical survey, July 2015, Research Report Series no. 41-2016, NGR: SU 6226 5971, ISSN: 2059-4453 (Online), Historic England

MAGIC Map (2021) Silchester Soilscape, Map Produced by Magic on 27th March 2021 using Ordnance Survey Projection OSGB36, 1:80,000 Grid Ref.: SU46076249, and Soilscape data from National Soil Resources Institute (Polygons showing 27 classes of soil – last updated 01/01/2005)

Mahmood, Z.U.W and Mohamed, C.A.R. (2010) Thorium in: Atwood, D.A. (Editor) (2010) Radionuclides in the Environment, pp: 247 – 255, John Wiley and Sons, Oxfordshire UK

Millard, A.R. and Hedges, R.E.M. (1995) The Role of the Environment in Uranium Uptake by Buried Bone, *Journal of Archaeological Science*, **22**: 239 – 250, <https://doi.org/10.1006/jasc.1995.0025>

Milsom, J. and Eriksen, A. (2011) The Geological Field Guide Series: Field Geophysics, Fourth Edition, pp: 1 – 32, Wiley-Blackwell, New Jersey USA

Moussa, M. (2001) Gamma-ray spectrometry: a new tool for exploring archaeological sites; a case study from East Sinai, Egypt, *Journal of Applied Geophysics*, **48**: 137 – 142, DOI: [https://doi.org/10.1016/S0926-9851\(01\)00077-5](https://doi.org/10.1016/S0926-9851(01)00077-5)

Nash, D. Jake, T. Ciborowski, R. Ulyyott, J. Pearson, M. Darvill, T. Greaney, S. Maniatis, G. and Whitaker, K. (2020) Origins of the Sarsen Megaliths at Stonehenge, *Science Advances*, **6** (31), DOI: 10.1126/sciadv.abc0133

NPL (2014) Good Practice Guide No. 30 – Practical Radiation Monitoring, Issue 2, National Physical Laboratory, ISSN: 1368-6550

NUVIA (2019) Calibration Certificate for Groundhog Detector GN08, Completed June 2019, Internal Report for NUVIA Limited UNPUBLISHED

NUVIA (2021) NUVIA UK Products: Groundhog®, www.nuvia.co.uk/product/Groundhog®, Accessed 21/02/2021

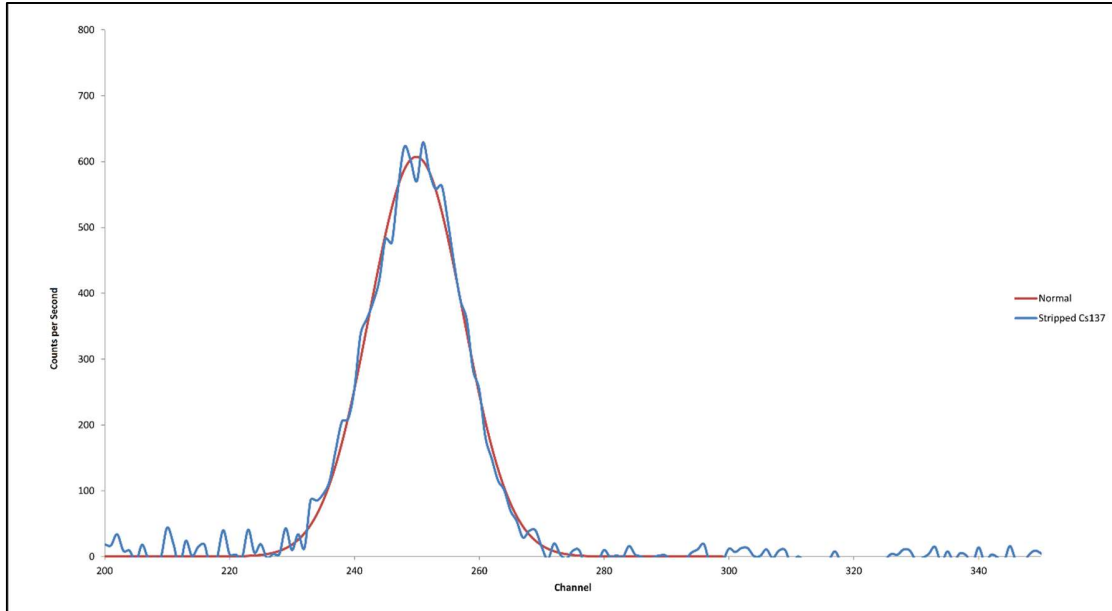
Ordnance Survey (1912) Little London, Sheet 1:10 560 (County Series 2nd Revision), Scale 1:10560 (TIF File), Last Updated 1st January 1912, Ordnance Survey, GB. Using: EDINA Historic Digimap Service <https://digimap.edina.ac.uk>, Created: November 2020

Peppe, D.J. (2013) Dating Rocks and Fossils using Geologic Methods, *Nature Education Knowledge*, **4** (10): 1

Pike, A.W.G. Hedges, R.E.M. and van Calsteren, P. (2002) U-Series Dating of Bone using the Diffusion-Adsorption Model, *Geochimica et Cosmochimica Acta*, **66** (24): 4273 – 4286, DOI: [https://doi.org/10.1016/S0016-7037\(02\)00997-3](https://doi.org/10.1016/S0016-7037(02)00997-3)

- Putiška, R. Kušnirak, D. Dostál, I. Lačný, A. Moješ, A. Hók, J. Pasteka, R. Krajňák, M. Bosansky, M. (2014) Integrated Geophysical and Geological Investigations of Karst Structures in Komberek, Slovakia, *Journal of Cave and Karst Studies*, *National Speleological Society Bulletin* **76** (3): 155 – 163
- Reinhardt, N. and Herrmann, L. (2019) Review Article – Gamma-ray spectrometry as a versatile tool in soil science: A Critical Review, *Journal of Plant Nutrition and Soil Science*, **182**: 9 – 27, <https://doi.org/10.1002/jpln.201700447>
- Ruffell, A. McKinley, J. Lloyd, C.D. and Graham, C.J. (2006) Th/K and Th/U Ratios from Spectra Gamma-Ray Surveys Improve the Mapped Definition of Subsurface Structures, *Journal of Environmental and Engineering Geophysics*, **11** (1): 53 – 61, <https://doi.org/10.2113/JEEG11.53>
- Ruffell, A. and McKinley, J. (2008) *Geoforensics*, Wiley, Blackwell, New Jersey USA.
- Ruffell, A. and Wilson, J. (1998) Near-Surface Investigation of Ground Chemistry using Radiometric Measurements and Spectral Gamma Ray Data, *Archaeological Prospection*, **5**: 203 – 215, DOI: [https://doi.org/10.1002/\(SICI\)1099-0763\(199812\)5:4<203::AID.ARP96>3.0.CO;2-D](https://doi.org/10.1002/(SICI)1099-0763(199812)5:4<203::AID.ARP96>3.0.CO;2-D)
- Sanjurjo-Sanchez, J. Chamorro, C.A. Alves, C. Sanchez-Pando, J.C. Blanco-Rotea, R. and Costa-Garcia, J.M. (2017) Using In-Situ Gamma Ray Spectrometry (GRS) Exploration of Buried Archaeological Structures: A case study from north-west Spain, *Journal of Cultural Heritage*, Published Online, DOI: 10.1016/j.culher.2018.05.004
- Schmidt, A. R. Linford, P. Linford, N. David, A. Gaffney, C.F. Sarris, A. and Fassbinder, J. (2015) EAC Guidelines for the use of Geophysics in Archaeology: Questions to Ask and Points to Consider, EAC Guidelines 2, Namur, Belgium: Europae Archaeologiae Consilium (EAC), Association Internationale san But Lucratif (AISBL), ISBN: 978-963-9911-73-4, 135p
- SPRS (2020) *Britannia Monograph Series*, Archaeology Data Service, Society for the Promotion of Roman Studies, DOI: <https://doi.org/10.5284/1049651>, Accessed 20th August 2020
- Trogu, A. Ranieri, G. Calcina, S. Piroddi, L. (2014) The Ancient Roman Aqueduct of Karales (Cagliari, Sardinia, Italy): Applicability of Geophysics Methods to Finding the Underground Remains, *Archaeological Prospection*, **21**: 157 – 168, DOI: 10.1002/arp.1471
- USNRC (2009) *Multi-Agency Radiation Survey and Assessment of Materials and Equipment Manual (MARSAME) (NUREG-1575), 'Supplement 1'*, Office of Nuclear Regulatory Research, US Nuclear Regulatory Commission (USNRC), Washington DC, January 2009
- Westminster Abbey (2020) Westminster Abbey – History: Architecture, www.westminster-abbey.org/about-the-abbey/history/architecture, Dean and Chapter of Westminster, Accessed 04/09/2020
- Wiley Online Library (2023) *Archaeological Prospection – Overview*, www.onlinelibrary.wiley.com/page/journal/10990763/homepage/productinformation.html, Accessed 02/06/2023
- Zheng, W. Li, X. Lam, N. Wang, X. Liu, S. Yu, X. Sun, Z. Yao, J. (2013) Applications of Integrated Geophysical Method in Archaeological Surveys of the Ancient Shu Ruins, *Journal of Archaeological Science*, **40**: 166 – 175

4.7 Supplementary Data



Source: Nuvia (2019)

Supplementary Figure S4.1 – Response Curve of Groundhog Detector GN08 to a 6 kBq Cs-137 Source as Part of Calibration Checks.

Supplementary Table S4.1 – Descriptions of the Four Sites Subject to Groundhog Surveying

Site	Survey Area (m ²)	Description
Site A (Urban)	4000 (uncollimated) 2000 (collimated)	The urban area (Site A in Figure 4.2) surveyed was located within the fenced off area of the 2019 University of Reading Field School, a short distance southeast from the Amphitheatre and close to the bath house. The chosen survey area is known to contain a road junction and the remains of buildings – possibly shops and workshops as discussed in the antiquary reports presented in Creighton and Fry (2016). The area was selected as it was hoped that the road junction would generate a clear linear anomaly in the radiation maps, achieved by the concentration of construction material that had contrasting radiological properties to surrounding substrate. This inference is based on the findings from previous magnetic, GPR and earth resistance surveys, where the resultant data sets clearly show these features.
Site B (Inhumations/ Cremations)	4000 (uncollimated)	This survey area (Site B in Figure 4.2) is located outside of the Roman walls, close to the West Gate and is known to contain several cremations as summarised in Creighton and Fry (2016), Chapter 6 – Exterior 13. It is also possible that some inhumations exist within the area, but this is not confirmed. This site was selected to test whether the cremation of human remains could result in sufficient concentration of naturally occurring radionuclides as to be detectable through radiation surveys.
Site C (Temple)	1500 (uncollimated)	The third site chosen (Site C in Figure 4.2) was a paddock known to contain the western edges of two temples and a Temenos wall/ ditch. The latter feature surrounded the temples and a modern church. Previous ground penetrating radar surveys yielded high quality data/ images, indicating that these structures are well preserved (Fulford <i>et. al.</i> 2018) and therefore a valuable study site.
Site D (Kilns)	2000 (collimated) 2500 (uncollimated)	The kiln site (Site D in Figure 4.2) is situated outside of the Roman town in nearby Little London. The site has been excavated during earlier expeditions, during which two brick-built kilns were unearthed (Fulford, Pankhurst, Wheeler and Machin 2017). This site was selected as it was hoped that the naturally occurring radioactive material present in the fired brick of the kilns would generate a sufficient contrast to the surrounding material.



CHAPTER 5

Radiating Encouragement:
Further Investigation into the
Application of Gamma Ray
Spectroscopy for
Archaeological Prospection
at the Roman Town of
Silchester

5 RADIATING ENCOURAGEMENT: FURTHER INVESTIGATION INTO THE APPLICATION OF GAMMA RAY SPECTROSCOPY FOR ARCHAEOLOGICAL PROSPECTION AT THE ROMAN TOWN OF SILCHESTER

5.1 Introduction to Paper (as published in *Archaeological Prospection*, Vol 31(3))

This paper forms Chapter 5 of this thesis. It was submitted to *Archaeological Prospection* in December 2023. At the time of thesis submission, this paper has been accepted for publication, and has undergone final proofing/ typesetting and is now awaiting publication.

The paper presents the findings from two additional surveys undertaken at Silchester Roman Town. Building on the recommendations of the preliminary study, this research employs a vehicle mounted Groundhog system to survey an analogous set of targets, thereby testing the scalability and repeatability of the technique. The selected targets, located in Insulae VII, XXXV and XXXIII, included roads, buildings and a distinctive circular temple.

The gamma radiation distribution maps presented in this paper were created using Geoplot. This provided a valuable opportunity to test various tools including gap fill and multiple filters to identify potential methods for improving image quality. Additionally, visualisations were created using individual energy windows to explore whether specific radionuclides or energy ranges were responsible for the observed anomalies, and if isolating these could better highlight the targeted features.

Methodology Rationale

The decision to use a vehicle-mounted Groundhog system was driven by the conclusions and recommendations of the previous chapter. This system significantly increased the area that could be surveyed in a single day.

The trial use Geoplot was influenced by ongoing challenges with gaining access to the bespoke ArcGIS applications, created by Nuvia, normally used to process Groundhog data. The limited

number of licences to ArcGIS with the necessary applications combined with its use on time-based commercial projects, often made it difficult to find time slots to learn how to use the software and process data in a timely manner. Geoplot proved to be a highly effective alternative. Although it did not allow for spectral interrogation or the automatic generation of count rate distribution graphs, this was not critical to my research. The key output was the visualisations that could effectively be created in Geoplot. Count rate distribution graphs were created in Excel, using raw data. Further, Geoplot offered a number of benefits including the range of filters and the availability of the software to the wider archaeological community, facilitating the replication and recreation of this work by others.

Journal Rationale

The journal *Archaeological Prospection* was selected for publication as its aims and scope continue closely align with the research aim of this project. The previous paper submitted to *Archaeological Prospection* was well received, and it seemed fitting to publish the findings of the follow up work with the same journal.

5.2 Confirmation of Candidate Contribution

Victoria Robinson: Conceptualisation, literature review, methodology development, data collection, data processing, data analysis, writing – original draft, incorporation of peer reviewer comments.

Robert Clark: Preparation of Groundhog equipment, supporting data processing.

Dr Stuart Black: Conceptualisation, supporting data analysis, writing – review and editing.

Dr Robert Fry: Conceptualisation, permissions for access to Silchester, fieldwork setup, supporting data analysis, writing – review and editing.

Dr Helen Beddow: Conceptualisation, writing – review and editing.

Professor Mike Fulford: Provision of supporting data (unpublished)

5.3 Published Paper

5.3.1 Keywords

Archaeological Survey, Natural Radioactivity, Gamma Spectrometry, Gamma Ray Surveying, Nuvia Groundhog®, Silchester, Vehicle Mounted, Integrated Techniques

5.3.2 Abstract

This study builds on a preliminary investigation into the efficacy of gamma radiation surveying as a complementary tool for archaeological prospection. Improved surveying and data processing methods were implemented, including the use of a vehicle-mounted Groundhog surveying system, use of alternative software tools and examination of the impacts of individual radionuclides. The study focuses on a range of targets within *Insulae* VII, XXXV and XXXIII in Silchester Roman town, Hampshire. Targets of interest included a polygonal temple, a house, ditches (including an Iron Age defensive ditch) and several Roman roads.

While the survey revealed no measurable differences in the gamma radionuclide content of less substantial structures (such as the temple and house) and the surrounding soil, it successfully delineated major structures. The Roman roads, Iron Age defensive ditch and potentially an indication of a historic field boundary not present in modern records were clearly visible in the generated visualisations. The roads and field boundary appear as distinct linear anomalies of depleted radioactivity. The location of the Iron Age ditch correlates with an area of elevated radioactivity. Notably, the technique not only successfully identified archaeological features, but was also able to highlight differences in the properties of similar targets such as variations in road thickness. Further, the gamma radiation data indicates variations in the local geology attributable to historic changes in land use and geochemical composition.

This latest study corroborates the findings of the preliminary investigation, demonstrating replicability, scalability and ability to enhance output data quality. Further research, including sampling and non-destructive analysis of materials from the site, is needed to better explain observed results.

5.3.3 Introduction

Multiple geophysical survey methods have been applied on a global scale as a non-destructive method of identifying and analysing features of archaeological interest for over 70 years (Wynn 1986, Jordan 2009, Cuenca-Garcia 2018). As noted by Jordan (2009), an extensive amount of data has been accrued over this period, demonstrating the successful application of these techniques in supporting archaeological investigations. However, the effectiveness of each method is dependent on the ability to measure clear differences in the physical properties of potential targets and surrounding substrate, and susceptibility to interference from modern features (Gaffney and Gater 2011, Milsom and Eriksen 2011, Ruffell and McKinley 2008). Selection of an optimal geophysical technique most likely to yield significant contrasts must therefore be managed on a site-by-site basis. Consideration must be given to the physical characteristics of anticipated targets, the surrounding substrate, target size and presence of modern features that could cause interference (Gaffney and Gater 2011, Ruffell and McKinley 2008).

To improve data fidelity, multiple geophysical survey methods measuring different physical properties, and with different susceptibilities, can be applied. Multiple studies demonstrating the effectiveness of using complementary geophysical methods for the prospection and mapping of archaeological sites are available in the published literature. Key benefits associated with the application of complementary geophysical techniques at a site include improving the accuracy of data interpretation and increasing the amount of data that can be retrieved to characterise a site beyond merely establishing the presence and position of archaeological features. This first point is exemplified in a study by Cuenca-García (2018). Here, multiple geophysical techniques were consistently applied to three contrasting sites of archaeological interest across Scotland. Techniques included fluxgate gradiometer, electromagnetic induction, Ground Penetrating Radar (GPR) and earth resistance surveys (Cuenca-García 2018). Geochemical analysis of soil samples taken from each site was also undertaken to aid geophysical data interpretation (*ibid*). The selected sites contained known targets including a Viking Longhouse, Iron Age ditches and Neolithic/ Bronze Age closures. The findings from the study highlighted the benefits of implementing complementary techniques. This is best demonstrated in data from the survey of the Viking Longhouse. The Fluxgate Gradiometer survey was unable to detect the target through the deep windblown sands but was able to detect midden deposits that may have otherwise been missed (Cuenca-García 2018) – a false negative conclusion. In contrast, the GPR and

electromagnetic methods were capable of measuring the contrast between the longhouse and surrounding substrate (Cuenca-García 2018). The study highlights the value of such an approach in regions with more challenging geologies for archaeological prospection, and in particular those with significant heterogeneity in the soil overburden which can have the effect of shielding responses or creating noise in the output data.

Indeed, the author notes that in areas where significant variability exists, “*surveys based on a single technique... have a high chance of being disappointing...*” (Cuenca-García 2018, pg. 70). A later paper by Porcelli *et. al.* (2020) further highlights the importance of utilising multiple datasets to aid interpretation. Within this paper, Porcelli *et. al.* (2020) refers to a GPR survey of Tutankhamun’s tomb, undertaken to confirm an earlier theory that it may be part of a larger tomb infrastructure belonging to Queen Nefertiti. This preliminary GPR survey appeared to confirm this theory, with the findings published as the ‘discovery of the century’ (Porcelli *et. al.* 2020). However, two subsequent GPR surveys covering the same area, including one undertaken by the original authors, showed that this original conclusion was incorrect, and that there were no further features of interest (Porcelli *et. al.* 2020) – a false positive result. This second paper highlights the potential vulnerability of using a single technique, and how even different data sets using the same technique can lead to conflicting conclusions.

A study by Simon *et. al.* (2015) highlights the value of integrating different geophysical techniques to improve site characterisation, recognising that a single technique will only be able to generate data on one specific parameter of the site. In this study, the authors applied a combination of geophysical techniques to investigate a Neolithic site in Thessaly, Greece. Techniques gainfully employed included magnetic surveys, electrical tomography and ground penetrating radar (Simon, *et. al.* 2015). The combination of techniques yielded data with greater interpretive value. Useful insights into the presence and location of Neolithic structures, depth profiles of these features and indications of the geomorphology and sediment diversity of the area were provided (Simon, *et. al.* 2015). Further, the techniques applied facilitated a proportionate approach to surveying and the ability to gain the most amount of information possible within resource constraints. Magnetic and electrical methods enabled the efficient and effective surveying of a substantial area at a useful resolution (Simon, *et. al.* 2015). GPR, a higher resolution technique, could then be applied to

much smaller areas, targeting features most likely to benefit from this higher resolution (Simon, *et. al.* 2015).

In summary, the application of multiple geophysical techniques in archaeological prospection follows a philosophy similar to that of James Lovelock’s insightful Gaia theory; that when these different complex techniques are applied cooperatively, the value of the combined data should be greater “than the sum of its parts” (Lovelock 2020). Building on this philosophy, the authors of this paper aim to assess an alternative non-intrusive survey method’s effectiveness in archaeological prospection, and its ability to contribute to this multi-technique approach. Specifically, the use of portable gamma radiation systems to measure any contrasts in concentrations of naturally occurring radioactivity in archaeological targets and the surrounding substrate. If successful, the use of gamma surveying methods could add to the existing ‘toolbox’ of non-intrusive archaeological prospection methods and may even facilitate improved interpretation of acquired data.

This research is the first reporting of a vehicle-mounted gamma radiation survey conducted at an archaeological site, for the purpose of prospection, available within the published literature. Our study successfully demonstrates the repeatability and scalability of the method, as well as an ability to apply multiple processing methods to generate high quality visual outputs that are novel, and that show significant promise for archaeological and land-use investigations.

5.3.4 Building on a Preliminary Investigation at Silchester

Following an earlier study, the authors published findings from a preliminary investigation exploring the efficacy of using gamma radiation surveying methods to support the identification of buried archaeological features (Robinson, *et. al.* 2022). This approach is based on the principle that naturally occurring radioactive material is ubiquitous in the environment (IAEA 2023) and that human activity can cause measurable changes in the concentrations of this radioactivity. This includes for example, importing and depositing (construction) materials from other locations, using clays which are naturally rich in naturally occurring radionuclides to make bricks (Aliyev 2004, IAEA 2003) and other industrial activities. The study focussed on targets within Silchester Roman Town. This location was selected due to the extensive geophysical and archaeological data

available for the site (Creighton and Fry 2016, Fulford 2021). This provided a valuable opportunity to compare gamma surveying data against this existing and well-understood information.

In the preliminary study (Robinson, *et. al.* 2022), gamma radiation surveys were undertaken using a hand-held gamma surveying system in both a collimated and uncollimated configuration to target four small areas across the site. Each contained a different target type. The system used was a Groundhog® Fusion system, developed, owned and operated by Nuvia Limited. The Groundhog® Fusion system (subsequently referred to here as Groundhog®) is part of a family of rugged, portable gamma radiation detection systems with spectrometric capability. The key components of Groundhog® used for this study are presented in Section 5.1.6. The system can be deployed in various configurations including collimated, uncollimated, vehicle mounted (using a bank of gamma detectors) or hand-held (single gamma detector). Groundhog systems are traditionally used in the nuclear industry for mapping out anthropogenic radioactive contamination in the environment.

Results using a hand-held gamma detector from this earlier investigation at Silchester showed varying results. Gamma radiation data from two of the areas; an 'urban' site from the centre of the Roman Town and an area containing cremations/ inhumations from just outside the Late Roman Town walls, failed to distinguish any archaeological features (Robinson, *et. al.* 2022). However, the other two sites; a temple area in the east side of the site, and an industrial area in nearby Little London, yielded positive results. Here, the Groundhog® system was able to identify man-made features (both archaeological and more modern) that were also visible within extant fluxgate gradiometer and GPR data. Features identified included a Temenos wall/ ditch bounding a Roman temple and an infilled clay pit (Robinson, *et. al.* 2022). The results suggested that gamma radiation surveys could be used to support the identification of some buried archaeological features and could add value to a multi-method geophysical approach to a site's identification and interpretation. Completion of this pilot study highlighted a number of opportunities for potentially improving the quality and efficiency of survey outputs. This included improving the scalability of the technique by using Nuvia's vehicle mounted Groundhog® system and applying different data processing methods. This paper presents the results of work testing these variables.

Aspects for Further Investigation

Completion of the first set of gamma surveys highlighted several opportunities for further work to test:

- Whether the findings from the first study could be replicated for other analogous targets;
- Whether the technique could be scaled up to cover a larger area within a similar period of time; and
- Methods for improving the quality of processed data used for interpretation.

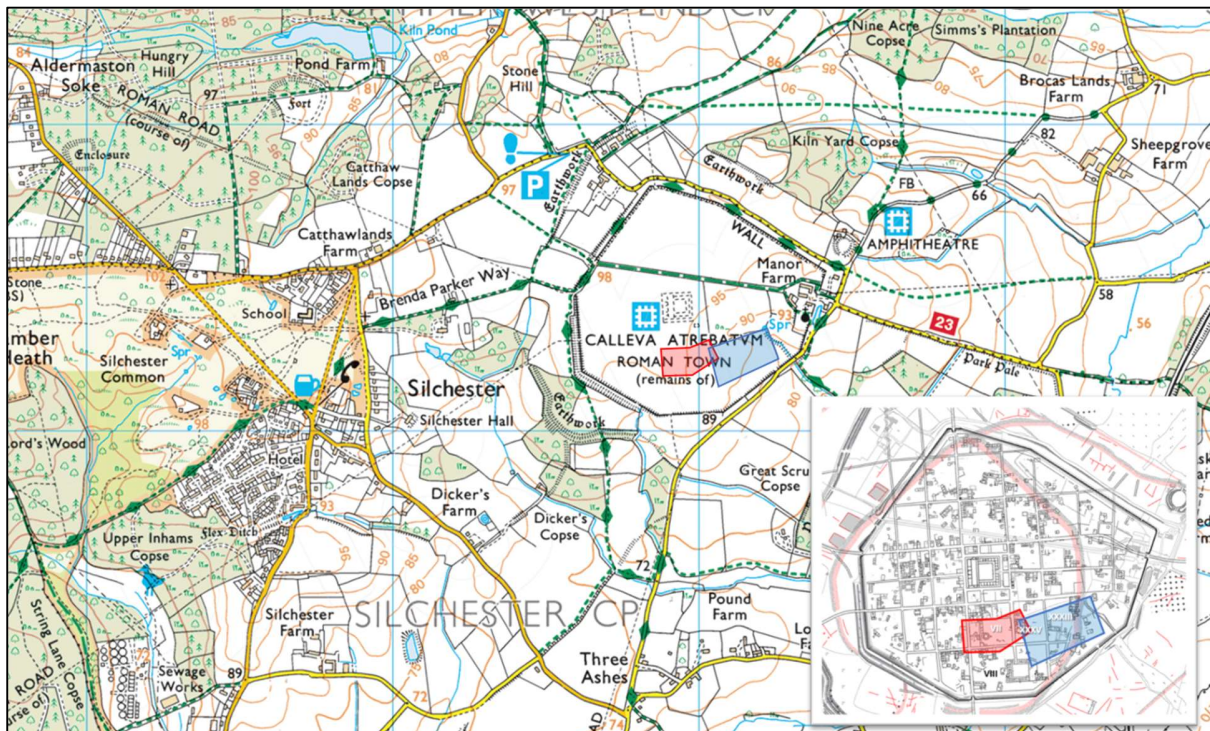
Two subsequent surveys were therefore undertaken at a different location within Silchester's boundary walls. The new location offered analogous targets, including the Roman road infrastructure, a 16 sided temple structure and a major defensive Iron Age Ditch to test replication. Scalability was tested through the deployment of the vehicle mounted Groundhog® system which is capable of operating 3 gamma detector units simultaneously and using a traversing speed of ~1 m/s, is able to cover approximately 1.4 – 2 ha/day. The collected data was processed using Geoplot 4 (Geoscan Research), enabling further experimentation with data processing. Finally, data from the two surveys were normalised with the intent of integrating the two data sets.

5.3.5 Current Study Site and Existing Data

The study site is situated within the Roman Town of Silchester (Calleva Atrebatum) (Figure 5.1). The town is located approximately two kilometres to the west of the current day village of Silchester, Hampshire, in south-east England. The site has a long history of occupation, dating back to the Iron Age (Fulford 2021). Indeed, one of the targets selected for this study is an Iron Age ditch that formed part of a large defensive enclosure, encompassing an area of ~38 ha (*ibid*). The positioning of the later Roman town broadly aligns with this enclosure (Fulford 2021). The Roman town of Silchester hosted various buildings and supporting infrastructure; from domestic dwellings to workshops, shops, temples and road networks (Creighton and Fry 2016, Fulford 2021). The roads divided the town into *insulae*, each generally containing a mixture of building types. It was this diversity of target type, combined with the extensive geophysical and archaeological data already available for the site that cemented Silchester as an optimal case-study for this research project. This data has been acquired from over 150 years of systematic

excavations at the site, starting principally with Reverend James Joyce in the 1860s (Creighton and Fry 2016) and decades of geophysical survey initiated in the 1950s (Creighton and Fry 2016).

The targets selected for this study are located across *Insulae* VII and XXXV to the west and *Insulae* XXXIII and XXXII to the east.



Source: Adapted from Digimap (2023) and Creighton and Fry (2016)

Figure 5.1 – Survey areas one and two, highlighted in red and blue respectively, in the context of Silchester Roman Town and surrounding area. Inset: *Insulae* covered by the survey area.

Insulae VII and XXXV

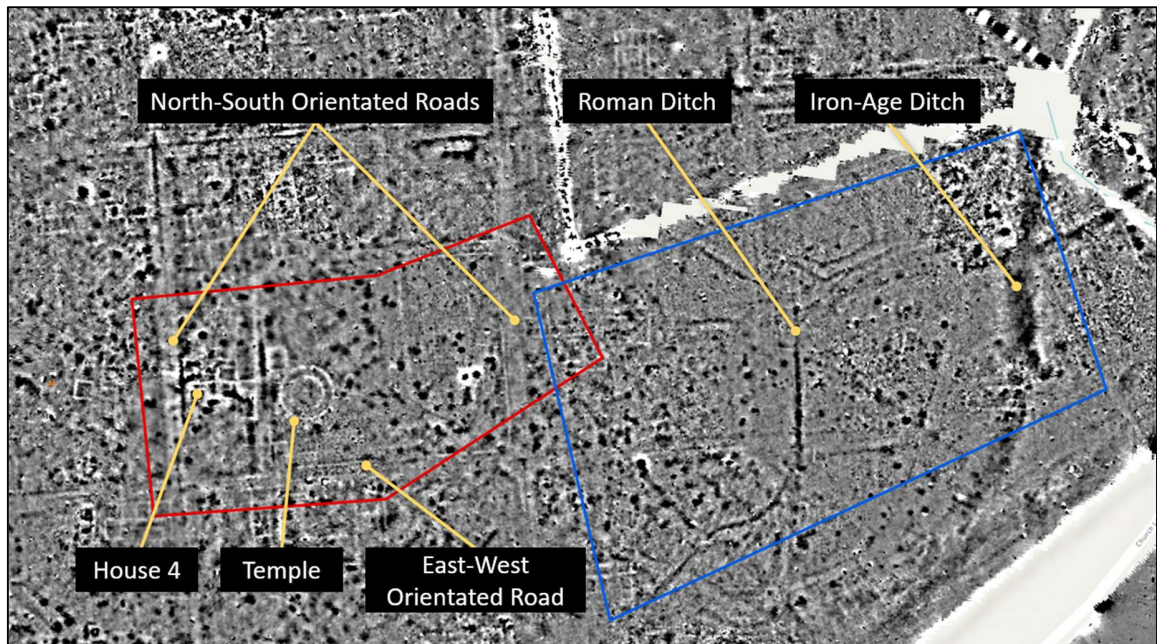
The first survey location (Area 'A'), outlined in red in Figure 5.2, is a 0.6 ha area spanning *Insulae* VII and XXXV and contains three targets of interest (Figure 5.2). The first target is an anomaly broadly circular in shape, identified as a temple of stone construction, including ironstone quoins (Fulford 2021, Ward 1911). This feature comprises two concentric shapes; the outer being a 16-sided polygonal wall and an inner circular structure with a total maximum diameter of ~20 m (Creighton and Fry 2016). Although the foundations of this temple have previously been described as 'slight' (Creighton and Fry 2016), they produce a clear circular anomaly in the fluxgate gradiometer (Figure 5.2) and GPR data. The latter suggesting a depth of 1.57 and 0.23

metres below the soil surface (Linford, Linford and Payne 2019). It was therefore hoped that the structure would be substantial enough to support detection of a contrast in naturally occurring radioactive material relative to the surrounding substrate. In addition to the temple, there is 'Insula VII House 4'; an eight-roomed house (Creighton and Fry 2016), and sections of road in both north-south and east-west orientations. One of these roads is the major north-south road of the Town, linking its North and South Gates (Fulford 2021). It is understood that House 4, as per other buildings on site, is predominantly of flint rubble construction with brick corner stones (Creighton and Fry 2016) and therefore of more typical construction to other buildings in the Town compared to the temple. It was identified as a good target for the gamma radiation survey due to its shallow depth (approximately 30 cm below ground level) and its ability to generate a prominent magnetic anomaly in the extant Fluxgate Gradiometer data (Linford, Linford and Payne 2019, Creighton and Fry 2016). The roads appear to be located at similar depths to the temple, as suggested by GPR data (Linford, Linford and Payne 2019). The roads predominantly consist of compacted gravel extracted from quarries west of the Roman Town (Fulford 2021). The roads and temple targets were of particular interest to the authors. In the previous study by Robinson, *et. al.* (2022), the roads in *Insula XXXIV* failed to generate a measurable difference in gamma emissions relative to the surrounding substrate. The authors wished to explore whether these findings would be repeated for roads in a different area of the Silchester site, or if different behaviours would be observed. The temple structure provided a novel target type of significant size to further test the efficacy of the Groundhog system.

Insulae XXXIII

A larger ~1.4 ha area (Area 'B'), outlined in blue in Figure 5.2, was targeted in an adjacent space spanning *Insulae XXXIII* and *XXXII*. This site was selected due to the presence of two key features clearly visible within the extant geophysics data: a large (Iron Age) defensive ditch running down the east of the survey area and a suspected Roman ditch for a drain or water supply (Figure 5.2). The Iron Age ditch was excavated in 2019 which demonstrated that it terminates at 4.8 m below the ground surface (Fulford, *et. al.* 2019). The ditch was selected for this study as it is analogous to targets clearly visible in the previous study: the ditch features associated with the temenos wall and the infilled clay pit. The Roman ditch offered a clear linear anomaly which turns into a long sweeping curve at the southern end of the survey area. It introduces a new target type to this research project and an opportunity to further test the efficacy of this technique.

It is noted that both study areas also contain other features such as large pits, wells, minor roads and structures that may also form targets of interest. However, due to their smaller size, they are less likely to generate significant contrasts in background radioactivity compared to the surrounding soil.



Data Source: Fluxgate Gradiometer Data from Creighton and Fry (2016).

Figure 5.2 – Close-up view of the survey areas overlaying the fluxgate gradiometer data (+/- 7nT – black high to white low). The figure shows the targets present within Area A (outlined in red) and Area B (outlined in blue).

5.3.6 Methodology

Overview of Equipment Used

The use of a vehicle mounted system facilitated the simultaneous operation of three Groundhog® gamma detector units (Figure 5.3). The Groundhog® units each contain a 76 mm x 76 mm sodium iodide (NaI) scintillation type gamma detector and spectrometer. The NaI detectors have an operating energy range of approximately 15 – 3000 keV. The units are linked to a mapping grade GPS unit and data logger in the form of an ultra-mobile personal computer (UMPC). One gamma spectrum measurement is recorded by the system every second, along with corresponding positioning data.

With the deployment of three detectors, it is possible to achieve the simultaneous collection of three gamma radiation measurements per second, with each gamma detector spaced one metre apart. This contrasts significantly with the hand-held system's capacity for collecting one gamma radiation measurement per second, highlighting the enhanced efficiency afforded by the vehicle mounted configuration.

Site Surveys

Vehicle mounted surveys were completed on 18th August 2022 and 16th May 2023. The second survey was originally unplanned and undertaken to fill in a substantial gap in the data on the eastern side of the survey area as a result of a GPS signal failure during the original survey (Area B) (Figure 5.4).

In advance of each deployment of the vehicle mounted system, the three Groundhog[®] detector units were subject to full calibration, in accordance with Nuvia procedures. These annual calibration checks are essential to ensure that each unit is performing as expected and fit for purpose, thereby reducing the risk of introducing systematic errors. The Nuvia procedures are based on the National Physics Laboratory's Good Practice Guide 14 (Lee and Burgess 2014). The calibration process measured the gamma detectors' responses against background gamma radiation and a 5.72 kBq Cs-137 check source for a period of 600 seconds each. This confirmed that the gamma detectors were operating within acceptable ranges and therefore generating reliable data. The calibration checks confirmed that the detectors had an efficiency (i.e., the ratio of light pulses generated by the NaI crystal relative to the number of gamma rays emitted by the check source) of ~18 counts per second (cps) in the Cs-137 (662 keV) photopeak and a net value of 3.17 cps which is well within the acceptable range of 2.93 – 3.24 cps. It was further confirmed that the detectors were operating with an energy resolution (i.e. the detector's ability to differentiate between energy peaks in a spectrum) of 7% at full width half maximum amplitude (FWHM). Again, this was within the acceptable range of 6.50 – 8.00%.

On the morning of each survey, the Groundhog[®] system was subject to additional equipment function checks. These were undertaken in accordance with Nuvia's internal Method Statement. Key activities included:

- Vehicle safety checks.
- Ensuring equipment has been subject to the necessary electrical safety checks.
- Visual checks of equipment and cables to ensure they are in good physical condition and that batteries have full charge.
- Functional checks of the Groundhog® system to ensure the GPS receiver and gamma radiation detectors were operating correctly. This included checking the responses of the detector unit, checking functionality of the necessary software tools, and that the GPS unit was receiving a sufficiently strong signal.

As the survey areas were located in a large open field, a detailed walk-round was not required. It could be seen that there were no obstructions or hazards that could impact on vehicle access. It was however noted that one small area close to the Iron Age ditch was heavily rutted. Whilst it was acknowledged that this would not impact on vehicle progress, suddenly dropping into a deep rut could trigger an ‘excess speed’ alarm on the UMPC. It could also potentially shock the NaI crystals of the detector units, leading to an erroneous measurement.

To facilitate the vehicle survey, the three gamma radiation detectors and GPS antenna were fixed in place using a mounting frame attached to the front of the Land Rover (Figure 5.3). The frame ensures that the detectors are securely positioned 1 metre apart at a consistent height of ~30 cm. The corners of the targeted survey areas, shown in Figure 5.2, were marked out with siting poles positioned using a Leica GS16 RTK GNSS unit.

The gamma radiation surveys were completed by driving around the perimeter of one of the pre-determined survey areas and gradually working inwards towards the centre, following the tyre tracks of the previous circuit to avoid introducing gaps in the measurements. Several passes of the centre of each survey area were made due to the turning circle of the vehicle. A constant slow speed of approximately 1 m s^{-1} was maintained by placing the vehicle in first gear on a low transfer case setting (‘low range’), thereby avoiding the need to apply acceleration. Maintaining this speed facilitated the collection of at least one gamma radiation measurement per square metre for each detector. This speed, combined with the simultaneous use of three detectors enabled the collection of three radiation measurements every second, covering an area of three

square metres. On completion of one survey area, the vehicle was relocated to the second pre-defined survey area (August 2022 survey only) and the process repeated.



Source: Author Photograph

Figure 5.3 – View of the Nuvia survey vehicle, fitted with three Groundhog® Detectors and GPS system secured to the front. The detectors are spaced 1 m apart and positioned ~20 cm above ground level.

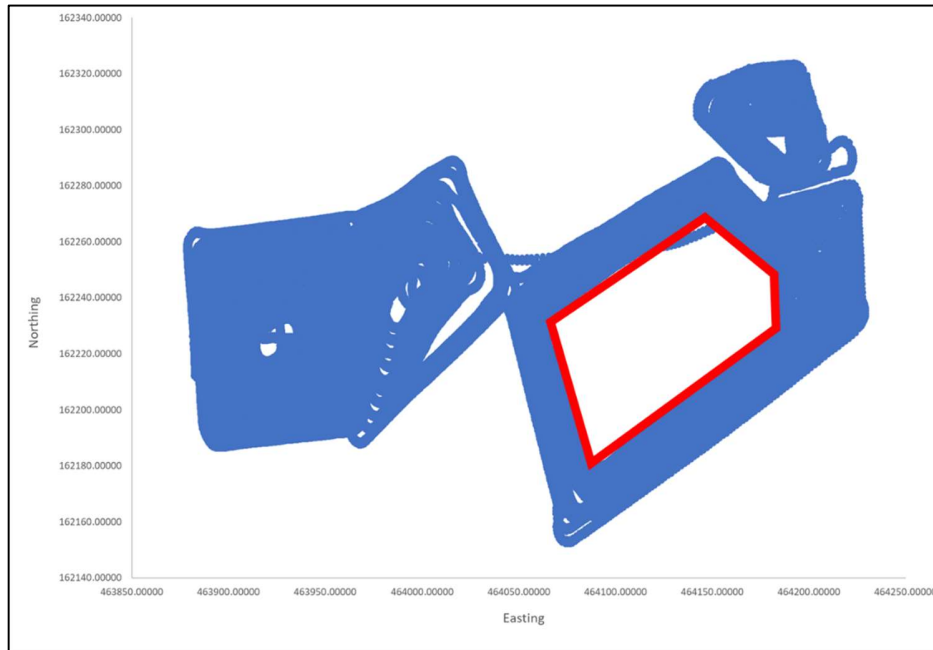
Data Processing

During the August 2022 and May 2023 surveys, gamma radiation and GPS measurements were automatically logged on the UMPC set up in the cab of the vehicle. At the end of each survey, this data was transferred to a stand-alone desktop computer for quality checks and preliminary processing.

As per the previous study, Microsoft Access (v. 16.0.14131.20278) was used to compile the data, with post processing to improve the quality of location data undertaken in GrafNav (v. 8.3). RINEX data from the Hartley Witney (HART) OS Reference Station was used for differential correction.

Further quality checks, including checks on the completeness of the data, highlighted the significant gap in the August 2022 data within Area B. Later investigation showed that this affected an area of ~5,500 m² (Figure 5.4); nearly a third of the eastern portion of the survey area, for which corresponding gamma data could not be plotted. This missing data informed the decision to resurvey the eastern side of the survey area to fill in this gap (Area B). With the exception of the missing GPS points, the remainder of the August 2022 and subsequent May 2023 positional data was excellent, achieving centimetre accuracy. Finally, quality checks also highlighted seven erroneous gamma radiation measurements in the May 2023 data. These values were an order of magnitude higher than the average readings in the data set. The anomalous data points can be attributed to a physical shock to one of the NaI crystals in a detector unit; likely due to driving over the ruts or contacting tufts of long grass. It is considered improbable for measurements exceeding 3000 cps to occur naturally in an area with typical background radioactivity for the region. Notably, these elevated readings affected only one detector at a time. If there was a point source of elevated radioactivity in the ground, we would expect multiple detectors to record similarly high values. In consequence, these erroneous measurements were removed from the dataset.

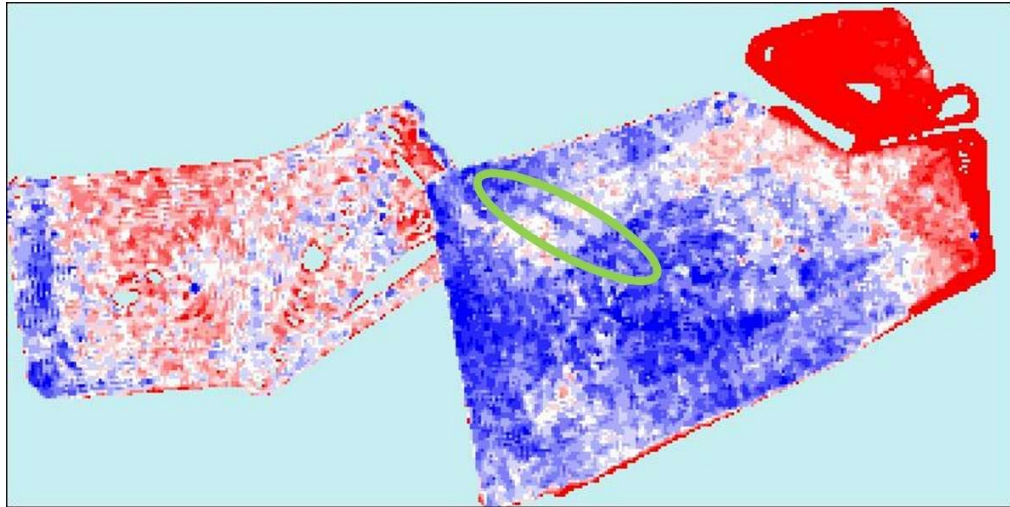
Finally, both the August 2022 and corrected May 2023 data sets were exported as dBase database (.dbf) files for further processing.



Source: Generated from primary data

Figure 5.4 – Plot of the GPS/ gamma radiation data points (blue) collected during the August 2022 survey, highlighting the area affected by missing GPS data (outlined in red)

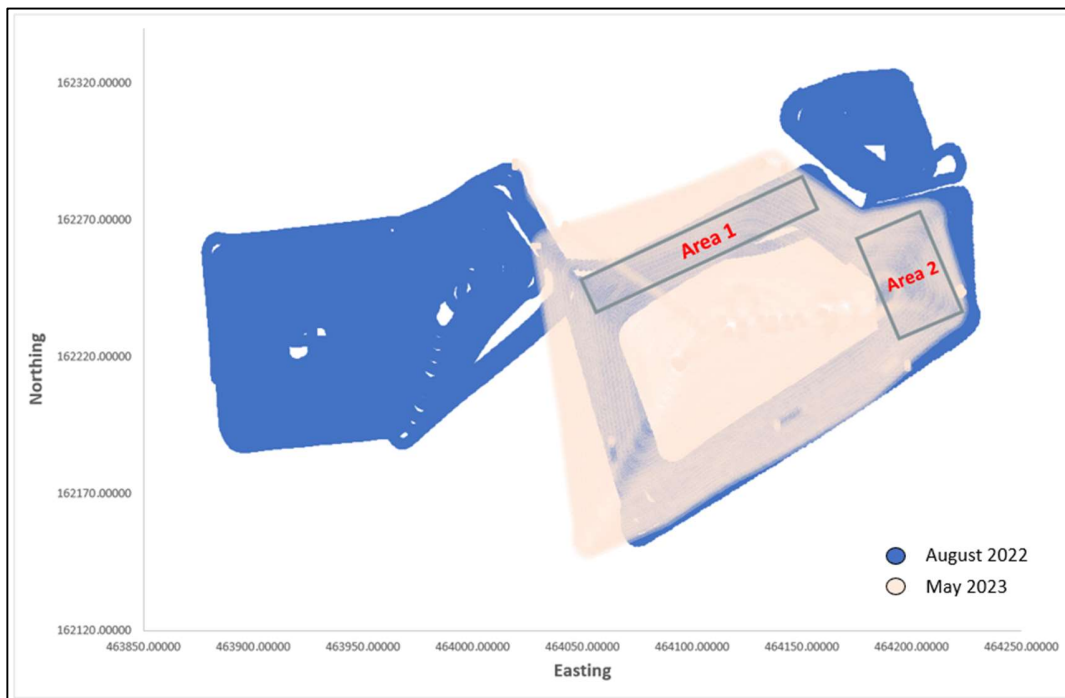
The original strategy for processing the data was to combine the August 2022 and May 2023 data sets to create a single set of visualisations. This was accomplished using the Geoplot software tool (version 4). However, this was found to be non-viable. The data could not be integrated, with areas of overlaying measurements obscuring any potential anomalies present. As shown in Figure 5.5, the overlaid measurements actually created false positives, showing linear anomalies that were attributable to vehicle movements.



Source: Created from Primary Data

Figure 5.5 – Preliminary attempt at creating visualisations by combining the August 2022 and May 2023 datasets. This shows how the overlaid data is obscuring any anomalies, and indeed creates false positives as highlighted in the green oval.

To establish the cause of this incompatibility, gamma radiation measurements from two areas of overlap were samples (Figure 5.6) and subject to a two-tail t-test, assuming unequal variances. The hypothesised mean difference was set at 0, assuming that there would be no significant difference in background gamma radiation measurements. A significance value of 0.05 was also set. As shown in Table 5.1, both sample areas confirm that the two data set are significantly different, with P values of <0.05. After identifying a significant difference, the August 2022 data which demonstrated a higher mean background gamma radiation value, was normalised against the May 2023 data. Multiple normalisation methods were applied, including subtracting the minimum value from each entry in the combined dataset and dividing by the range, dividing all values by the mean of the August 2022 and May 2023 mean values, and dividing by mean and median values. None of these approaches addressed the problem. Consequently, a decision was made to process the August and May datasets separately, with resultant visualisations combined post-processing.



Source: Created from primary data

Figure 5.6 – Plot of the GPS/ gamma radiation data points collected during the August 2022 and May 2023 surveys. Areas 1 and 2 denote where data was sampled for statistical analysis.

Table 5.1 – Results from a two-tailed t-test for sub-sets of overlapping data from the August 2022 and May 2023 surveys as shown in Figure 5.6

Parameters	Area 1		Area 2	
	Aug-22	May-23	Aug-22	May-23
Mean (cps)	225	189	237	199
Variance (cps)	310	239	359	259
Observations	3171	3264	2404	2950
Hypothesized Mean Difference	0		0	
df	6276		4727	
t Stat	87.11		77.69	
P(T<=t) one-tail	0.000		0.000	
t Critical one-tail	1.65		1.65	
P(T<=t) two-tail	0.000		0.00	
t Critical two-tail	1.96		1.96	

Source: Created from primary data

In the preliminary study by Robinson, *et. al.* (2022), gamma radiation data heatmaps were created exclusively in a bespoke add-on of ArcGIS, managed by Nuvia Limited. These heatmaps allowed the authors to identify anomalies that aligned with known archaeological features. However, for the purposes of this research project, a different software solution, Geoplot (version 4) was

selected to plot the gamma data and create the visualisations. This choice not only enabled the exploration of alternative processing methods, but also offered opportunities for enhancing image quality. Further, this approach utilised a widely used software programme that does not require bespoke add-ons, improving accessibility.

Geoplot 4 offers a broad range of processing tools to enhance image quality. Work was therefore undertaken to explore which tools, or combination of tools, would generate the best quality visualisations. Different processing tools were applied to the total gamma counts per second recorded during both the August 2022 and May 2023 surveys. Care was taken to achieve an optimal balance between enhancing image quality to draw out anomalies and excessively altering the output, reducing fidelity to the original data sets. Colour palette 09 (+/-2 standard deviations) was found to be the most compatible with all processing methods to highlight the anomalies.

As a baseline, a single application of GPS Gap Fill was applied to the data. Subsequently, different data enhancement and smoothing filters (either a single application or combination of: Wallis, Median, Low Pass and High Pass filters) were tested on the raw dataset, (Figure 5.7). The Wallis filter was found to optimise and enhance anomalies, that align with known archaeological features, in the dataset without overly smoothing the data.

Interrogation of the output images identified the combination of 'GPS Gap Fill + Wallis Filter' as the optimal method for processing the data. It created a smooth image capable of drawing out anomalies without excessive deviation from the raw data (Figure 5.7, Figure 5.9). This method was therefore applied to all subsequent processing.

Expanding on the data processing methods applied in the preliminary Silchester study (Robinson, *et. al.* (2022), the authors completed a more comprehensive analysis by investigating the specific impact of individual radionuclides on the observations from the 'total gamma counts' visualisations. Targeted radionuclides included both naturally occurring primordial radionuclides, namely potassium-40, uranium-238 and thorium-232, and the anthropogenic caesium-137. Further, the authors examined energy windows that aggregated measurements falling below the caesium-137 energy range ('Below Window') and above it ('Above Window'). Targeting of these individual radionuclides was achieved by importing data from individual regions of interest into

Geoplot. The ability to explore the impact of individual radionuclides has the exciting potential to offer additional interpretive value for more traditional geophysical surveys of archaeological deposits. By generating visualisations for each radionuclide, it may be possible to make inferences on the materials used on the construction of features identified as being of archaeological interest. For example, elevated concentrations of uranium and thorium may indicate the presence of granitic features, whereas concentrated areas of depleted radioactivity across all radionuclides may suggest features comprising sedimentary rock such as flint. More broadly, the behaviours of individual radionuclides may help characterise the geological history of the area, as evidence in studies such as that undertaken by Kozhevnikov, *et. al.* (2018).

As illustrated in Table 5.2, each radionuclide can be identified through its characteristic energy range. When a gamma radiation measurement is registered by a detector, it is assigned to the corresponding energy window. It is further noted that where radionuclides do not undergo decay through emission of gamma photons, a proxy daughter radionuclide emits gamma photons is used, as shown in Table 5.2.

Table 5.2 – Regions of Interest Subject to Interrogation via Geoplot¹

Region of Interest	Energy Range (keV)
Total Gamma	0 – 3000
Potassium (K) (via ⁴⁰ K)	1400 – 1600
Uranium (U) (via ²¹⁴ Bi)	1600 – 1900
Thorium (Th) (via ²⁰⁸ Tl)	2500 – 3000
Caesium (Cs) (via ¹³⁷ Cs)	581 – 740
Below (¹³⁷ Cs) Window	0 – 530
Above (¹³⁷ Cs) Window	760 – 3000

Source: Davies (2015)

¹ Each gamma ray photon emitted by a decaying radionuclide has a specific energy, typically measured in keV. This energy is unique to the source radionuclide (IAEA 2017). The energies of these gamma photons therefore act as a fingerprint, supporting the characterisation of radioactive material. Where there are multiple radionuclides present that emit gamma ray photons with similar energies, it may be difficult to differentiate between them, depending on the resolution of the detector used. For example, the radionuclides Pb-214, which emits gamma ray photons with energies of 295 keV and 351 keV, and Bi-214, which emits gamma ray photons of 609 keV and 665 keV (IAEA 2008) would fall into the Cs-127 region of interest of 581 – 740 keV, as shown in Table 5.2, for the Groundhog NaI gamma detectors. It is the ability to differentiate between these peaks that determines the resolution of the detector.

5.3.7 Results

The use of the vehicle-mounted Groundhog® system significantly increased the area that could be practically surveyed in a day. In the preliminary study by Robinson, *et. al.* (2022), where Groundhog® was deployed in a hand-held configuration, a total of ~16,000 m² was surveyed over a 2-day period. As shown in Table 5.3, approximately 23,500 m² was surveyed in a single day in August 2022, using the vehicle-mounted system. It is acknowledged that the efficiency of the hand-held surveys was impacted by the need to relocate between survey areas and the need to set up transect guides at each site. However, even once this inefficiency has been accounted for, it can be seen that the vehicle-mounted system significantly improves the scale of survey achievable. This supports the well-established findings from the commercial application of the Groundhog® system where it is known that a typical hand-held survey can cover hundreds to thousands of square metres (~15,000 readings per person/day) to tens of thousands of square metres per day (>50,000 readings per day).

Using the vehicle-mounted system also yielded a slight improvement in measurement density, increasing from a mean density of 1.3 measurements per square metre using the hand-held system (Robinson, *et. al.* 2022) to a mean of 2.2 measurements per square metre using the vehicle mounted system as shown in Table 5.3. This improvement is attributable to the degree of overlap achieved during each pass of the Land Rover. This outlines the summary statistics for the August 2022 and May 2023 surveys, as well as those from the July 2019 survey of the Urban Area (Robinson, *et. al.* 2022), which is analogous in terms of target types to the current survey areas. The total number of measurements recorded during each survey as well as minimum, maximum and mean readings collected are presented. Notably, the data from the May 2023 survey exhibits a closer resemblance to the July 2019 survey data than to the August 2023 data, the latter being collected during an extreme (high temperature) weather event. The two-tailed t-test applied to the data sets (Table 5.1) confirmed that the differences in the values observed for the August 2022 and May 2023 surveys are statistically significantly different.

Table 5.3 – Summary statistics for the August 2022 and May 2023 surveys shown against the July 2019 Urban Area survey for comparison. This highlights the improved survey density achieved by the vehicle mounted system.

Parameter	August 2022	May 2023	July 2019
Total Area Surveyed (m ²)	~23,500	~18,000	~4000
Total No. Measurements	44,161	45,168	5255
Average No. Readings/ m ²	1.9	2.5	1.3
Minimum Total Gamma (cps)	132	124	163
Maximum Total Gamma (cps)	310	264	274
Mean Total Gamma (cps)	212	186	217
Standard Deviation	24	16	16

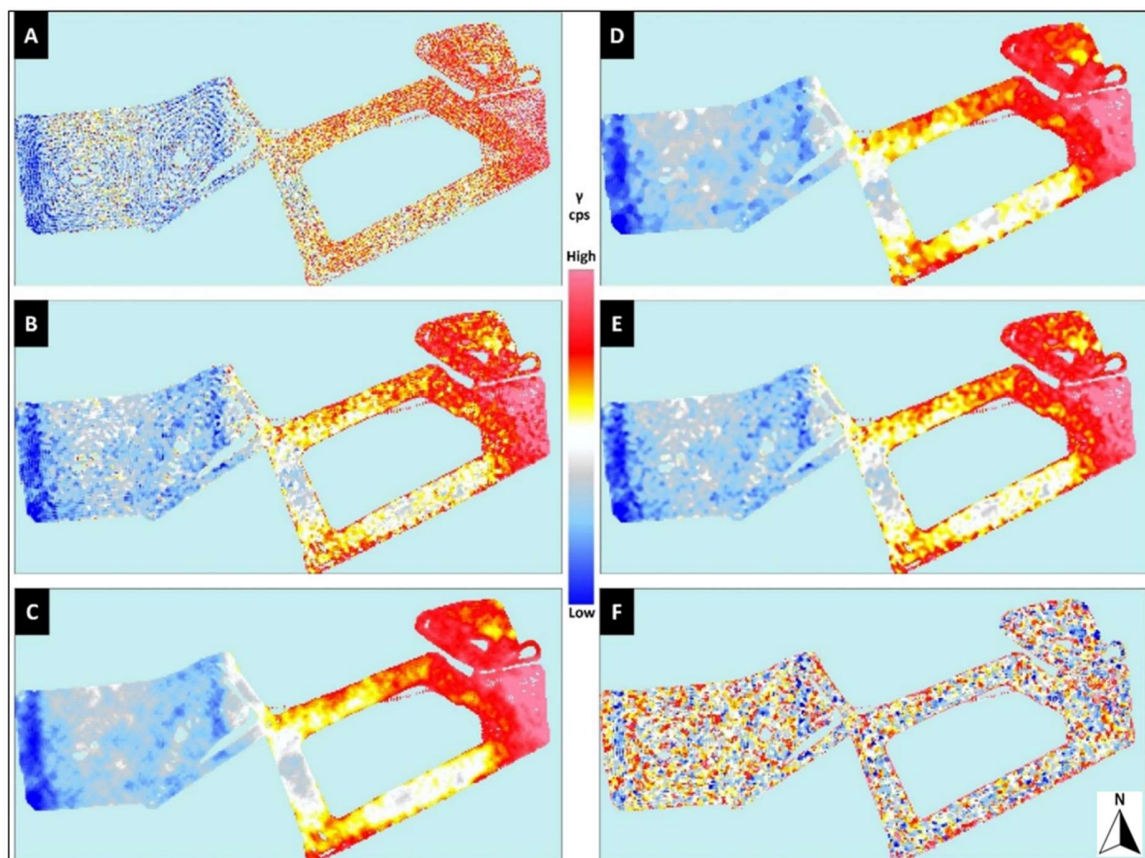
Source: July 2019 data is taken from Robinson *et. al.* (2022)

Total Gamma Emissions

Figure 5.7 presents the visualisations generated through the processing of total gamma counts recorded during the August 2022 survey. This figure reveals the impact of applying different processing tools on data quality.

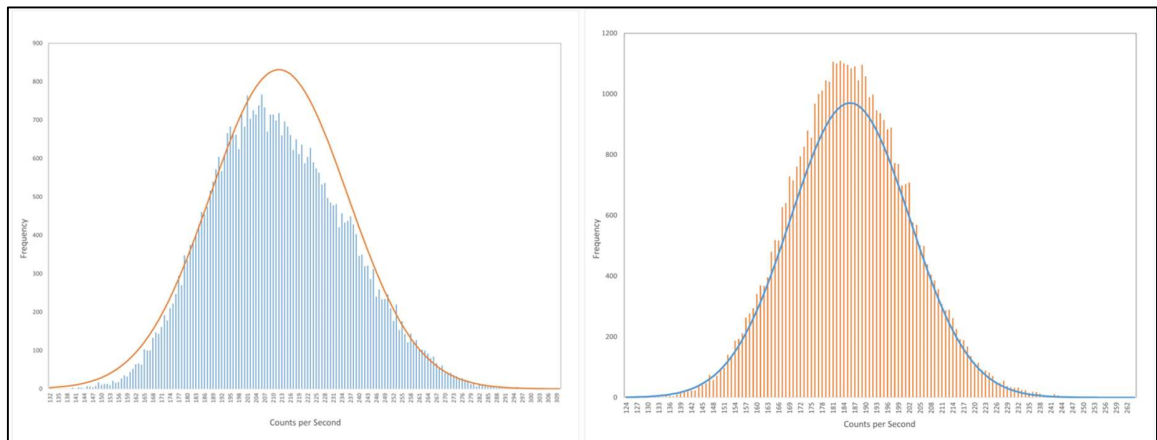
The total gamma dataset from August 2022 identified two clear feature types within the survey area. These are clearly visible in both the raw data (Figure 5.7a) and processed data (Figures 5.7c – 5.7f). The first relates to the presence of linear anomalies on the western extent of each dataset associated with Area A. There are two distinctive north-south aligned anomaly and a less-well defined east-west anomaly running along the bottom of the area. These anomalies align very closely with known Roman roads clearly visible in the fluxgate gradiometer data (Figure 5.2). These linear anomalies are present as areas of depleted radioactivity. The second anomaly of note is the clear transition from an area of generally low background radioactivity (~130 – 190 cps) in Area A, to a gradual increase in Area B, peaking at ~250 – 300 cps on the far eastern side of Area B. This observation is confirmed in the count rate distribution graph (Figure 5.8) which shows that gamma data from the August 2022 survey is not normally distributed. The chart demonstrates a bias towards lower counts per second, which will be influenced by the missing data from Area B where higher counts dominate. The transition from an area of lower background radioactivity in Area A to higher background radioactivity in Area B aligns with a historic field boundary running down the centre of the survey area. The localised area of elevated radioactivity in the far eastern side of Area B may be suggestive of a change in the hydrogeological conditions. These findings are explored further in Section 5.5.

It is recognised that none of the data processing methods were able to delineate the circular anomaly of the temple or House 4, which were the other key features of interest in this area. This may be anticipated, given the comparatively less substantial structures of these features relative to the roads, and considering the survey’s spatial resolution. However, it is noteworthy that there is also an absence of any localised areas of either depleted or elevated levels of radioactivity that could be associated with these structures.



Source: Created from primary data

Figure 5.7 – Impact of different Geoplot processing tools on image quality for August 2022 total gamma counts (cps). The methods presented here are: ‘No Processing’ (A), ‘GPS Gap Fill’ (B), GPS Gap Fill + Wallis Filter (C), GPS Gap Fill + Median Filter (D), GPS Gap Fill + Low Pass Filter (E) and GPS Gap Fill + High Pass Filter (F). The GPS Gap Fill + Wallis Filter (C) was identified as the preferred processing method.



Source: Created from primary data

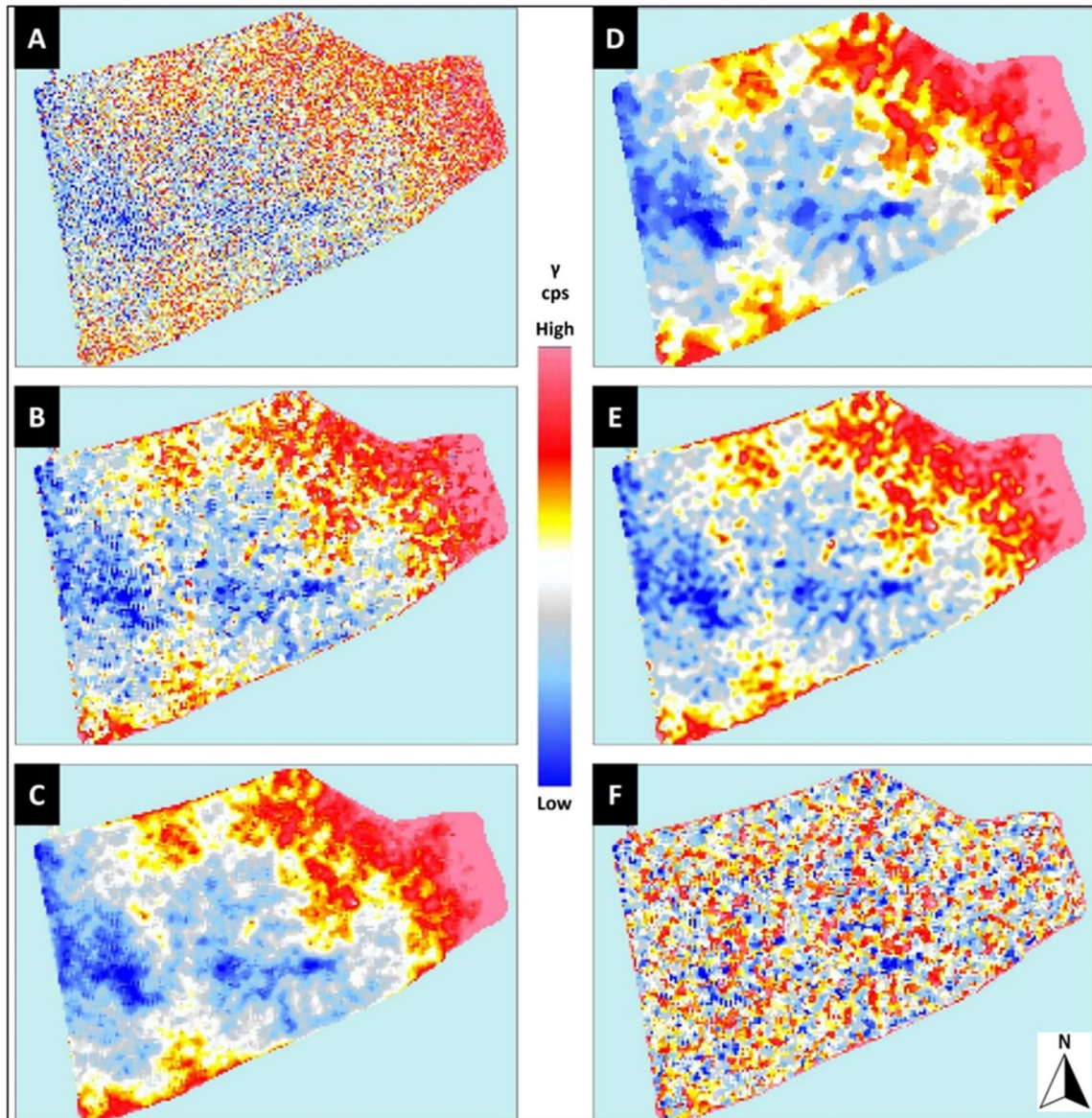
Figure 5.8 – Count rate distribution graphs for the August 2022 (left) and May 2023 (right) datasets. The August 2022 chart indicates that the background radioactivity is not normally distributed.

Visualisations generated for the May 2023 data which focussed solely on Area B are presented in Figure 5.9. As observed for the August figures, it is evident that various anomalies can be identified. Notably, two linear anomalies are visible to varying degrees in all images: one running north to south and the other running east to west. These anomalies, which appear as areas of depleted background radioactivity, again correspond closely to Roman roads as depicted in the existing fluxgate gradiometer data (Figure 5.2). Interestingly, the May 2023 visualisations reflect the same localised area of radioactivity present in the far east side of Area B, as observed in the August 2022 data. Again, this is reflected in the count rate distribution graph for May 2023 (Figure 5.8) which suggests data is not normally distributed, with a bias towards moderate count rates. It is noted that the area containing the highest concentrations of radioactivity on the far-right of the images broadly aligns with the Iron Age Oppida bordering the area.

Again, not all anomalies visible in the Fluxgate Gradiometer data are present in the gamma radiation heat maps. In particular, there is no indication of the presence of the smaller ditch or culvert running through the centre of this survey area.

As might be expected, those filters capable of smoothing the data and drawing out weaker anomalies have yielded the best results for both data sets. Notably, the Wallis (Figures 5.7c and 5.9c), Median (Figures 5.7d and 5.9d) and Low Pass (Figures 5.7e and 5.9e) filters have effectively reduced the 'noise' present and drawn out the linear anomalies associated with the Roman roads without obscuring any detail. In contrast, the high pass filter which acts to remove low frequency

large scale spatial detail (Geoscan 2014) has had a negative impact on image quality, obscuring features otherwise visible (Figures 5.7f and 5.9f).



Source: Created from primary data

Figure 5.9 – Impact of different Geoplot processing tools on image quality for May 2023 total gamma counts (cps). The methods presented here are: ‘No Processing’ (A), ‘GPS Gap Fill’ (B), GPS Gap Fill + Wallis Filter (C), GPS Gap Fill + Median Filter (D), GPS Gap Fill + Low Pass Filter (E) and GPS Gap Fill + High Pass Filter (F). The GPS Gap Fill + Wallis Filter (C) was identified as the preferred processing method.

Understanding the Impact of Individual Radionuclides

Figures 5.10 and 5.11 provide visualisations for the contributions of individual radionuclides within the August 2022 and May 2023 surveys respectively. Interestingly, visualisations for the potassium, thorium and caesium energy window data collected during the August 2022 survey (Figures 5.10 a, c and d) reflect the findings of the total gamma count data; that count rates increase as you move eastwards across the survey areas.

For both the August 2022 and May 2023 surveys, the roads are faintly visible within the potassium energy window (Figures 5.10a and 5.11a), albeit to a lesser degree in the August 2022 figures. This may be due to the generally higher number of counts attributable to potassium in the May survey, making any shielding effects from the roads more prominent.

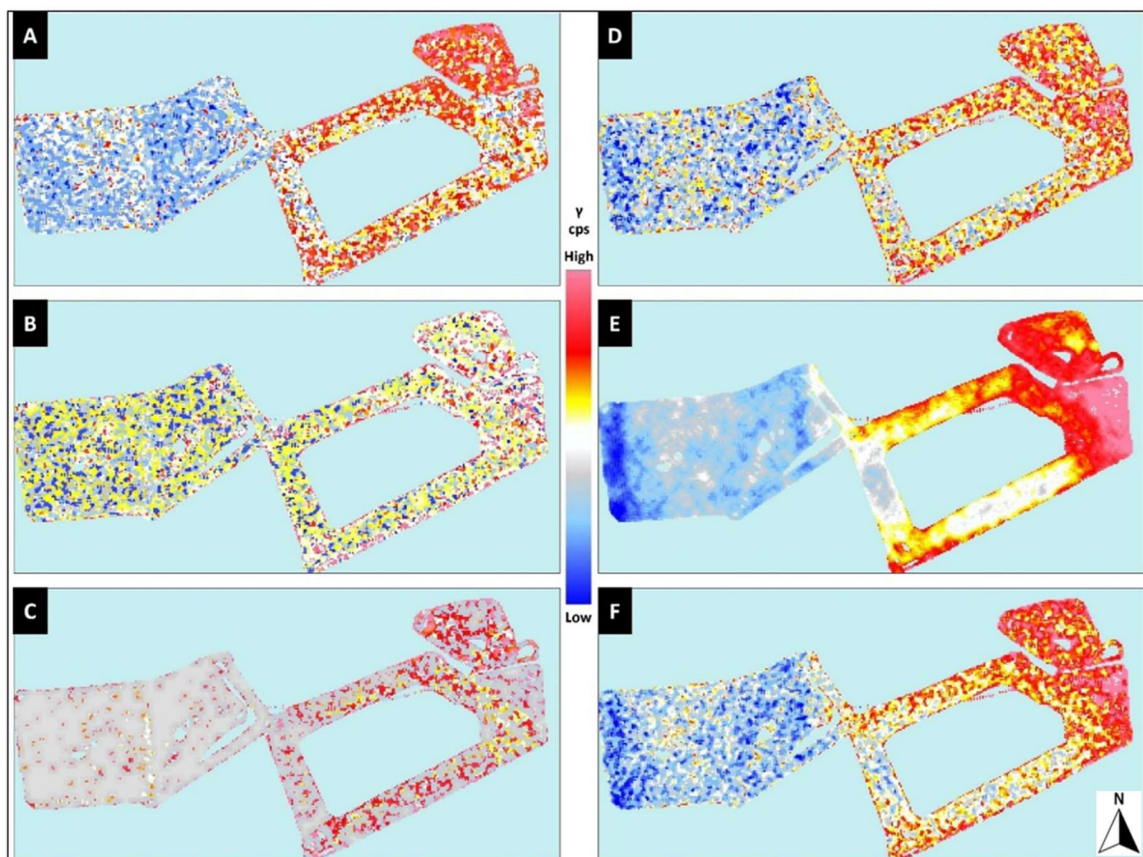
Uranium and thorium appear to be broadly uniformly distributed across the survey areas in both the August 2022 (Figures 5.10b and 5.10c) and May 2023 (Figures 5.11b and 5.11c), with no anomalies visible.

The linear anomalies associated with the Roman roads are visible in the caesium data in the August 2022 visualisation (Figure 5.10d) and to a lesser extent in May 2023 (Figure 5.11d).

Data extracted from the 'below window' (Figures 5.10e and 5.11e) and 'above window' (Figures 5.11e and 5.11f) energy windows show that the contrast for the roads are most prominent here. Surprisingly, the below window visualisations generate the highest quality images, even though it covers the smallest energy range (0 – 530 keV, relative to the 730 – 3000 keV emissions captured in the 'above window' dataset). This is in part attributable to the detector capturing gamma rays emitted from a range of naturally occurring radionuclides with similar energies including Pb-214 (with gamma photon energies of 52.2, 241.9, 295.2 and 31.9 keV), Ra-226 (with a gamma photon energy of 186.2 keV) and U-238 (with gamma photon energies of 49.5 and 113.5 keV) (IAEA 2008). Further, it is noted that NaI detectors of the dimensions used within the Groundhog® system (76 mm x 76 mm) are particularly efficient in this energy window (Mirion 2023).

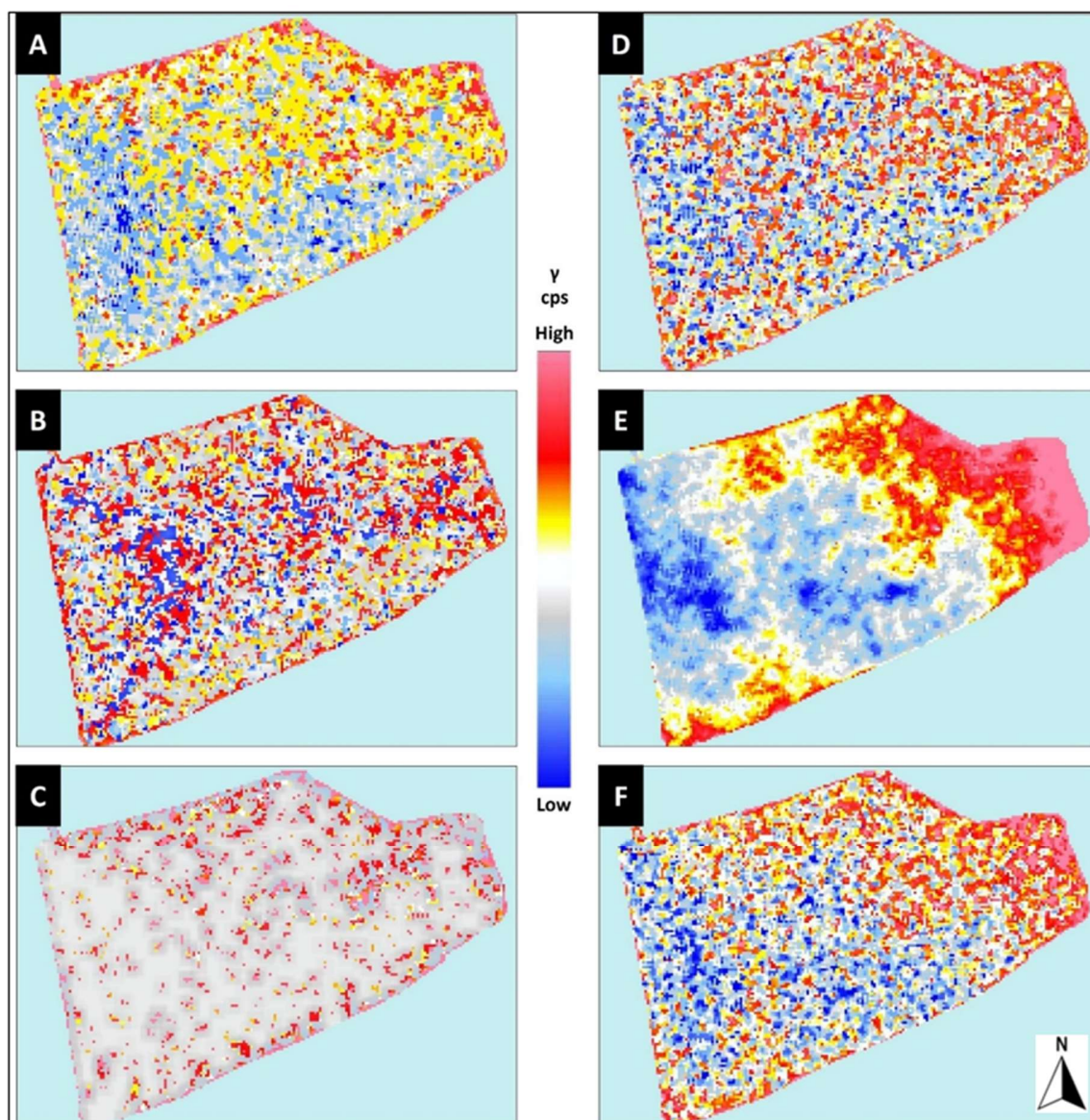
Figures 5.10 and 5.11 suggest that potassium and caesium have the greatest impact on the visibility of any sub-surface features. However, it is acknowledged that it is the total gamma

counts that provide the best quality images overall. This is particularly well demonstrated in Figures 5.12 and 5.13 which show the combined August 2022 and May 2023 total gamma visualisations overlaying the Fluxgate Gradiometer data of Creighton and Fry 2016. These figures clearly show the alignment of the Roman roads between the two types of data. Figure 5.13 also provides an overlay of building outlines for further context. This confirms the absence of other key features such as the temple.



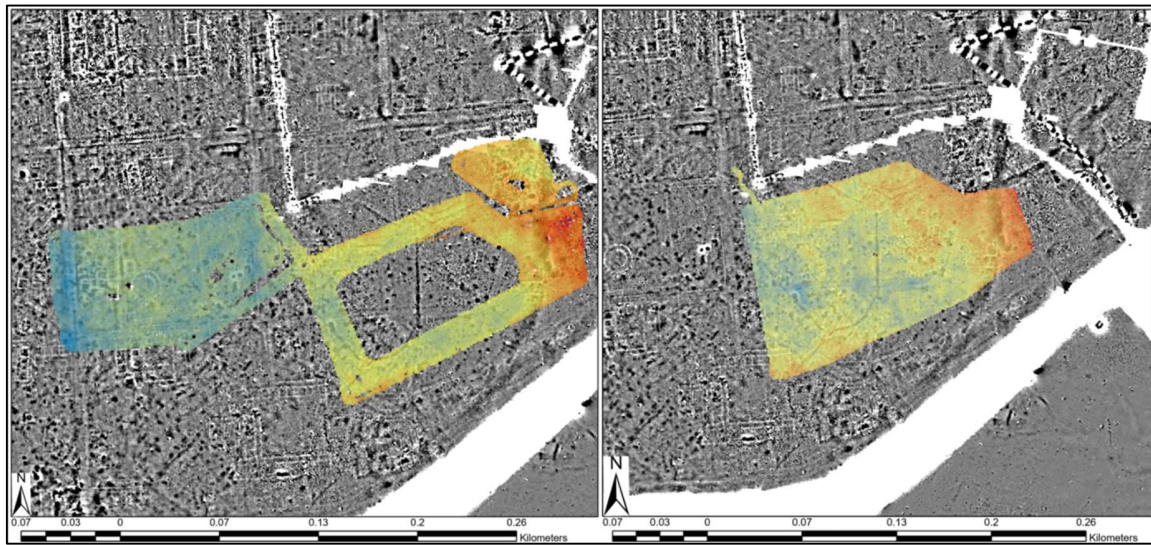
Source: Created from primary data

Figure 5.10 – Application of the GPS Gap Fill + Wallis Filter to the following regions of interest within the August 2022 dataset, as per Table 5.2: Potassium (A), Uranium (B), Thorium (C), Caesium (D), Below Window (E) and Above Window (F).



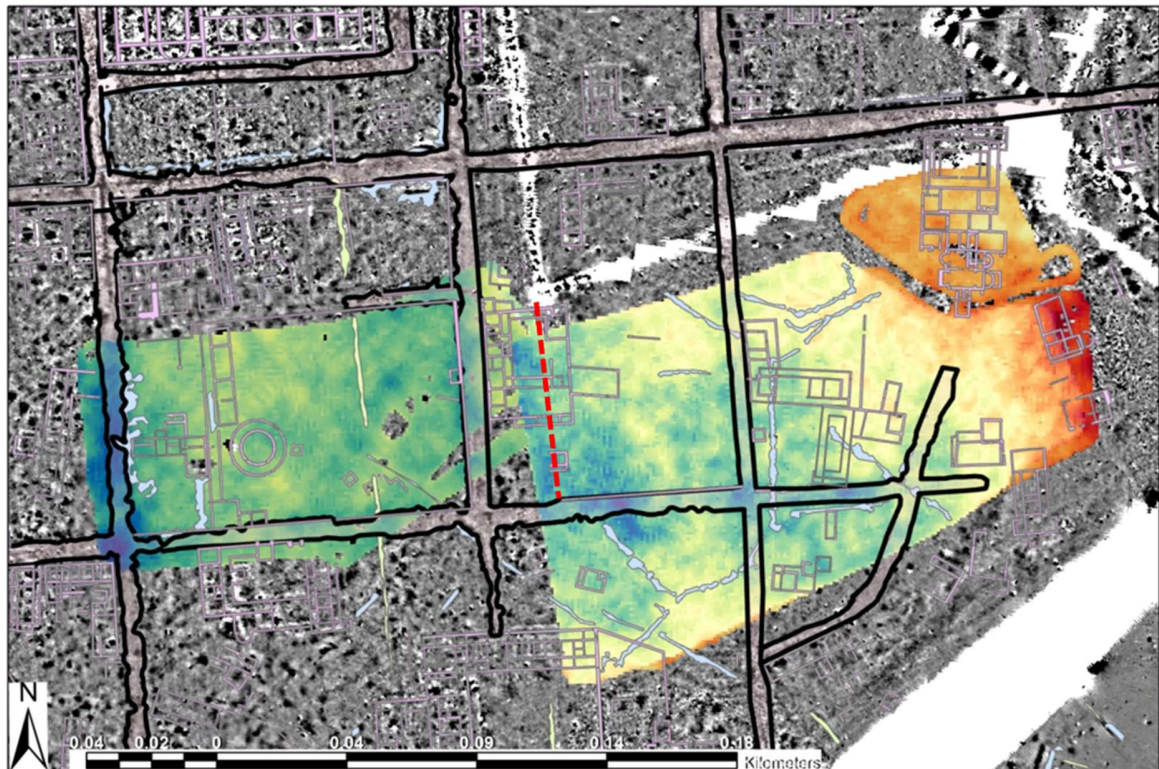
Source: Created from primary data

Figure 5.11 – Application of the GPS Gap Fill + Wallis Filter to the following regions of interest within the May 2023 dataset, as per Table 5.2: Potassium (A), Uranium (B), Thorium (C), Caesium (D), Below Window (E) and Above Window (F).



Data Source: Fluxgate Gradiometer Data from Creighton and Fry (2016).

Figure 5.12 – August 2022 (left) and May 2023 (right) Geoplot-processed data overlaid on existing Fluxgate Gradiometer data (± 7 nT – black high to white low), demonstrating the alignment of observed anomalies. Gamma radiation data has been set at 25% transparency to reveal underlying anomalies.



Data Source: Fluxgate Gradiometer data and building overlays from Creighton and Fry (2016).

Figure 5.13 – Combined August 2022 and May 2023 Geoplot-processed data overlaid on existing Fluxgate Gradiometer data ($\pm 7\text{nT}$ – black high to white low), with previously mapped features overlaid demonstrating alignment of the anomalies in the gamma radiation data with known features. Overlaid data includes the Antiquaries Great Plan (pink lines), the Fluxgate Gradiometer interpretation of the roads (black outlines), positive linear anomalies in the Fluxgate Gradiometer data (blue lines) and historic field boundary from 1759 (red dotted line).

5.3.8 Discussion

The surveys undertaken as part of this latest study underpin the findings of the preliminary investigation completed by Robinson, *et. al.* (2022). They have confirmed that portable gamma surveying methods can be effective at identifying features of archaeological interest. This is achieved by detecting measurable differences in concentrations of naturally occurring radioactive material present in or above archaeological targets and surrounding soil. However, as for the preliminary study, the August 2022 and May 2023 surveys have yielded mixed results.

Neither of the buildings or the thin linear Roman trench within *Insulae* VII, XXXV or XXXII were capable of generating measurable contrasts in radioactivity as to be distinguished in the

visualisations. This reflects the findings of the preliminary study which also failed to delineate the outlines of known buildings. It is possible that this is attributable to the less robust structures of these buildings, reducing their ability to create a sufficient contrast in background gamma radiation measurements. This effect may be exacerbated by the resolution of the surveys. Alternatively, it is possible that the materials of construction have a similar gamma radionuclide composition to the surrounding soil than observed for the roads. Whilst the difficulty in clearly delineating these less substantial features may be expected for these reasons, it is interesting that there are no general areas of localised increased or decreased counts attributable to the disturbance caused by this past activity. Further work is therefore planned to explore this finding through collection and analysis of samples of building materials and soils.

A welcome finding of this latest study was the ability to delineate road structures. This was not achieved in the preliminary study. In both the August 2022 and May 2023 data, roads appear as areas of low background radioactivity. Particular attention is drawn to the roads visible in the August 2022 'total gamma' visualisations (Figure 5.7). In all iterations of this image, Silchester's primary north-south road, visible on the left-hand side of each image is the most prominently featured, followed by a secondary north-south road to the right. In contrast, the east-west road is showing a very weak contrast and is incomplete in the gamma data. This variability is absent in the Fluxgate Gradiometer data shown in Figure 5.2. It is suggested that variations in the observed gamma radionuclide content of the roads may be indicative of varying thicknesses of road material which possesses a lower concentration of radioactive material relative to the surrounding soil. Consequently, it shields the gamma radiation emitted from the underlying soil to a different extent. This is supported by the work of Fulford, Clark and Pankhurst (2024) who note that the main north-south road is a substantial structure, measuring up to 7.6 m in width and approximately 1 m in thickness. In contrast, the east-west road is up to 6 m wide and 0.85 m thick (*ibid*). Another factor contributing to the observed variations in the gamma radionuclide content of the roads is the extent of material consolidation. Previous excavations revealed that the materials comprising the main north-south road had become cemented together, presenting a more solid mass (M. Fulford, personal communication). This increased consolidation, combined with the increased thickness in the road material, may have enhanced the shielding effect. The cause of this cementation process is unknown but may be attributable to the heavy use of this street and its accommodation of carts carrying substantial loads of up to 500 kg (M. Fulford,

personal communication). This discovery suggests that portable gamma radiation data collected as part of an archaeological investigation could aid interpretation of traditional geophysical survey outputs, enhancing the value of other non-intrusive surveys. This is particularly relevant when it is recognised that in the fluxgate gradiometer dataset, the clear delineation of the roads is largely attributable to the accompanying roadside ditches, rather than the deposition of the flint and gravel itself.

In addition to the linear anomalies attributable to the roads, another anomaly of interest is the transition from an area of lower radioactivity in Area A to higher activity in Area B. This is clearly visible in the August 2022 survey data (Figure 5.7). The point of transition – where Areas A and B connect, aligns closely with a historic field boundary visible in a 1759 plan of Silchester, as depicted in Figure 5.13. This boundary may be indicative of differing land uses which have caused changes in soil chemistry or composition, which in turn has influenced the adsorption/ retention of radionuclides. This field boundary may also be visible in the gamma radiation data. In the May 2023 survey, there is a north-south aligned linear anomaly, present as an area of depleted radioactivity, running along the left-hand edge of the survey area (Figure 5.9). Specifically, this appears to be attributable to localised reductions in concentrations of potassium, thorium and caesium (Figure 5.11). As shown in Figure 5.13, this linear anomaly does not align with any of the Roman roads, but does closely follow the 1759 boundary. It is noted that this boundary is not present in the later 1841 tithe map for the area (Hampshire Archives 2023a). However, the accompanying Tithe Award identifies the area within which the gamma radiation survey data sits as the “Watch Field and the Nine Acres” (Hampshire Archives 2023b). The area to the right of the 1759 field boundary is approximately nine acres in size. This further suggests that the two sides of this field remained distinct for an extended period, even though the physical field boundary was no longer present.

The area containing the highest levels of radioactivity, running along the right-hand edge of Area B is present in both the August 2022 and May 2023 data. This aligns closely with the location of the Iron Age ditch and an area prone to waterlogging.

The waterlogged area aligning with the Iron Age ditch is expected to have a different chemistry to the adjacent soil. This difference can influence the behaviour of any naturally occurring

radionuclides present. For example, uranium in soils is commonly found as a mobile form of UO_2 in its U(VI) state, particularly in slightly basic to acidic soils (Smedley and Kinniburgh 2023). However, under strongly reducing conditions, the uranium can be reduced to its U(IV) state, leading to its precipitation as an immobile form of UO_2 or otherwise become sorbed onto the surface of soil particles (Smedley and Kinniburgh 2023) thereby increasing uranium concentrations in the soil. The water logged area at Silchester could provide such conditions. Further, this area is rich in clay deposits, contributing to waterlogging. The Iron Age defensive ditch is cut into London Clay, eventually becoming infilled with a mixture of clays and anthropogenic deposits, including brick and organic materials (M. Fulford, personal communication). The location of the elevated radioactivity coincides with an area where the gravel capping over the London Clay had been eroded away (M. Fulford, personal communication). The presence of these clay deposits increase the chance of accumulating radionuclides such as caesium-137 which adsorbs strongly to clay particles (Ritchie 1998). The authors intend to further characterise this area as part of ongoing research to gain a better understanding of the geochemical properties of the area and how these properties vary across the site profile.

The equipment failure during the August 2022 survey and requirement to re-survey the eastern side of the site provided an additional opportunity to explore the impact of changing soil moisture content on the effectiveness of portable gamma surveying, recognising the potential for shielding from interstitial water. The August 2022 survey was conducted in what may be considered optimal ground conditions; minimal soil moisture following an extended period of very low rainfall and high temperatures. Indeed, evidence suggests that this was the fourth driest summer on record (McCarthy 2022). This contrasts with the meteorological conditions in May 2023, where the first half of the month saw rainfall levels exceed the mean value for the period 1991 – 2020 for the same month (Met Office 2023). As a result, soil moisture content and therefore potential for increased gamma radiation shielding was much higher in May. It might therefore be expected that the May 2023 survey would yield lower quality results. However, as seen in Figures 5.7 and 5.9, groundwater in this case does not appear to have a significant impact on data quality, with road structures clearly visible in both conditions. However, it is noted that this survey has resulted in generally lower levels of radioactivity recorded overall, which is expected to be attributable to a degree of shielding by interstitial water. It is recognised that this result in isolation is insufficient to draw any meaningful conclusions on this aspect and therefore further research is required to

fully understand the impact of groundwater conditions on gamma survey data quality in archaeological applications.

In addition to the aspects identified for further investigation already discussed, it is acknowledged that there are still multiple other areas that require further exploration. This includes conducting surveys at different locations to explore the impact of varying geologies, testing the responses of different target types (e.g. considering materials of construction, size and burial depths) and the completion of surveys in more controlled conditions to facilitate better control of individual variables.

5.3.9 Conclusions

This study has provided a valuable opportunity to further challenge the viability of portable gamma surveying as a contributory tool for non-intrusive archaeological propection. This has been achieved by:

1. Testing the replicability of the technique by surveying areas containing analogous target types to the preliminary study completed by the authors;
2. Testing scalability of the technique by applying a vehicle-mounted Groundhog® system; and
3. Exploring alternative data processing methods to improve the quality of the visualisations used to identify anomalies that could be attributable to archaeological features of interest.

Completion of this latest suite of gamma radiation surveys has confirmed that the method can be successfully scaled to encompass a much larger survey area without compromising data quality. As per the preliminary investigation, the latest surveys have yielded mixed results with the Groundhog® system successfully delineating some known archaeological features such as Roman roads, whilst failing to detect others such as buildings. Interestingly, the types of targets detectable have not been consistent between the two studies. In the preliminary study, roads and buildings could not be identified whereas ditches created clear anomalies. In this latest study, roads were consistently capable of generating anomalies within the gamma radiation data, whereas this was less successful for the ditches. Where the area of elevated radioactivity aligns

with the Iron Age ditch, there is some uncertainty as to whether the anomaly can be attributed to the ditch itself, or if it is indicative of ground disturbance associated with past excavations.

The strength of the anomalies associated with each road may indicate variations in either the depth of road material or construction materials, suggesting that gamma radiation data could aid interpretation of other geophysical survey outputs. This strengthens the argument that portable gamma surveying can add value to non-intrusive archaeological investigations.

There is notable uncertainty regarding the causes of some of the observed outcomes. This uncertainty relates to the absence of measurable differences in gamma radiation levels present in/ over archaeological targets (identified as being strong candidates) and surrounding soils, and the discrepancy in the types of targets discernible in the preliminary and current investigations. Consequently, additional investigations and research is imperative if these uncertainties are to be adequately addressed. This will be achieved through the direct radiochemical analysis of samples of soil and target material, and surveying of new archaeological sites.

The use of an alternative software tool, Geoplot, has provided a valuable opportunity to apply different processing tools to enhance the quality of visualisations generated. This was successful, with the Wallis Filter in-particular able to draw out anomalies without deviating too far from the raw data.

The ability to investigate the influence of individual radionuclides on the results observed has also produced interesting insight and may aid interpretation of the total gamma visualisations. This includes identifying areas of ground disturbance indicative of previous excavation works. It is believed that this area also warrants further explanation. Overall, this latest study has proven to be a successful progression of the preliminary investigation confirming that portable gamma surveying methods can identify archaeological features of interest. However, further work is now required to better understand what types of features are most amenable to this technique, and how it can be most effectively applied.

5.3.10 References

Please see Section 5.5

5.4 Conclusions and Next Steps

The second set of Silchester surveys has yielded positive results. Whilst it was not possible to delineate all targets surveyed (the buildings and temple), the Roman roads are clearly visible in the gamma radiation data. Exciting developments in this latest research include the ability to detect differences in the physical properties of the three identified roads, and the ability to detect differences in the radiochemical characteristics of the site. In one case, this is indicative of a possible historic field boundary.

The reasons why some archaeological features can create measurable differences in gamma radiation intensities whilst others cannot remain unclear. This is particularly perplexing when considering that roads surveyed during the preliminary investigation were undetectable, whereas those in this latest study were clearly identifiable. Further research is necessary to understand what may be causing this inconsistency. It is also recognised that to date, surveys have only been conducted within the Silchester site. It is therefore uncertain if the findings to date are unique to Silchester, or if similar results could be achieved at other archaeological sites. Recommendations for further work therefore include:

- Repeating Groundhog surveys at other archaeological sites within the UK, testing the method on different target types and geologies.
- Analysing archaeological and environmental samples to determine concentrations of naturally occurring radioactive material, to understand what might be causing measurable differences in radioactivity and to aid in the interpretation of heat maps.
- Using the insights gained from additional work to begin developing explanations for the observed results.

The following chapter addresses these recommendations. It presents the findings of Groundhog surveys undertaken at archaeological sites in Bisham and East Heselton, comparing these results with those from Silchester. X-ray fluorescence data from the analysis of archaeological and environmental samples is also included as part of the data analysis. The output from this next phase of research culminates in the development of a model that can be used to more effectively plan research at other archaeological sites, taking into account local geology and anticipated target types.

5.5 References

Aliyev, C. (2004) NORM in Building Materials, in: IAEA (2004) Naturally Occurring Radioactive Materials (NORM IV): Proceedings of an International Conference held in Szczyrk Poland, 17 – 21 May 2004, IAEA-TECDOC-1472, Vienna Austria

Creighton, J. and Fry, R. (2016) Silchester: changing visions of a Roman town: integrating geophysics and archaeology: the results of the Silchester mapping project, 2005 – 10, Britannia monograph series; no. 28, Society for the Promotion of Roman Studies, ISBN: 9780907764427, pp:486

Cuenca-Garcia, C. (2018) Soil geochemical methods in archaeogeophysics: Exploring a combined approach at sites in Scotland, *Archaeological Prospection*, **26** (1): 57 – 72, DOI: <https://doi.org/10.1002/arp.1723>

Davies, M. Clark, R. and Adsley, I. (2011) High-Density Gamma Radiation Spectrometry Surveys of Contaminated Land, Proceedings of the 14th International Conference on Environmental Remediation and Radioactive Waste Management, September 25 – 29, Reims, France

Davies, M. (2015) Health Physics Procedure HPP357 – Calibration of Groundhog Detectors, Issue A, September 2015, Internal Report for NUVIA Limited UNPUBLISHED

Digimap (2023) Silchester Overview, PDF Map, Scale 1:10000, Projection: British National Grid (EPSG:27700), OS Master Map, March 2023, Ordnance Survey using Digimap Ordnance Survey Collection, <https://digimap.edina.ac.uk/>, created 22nd October 2023

ESRI (2022) ArcGIS Pro: How inverse distance weighted interpolation works, <https://pro.arcgis.com/en/pro-app/latest/help/analysis/geostatistical-analyst/how-inverse-distance-weighted-interpolation-works.htm>, Accessed 14th January 2022

Fulford, M. Clarke, A. Eaton, J. Fry, R. Lambert-Gates, S. Machin, S. Pankhurst, N. and Wheeler, D. (2019) Silchester Roman Town: The Baths 2019, Department of Archaeology, University of Reading, Reading UK

Fulford, M. (2021) Silchester Revealed: The Iron Age and Roman Town of Calleva, Windgather Press, Havertown, ISBN: 9781911188865

Fulford, M. Clarke, A. and Pankhurst, N. (2024) (accepted for publication) Silchester Insula IX. Oppidum to Roman City, c. A.D. 85-125/50. Final Report on the Excavations 1997 – 2014, London, Society for the Promotion of Roman Studies, Britannia Monograph 37

Gaffney, C. and Gater, J. (2011) Revealing the Buried Past: Geophysics for Archaeologists, Tempus Publishing Ltd, Gloucestershire UK

Geoscan (2014) Geoplot Version 3.0 for Windows: Datasheet Issue 13, GPW300_13 PPX2, June 2014, http://www.geoscan-research.co.uk/Geoplot3_v13_Data_Sheet.pdf, Created June 2014, Accessed October 2023

Hampshire Archives (2023a) Plan of the Parish of Silchester in the county of Hants 1841, Accessed: October 2023

Hampshire Archives (2023b) Apportionment of the Rent-Charge in lieu of Tithes in the Parish of Silchester in the County of Southampton (sic), Published by Routledge London 1841, Accessed: October 2023

IAEA (2003) Extent of Environmental Contamination by Naturally Occurring Radioactive Material (NORM) and Technological Options for Mitigation, Technical Report Series No. 419, International Atomic Energy Agency, Vienna

IAEA (2023) Radiation in Everyday Life, <https://www.iaea.org/Publications/Factsheets/English/radlife>, International Atomic Energy Agency (IAEA), Accessed: 21/01/2023

Jordan, D. (2009) How Effective is Geophysical Survey? A Regional Review, *Archaeological Prospection*, **16**: 77 – 90, DOI: 10.1002/arp.348

Kozhevnikov, N.O. Kharinsky, A.V. and Snopkov, S.V. (2018) Geophysical prospection and archaeological excavation of ancient iron smelting sites in the Barun-Khal valley on the western shore of Lake Baikal (Olkhon region, Siberia), *Archaeological Prospection*, **2018**: 1 – 17, <https://doi.org/10.1002/arp.1727>

Lee, C.J. and Burgess, P.H. (2014) Good Practice Guide 14, The Examination, Testing and Calibration of Portable Radiation Protection Instruments, Issue 2, First Issued – 1999, Updated – 2014, National Physics Laboratory (NPL) Middlesex UK

Linford, N., Linford, P. and Payne, A. (2019) Silchester Roman Town Hampshire: Report on Geophysical Surveys June 2009, March 2014 and July 2015, Research Report No. 85-2019, Historic England, Portsmouth UK, ISSN: 2059-4453

Lovelock, J. (2000) Gaia: a new look at life on Earth, Oxford University Press, ISBN: 9780192862181

McCarthy, M. (2022) Guest Post: A Met Office review of the UK's record-breaking summer in 2022, Carbon Brief, <https://www.carbonbrief.org/guest-post-a-met-office-review-of-the-uks-record-breaking-summer-in-2022/>, Last Updated: 28/09/2022, Accessed: 17/08/2023

Met Office (2023) May 2023 Monthly Weather Report, https://www.metoffice.gov.uk/binaries/content/assets/metofficegovuk/pdf/weather/learn-about/uk-past-events/summaries/mwr_2023_05_for_print.pdf, Last Updated: May 2023, Accessed: October 2023.

Milsom, J. and Eriksen, A. (2011) The Geological Field Guide Series: Field Geophysics, Fourth Edition, Wiley-Blackwell, Sussex UK

Mirion (2023) Gamma and X-Ray Detection, <https://www.mirion.com/discover/knowledge-hub/articles/education/nuclear-measurement-fundamental-principle-gamma-and-x-ray-detection>, Mirion Technologies, Accessed 10th December 2023, Mirion Technologies, Harwell UK

Porcelli, F., Sambuelli, L., Comina, C., Spanò, A., Lingua, A., Calantropio, A., Catanzariti, G., Chiabrando, F., Fischanger, F., Maschio, P., Ellaithy, A., Airolidi, G., & De Ruvo, V. (2020). Integrated Geophysics and Geomatics Surveys in the Valley of the Kings. *Sensors (Basel, Switzerland)*, **20** (6): 1552, DOI: 10.3390/s20061552

Ritchie, J.C. (1998) ¹³⁷Cs use in estimating soil erosion – 30 years of research *in*: IAEA (1998) Use of ¹³⁷Cs in the Study of Soil Erosion and Sedimentation, IAEA-TECDOC-1020, International Atomic Energy Agency, Vienna, July 1998

Robinson, V., Clark, R., Black, S., Fry, R., & Beddow, H. (2022). Portable gamma ray spectrometry for archaeological prospection: A preliminary investigation at Silchester Roman Town. *Archaeological Prospection*, **29** (3): 353–367, DOI: <https://doi.org/10.1002/arp.1859>

Ruffell, A. and McKinley, J. (2008) *Geoforensics*, Wiley, Blackwell, New Jersey USA

Simon, F. X. Kalayci, T. Donati, J.C. Cuenca-García, C. Manataki, M. and Sarris, A. (2015) How efficient is an integrative approach in archaeological geophysics? Comparative case studies from Neolithic settlements in Thessaly (Central Greece), *Near Surface Geophysics*, **13** (6): 633 – 643, DOI: 10.3997/1873-0604.2015041

Smedley, P.L. and Kinniburgh, D.G. (2023) Uranium in natural waters and the environment: Distribution, speciation and impact, *Applied Geochemistry*, **148**: 1 – 63, <https://doi.org/10.1016/j.apgeochem.2022.105534>

Ward, J. (1911) *Romano-British Buildings and Earthworks*, Chapter 10, Volume 24 of Antiquary's Books, Methuen & Company Limited, North Yorkshire, ISBN: 0598613269,9780598613264

Wynn, J.C. (1986) A review of geophysical methods in archaeology, *Archaeology*, **1** (3): 245 – 257, DOI: 10.1002/gea/3340010302

Acknowledgements

This unique investigation was possible thanks to Nuvia Limited who provided access to the Groundhog® Fusion Vehicle Mounted System and supporting software tools. The authors wish to express their thanks and gratitude to Ben Kolosowski and the University of Reading for permitting and facilitating access to the Silchester site, and to Anthony Sweeney for helping to set up the equipment at Silchester.



CHAPTER 6

Exploring the Value of
Gamma Radiation Surveys in
Archaeological Prospection –
A Consolidating Study

6 EXPLORING THE VALUE OF GAMMA RADIATION SURVEYS IN ARCHAEOLOGICAL PROSPECTION – A CONSOLIDATING STUDY

6.1 Introduction to the Paper

Chapter 6 of this thesis comprises the third and final paper to be submitted to *Archaeological Prospection* for consideration. At time of writing, the manuscript is currently undergoing final review from co-authors in preparation for final submission.

This paper presents the findings from additional Groundhog surveys undertaken at two new archaeological sites; Bisham and East Heselton. Additionally, it includes portable x-ray fluorescence (pXRF) data for environmental and archaeological samples collected from these sites. The aims of this study are two-fold. Firstly, by conducting surveys at new sites with different geologies and target types, it is demonstrated that the findings from previous studies are not unique to Silchester, but can be applied more widely. Secondly, the results from the Bisham and East Heselton studies are compared and contrasted with those from Silchester, aiming to better understand the mechanisms behind the recorded observations. The pXRF data has been helpful in supporting this analysis.

Lessons learned from processing data from the second Silchester study (Chapter 5) have been applied to the Bisham and East Heselton data, aiding the generation of high quality gamma radiation distribution maps in Geoplot. These have successfully drawn out anomalies of archaeological interest at both sites.

A key outcome from this final study is the development of a model that can be used to help target archaeological sites that are most likely to yield positive results based on the physical characteristics of anticipated targets and soil type. The findings from the Groundhog surveys and pXRF analyses undertaken to date were used to identify conditions likely to produce strong positive anomalies (such as those found in East Heselton), strong negative anomalies (such as the Roman roads seen in the Silchester data) and a predicted 'region of invisibility' where variations in

gamma radiation activities between the targets and surrounding soil are undetectable. This model will need to be reviewed and refined as more data become available.

Methodology Rationale

The Bisham study was initially a pilot project undertaken with the primary aim of becoming familiar with the Groundhog equipment, setting up and undertaking surveys and processing the resultant data. There was no expectation that the survey would yield usable data, but rather that the experience gained would be used to inform the development of a more refined methodology for the planned hand-held survey at Silchester. However, as discussed in this paper, the Bisham study produced positive results, although the implications were not fully understood at the time. The methodology applied closely followed that deployed at nuclear licensed sites and proved effective. No changes were therefore required for the preliminary study at Silchester.

The vehicle-mounted survey at East Heselton was informed by the size of the target – a ladder settlement covering approximately four hectares. A vehicle-mounted survey was the only feasible method of surveying the entire area within the available time. The deployment method was informed by the experience gained from the first vehicle mounted survey at Silchester. Due to the quality of the outputs generated in Geoplot for the second Silchester study, the same approach was continued for the Bisham and East Heselton data, applying identical gap fill and Wallis filters.

Journal Rationale

As with the previous papers, the work undertaken in this study aligns with the aims and scope of *Archaeological Prospection* and is considered the best fit for publication of this final paper.

6.2 Confirmation of Contribution

Victoria Robinson: Conceptualisation, literature review, methodology development, data collection (Bisham, East Heselton), data processing, data analysis, writing – original draft, incorporation of peer reviewer comments.

Dr Stuart Black: Conceptualisation, supporting data analysis, writing – review and editing.

Dr Robert Fry: Conceptualisation, permissions for access to Bisham, fieldwork setup, supporting data analysis, writing – review and editing.

Dr Helen Beddow: Conceptualisation, writing – review and editing.

Robert Clark: Preparation of Groundhog equipment, supporting data processing.

Dr Philippe De Smedt: Writing – review and editing, data collection (East Heselton).

Jeroen Verhegge: Writing – review and editing, data collection (East Heselton)

6.3 Published Paper

6.3.1 Keywords

Archaeology, Bisham, East Heselton, Gamma Radiation Surveying, NUVIA Groundhog®, Radioactivity, Silchester, pXRF

6.3.2 Abstract

This study advances research on the efficacy of portable gamma radiation surveys in detecting buried archaeological features. The method aims to measure and visualise, through the production of gamma radiation distribution maps, small variations in gamma radiation intensities present in archaeological targets and surrounding soil. Gamma radiation surveys were conducted at three archaeological sites (Bisham, East Heselton and Silchester) using Nuvia Limited's Groundhog® system. Portable XRF data from the analysis of environmental and archaeological samples were used to aid interpretation of the survey data.

The gamma radiation surveys successfully identified larger and distinctive features (both archaeological and geological), with clear anomalies visible in the gamma radiation distribution maps for all three sites. However, not all archaeological targets visible in the extant geophysical data were detectable in the gamma radiation surveys. The research has highlighted the value of being able to interrogate data from individual energy windows with some (including the 'Above Window' and 'Below Window' energy windows) drawing out anomalies more effectively than the total gamma radiation data. The XRF analyses provided valuable insights for interpreting these findings.

Our research has shown that portable gamma surveying methods show significant potential in assisting geophysical data interpretation, revealing additional insights into soil conditions, the physical characteristics of archaeological features, and historic field boundaries. This technique may not be comparable to existing geophysics methods in terms of its ability to consistently and reliably identify archaeological features. However, it presents promising opportunities for improvement and further exploration.

6.3.3 Introduction

The potential for ancient human activities to cause measurable and preservable variations in naturally occurring radiation, thereby enabling the identification of buried archaeological features using portable gamma radiation surveying methods, prompted the authors to undertake a programme of preliminary research aimed at exploring this previously unexamined hypothesis. These preliminary investigations were broadly successful. The methodologies applied were reviewed and refined, testing the scalability and repeatability of the technique by progressing from hand-held to vehicle-mounted gamma radiation surveys and surveying multiple analogous targets at the same site. Additionally, the impact of conducting collimated (shielded) and uncollimated surveys was explored. Building on the positive results from the preliminary studies, further gamma radiation surveys were conducted at two additional archaeological sites. This paper presents the findings from these additional surveys, consolidates the new information with the insights gained from the preliminary studies and interrogates the combined data to better understand the factors driving and influencing the observed results.

The preliminary research undertaken focussed on the Roman town of Silchester. Here, gamma radiation surveys were conducted at multiple locations using a portable gamma radiation detection - Nuvia Limited's Groundhog Fusion® (Groundhog®) system.

The subsequent sub-section briefly explores the outcomes of the research undertaken at Silchester using the Groundhog® system, the results of which were mixed, but positive overall. The generated gamma radiation distribution maps effectively delineated several archaeological features including roads and ditches. Further, the data yielded additional insights into the archaeological and geological context of the Silchester site as explored below. The findings from the Silchester surveys highlighted the need for further work to better ascertain the technique's efficacy and understand the observed results. Specifically, why certain features are discernible in the gamma radiation distribution maps whilst others remain elusive.

In an effort to address these uncertainties, data collected from gamma radiation surveys undertaken by the authors at three distinct archaeological sites of interest was sourced; Silchester in Hampshire, as covered in previous published works, Bisham in Berkshire and East Heselton in

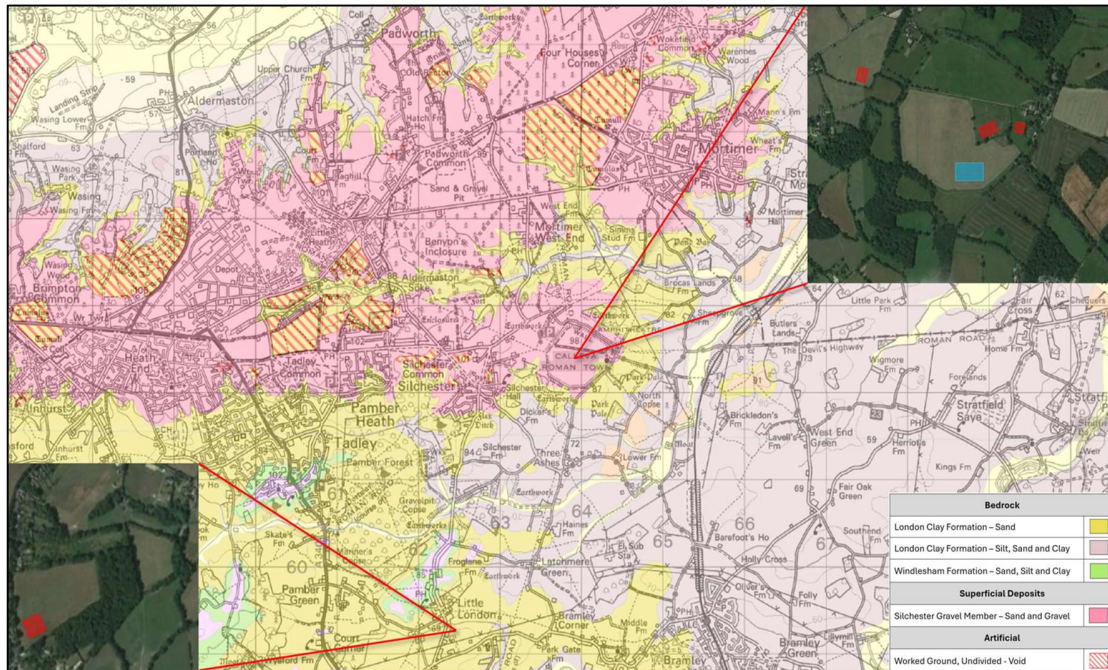
Yorkshire. Further, the scope of work was expanded to include analysis of different material types using pXRF, aiding in data interpretation.

The research presented here aims to build on the preliminary studies at Silchester, to provide greater insight in to the value of gamma radiation surveying as an adjunctive non-intrusive method for archaeological prospection. Further, this study endeavours to explore how the variability in the radiological properties of different geologies and soil types contribute to the creation of distinct anomalies in gamma radiation distribution maps, and influence the ability to delineate archaeological features. These aims have been pursued through the completion of further gamma radiation surveys at other archaeological sites and applying new/ additional analytical methods including the portable x-ray fluorescence (pXRF) analysis of materials collected from these sites. The pXRF analyses in particular sought to identify potential correlations between the radiological composition of soils and the materials used in the construction of the archaeological targets present at the site.

Overview of Current Findings (Background and Context)

The Groundhog® system was deployed at Silchester in various configurations and environmental conditions, targeting multiple types of archaeological feature at multiple locations (Figure 6.1) (Robinson et al. 2022; Robinson et al. 2024). This broad approach was chosen due to the uncertainty regarding the optimal configuration of Groundhog in an archaeological context and the types of targets that could influence gamma radiation intensity measurements.

Configurations tested included using a single hand-held detector with and without collimation (directional shielding), as well as a vehicle mounted system equipped with three detectors. Surveys were conducted in both typical seasonal climatic conditions and a period characterised by extreme high temperatures and low rainfall. Archaeological features of interest included roads, ditches, buildings, temples, kilns, cremations and inhumations. Additionally, an area containing a modern infilled claypit was surveyed. Different methods of data processing were also explored. Initially, gamma radiation distribution maps were generated using a bespoke ArcGIS add-on developed by Nuvia Limited. Subsequently, Geoplot (Version 4) was successfully deployed to create the high quality visual outputs.



Source: Adapted from Digimap (2024b) and Google Earth Pro (2021)

Figure 6.1 – Silchester survey areas (inset) in the context of the surrounding area and local geology. Survey areas outlined in red are those from the 2022 study. The area outlined in blue denotes the location of the August 2022/ May 2023 surveys.

The generated gamma radiation distribution maps proved to be highly insightful. When assessing the technique’s ability to delineate archaeological features, the gamma radiation distribution maps demonstrated that it is possible to detect objects and structures that have a measurably different radioactivity profile to the surrounding soil. Targets successfully identified included roads, ditches and areas of historic land disturbance. However, the results were inconsistent, with some feature types showing no significant contrast in gamma radiation intensities relative to the surrounding soil. These included buildings (domestic and a temple), cremations/ inhumations and small pits. Further work is therefore required to discern which target types and environmental conditions are most conducive to this type of survey. In addition to the identification (or lack thereof) of archaeological targets, the visual outputs from this research provided additional insights that warrant further exploration:

- **Insight into the physical properties of some archaeological features:** In the Robinson, *et. al.* (2024) study, surveys conducted in August 2022 and May 2023 revealed the presence of three Roman roads. Each road appeared with differing clarity. Further investigation demonstrated that the road that appeared most clearly in the gamma radiation

distribution map also had the greatest thickness and level of consolidation. This road provided the greatest level of gamma radiation contrast relative to the surrounding soil, likely due to the much lower concentrations of radioactive material present in its construction materials, relative to the surrounding soil. In consequence, this road presented as a clear area of depleted radioactivity. This insight was not present in the fluxgate gradiometer data of the same area.

- **Identification of transitions in geology and historic land boundaries:** The gamma radiation distribution maps presented in Robinson *et. al.* (2024) were able to identify two non-archaeological features; a potential historic field boundary (presenting as a linear anomaly of depleted radioactivity) and a transition in ground conditions from typical well-drained soils to a waterlogged area characterised by elevated radioactivity. Neither of these features appeared in the fluxgate gradiometer data.
- **Resilience to soil moisture content:** Results from the August 2022 and May 2023 study (*ibid*) suggest that the technique demonstrates resilience to variations in soil moisture content. Resurveying of an area in May 2023 (a period of higher than average rainfall), compared to August 2022 survey where extreme dry conditions were observed, both surveys were able to delineate the same archaeological features and general gamma radiation patterns.
- **Optimised configuration** – Both the hand-held and vehicle survey methods yielded good quality data and successfully identified archaeological targets. However, the authors suggest that the vehicle mounted system may offer a more practicable solution where vehicle access is permitted. Findings from Robinson, *et. al.* (2024) suggest that the vehicle-mounted system is capable of covering approximately ten times the area of a hand-held system over a comparable period of time and achieves a higher sampling density. However, the hand-held system remains a viable technique for smaller areas or culturally sensitive sites where vehicle access is not approved or practicable.
- **Flexibility in data processing** – Research (Robinson, *et. al.* (2024)) has demonstrated that visual outputs can be created using both bespoke and commercially available software tools. Whilst Geoplot does not allow detailed interrogation of the data (e.g., spectral analysis of areas of interest), it is capable of generating high quality visual outputs that are key to this research. Further, it supports the considered application of filters to enhance these visual outputs.

Further detail on the findings from the preliminary and follow-up surveys at Silchester can be found in Robinson, *et. al.* (2022) and Robinson *et. al.* (2024) respectively.

6.3.4 Looking Further Afield – New Study Sites

The previous research conducted by the authors centred on the Roman town of Silchester, as it was identified as an optimal location for testing the efficacy of portable gamma surveying methods for archaeological prospection. The extensive archaeological research already undertaken at the site, both through geophysical surveying and excavation, provided a comprehensive dataset against which gamma radiation data could be compared. Additionally, Silchester contains a diverse range of archaeological features enabling the authors to test the Groundhog[®] system's ability to delineate different target types.

To provide further confidence that the findings from Silchester were not unique, and to validate Groundhog's[®] performance in varied settings, it was necessary to test the system in other locations. Due to the early phase of this research, it was necessary to select sites that had already been subject to geophysical survey and known to contain archaeological targets. This provided reference datasets against which the gamma radiation results could be compared. Additionally, selecting sites with distinct geological and soil characteristics from Silchester was considered valuable.

Two UK-based sites were identified for surveying; Bisham in southeast England and East Heselton in the northeast. These sites presented contrasting geological conditions and local environments. The archaeological features at these sites were also different to those at Silchester, further ensuring the generation of good, comparative data sets. Like Silchester, East Heselton has been subject to extensive archaeological study with data sets available via multiple sources including the Archaeological Data Service (ADS 2013), LRC (2024a), LRC (2024b), Powlesland (2008), Verhegge, *et. al.* (2023) and the Heselton Interactive Map (University of Arkansas 2024). In contrast, Bisham was less well studied at the time, although previous geophysical surveys confirmed the presence of archaeological features of interest.

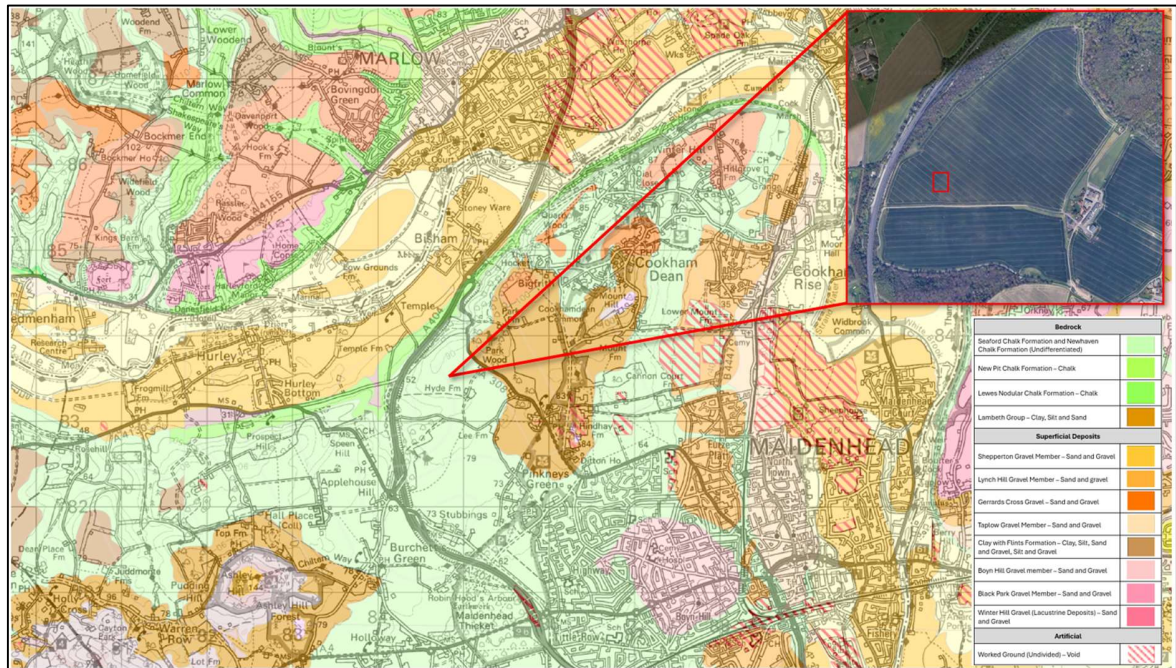
Further information on each of the targeted sites is summarised below.

Bisham

The village of Bisham is situated within Berkshire, approximately 5 km northwest of Maidenhead. The area sits on a bedrock of chalk overlain by sand and gravel deposits (BGS 2024). The region is characterised by a mosaic of farmland and an area ancient woodland that is believed to have been an original part of Britain's 'wildwood' (Woodland Trust 2024). The gamma radiation survey was undertaken in an area of arable land within Hyde Farm used for growing crops such as winter wheat (Randall Farms 2024) (Figure 6.2).

Archaeological evidence suggests that Bisham has a long history of occupation dating back to the Iron Age (Humphreys 2019). These discoveries, spanning the Iron Age and Roman periods, includes various artefacts including pits, ditches, post holes, as well as evidence of round houses and burials (Humphreys 2019). A previous geophysical survey enabled the authors to target an area for gamma radiation surveying known to contain several archaeological features of interest as shown in Figure 6.6. The area selected for surveying contains a chalk pit (Iron Age), Medieval burial, and what is believed to be a historic field boundary, though the age of the latter remains uncertain.

The survey at the Bisham site was completed by the authors as a pilot study. It provided a valuable opportunity to test the equipment and survey methodology developed for the preliminary investigation at Silchester (Robinson *et. al.* 2022).



Source: Adapted from Digimap (2024b) and Google Earth Pro (2021)

Figure 6.2 – Bisham survey area (inset), outlined in red, in the context of the surrounding area and local geology.

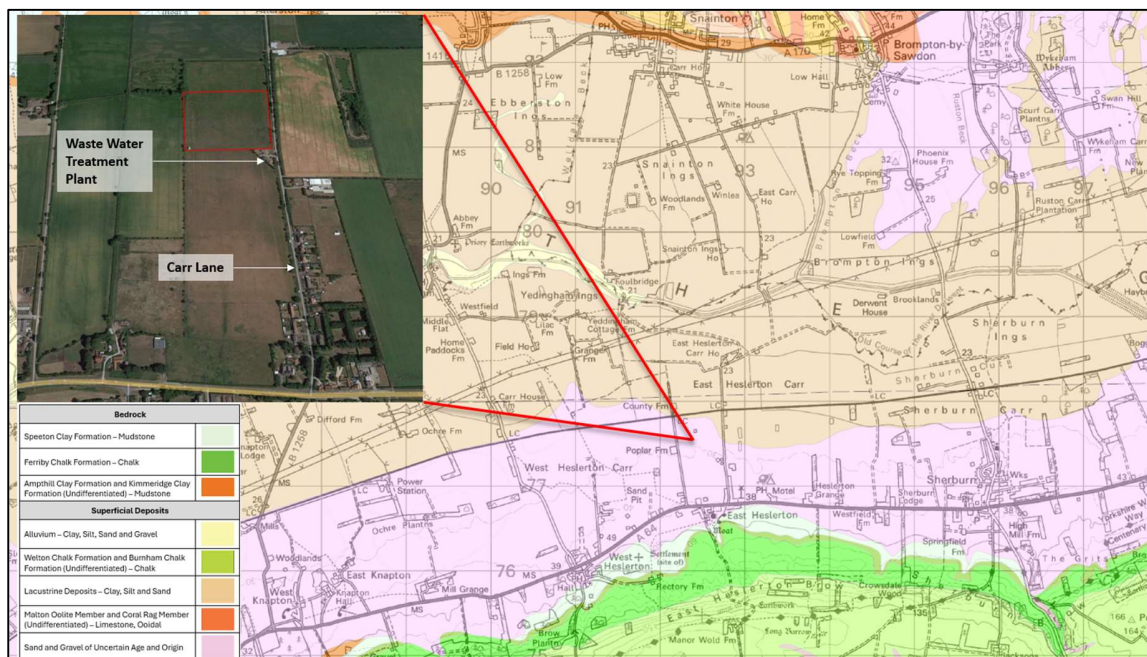
East Heselton

East Heselton is a small village in North Yorkshire, situated approximately 15 km northeast of the village of Malton, and 17 km southwest of Scarborough. Together with neighbouring West Heselton, the village sits within the Vale of Pickering; a known area of archaeological importance (Cooke 2012, LRC 2024a). The local geology is dominated by windblown sands and glacially deposited sands and gravels overlaying a bedrock of Amphill and Kimmeridge Clay formations (BGS 2024).

The site has a long and continuous history of human occupancy dating back to the Neolithic period (Cooke 2012, NRC 2024), with evidence of settlements covering the Bronze Age, Iron Age and Roman periods. Evidence of settlement is characterised by the presence of roundhouses, ladder settlements, cemeteries and associated artefacts (Cooke 2012, LRC 2024b). The true richness of the region's history was revealed through the efforts of the Heselton Parish Project; one of the largest and most enduring field archaeology projects in the UK (Powlesland 2008).

Chapter 6 - Exploring the Value of Gamma Radiation Surveys in Archaeological Prospection – A Consolidating Study

The area of East Heselton subject to gamma radiation surveying was limited to a four hectare section of a field that forms part of Manor Farm. As shown in Figure 6.3, the survey area is bounded by Carr Lane to the east and a waste water treatment plant at its southeastern corner. The survey site is known to contain an archaeological feature of interest; a late Iron Age/ early Roman ladder settlement as shown in Figure 6.10. This area is characterised by a unique geology. Whilst the majority of the field comprises wind blown and glacial sand/ gravel deposits typical for the area, the northeast corner transitions to an area of “silty, organically enriched soils” (Baldwin & Opitz 2022) with an increased water content.



Source: Adapted from Digimap (2024a) and Google Earth Pro (2018)

Figure 6.3 – East Heselton survey area (inset), outlined in red, in the context of the surrounding area and local geology.

6.3.5 Methodology

Gamma Radiation Surveys

All surveys completed were undertaken using Nuvia's Groundhog® system. Groundhog® is a rugged, portable gamma radiation detection system with spectrometric capability (Robinson, et. al. 2022; Robinson et al. 2024). It utilises sodium iodide (NaI) type detectors in conjunction with a mapping grade GPS system, spectrometer and data logger (an ultra-mobile PC or UMPC) to collect one gamma spectrum per second and associated positional information. Raw gamma radiation data is presented in counts per second (cps). The most commonly used values are the total counts per second. However, individual energy windows can also be targeted and interrogated. The collated data can be processed to generate multiple outputs. Of particular relevance to this research is the ability to generate 'gamma radiation distribution maps' capable of revealing areas of varying radioactivity. Groundhog® was developed by Nuvia for use in the nuclear industry for the identification and mapping of man-made contamination within buildings and the wider environment. Consequently, the adaptation of Groundhog® for use in an archaeological context highlights the truly interdisciplinary nature of this research.

The selection of survey areas at Bisham and East Heslerton was informed by a combination of factors including existing geophysical data (from magnetic and Frequency Domain Electromagnetic (FDEM) surveys respectively), site characteristics and the chosen survey method. At Bisham, the decision was made to deploy Groundhog in a hand-held configuration, preferring the minimally intrusive approach due to the use of the site for commercial crops cultivation and being cognisant the early stage of research. Further, the archaeological features of interest identified in the extant magnetometer survey data (Figure 6.6) were located in close proximity to one another, leading to the selection of a relatively small survey area of 5000 m² (0.5 ha). In contrast, the survey of East Heslerton benefitted from being deployed in a Groundhog in a vehicle-mounted configuration, building on the findings of the previous studies at Bisham and Silchester. Experience gained from the earlier vehicle-mounted Groundhog survey at Silchester confirmed that this approach was capable of covering much larger areas in a comparable time-frame to hand-held surveys. This approach facilitated the targeting of a large area of 40,000 m² (4 ha), encompassing the entire Roman ladder settlement and geological transition as observed in the FDEM data (Figure 6.10). For both sites, GLONASS+GPS technology was used to accurately delineate the survey boundaries in the field, with marker poles set in each corner.

Bisham Hand-Held Survey

As a hand-held survey was conducted at Bisham, only a single Groundhog Fusion unit was required. This comprises a 76 mm x 76 mm sodium iodide (NaI) gamma radiation detector (with an operating energy of ~15 – 3000 keV) and spectrometer connected to a mapping grade GPS system and UMPC. No collimation was applied to the detector.

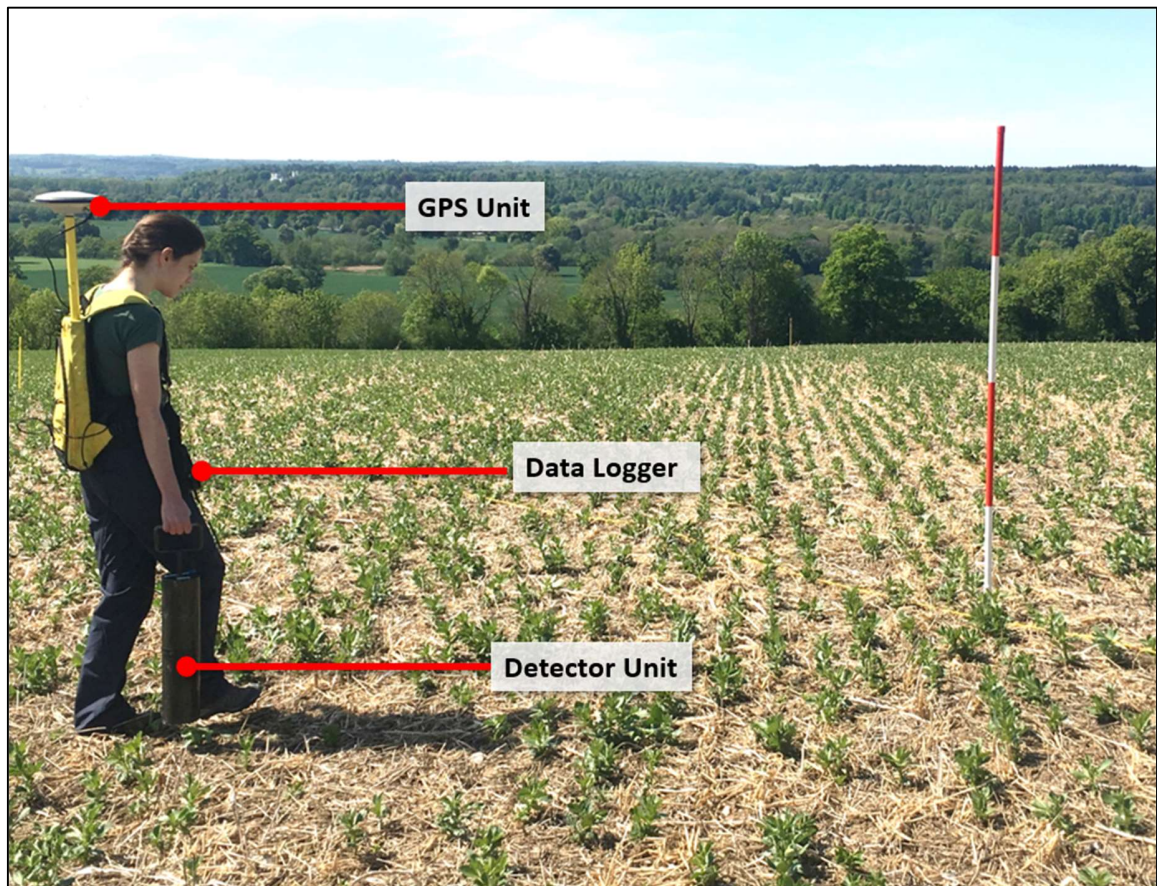
Before deployment, the unit was subject to the required annual calibration and pre-use functional checks; both in accordance with Nuvia procedures. The annual calibration checks measure the detector's response against background radiation and a ~5.7 kBq Cs-137 check source, each for a duration of 600 seconds. This ensures that the unit is operating within its expected efficiency (i.e. the ratio of the number of light pulses generated by the NaI crystal to the number of gamma rays emitted by the check source over a defined period) and energy resolution (the ability to differentiate between different energy peaks in a spectrum) and therefore able to generate reliable data. Results of the annual calibration test confirmed that the detector was performing within an acceptable efficiency range of 2.93 – 3.24 cps at 3.21 cps kBq⁻¹. Additionally, the energy resolution was measured as 7.2% at Full Width Half Maximum (FWHM) amplitude, which is within the acceptable range of 6.50 – 8.00%.

On the morning of the survey, functional checks confirmed that all required components were in place, that batteries (and spares) were fully charged and all detector unit components, including the GPS unit and UMPC, were operating correctly and safely.

The Bisham survey was completed on the 13th May 2019 in dry conditions with a maximum temperature of 21°C. On arrival at the site, a walk-round was undertaken to confirm that there were no trip hazards or other obstacles that could impede the survey. No issues were identified. To establish the transect route, ropes marked at 1 metre intervals were positioned along the perimeter of the survey area in an approximately east-west orientation, utilising the corner markers as reference points.

The survey was completed by moving the detector unit along 1 metre transects at a walking speed of approximately 1 metre per second. A gamma radiation and GPS measurement was

automatically recorded by the UMPC every second, generating a GPS-positioned radiation measurement for every square metre of the survey area. As shown in Figure 6.4, the detector unit was carried to the side of the body with the arm straight. This allowed the face of the detector to remain at a consistent height of approximately 20 cm above the ground surface. The GPS unit and supporting infrastructure was carried in a backpack.



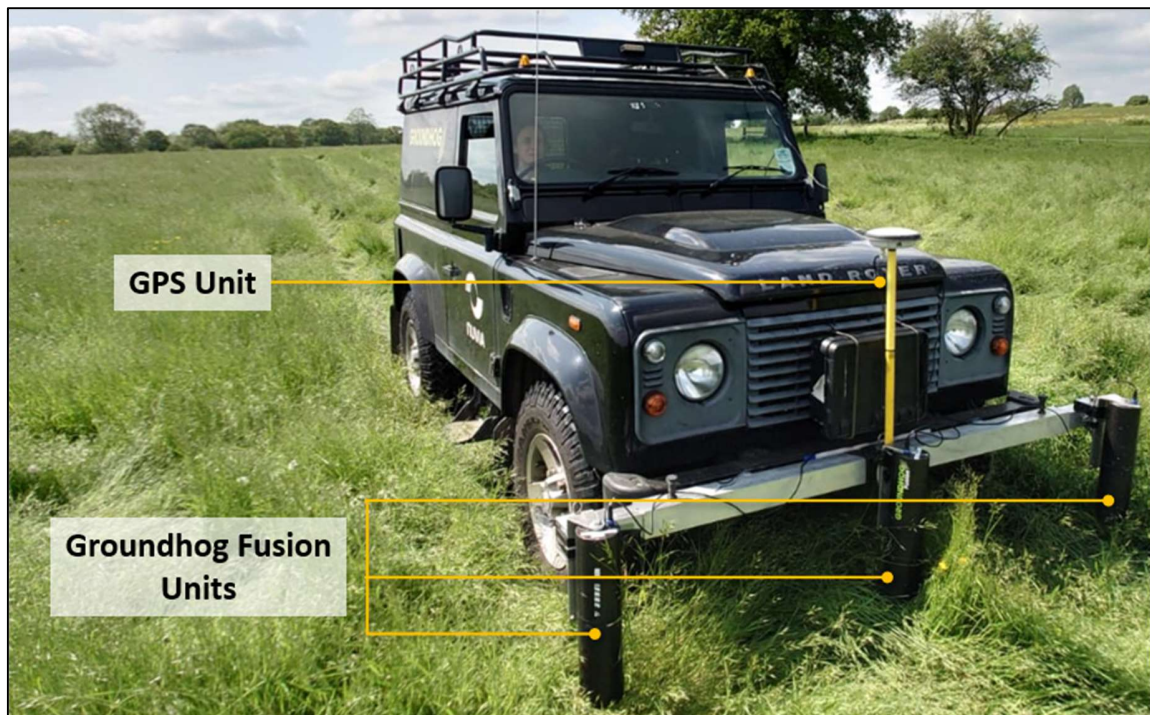
Source: Personal Photograph

Figure 6.4 – Groundhog deployed at Bisham in a hand-held configuration. The detector unit is carried against the body with a straight arm, maintaining the face of the detector ~20 cm above the ground surface. The data logger (UMPC) is attached to the backpack enabling hands-free use.

East Heselton Vehicle-Mounted Survey

The East Heselton site was surveyed using Groundhog® in a vehicle-mounted configuration. This arrangement enabled the simultaneous operation of three Groundhog® units mounted to the front of the vehicle, in conjunction with the GPS antennae (Figure 6.5). A mounting frame ensured a consistent spacing of 1 metre between the units. The UMPC was securely stowed in the cabin of

the vehicle. Similar to the procedures followed for the Bisham survey, all three units underwent annual calibration and pre-use checks applied for the Bisham survey. The performance of the three detectors is summarised in Table 6.1. All three detectors passed their annual calibration checks. It is however noted that the second detector reported a Cs-137 Photopeak net cps/kBq value of 3.34, slightly exceeding the acceptable range. Additionally, the third detector (GN08) exhibited a slightly elevated FWHM value; again above the typical acceptable range for this parameter. However, the technician who conducted the calibration checks, as indicated in the calibration certificates, affirmed that the units were still performing acceptably and generating accurate data. Pre-use checks confirmed the correct and safe operation of all equipment on the day of the survey.



Source: Personal Photograph

Figure 6.5 – Groundhog Configuration used at the East Heselton site. The three gamma detector units along with the GPS antennae can be seen fixed to the front of the vehicle.

Table 6.1 – Overview of the Results from the annual calibration checks for the three detectors used in the East Heselton Survey. Results are presented for the efficiency (net cps values) and energy resolution (FWHM) of the detectors.

Detector No./ Name	Cs-137 Photopeak – Net cps	Cs-137 Photopeak – Net cps/kBq	Acceptable Range – cps/kBq	FWHM	Acceptable Range – FWHM
1 / GN01	18.13	3.17	2.93 – 3.24	7.0%	6.5 – 8.0%
2 / GN06	19.13	3.34		7.6%	
3/ GN08	18.35	3.21		8.2%	

Source: Created from primary data

The survey was conducted on the 15th September 2022 in dry conditions with a maximum temperature of 15°C. The site had experienced minimum rainfall; less than 1 mm of rain over the previous four days, supporting optimal survey conditions. An initial walk-round of the site confirmed flat terrain and no hazards or features that could impede the survey. Surveying involved manoeuvring the vehicle along the perimeter of the survey area, guided by the corner markers. To maintain a target speed of approximately 1 m/s, the vehicle transmission was set to low range. This facilitated steady movement without the need to apply acceleration, thereby minimising variability.

After completing each lap of the survey area, the vehicle was incrementally moved inward, aligning the passenger-side tyres with the tracks left by the driver-side tyres from the previous pass, ensuring overlap. As per the Bisham study, one GPS measurement and one gamma radiation measurement was collected per second for each unit. With three units operating concurrently, it was possible to collect three gamma radiation measurements every second, ensuring a minimum of 1 GPS-positioned gamma measurement for every square metre of the survey area. Overlapping each vehicle pass supported an increase in sampling density overall.

Data Processing

All gamma radiation and GPS data were automatically recorded on the UMPCs deployed during the Bisham and East Heselton surveys. On completion, the datasets were downloaded to a stand-alone desktop computer enabling the completion of several data management activities before progressing to create the gamma radiation distribution maps. These tasks included post-processing of GPS data to provide centimetre accuracy, data quality checks and integration of the GPS and gamma radiation data.

Following the methodologies outlined in Robinson, *et. al.* 2022 and Robinson, *et. al.* 2024, Microsoft Access (v. 16.0.14131.20278) was the primary tool for compiling the data. Post processing to improve the quality of location data was undertaken in GrafNav (v. 8.3). RINEX data obtained from the Amersham (AMER) and Scarborough (SCAU) OS Reference Stations were used for differential correction for the Bisham and East Heslerton GPS datasets respectively. Integrated datasets were exported as dBase database (.dbf) files for further quality assurance and processing. Quality checks verified the completeness of both datasets, confirming the absence of anomalous values that would be indicative of a malfunction within the Groundhog® system during surveying.

Geoplot 4 was used to generate gamma radiation distribution maps for both data sets. To generate the highest quality images, GPS Gap Fill and the Wallis filter were applied to enhance anomalies present in the data. This decision was informed by prior research conducted by the authors to establish an optimal strategy for creating high-fidelity images capable of highlighting relevant features whilst preserving the integrity of the original data. The findings from this work are presented in Robinson, *et. al.* (2022). A colour palette proved most effective for drawing out features of interest in the Bisham data, whereas for East Heslerton it was most effective at emphasising geological features. However, it was observed that a greyscale palette was more effective at delineating anomalies potentially associated with the ladder settlement in East Heslerton. This is possibly due to the limited contrast in gamma radiation measured between the archaeological feature and surrounding substrate.

Gamma radiation distribution maps were generated for the above window, below window, potassium, uranium, thorium, caesium energy windows as well as the total counts.

In addition to the gamma radiation distribution maps, count rate distribution graphs were generated for each dataset to complement the analysis and aid interpretation.

Sample Analysis

To aid interpretation of the Groundhog® data collected across the Silchester, Bisham and East Heslerton sites, various material samples recovered from Silchester were subject to pXRF analysis. The primary aim of this analysis was to confirm the presence of any variations in the concentrations of naturally occurring radionuclides, specifically potassium, uranium and thorium,

across the different material types found at the Silchester site. This in turn, would help validate the findings from the Groundhog® surveys. Quantities of the following materials were collected and subject to analysis:

- Soil (3 samples) – representative of the soil matrix encompassing the archaeological features at Silchester.
- Gravel (1 sample) – Analogue of the construction material used in the Roman roads at Silchester.
- Flint (1 sample) – Analogue of the construction material used in the Roman roads at Silchester.
- Tile (1 sample) – Analogue of tiles and bricks used elsewhere at the Silchester site.

Samples from Silchester were selected for analysis due to the pronounced contrasts observed in gamma radiation measurements between archaeological targets and surrounding soil, particularly evident in the gamma radiation data presented in Robinson, *et. al.* (2024). Further, the extensive excavation work already undertaken at Silchester facilitated the collection of a variety of material types for analysis without causing further disruption to the site. This was considered beneficial, recognising the status of all three study locations as active agricultural sites.

It is important to acknowledge the limitations of the approach applied to sample collection. The aim of this analysis was not to accurately characterise the survey area and the targets within it. Rather, the aim was to explore the relative contrast in the radiochemical composition of the different materials to better understand the anomalies being generated. It is recognised that there will be variability in the soil composition across the Silchester site, and the potentially diverse sources (and therefore composition) of the gravel and flint present in the roads compared to that found elsewhere on site. However, it is believed that the materials subjected to pXRF analysis serve as sufficient analogues to provide valuable insights into the composition of the different material types and contrasts in their radiochemical composition, thereby aiding the interpretation of the gamma radiation data.

Soils were fully dried prior to analysis to minimise the risk of x-ray attenuation or scattering from soil moisture. Soil residues were removed from the surface of the gravel, flint and tile samples to

ensure the resultant data was reflective of the material of interest. Three sub-samples of the soil, gravel and flint were taken and placed into sample capsules to a minimum sample depth of 150 mm. This ensured that an 'infinite thickness' was achieved, and ensured full containment of the primary and secondary x-rays within the sample. The capsules used a mylar film base as this incurs only negligible attenuation effects for most contaminant x-ray lines (Kalnicky and Singhvi 2001). The capsules were analysed with the pXRF secured in a benchtop test stand, and connected to a desktop computer. This offered multiple benefits including greater precision for analysing smaller samples, direct transfer of analytical data to the computer minimising the risk of data loss or transposing errors, and remote operation thereby maximising operator distance from the x-ray source. The same method was applied to the gravel and flint samples that were placed on mylar film within the test stand.

It was not possible to place the tile in the test stand due to its size. Instead, the sample was analysed with the pXRF in a freehand configuration,. The tile was analysed in two separate locations – on its external surface which was exposed to soil contamination and weathering over time, and its internal surface which is more representative of the bulk material.

All samples were analysed using a Thermo Scientific Niton XL3-700 portable XRF analyser for a period of 120 seconds. The instrument was previously calibrated to include the widest suite of elements, especially those of interest to this study – potassium, uranium and thorium. The results, which were recorded in parts per million (ppm) (uranium and thorium) and percentage (potassium) were averaged across the sub-samples for each material.

To further enhance the data sets available for interpretation, the authors have compared the values obtained for the soil samples with pXRF data for surface soils collected from boreholes using an auger, in the East Heselton survey area, by De Smedt and Verhegge (2022) and published characterisation data from the UK Soil Observatory (UKSO 2024) covering the Bisham site. The boreholes were collected from within the confines of the survey area presented in Figure 6.3. As with the Silchester data, three pXRF readings were taken for each soil sample. Their averages are presented within this paper for comparison.

6.3.6 Results

The gamma radiation surveys undertaken at the Bisham and East Heslerton sites successfully identified features of archaeological interest, corroborating findings from the previous studies at Silchester. Transitions in geochemical conditions and, to a lesser extent, archaeological targets were discernible in the gamma radiation distribution maps. Additionally, the results from the pXRF analysis of the various materials recovered from the Silchester site aided in interpreting Groundhog data. Specifically, they supported the hypothesis proposed by the authors that gravel and flint used in the construction of roads in Silchester contain lower concentrations of naturally occurring radionuclides relative to surrounding soils.

Bisham Survey

A total of 9703 gamma radiation measurements were collected over the 5000 m² survey area, leading to an average sampling density of ~2 measurements per square metre. This is likely due to the detector traversing the site at a speed lower than 1 metre per second and possible overlapping of the detector along the transects. A full suite of summary statistics is presented in Table 6.2. Post-processing of the GPS data confirmed that the quality of this data was excellent, achieving centimetre accuracy.

The gamma radiation distribution map for Bisham is presented in Figure 6.6. The original magnetometer survey data (Figure 6.6a) adjoins an overlay of the gamma radiation data (Figure 6.6b) to demonstrate how the anomalies align. A clear transition from generally low radioactivity in the west to higher radioactivity east can be seen. However, reduced gamma radiation counts are observed towards the eastern edge of the site. The area with the highest gamma radiation intensities aligns closely with a linear anomaly present in the magnetometer survey data, with values reducing as distance from this feature increases.

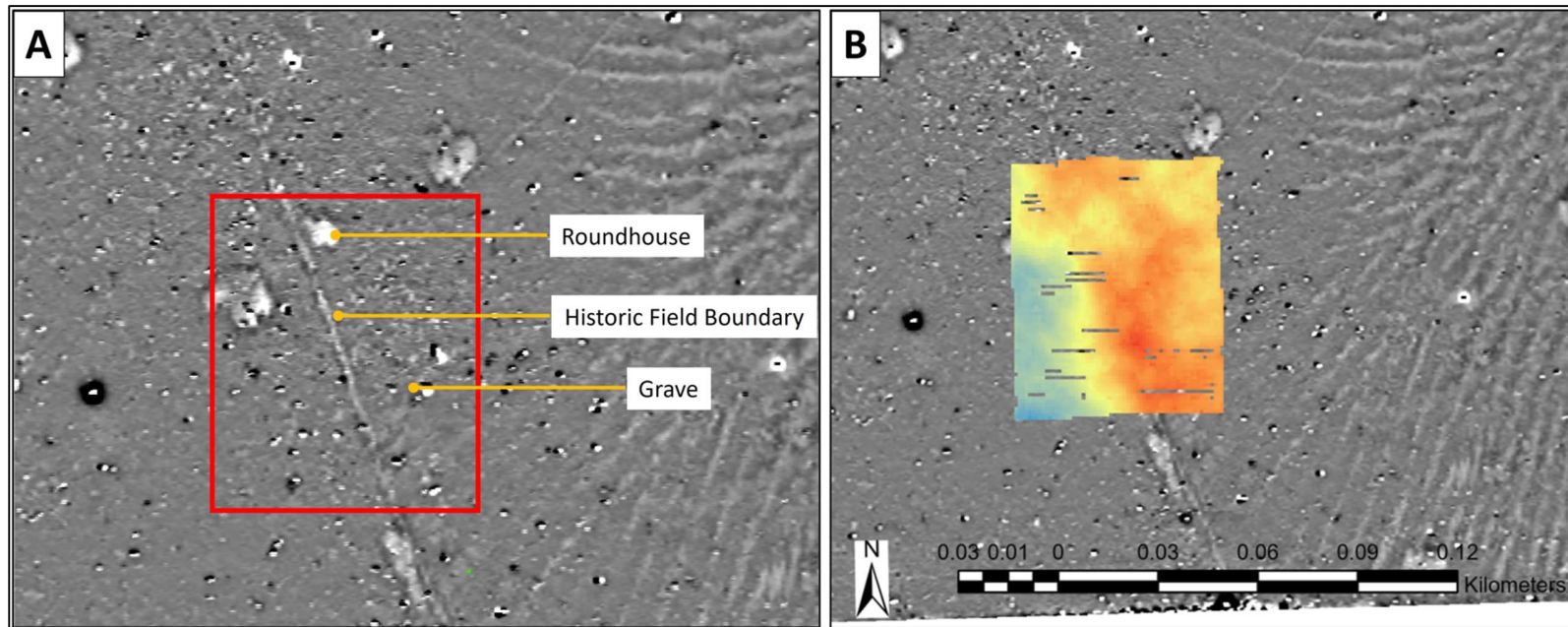
To help identify anomalies in the Bisham data, gamma radiation distribution maps were created for each energy window set within the Groundhog® system (Figure 6.7). Each energy window monitors and counts the number of incident gamma photons corresponding to its specific energy range. Since the energy of a photon is unique to its source radionuclide, it is possible to identify specific radionuclides present in a surveyed area. Figure 7 shows that the potassium, uranium, thorium and caesium energy windows yield low-quality visualisations, showing significant 'noise'.

In contrast, the below window energy window, which records all incident radiation between 0 – 530 keV, yields the highest quality image second only to the total gamma window which sums the counts from all energy windows. The below window distribution map highlights an area of elevated radioactivity situated in the lower half of the image. Unfortunately, none of the distribution maps were able to delineate the location of the grave or chalk pit targets visible in the magnetometer survey data.

The findings from looking at data from the individual energy windows are consistent with those from the August 2022 and May 2023 surveys at Silchester (Figures 6.12 and 6.13). At Silchester, the energy windows for individual radionuclides, and in particular thorium, produced low-quality images, whereas the above and below window energy windows generated distribution maps that more clearly highlighted targeted archaeological features. The main difference for the Silchester data, is that above window data generated the better distribution map capable of drawing out the Roman roads.

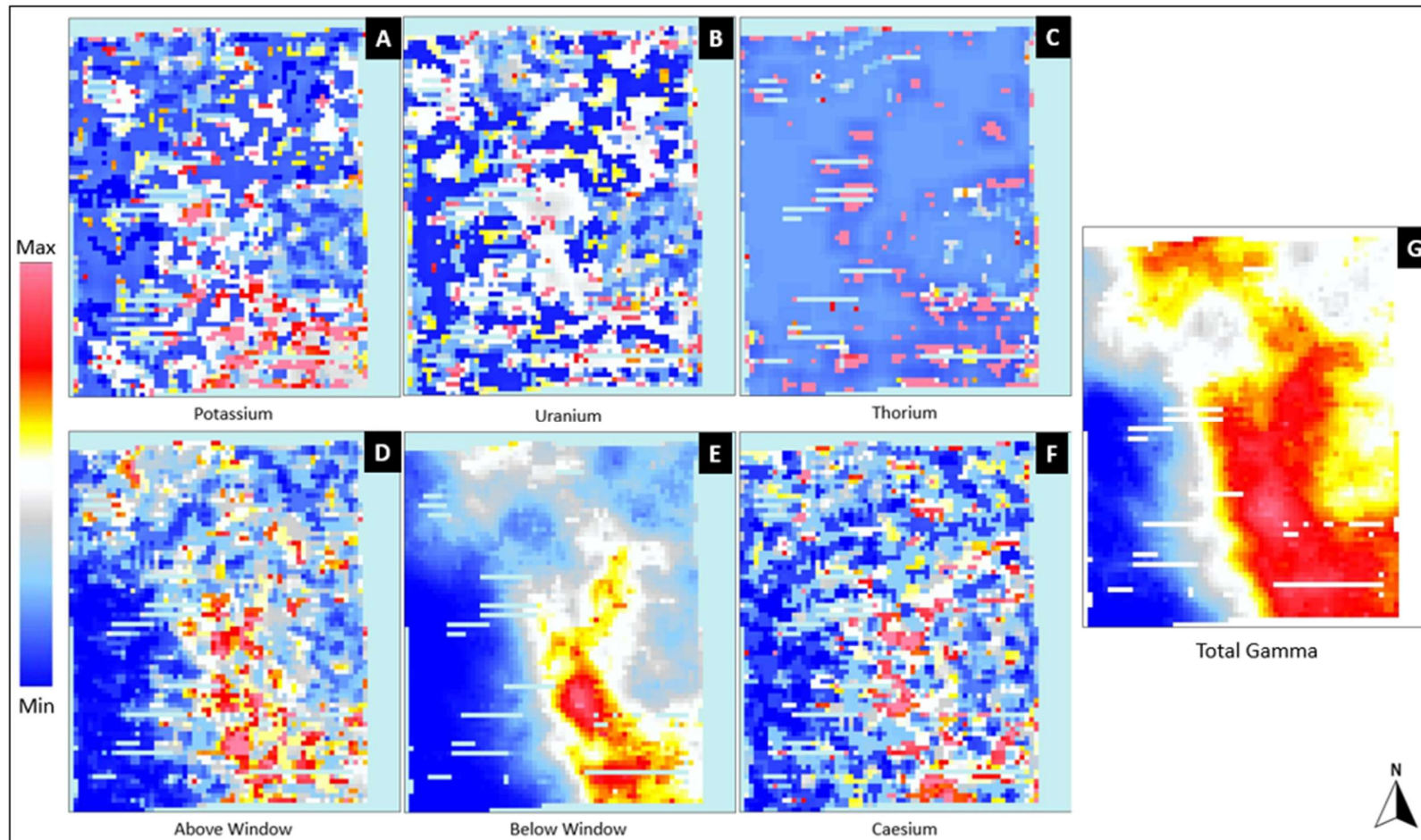
The count rate distribution graph for the radiation data used to generate the gamma radiation distribution map, shown in Figure 6.8, demonstrates a non-normal distribution which supports this observation. The mean count rate for the site is 165 cps, which is lower than the typical background values of 200 – 300 cps observed in the UK (Davies *et. al.* 2011) Although the source of the linear anomaly is believed to be a historic field boundary, there is no evidence to support this. There are no physical indicators are visible at the site, and historic records dating back to the first half of the 19th century (Figure 6.9) also fail to identify any such boundary.

There are no clear anomalies in the gamma radiation data that align with either the chalk pit or grave site identified in the magnetometer survey data (Figure 6.2).



Source: Modified from (UoR 2024)

Figure 6.6 – (A) Fluxgate magnetometer survey (± 7 nT – white high to black low) showing the features targeted in the gamma radiation survey; a chalk pit, Medieval burial and historic field boundary. The survey area is outlined in red. (B) Gamma radiation distribution map overlaying the existing magnetometer survey data for Bisham, highlighting a clear transition from an area of higher radioactivity towards the eastern side of the survey area to an area of lower activity in the west.



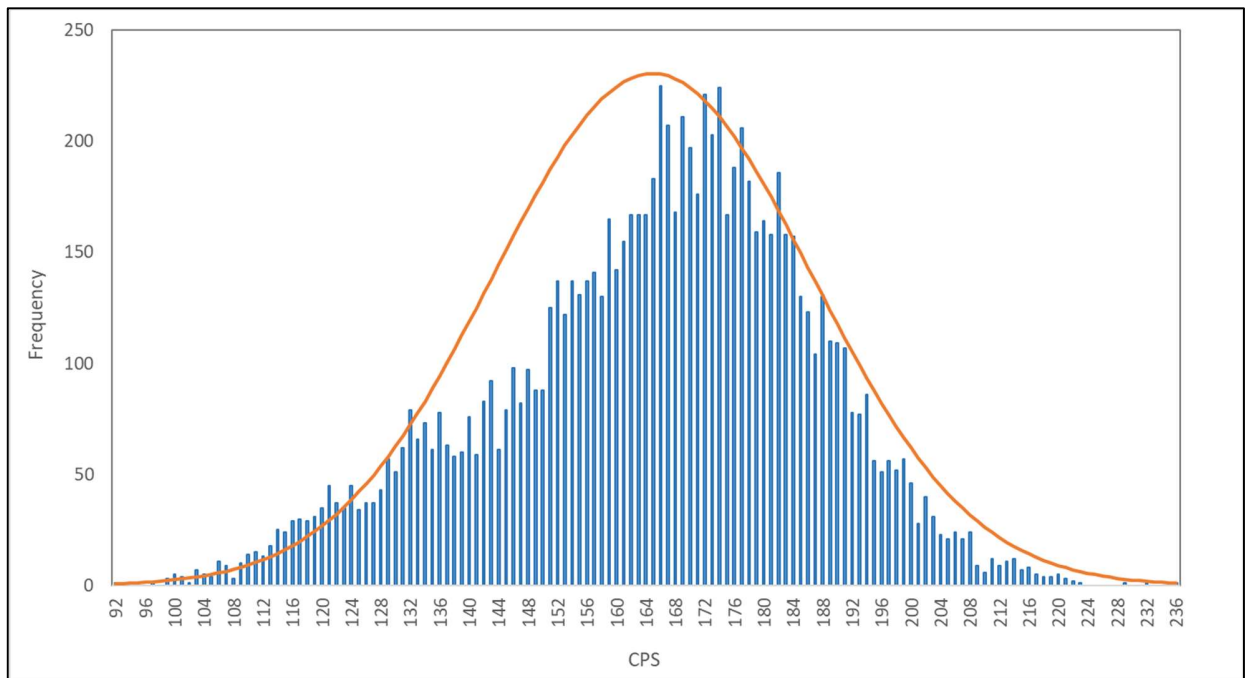
Source: Created from primary data

Figure 6.7 – Composite figure revealing the impact of different energy windows on the clarity of the linear anomaly at the Bisham site. (A) Potassium (1400 – 1600 keV), (B) Uranium (1600 – 1900 keV), (C) Thorium (2500 – 3000 keV), (D) Above Window (760 – 3000 keV), (E) Below Window (0 – 530 keV) and (F) Caesium (581 – 740 keV) energy windows are shown against the Total Gamma data (G) image. All images utilised GPS Gap Fill + Wallis Filter.

Table 6.2 – Summary Statistics from the gamma radiation survey of the Bisham Site. Values are provided for total gamma only.

Parameter	Bisham
Min (cps)	92
Max (cps)	236
Mean (cps)	165
Range (cps)	144
No. Measurements	9703
Area Surveyed (m ²)	5000
No. Measurements/ m ²	2.0

Source: Created from primary data



Source: Created from primary data

Figure 6.8 – Count rate distribution graph for the Bisham survey, suggesting the background radiation data are not normally distributed.



Source: ARCHI UK (2024)

Figure 6.9: View of the Bisham survey area dating to c. 1805 – 1845. No field boundaries or other geological features aligning with the anomalies found in the gamma radiation or magnetometer survey data can be seen. The approximate location of the survey area in Bisham is outlined in red.

East Heselton Survey

Due to the use of the vehicle mounted system at East Heselton, it was possible to cover a much larger area to Bisham - ~40,000 m² in a single day. This yielded over 63,000 gamma radiation measurements, achieving an average sampling density of 1.6 measurements per square metre. Whilst lower than achieved for Bisham due to the higher speed of the vehicle, this is still higher than the 1 measurement per square metre targeted. With a value of 221 cps, the mean count rate for the site is within the 200 – 300 cps normally expected for the UK, as noted previously, albeit towards the lower end of this range. A full set of summary statistics for East Heselton is provided in Table 6.3.

The gamma radiation distribution map for East Heselton is presented in Figure 6.10. The first image within this figure (Figure 6.10a) is the extant FDEM In-Phase Magnetic Susceptibility data of the 1 m Perpendicular Coil configuration, included for comparison purposes. Three variants of the

gamma radiation distribution map were created to help draw out any anomalies. The first variant (Figure 6.10b) uses a greyscale palette, enhancing some linear anomalies (circled in blue) that may be attributable to the ladder settlement, or possibly aligning with the c. Medieval ploughing direction. If this is the case, than this is the first example of a positive anomaly within this study. It is acknowledged that the gamma radiation data does not accurately delineate the ladder settlement as observed in the FDEM data (Figure 6.10a). However, the anomalies identified, if targeted for excavation, would likely yield positive results. Linear anomalies in the corners of this image (circled in orange) are likely an artefact of the Groundhog® vehicle manoeuvring around site. This can result in an increased number of measurements taken in these areas, skewing the results. The second variant of the gamma radiation distribution map (Figure 6.10c) more effectively draws out a large anomaly – an area of depleted radioactivity in the north-eastern corner of the site. This anomaly, which is also partially visible in the FDEM data, aligns with the previously discussed area of silty and organically enriched soil. The linear anomalies identified in Figure 6.10b, which broadly align with sections of the ladder settlement, are visible in Figure 6.10c, but with less clarity. The third variant (Figure 6.10d) presents the Below Window gamma radiation data which was found to be particularly effective at drawing out the ‘Γ’ shaped anomaly. This figure is particularly effective at highlighting that this is a positive anomaly. The Below Window data has been set at 65% transparency and overlaid on the FDEM data to better show the alignment of this anomaly with the ladder settlement.

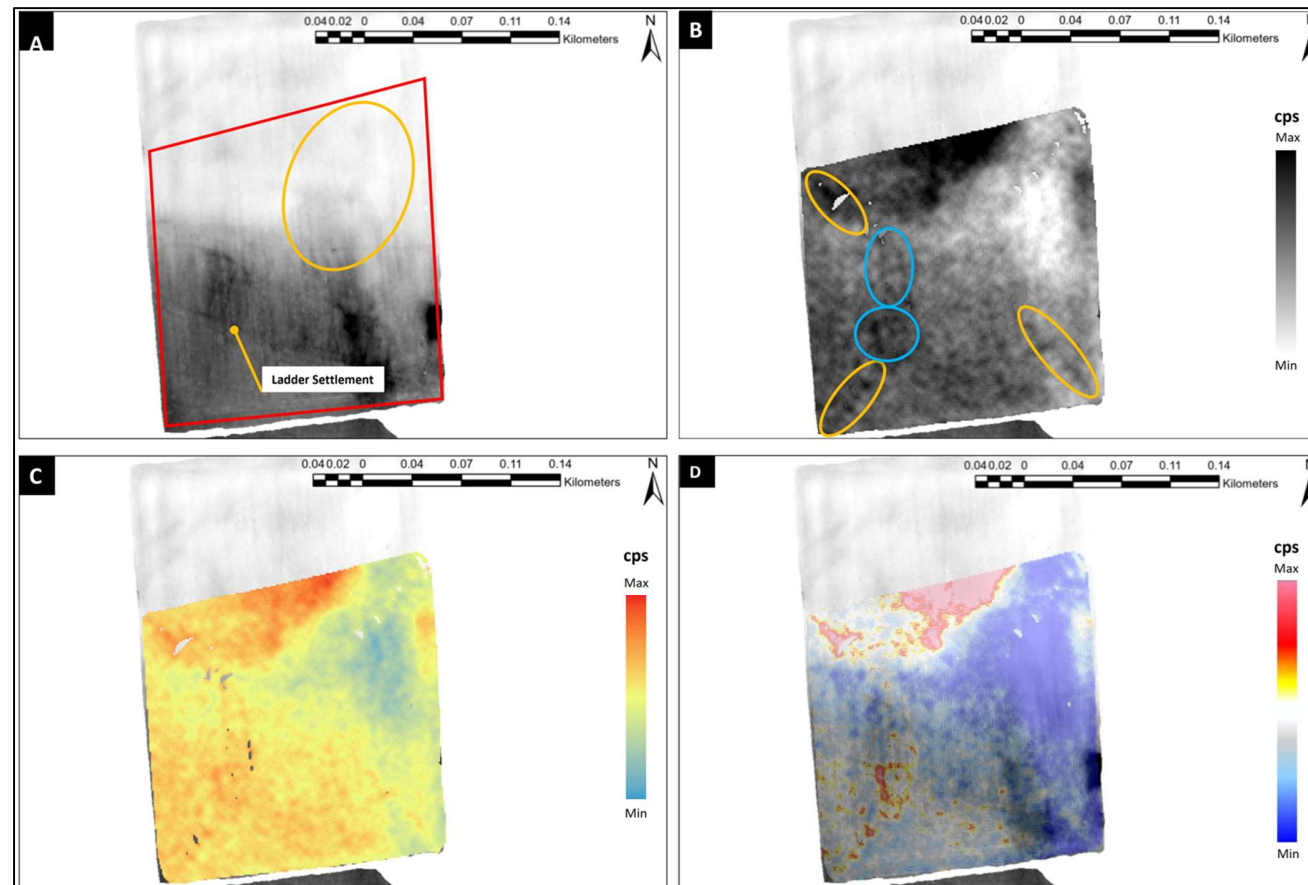
Gamma radiation distribution maps have been produced for the individual energy windows. As observed in the Bisham and Silchester datasets, the distribution maps for potassium, uranium, thorium and caesium energy windows contain a lot of ‘noise’ and fail to delineate any archaeological features. However, the distribution map for the caesium energy window can delineate the large anomaly in the north-east corner. Again, the data from the below window energy window has created a high-fidelity distribution map. The ‘Γ’ shaped anomaly is particularly visible here. The other linear anomaly just above this is also visible, albeit to a lesser extent. For the East Heslerton site, the below window gamma radiation distribution map appears more effective than total gamma at highlighting archaeological features.

Despite the significant area of depleted radioactivity in this survey, the count rate distribution graph for this data set (Figure 6.14) indicates a normal distribution pattern.

Table 6.3 – Summary statistics from the gamma radiation survey of the East Heslerton Site. Values are provided for total gamma only.

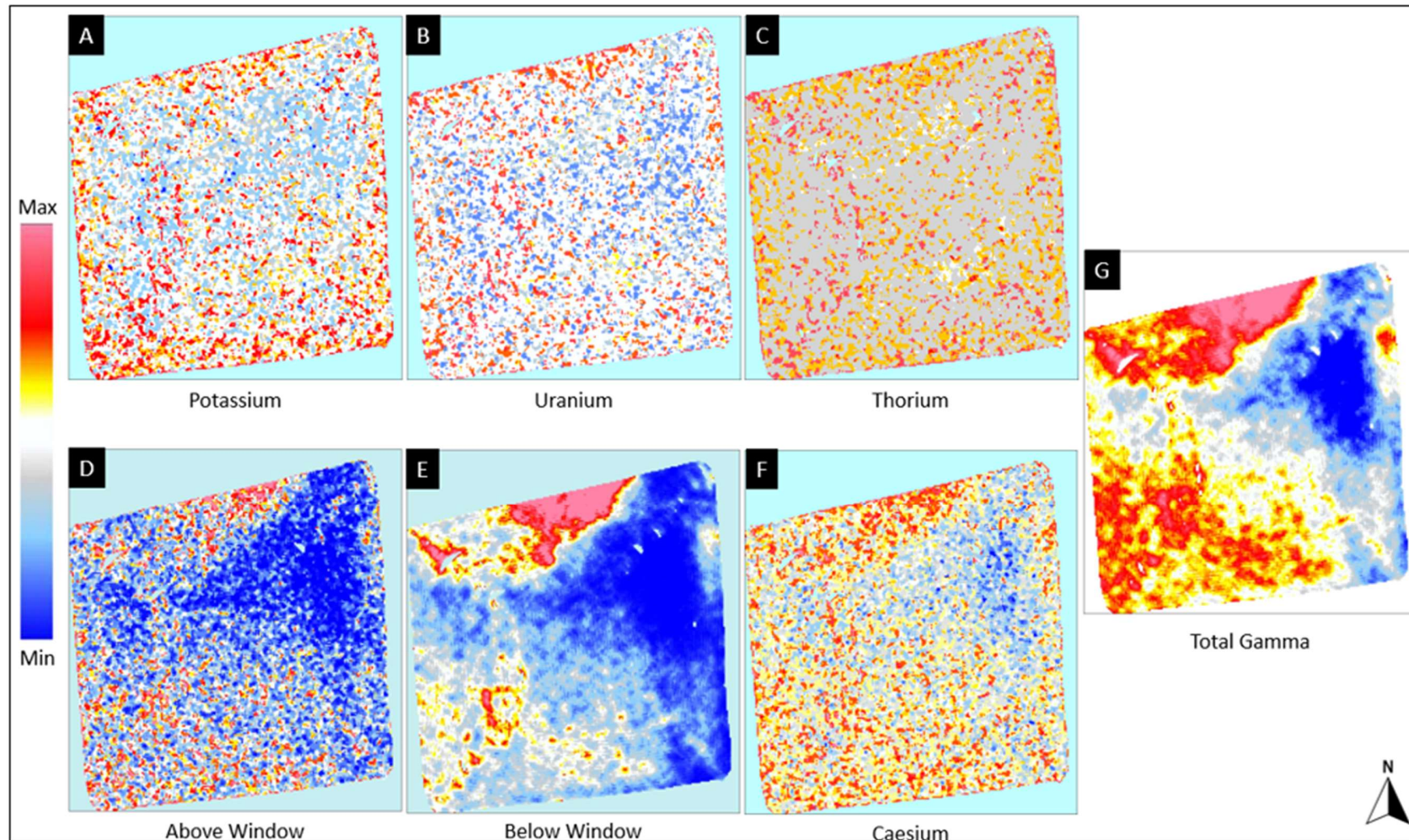
Parameter	East Heslerton
Min (cps)	141
Max (cps)	308
Mean (cps)	221
Range (cps)	167
No. Measurements	63,133
Area Surveyed (m ²)	40,000
No. Measurements/ m ²	1.6

Source: Created from primary data



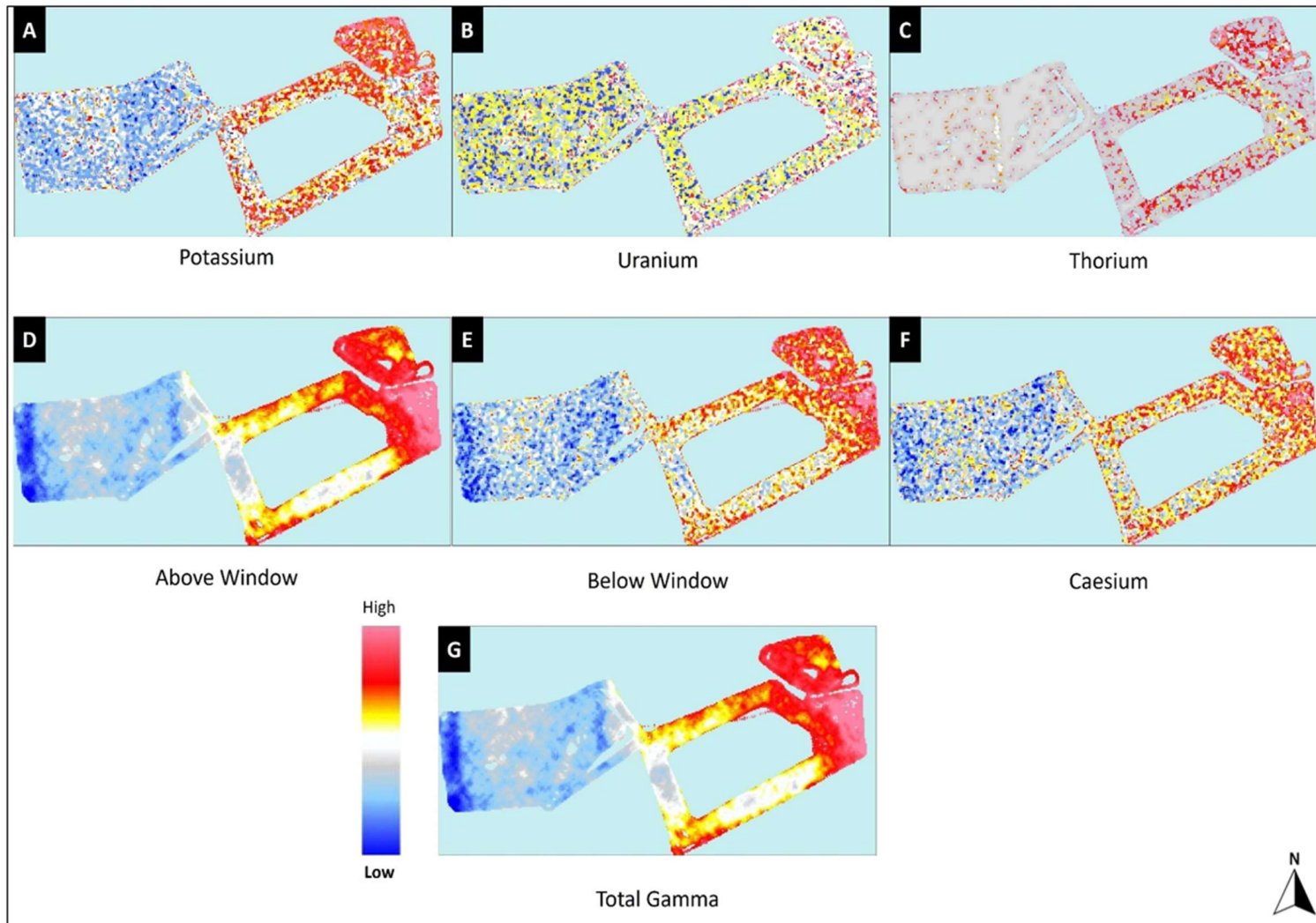
Source: Modified from Verhegge, et. al. (2023)

Figure 6.10 – Comparison of the Frequency Domain Electro Magnetic (FDEM) survey data (PRHIP: +/- 3 mS/m - white high to black low) (A) which reveals the Roman ladder settlement (bottom left) and transition in geological conditions (top right – circled in orange) within the survey area (outlined in red), with overlaid gamma radiation data for the East Heselton site in greyscale (B) and colour (C) palettes. Gamma radiation data (GPS Gap Fill + Wallis Filter) reveals linear anomalies on the western side of the survey area, broadly correlating with the ladder settlement evident in (A). These anomalies are more discernible in the greyscale palette (B) and are circled in blue. However, diagonal linear lines emanating from the corners of the survey area (circled in orange) likely result from vehicle manoeuvring and are considered artefacts. A distinct area of depleted radioactivity is observed in the northeastern corner of the survey area and is particularly pronounced in the colour palette (C). To further highlight this, the below window gamma data (D) is shown overlaying the ladder settlement at 65% transparency to highlight the relative locations of the linear anomalies in the gamma data and the ladder settlement.



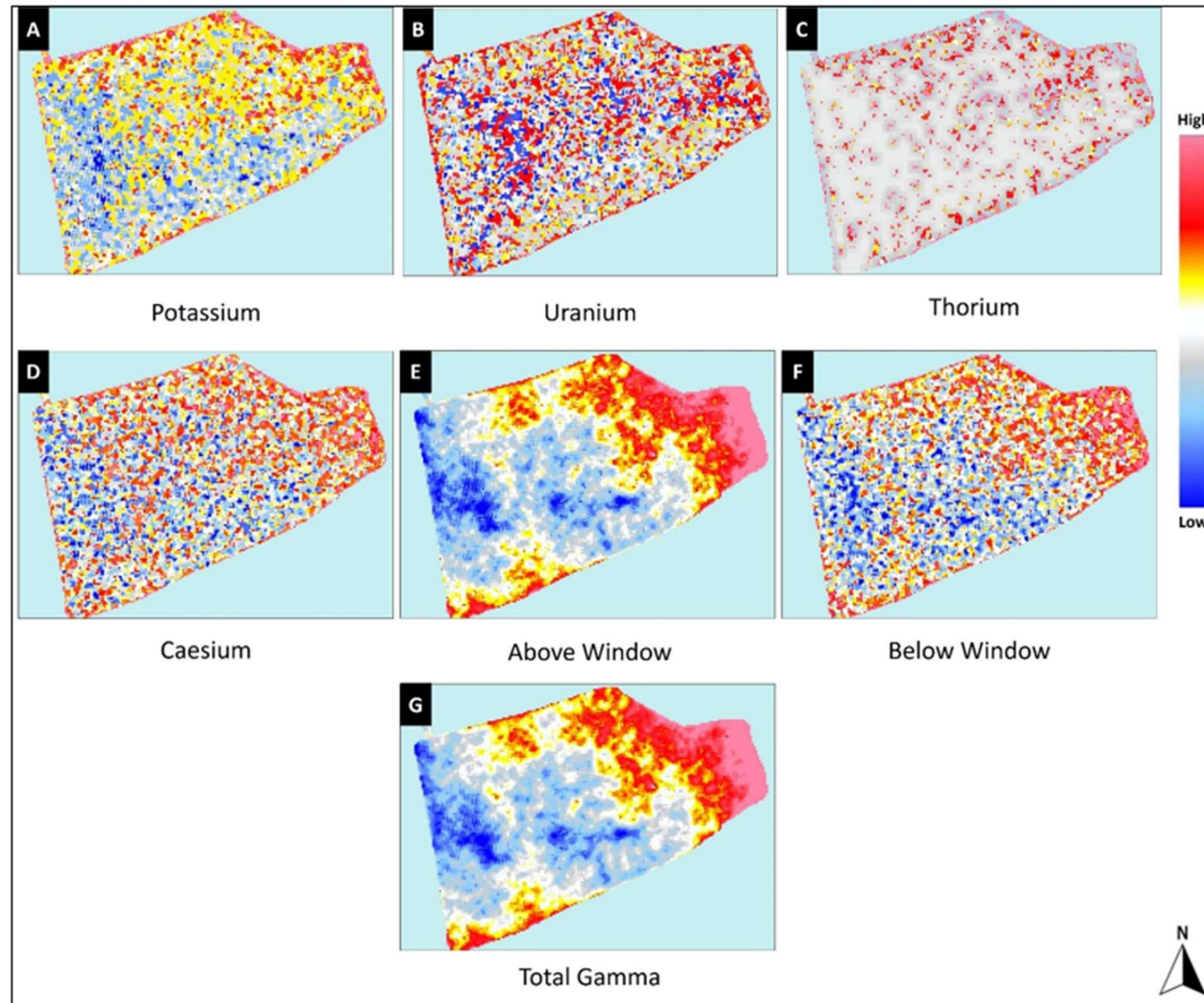
Source: Created from primary data

Figure 6.11 – Composite figure revealing the impact of different energy windows on the clarity of the linear anomaly at the East Heslerton site. (A) Potassium (1400 – 1600 keV), (B) Uranium (1600 – 1900 keV), (C) Thorium (2500 – 3000 keV), (D) Above Window (760 – 3000 keV), (E) Below Window (0 – 530 keV) and (F) Caesium (581 – 740 keV) energy windows are shown against the Total Gamma data (G) image. All images applied GPS Gap Fill + Wallis Filter



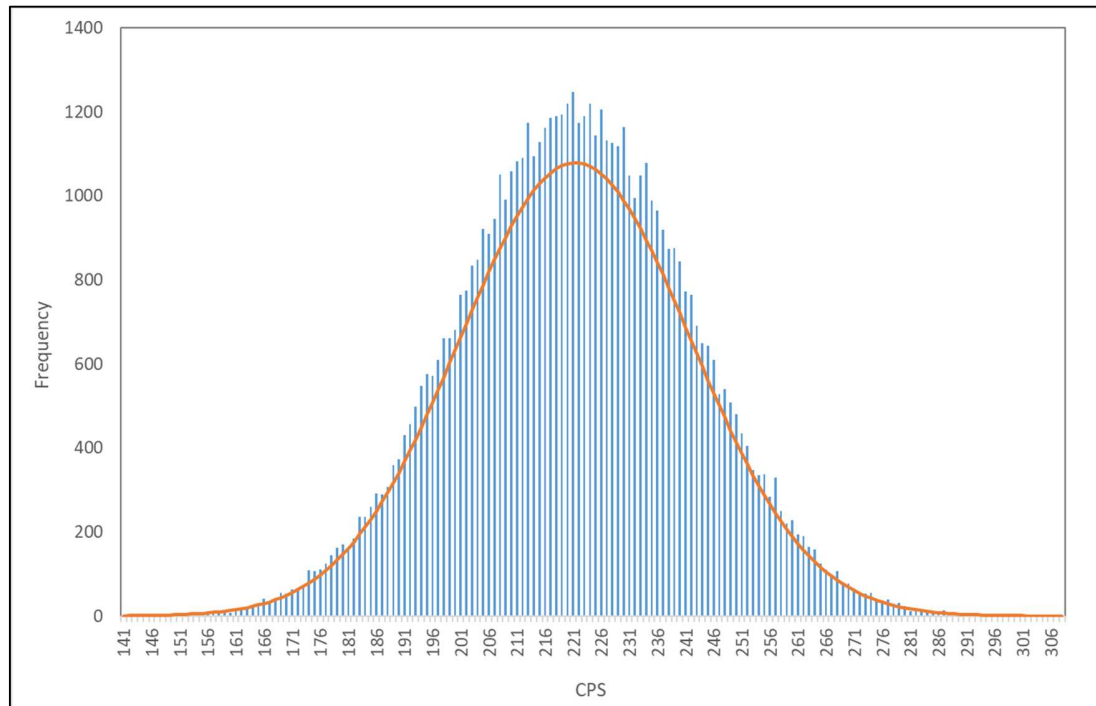
Source: Adapted from Robinson et. al (2024)

Figure 6.12 – Composite figure revealing the impact of different energy windows on the clarity of the linear anomaly at the Silchester site (August 2022 survey). (A) Potassium (1400 – 1600 keV), (B) Uranium (1600 – 1900 keV), (C) Thorium (2500 – 3000 keV), (D) Above Window (760 – 3000 keV), (E) Below Window (0 – 530 keV) and (F) Caesium (581 – 740 keV) energy windows are shown against the Total Gamma data (G) image. All images applied GPS Gap Fill + Wallis Filter.



Source: Adapted from Robinson *et. al* (2024)

Figure 6.13 – Composite figure revealing the impact of different energy windows on the clarity of the linear anomaly at the Silchester site (May 2023 survey). (A) Potassium (1400 – 1600 keV), (B) Uranium (1600 – 1900 keV), (C) Thorium (2500 – 3000 keV), (D) Above Window (760 – 3000 keV), (E) Below Window (0 – 530 keV) and (F) Caesium (581 – 740 keV) energy windows are shown against the Total Gamma data (G) image. All images applied GPS Gap Fill + Wallis Filter.



Source: Created from primary data

Figure 6.14 – Count rate distribution graph for the East Heselton survey, suggesting the background radiation data are normally distributed.

Portable XRF Data from Silchester and East Heselton Samples

Average concentrations of uranium, thorium and potassium from the Silchester and East Heselton environmental and archaeological samples are presented in Table 6.4. Values for Bisham, taken from published data, are also provided for completeness. Concentrations of uranium and thorium have been calculated using the following IAEA conversion factors (IAEA 2003a):

- 1 ppm uranium = 12.35 Bq/kg
- 1 ppm thorium = 4.06 Bq/kg
- 1% potassium-40 = 313 Bq/kg

The percentage of potassium-40, used to calculate the Bq/kg values, has been estimated based on the assumption that potassium-40 constitutes 0.012% of naturally occurring potassium (HPS 2001). Cells marked '<LOD' indicate where element concentrations are below the limits of detection.

The data presented in Table 6.4 suggest that Silchester and Bisham share broadly similar radiological characteristics, with comparable concentrations of potassium, uranium and thorium. This similarity is reasonably expected, noting their close proximity (less than 30 miles apart) and similar geologies with superficial deposits dominated by sand and gravel. In contrast, data from the East Heselton site indicate much lower background radioactivity concentrations. All uranium measurements are below the limits of detection, and only four of the 13 samples analysed yielded positive values for thorium, with seven positive results for potassium. These low values can be attributable to the local geology, which is dominated by wind blown and glacial sand deposits which typically contain lower concentrations of naturally occurring radioactive material relative to soil (IAEA 2003b). The extent of the sandy deposits in this area is further evidenced by the inability to grow crops due to poor water retention (D. Lumley, personal communication, October 2022) necessitating the land's use as pasture. Based on this data alone, it may be concluded that the geologies of the Bisham and Silchester sites are more amenable to identifying targets containing very low radioactivity concentrations, whereas targets with higher concentrations of naturally occurring radioactivity would be more readily identifiable at East Heselton.

When comparing the Silchester soil samples against the gravel, flint and tile samples, it is evident that the tile sample provides the greatest contrast, containing approximately double the amount of potassium, uranium and thorium relative to the soil. Therefore, features constructed from tile and brick (a similarly clay-dominant product) would be expected to appear in gamma radiation distribution maps as positive anomalies. The elevated concentrations of radionuclides within the tile can be explained by its high clay content. Clays are effective adsorbents of radionuclides with the dominant mechanism being ion exchange (Maes *et. al.* 2021). The cationic radionuclides are adsorbed to the negatively charged surfaces of the clay minerals (Maes *et. al.* 2021).

Flint, a form of quartz (silicon dioxide) typically contain low concentrations of uranium and thorium (<10 – 40 Bq/kg and <8 – 25 Bq/kg respectively) and moderate concentrations of potassium-40 (<300 – 400 Bq/kg) (IAEA 2003b). This is largely supported by the pXRF analysis of the flint samples from Silchester which show a similarly low Th/U ratio. Whilst the uranium concentrations are broadly comparable to the soil values, thorium is present at concentrations of around 50% of those found in the soil. Potassium concentrations are significantly lower, at just 5% of the concentration found in the soil. A similar trend can be seen in the pXRF measurements for the gravel, the composition of which is determined by the local bedrock (London Clay Formation and sand deposits). The gravel has a potassium concentration of approximately 50% of that observed in the soil. Whilst uranium concentrations within the gravel were at levels below the limit of detection, the thorium concentrations were present at concentrations comparable to those found in the flint. Based on this data, it may be expected that features comprising flint and gravel would appear in gamma radiation distribution maps as negative anomalies.

Table 6.4 – Results of pXRF analysis showing the average concentrations of naturally occurring uranium (U), thorium (Th) and potassium-40 (K-40) in environmental and archaeological samples from Silchester and East Heselton. For Silchester, mean concentrations (\pm error) are calculated from triplicate measurements per sample. For East Heselton, values represent average concentrations (\pm error) across each borehole. Mean soil concentrations of U, Th and K for the Bisham site (published data) are included for completeness. Isotope ratios (Th/K, Th/U and U/K) for all measurements are also presented.

Location	Sample / Borehole Ref.	Material Type	U-238 (Bq/kg)	Error (+/-)	Th-232 (Bq/kg)	Error (+/-)	K-40 (Bq/kg)	Error (Total K) (+/-)	Ratios		
									Th/K	Th/U	U/K
Silchester (personal data)	12276	Soil	<LOD	3.29	20.60	1.55	307.59	190.06	<u>0.07</u>	0	0
	12260	Soil	45.02	2.97	19.27	1.59	301.41	195.91	<u>0.06</u>	0.43	0.15
	12266	Soil	<LOD	3.34	23.12	1.61	350.77	212.23	<u>0.07</u>	0	0
	Soil – Mean	Soil	15.01	39.80	21.00	6.42	319.92	199.44	<u>0.07</u>	1.40	0.05
	0324-1	Gravel	<LOD	2.55	11.16	1.40	90.77	103.54	<u>0.12</u>	N/A	N/A
	0324-2	Flint	33.58	1.92	11.08	1.74	11.14	56.52	<u>0.99</u>	0.33	3.01
	0324-3	Tile	91.34	3.54	59.58	2.40	832.03	417.55	<u>0.07</u>	0.65	0.11
East Heselton (De Smedt and Verhegge, (2022))	22-484	Soil	<LOD	-	0.0073	20.29	<LOD	-	<u>N/A</u>	<u>N/A</u>	<u>N/A</u>
	22-485	Soil	<LOD	-	<LOD	-	<LOD	-	<u>N/A</u>	<u>N/A</u>	<u>N/A</u>
	22-486	Soil	<LOD	-	<LOD	-	113.13	102.00	<u>N/A</u>	<u>N/A</u>	<u>N/A</u>
	22-487	Soil	<LOD	-	0.0073	20.29	73.69	93.00	<u>9.91E-05</u>	<u>N/A</u>	<u>N/A</u>
	22-488	Soil	<LOD	-	<LOD	-	138.30	110.00	<u>N/A</u>	<u>N/A</u>	<u>N/A</u>
	22-489	Soil	<LOD	-	0.0049	16.23	<LOD	-	<u>N/A</u>	<u>N/A</u>	<u>N/A</u>
	22-490	Soil	<LOD	-	<LOD	-	<LOD	-	<u>N/A</u>	<u>N/A</u>	<u>N/A</u>
	22-491	Soil	<LOD	-	<LOD	-	<LOD	-	<u>N/A</u>	<u>N/A</u>	<u>N/A</u>
	22-492	Soil	<LOD	-	<LOD	-	38.76	101.00	<u>N/A</u>	<u>N/A</u>	<u>N/A</u>
	22-493	Soil	<LOD	-	<LOD	-	<LOD	-	<u>N/A</u>	<u>N/A</u>	<u>N/A</u>
	22-494	Soil	<LOD	-	<LOD	-	21.63	85.00	<u>N/A</u>	<u>N/A</u>	<u>N/A</u>
	22-495	Soil	<LOD	-	<LOD	-	43.91	94.00	<u>N/A</u>	<u>N/A</u>	<u>N/A</u>
	22-496	Soil	<LOD	-	0.0061	16.23	72.57	105.00	<u>8.41E-05</u>	<u>N/A</u>	<u>N/A</u>
Soil – Mean	Soil	<LOD	-	0.001966	5.62	38.61	98.57	<u>5.09E-05</u>	<u>N/A</u>	<u>N/A</u>	
Bisham (UKSO 2024)	N/A	Soil (Mean)	17.91	2.11	27.83	1.70	251.65	0.10	0.11	1.55	0.07

6.3.7 Discussion

In this study, the efficacy of portable gamma radiation survey methods as a supportive archaeological prospection tool has been tested. This has been achieved by deploying Nuvia's Groundhog® system at sites of archaeological interest in Bisham and East Heselton. This builds on previous research undertaken by the authors at the Roman town of Silchester, creating a more robust body of evidence for interrogation and interpretation. The scope of the research has been expanded to include x-ray fluorescence analysis of environmental and archaeological samples collected from Silchester and East Heselton. This has been undertaken to obtain indicative values of potassium, uranium and thorium concentrations present to aid interpretation of the outputs from the gamma radiation surveys.

Results suggest that portable gamma radiation survey methods can effectively identify certain archaeological features and geological transitions potentially attributable to past human activities. Of particular value with this technique is the ability to 'slice' the data by creating gamma radiation distribution maps for individual energy windows. This not only provides an additional opportunity to draw out anomalies that might otherwise have been lost in the total gamma data, but also provides some insight into what might be causing any anomalies present in the data.

The detection of anomalies in the gamma radiation distribution maps from the Bisham and East Heselton surveys, that correspond to anomalies identified in existing geophysical (magnetic and FDEM) data, validates the applicability of the method at different sites. It confirms that the positive results achieved from previous studies undertaken by the authors are not unique to Silchester, but instead have a broader applicability. The results from the Bisham and East Heselton surveys are promising. However, it is recognised that the Groundhog system was not capable of delineating all targets surveyed. Possible causes for this lack of differentiation include an inadequate spatial resolution, the burial depth of the targets and the materials used in target construction containing concentrations of naturally occurring radioactivity comparable to those in the surrounding soil. Whilst linear anomalies identified within the East Heselton gamma radiation distribution map would likely support successful targeting of excavations, the full ladder settlement was not clearly identifiable. At Bisham, the chalk pit and grave site remained elusive.

Further work is therefore required to understand the optimal conditions in which gamma radiation survey methods can be successfully deployed.

The data obtained from pXRF analyses has support the findings from the gamma radiation surveys. For example, it was confirmed that the gravel and flint from Silchester contain lower concentrations of naturally occurring radioactivity relative to the surrounding soils. This underpins the results of previous surveys at Silchester where roads, comprising gravel and flint, were present as areas of depleted radioactivity within the gamma radiation distribution map. It is however recognised that there were significant limitations in the Silchester pXRF data; notably that the samples collected were not from the areas subject to gamma radiation surveying. As part of future work, the authors intend to target sites where archaeological and environmental samples are collected from the areas subject to surveying. Despite these limitations, it is believed that the pXRF results provide valuable early insight and supporting data.

Bisham Survey

The survey of Bisham demonstrated the efficacy of the hand-held Groundhog® system for smaller and/ or more culturally sensitive areas. The survey achieved a good sampling density – above the target 1 measurement per square metre within the time available. Application of the same data processing methods in Geoplot as used in the Robinson *et. al.* (2024) study again resulted in the generation of a high-quality gamma radiation distribution map that accurately reflected the raw data.

The clear linear anomaly associated with the suspected historic field boundary is analogous to previous findings at Silchester, where similar behaviours were observed at what was also suspected to be a historic field boundary. As for Silchester, the cause of the elevated gamma radiation levels associated with the anomaly at Bisham is unknown. The area of depleted radioactivity along the western edge of the survey area is at a slightly lower elevation (approximately 5 metres) relative to the eastern edge. This might suggest that any naturally occurring radioactivity in solution flowing down hill is being held up at this boundary area by some mechanism such as a change in physical composition or chemistry of the soil.

The failure to detect the Iron Age chalk pit and grave was disappointing. This may be due to the small size of these targets, depth of burial or lack of contrast in the amount of radioactivity present in the targets relative to the surrounding soil. It is however noted that a ground penetrating radar survey of the site also failed to locate the grave; rather, it was only identified as a magnetic anomaly in the magnetic data due to the grave goods associated with the grave (Bunker and Thomas 2022).

East Heselton Survey

The use of the vehicle-mounted system at East Heselton supported the surveying of a much larger area than achieved for Bisham, without compromising on sample density. Again, the use of Geoplot with minimal processing resulted in the creation of high-quality gamma radiation distribution maps capable of drawing out anomalies of interest. Colour and monochrome palettes were used to good effect to draw out these anomalies.

As for Bisham, the results from the East Heselton survey were mixed. The ladder settlement creates a clear anomaly in the FDEM data, particularly the magnetic susceptibility and magnetometer data, and to a lesser extent, electrical conductivity data. However, is not clearly discernible in the gamma radiation data, although some linear anomalies in the area were identified. This may be due to the materials used in the ladder settlement containing similar concentrations of radioactive material to the surrounding soil, a shielding effect from overlaying soil, or inadequate spatial resolution. Targeting the linear anomalies found in the approximate vicinity of the ladder settlement, as identified in the gamma radiation data, for excavation would likely yield positive results. However, it is acknowledged that without prior knowledge of the archaeological feature present in the ground (as shown in the FDEM data) these anomalies could be easily overlooked. Equally, the linear anomalies present in the corners of the survey area – artefacts of the turning motion of the Groundhog vehicle – have caused false positives which are misleading without prior knowledge of the site and awareness of the Groundhog® system. The results from this survey therefore highlight the importance of critically appraising the data, avoiding over-processing of data to draw out buried ‘features’ and the value of applying multiple survey methods at a site to aid accurate interpretation. In future surveys, it may be possible to remove these artefacts by traversing the site along transects, rather than driving in a circular

pattern. However, this would only be possible at sites where there is enough space to turn the vehicle at the end of each transect, ensuring correct positioning.

A noteworthy outcome of the East Heselton survey is the ability of the gamma radiation data to clearly delineate the changing geological/ geochemical conditions within the north-east corner of the site, which have created measurable changes in the radiochemical composition of the area, with counts count rates almost halving from an average of 221 cps to ~140 cps in this transitional area. Such insights may be useful in understanding the geological contexts of sites as part of archaeological investigation.

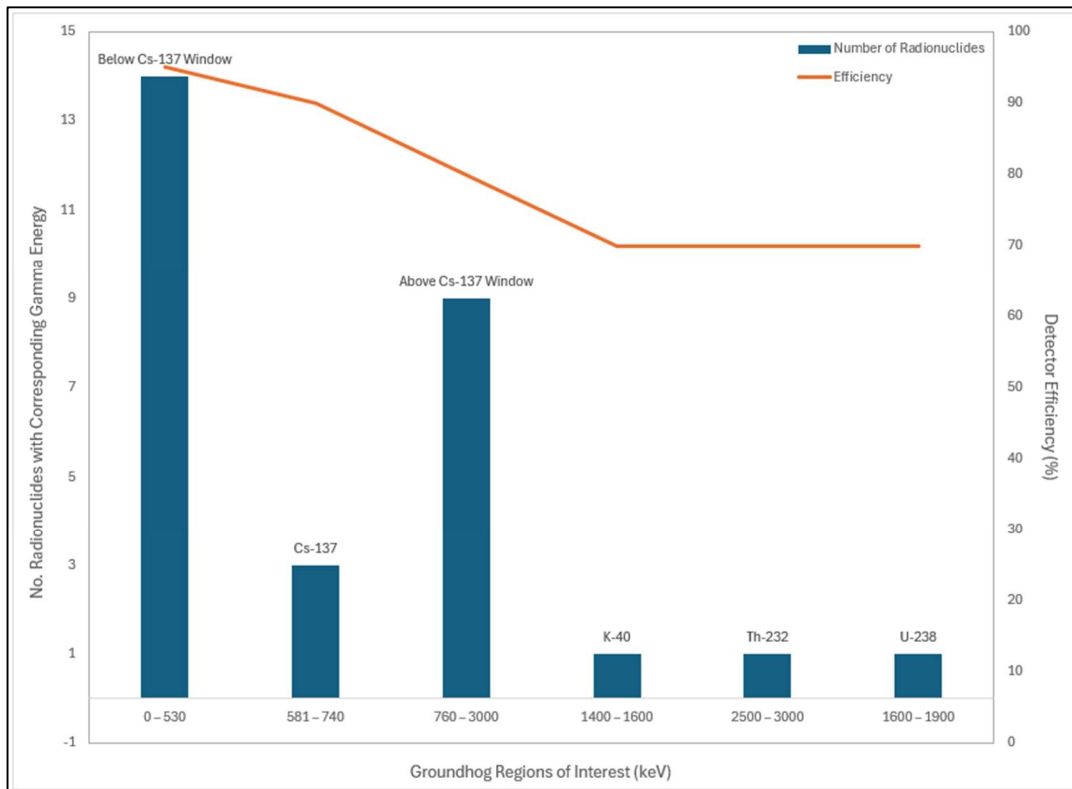
Building on Preliminary Studies – Further Aspects for Consideration

To better understand which of the main radionuclides of interest (potassium-40, uranium-238 and thorium-232) are contributing to the results obtained, a consideration of what the gamma detector is measuring is required. As shown in Table 6.5, there are six gamma emitters in the uranium-238 decay chain, with 12 corresponding characteristic gamma energy peaks. Thorium-232 has four gamma emitters within its decay chain with 13 characteristic gamma energy peaks. The majority of these energy peaks are less than 1000 keV. In contrast, potassium-40 has only one gamma energy peak at 1460 keV. The 76 x 76 mm (3" x 3") NaI detector within the Groundhog® system has the highest adsorption efficiencies for gamma rays with energies in the region of ~350 – 1000 keV, as shown in Figure 6.15. This suggests that those radionuclides with lower energies (i.e. those within the uranium and thorium decay chains) will have the biggest influence in the creation of gamma radiation distribution maps and the detection of any anomalies present. It is these radionuclides then, that are of particular interest moving forward. In contrast, potassium-40 is expected to have the smallest influence.

Table 6.5 – Overview of the gamma emitters and their peak energies from the potassium-40, uranium-238 and thorium-232 decay chains.

Potassium-40		Uranium-238		Thorium-232	
Isotope	Gamma Peak (keV)	Daughter Isotope	Gamma Peak (keV)	Daughter Isotope	Gamma Peak (keV)
K-40	1460	Th-234	63.3	Ac-228	93.4
			92.6		911.1
Pa-234m	100	209.3			
Ra-226	241	338.3			
Pb-214	295.2	Pb-212	238.6		
			351.9	727.2	
Bi-214	609.3	Bi-212	84.2		
			1764.5	277.4	
			1120.3	510.8	
			1238.1	583.1	
Pb-210	46.5	Pb-210	860.5		
			2204.2	2614.7	

Source: Created from primary data

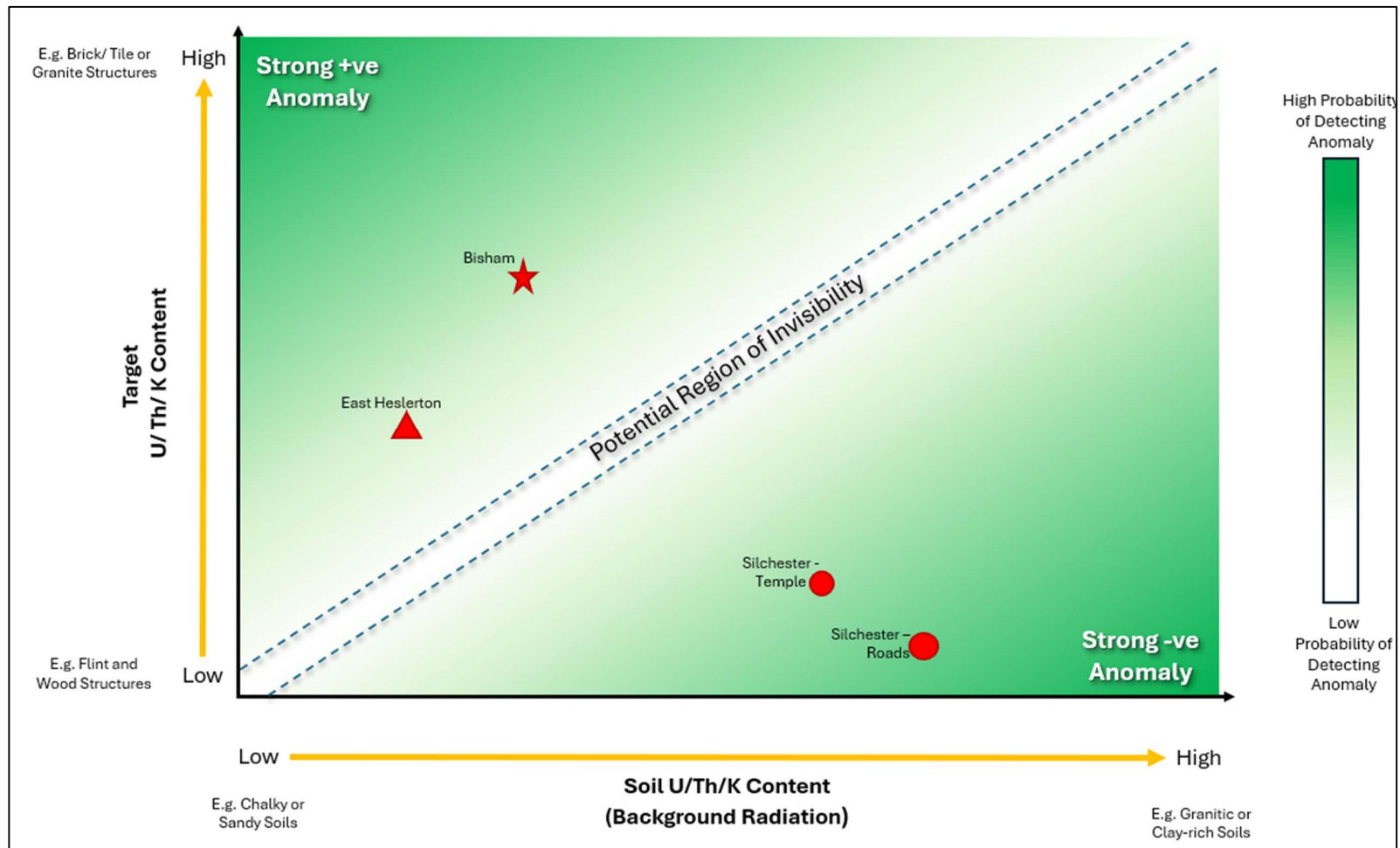


Source: Detector Efficiency Data from Mirion Technologies (2024)

Figure 6.15 – Histogram showing the distribution of radionuclides of interest for this study across the Regions of Interest (ROI) in the Groundhog system. The absorption efficiency of the detector for each ROI is also presented. Most radionuclides are concentrated within the lower energy windows, where the Groundhog system demonstrates the highest efficiency.

Utilising the findings from the research undertaken to date, a model broadly defining optimal conditions for conducting gamma radiation surveys in support of archaeological prospection has been developed by the authors (Figure 6.16). Using data from the Groundhog® surveys at Silchester, Bisham and East Heselton, alongside the preliminary pXRF data and insights into the main isotopes of interest, the model visualises the conditions most likely to generate significant contrasts between archaeological targets and surrounding substrates. Negative results – instances where archaeological targets could not be delineated in the gamma radiation survey data – have informed the inclusion of a “region of invisibility” within this model. This represents conditions where there is no measurable difference in radioactivity present in targets and soils, rendering buried archaeological features undetectable. The approximate positions of the Bisham, Silchester and East Heselton sites have been plotted as a demonstration.

With continued surveying at various sites, better targeted sampling of soils and archaeological materials, and resultant accumulated data, it will be possible to refine the parameters of this model. Enhancements, such as better defining the width of the region of invisibility will support improved planning of gamma radiation surveys. Ultimately, the refined model aims to produce higher-quality data that can effectively complement traditional geophysical methods.



Source: Personal image

Figure 6.16 – Model depicting optimal conditions for conducting gamma radiation surveys in archaeological prospection, along with a ‘potential region of invisibility’ where the contrast in naturally occurring radioactivity between archaeological targets and surrounding substrate is minimal. Approximate locations of Silchester, Bisham and East Heslerton are shown. The figure demonstrates how the gravel/ flint roads of Silchester would yield a reasonable negative contrast relative to the surrounding soil, as seen in the gamma radiation surveys.

6.3.8 Conclusion

By deploying the Groundhog® system to a broader range of archaeological contexts across the UK, it has been possible to obtain further unique and independent datasets capable of supporting the original research aim of determining the efficacy of gamma radiation survey methods in archaeological prospection. This approach also confirmed that positive results from previous surveys undertaken by the authors were not unique to Silchester indicating a wider applicability for this method. By continuing to deploy Groundhog® in both hand-held and vehicle mounted configurations, it has been possible to demonstrate that both techniques can be deployed to create high-quality data sets. This provides flexibility to use the most appropriate survey method taking into account the size, accessibility and sensitivity of the target area.

The inability to consistently identify anomalies in the gamma radiation data that align with the targeted archaeological features, highlights the inevitable difficulty of measuring subtle differences in radiological signals from materials containing similarly low concentrations of naturally occurring radioactive material. However, this consolidation study and creation of the indicative model identifying the optimal surveying conditions, offers a promising start point for future optimal targeting of archaeological sites for gamma radiation survey.

This novel research indicates that while portable gamma surveying methods have not yet achieved the consistent and high-quality feature detection capability of traditional geophysical techniques, they hold clear potential for supporting the interpretation of geophysical data. The gamma radiation data provide additional insights into soil conditions, the physical characteristics of archaeological features, the location of historical field boundaries and their influence on soil conditions. In consequence, this technique presents promising opportunities for improvement and further exploration. Most notably in targeting new archaeological sites with differing geological conditions and targets, deploying different detector types, improving survey methods and collecting more representative environmental and archaeological samples for detailed analysis.

6.3.9 References

Please see Section 6.5.

6.4 Conclusions and Next Steps

As with the Silchester studies, the surveys undertaken at Bisham and East Heslerton yielded mixed results. As both sites, anomalies were identified that broadly aligned with known archaeological features. However, not all targets (including the grave and chalk pit) were identified. At East Heslerton, a change in the hydrogeological characteristics of the site was also identified.

This final study has begun to provide some explanations for the observed results. Across the three sites, archaeological features with lower concentrations of naturally occurring radionuclides appear to be responsible for the clearest anomalies in the gamma radiation distribution maps. Size also appears to be a factor, with larger targets such as roads and walls generating measurable differences in radioactivity. Smaller targets, such as individual houses and inhumations do not appear to offer sufficient contrast using the survey methods applied thus far.

It is acknowledged that this research project has only just begun to explore the efficacy of portable gamma surveying as an additional tool for archaeological investigations. Valuable insights have been obtained that support the use of this technique. However, extensive research is still required to help understand the observations made to date, and to better delineate the specific conditions where this technique will add the most value. Chapter 7 discusses this in more detail, with an outline plan for future work and areas that require further exploration.

6.5 References

ADS (2013) Series: The Landscape Research Centre unpublished report series, ADS Digital Resource 1990 – 2013,

[https://archaeologydataservice.ac.uk/library/browse/series.xhtml?recordId=10469,Archaeological Data Service/ Landscape Research Centre](https://archaeologydataservice.ac.uk/library/browse/series.xhtml?recordId=10469,Archaeological%20Data%20Service/Landscape%20Research%20Centre), Accessed 05/01/2024

ARCHI UK (2024) 1805 – 1845: Earliest British Ordnance Survey 1 inch to 1 mile – Early Georgian OS Map showing the area of Bisham, Berkshire, Latitude 51.557985 Longitude -0776823 NGR, https://www.archiuk.com/cgi-bin/get_victorian_old_maps_of_the_british_isles_ordnance_survey_1inch_1mile.pl?map_location=&ngr=&search_location=Bisham,%20Berkshire,%20SU8585,%20SU%2085%2085&os_series=0&is_sub=&pwd=&latitude=51.557985&longitude=0.776823&placename=Bisham&TownName=BISHAM&county=Berkshire&postcode=, Accessed 01/03/2024

Baldwin, E. and Opitz, R. (2022) ipaast-czo case study: Manor Farm, Yorkshire, <https://ipaast-czo.glasgow.ac.uk/index.php/case-studies/>, Interoperable Precision Agricultural and Archaeological Sensing Technologies (ipaast), Last Updated: 2022, Accessed: 05/01/2024

BGS (2024) British Geological Survey Geology Viewer https://geologyviewer.bgs.ac.uk/?_ga=2.4452917.789100064.1706879541-425405615.1706879541, Accessed: 05/01/2024

Bunker, M. and Thomas, G. (2022) The Marlow Warlord: An Early Medieval Sentinel Burial of the Middle Thames, University of Reading, United Kingdom

Cooke, L. (2012) Vale of Pickering Statement of Significance, Report Prepared for English Heritage (Yorkshire and Humber Region), https://lucooke.files.wordpress.com/2011/12/vop-sos_final_may2012.pdf, Last Updated: 2012, Accessed: 05/01/2024

De Smedt, P. and Verhegge, J. (2022) pXRF Data for Soil Samples from the East Heselton survey area. Samples collected and analysed in 2022. Data Obtained in 2024, via personal communication.

Davies, M. Clark, R. and Adsley, I. (2011) High-Density Gamma Radiation Spectrometry Surveys of Contaminated Land, Proceedings of the 14th International Conference on Environmental Remediation and Radioactive Waste Management, September 25 – 29, Reims, France

Digimap (2024a) “East Heselton in Context”, PDF Map, scale 1:50,000, May 2024, Geology Map using DiGMap GB-50 Rock Unit and Ordnance Survey (AC0000851941) using Digimap Ordnance Survey Collection, <https://digimap.edina.ac.uk/>, created 30/05/2024

Digimap (2024b) “Bisham in Context”, PDF Map, scale 1:50,000, May 2024, Geology Map using DiGMap GB-50 Rock Unit and Ordnance Survey (AC0000851941) using Digimap Ordnance Survey Collection, <https://digimap.edina.ac.uk/>, created 30/05/2024

Google Earth Pro (2018) East Heselton, 54°10'57.27"N 0°34'48.56"W, elevation 31 m, 2D map, imagery date 01/07/2018, viewed 10/02/2024

Google Earth Pro (2021) Bisham, 51o32'27.37"N 0o46'19.34"W, elevation 76 m, imagery date 16/07/2021, viewed 10/02/2024

HPS (2001) Human Health Fact Sheet – Potassium 40, <https://hpschapters.org/northcarolina/NSDS/potassium.pdf>, Health Physics Society (HPS), Last Updated: October 2001, Accessed: 28/04/2024

Humphreys, O. (2019) Archaeology in East Berkshire: A Resource Assessment, Report to the Ardeola Charitable Trust, University of Reading, <https://research.reading.ac.uk/middle-thames-archaeology/wp-content/uploads/sites/180/2021/02/East-Berks-Resource-Assessment-FINAL-1.pdf>, Last Updated: 22/01/2019, Accessed 09/02/2024

IAEA (2003a) Guidelines for Radioelement Mapping using Gamma Ray Spectrometry Data, IAEA-TECDOC-1363, International Atomic Energy Agency, Vienna, July 2003

IAEA (2003b) Extent of Environmental Contamination by Naturally Occurring Radioactive Material (NORM) and Technological Options for Mitigation, Technical Report Series No. 419, International Atomic Energy Agency, Vienna

Kalnicky, D.J. and Singhvi, R. (2001) Field Portable XRF Analysis of Environmental Samples, *Journal of Hazardous Materials*, **83** (1 – 2): 93 – 122, [https://doi.org/10.1016/S0304-3894\(00\)00330-7](https://doi.org/10.1016/S0304-3894(00)00330-7).

LRC (2024a) Heselton Research Project – The Aims, Objectives and Research Design for the Heselton Parish Project, www.landscaperesearchcentre.org/settle/Res_des/Hpdesign.htm, Landscape Research Centre (LRC), Accessed 05/01/2024

LRC (2024b) East Heselton, www.landscaperesearchcentre.org/html/east_heselton.html, Landscape Research Centre (LRC), Accessed 06/01/2024

Maes N., Glaus M., Baeyens B., Marques Fernandes M., Churakov S., Dähn R., Grangeon S., Tournassat C., Geckeis H., Charlet L., Brandt F., Poonosamy J., Hoving A., Havlova V., Fischer C., Scheinost A., Noseck U., Britz S., Siitari-Kauppi M., Missana T. (2021): State-of-the-Art report on the understanding of radionuclide retention and transport in clay and crystalline rocks. Final version as of 30.04.2021 of deliverable D5.1 of the HORIZON 2020 project EURAD. EC Grant agreement no: 847593.

Mirion Technologies (2024) Gamma and X-Ray Detection, <https://www.mirion.com/discover/knowledge-hub/articles/education/nuclear-measurement-fundamental-principle-gamma-and-x-ray-detection#:~:text=The%20high%20of%20iodine,diameter%20by%203%20in>, Mirion Technologies, Accessed 28/04/2024

Powlesland, D. (2008) Why Bother? Large Scale Geomagnetic Survey and the Quest for “Real Archaeology” IN Powlesland, D. (2008) Seeing the Unseen, Geophysics and Landscape Archaeology, First Edition, CRC Press, Florida USA, ISBN: 9780429207372

Randall Farms (2024) Farming, <https://www.randallfarms.co.uk/farming/>, Randall Farms Regenerative Rural Business, Accessed 09/02/2024

Robinson, V., Clark, R., Black, S., Fry, R., & Beddow, H. (2022). Portable gamma ray spectrometry for archaeological prospection: A preliminary investigation at Silchester Roman Town. *Archaeological Prospection*, **29** (3): 353–367, DOI: <https://doi.org/10.1002/arp.1859>

Robinson, V. Black, S. Fry, R. Beddow, H. and Fulford, M. (2024) Radiating Encouragement: Further Investigation into the Application of Gamma Ray Spectroscopy for Archaeological Prospection at the Roman Town of Silchester, *Archaeological Prospection*, **31** (3): 249 – 266, DOI: <https://doi.org/10.1002/arp.1950>

UKSO (2024) UK Soil Observatory Map Viewer – Potassium, Uranium, Thorium, https://map.bgs.ac.uk/arcgis/services/UKSO/UKSO_BGS_NSI/MapServer/WmsServer?, UK Soil Observatory (UKSO), Accessed 03/06/2024

University of Arkansas (2024) Heselton Atlas, <https://lrc.cast.uark.edu/map>, University of Arkansas, Accessed 22/12/2024

UoR (2024) University of Reading Survey of the Bisham Site – Unpublished Data, accessed: April 2024

Verhegge, J. Van Parys, V. Baldwin, E. Optiz, R. and De Smedt, P. (2023) IPAAS East Heselton FDEM (Version 1) [Data Set], Zenodo, <https://zenodo.org/records/7741749>, DOI: 10.5281/zenodo.7741749, Accessed: 12/01/2024

Woodland Trust (2024) Bisham Woods, Cookham Dean Maidenhead, <https://www.woodlandtrust.org.uk/visiting-woods/woods/Bisham-woods/>, The Woodland Trust, Accessed 09/02/2024

Yusof, M.Y.D. Idris, M.I. Mohamed, F. and Nor, M.M. (2020) Adsorption of Radioactive Element by Clay: A Review, Institute of Physics Conference Series: *Materials Science and Engineering*, **785** 012020, DOI: 10.1081/1757-899X/785/1/012020

Acknowledgements

This unique investigation was possible thanks to NUVIA Limited who provided access to the Groundhog® Fusion System and supporting software tools. The authors wish to express their thanks and gratitude to the University of Reading for providing access to the Silchester site, and to Dominic Powlesland and the Universities of Glasgow and Ghent for their insights, support and facilitating access to the East Heselton Site.



CHAPTER 7

Discussion

7 DISCUSSION

This research provides new insights into the efficacy of portable gamma survey methods as a complementary tool for archaeological prospection. Results indicate that some archaeological targets exhibit measurably different radioactivity levels relative to the surrounding soil, resulting in clear anomalies visible in the gamma radiation distribution maps derived from the survey data. This supports the hypothesis posed in Chapter 1. However, results to date are not consistent, as many features fail to show such measurable differences in radiological composition. Overall, results have been positive, leading to the development of a model that can be used to better help plan future gamma radiation surveys, based on the radiological characteristics of the soil and anticipated target type as presented in Chapter 6. This model builds on a more high-level version of a chart presented in Chapter 3. The findings from the Bisham, Silchester and East Heslerton plots was used to more accurately define conditions leading to strong positive and negative contrasts as well as to identify a ‘region of invisibility’ where insufficient contrast in the radiological characteristics of archaeological targets and surrounding soil prevents detection of these buried features.

7.1 Introduction

As explored in Chapter 1, the overarching aim of this research was to test the hypothesis that past human and geological processes can cause measurable variations in concentrations of naturally occurring radioactive material relative to the surrounding soil. Further, it was believed that by measuring these differences, it would be possible to detect structures and objects of archaeological interest. This hypothesis was tested by deploying portable gamma radiation survey methods developed for use in the nuclear industry.

This thesis demonstrates how a combination of fieldwork, laboratory analysis and literature reviews have been successfully applied to collect the right type and quantity of data to help address the overarching research aim. The collated information has provided valuable insights into the efficacy of the gamma radiation surveying as a complementary method for archaeological investigation, and has improved our understanding of factors that may be contributing to variations (or lack thereof) in observed radioactivity.

This chapter seeks to further highlight key findings from the research undertaken and explore the possible factors influencing the observations made. Reflections on the limitations of the methodologies applied and challenges faced are presented. The chapter concludes by providing recommendations on future work to build on these early findings.

7.2 Key Findings

The literature review for this thesis (**Chapter 2**) fulfilled two key functions. Recognising the diverse nature of this research project, the first function was to provide key contextual information on the following concepts:

- The presence of naturally occurring radioactivity in the environment;
- Methods of measuring this radioactivity (with a focus on Nuvia's Groundhog system);
- Potential mechanisms for accumulating naturally occurring radioactivity in archaeological targets; and
- The value of applying multiple non-intrusive surveying methods in archaeological investigations.

This was undertaken to provide a solid foundation upon which to build the subsequent chapters, and to gain an early indication of the feasibility of the study. The second function was to investigate the extent to which the application of portable gamma radiation survey methods have been applied to archaeological investigations. This second phase was key to understanding the gaps in the published literature, areas for improvement and how this research could make a new and original contribution to the existing body of knowledge. Reviewing existing studies would also provide further indication of the feasibility of the proposed research project.

The study highlighted the value of conducting non-intrusive investigations; from obtaining important contextual information without disrupting the site, to supporting the effective targeting of intrusive investigations to maximise data collection. The study also highlighted the vulnerabilities of geophysical methods that can lead to false positive (Type 1 error) or false negative (Type 2 error) results during interpretation. This supported the supposition that applying more than one geophysical method at a site can be highly beneficial. Such an approach generates multiple, complementary datasets that can be compared and contrasted. This, in turn, improves

the quality of data interpretation by reducing the risk of Type 1 and Type 2 errors, improving confidence in the conclusions drawn.

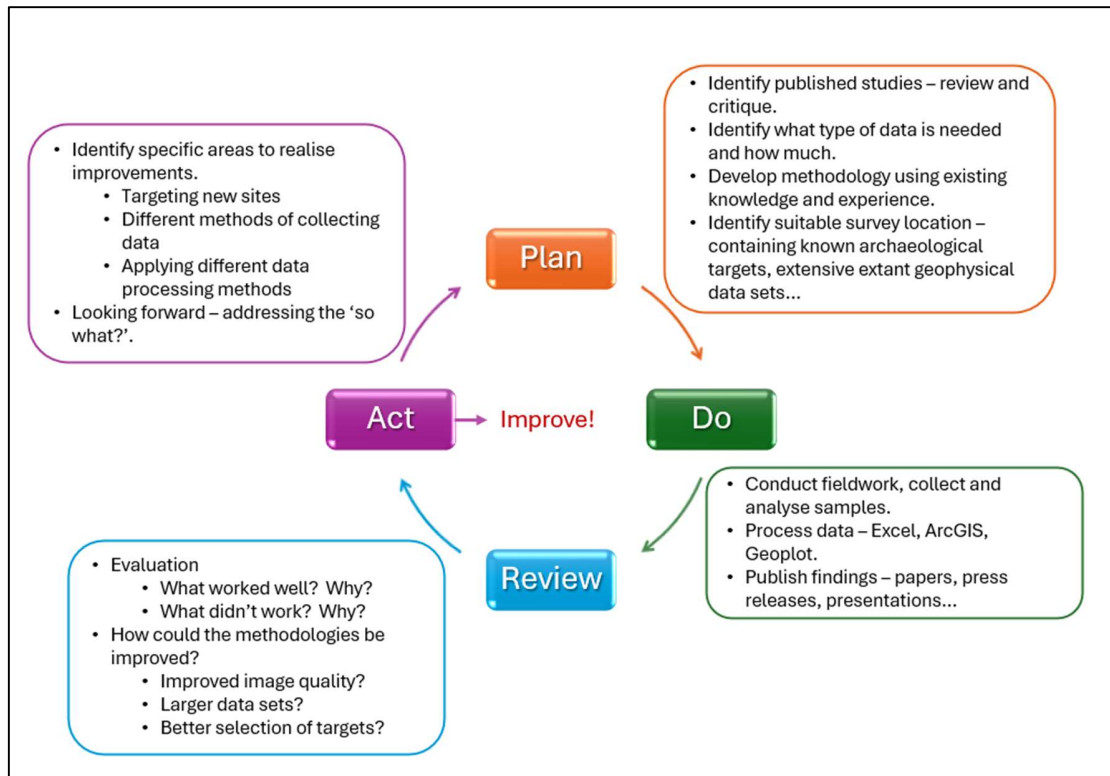
The output of this part of the review supported the use of gamma radiation surveying as a complementary tool in the existing toolbox of geophysical methods. The literature identified viable mechanisms for creating measurable differences in radioactivity between targets and surrounding soil. These mechanisms include the import of construction materials from other areas and the processing of materials for construction, which can concentrate naturally occurring radioactivity (e.g., during brick formation). Further, the literature review supported the idea that conducting a gamma radiation survey of an archaeological site enables the collection of a unique data set that could aid in the interpretation of outputs from other geophysical surveys.

The second phase of the literature review highlighted the scarcity of published information in this area of research. Fewer than ten studies associated with radiological investigations of archaeological sites were found in the published literature. All referenced studies utilised static radiation survey methods. A number of shortfalls were identified within these studies, ranging from unclear or incomplete methodologies to a lack of investigation into the underlying causes for the results obtained.

The outcome from this phase of the literature review was as positive as it was challenging. The limited research on the application of (portable) gamma radiation survey methods for archaeological prospection created multiple avenues of exploration for this research project. At the same time, this meant that the study had a potentially broad scope and could easily lose focus and traction. Further, there was no clear methodology to follow and build on. This necessitated the application of an iterative approach to the project strategy as summarised in Figure 7.1. The baseline methodology for conducting the gamma radiation surveys was informed by the methodology for deploying Groundhog in a nuclear industry context, and applied in a preliminary study as explored in Chapter 3. The lessons learned and data gaps were used to inform a revised approach; a process that was repeated as the project progressed. This resulted in several positive outcomes including:

- The successful deployment of Groundhog in a vehicle-mounted configuration;

- The discovery that Geoplot could be used to generate high-quality gamma radiation distribution maps; and
- The successful completion of pXRF analyses to aid interpretation of Groundhog outputs.



Source: Personal image

Figure 7.1 – Overview of the iterative approach to developing the strategy and methodology for this project.

The findings from the preliminary study at Silchester, using Groundhog in a hand-held configuration, (**Chapter 4**) provided an early indication that the technique may be viable. Results showed that the technique was capable of delineating several buried features, including a temenos wall (negative anomaly), and an infilled clay pit (negative anomaly). It is possible that the survey also highlighted the location of a kiln, identified as a positive anomaly. However, there is a high level of uncertainty with this interpretation, as the linear anomaly identified in the data could also be explained as an artefact of interpolation. The study also highlighted that several targets could not be identified, including roads, buildings, cremations and inhumations. Further, only small areas could be surveyed over a two-day period. This influenced the decision to survey a different area of Silchester using Groundhog in a vehicle mounted configuration to explore repeatability and scalability.

Chapter 5 presented the results from this second study. Again, mixed results were obtained, with some targets failing to create a measurable contrast in radioactivity; most notably a house and temple. The roads in this area created distinctive negative anomalies, which was unexpected based on the results of the preliminary study. The cause of this discrepancy is not known. This second study also revealed transitions in the radiochemical composition of the soil itself, in one case suggesting the presence of a historic field boundary not visible in the magnetometer survey data. The ability to map changes in the radiochemical composition of the soil was replicated in the Bisham and East Heselton surveys (**Chapter 6**). Again, the gamma data was able to delineate a suspected historic field boundary, this time at Bisham. However, as with previous studies at Silchester, smaller targets were indistinguishable. The ladder settlement at East Heselton was not as clearly delineated in the gamma radiation data as it was in the geophysical surveys. However, it was concluded that if an intrusive investigation were planned, targeting the positive anomalies highlighted in the gamma radiation distribution map would likely have led to the settlement being found. Results from the three studies suggest that size is a potentially significant factor in determining the success of a survey, and that with the current techniques and technologies, only larger more robust features can be delineated. However, this research has shown that gamma radiation surveys can provide other potentially valuable contextual information such as historic changes in land use (as observed in Silchester and Bisham), transitions in geological conditions (as observed in Silchester and East Heselton) and possible insights into the thickness and consolidation of materials (as seen in the Roman roads at Silchester) that are not always identified in traditional geophysical surveys.

Overall, the research undertaken to date has highlighted that whilst portable gamma radiation surveying may be a valuable tool to support non-intrusive archaeological investigations, there remains a high level of uncertainty. It has been possible to demonstrate that Groundhog can delineate some archaeological features. However, it is not yet fully understood why the technique is effective for some targets and not others, although target size does appear to be one factor.

The following section explores the difficulties encountered, limitations of the methodologies applied and how they were managed. We will then proceed to a more detailed evaluation of the results.

7.3 Limitations and Impacts of the Selected Methodology

Table 7.1 provides an overview of challenges faced, the limitations of the methodologies applied, any impacts on the study and how they were managed. Many of these challenges were identified in advance of the project, making the content of this table somewhat comparable to that in Table 3.1. However, some challenges that arose during the course of this research, such as the Covid-19 pandemic, were unforeseen and are included here for completeness.

Table 7.1 – Overview of challenges and limitations of the methodologies applied, impacts on the study and mitigation measures applied.

Challenge/ Limitation	Impact on Study	Mitigation Strategy
Limited number of analogous studies, and no existing published studies where portable surveying methods have been applied.	No supporting information that could inform methodology development. Challenging to define where this research fits into the current body of knowledge.	Development of an iterative strategy that built on methods applied in the nuclear industry, and gradually built on lessons learned from each study.
Limited access to Groundhog equipment due to deployment on commercial projects.	Scheduling of fieldwork dependent on equipment availability.	Early planning of fieldwork, and booking out of equipment at the earliest opportunity.

Challenge/ Limitation	Impact on Study	Mitigation Strategy
<p>Did not re-survey the same area to more reliably test different variables, e.g.,:</p> <ul style="list-style-type: none"> • Wet vs dry conditions • Vehicle mounted vs hand-held Groundhog configuration • Collimated vs uncollimated surveys • Different sampling densities • Repeating the same standard method 	<p>Degree of uncertainty regarding key factors influencing the outcome of a survey. For example, conducting a collimated survey of the kilns in the preliminary Silchester study could have yielded clearer results.</p>	<p>Multiple areas of Silchester were surveyed, targeting analogous target types to test repeatability and scalability simultaneously.</p> <p>It is however recognised that the completion of repeat surveys at the same area will yield valuable additional data to contribute to our understanding of the efficacy of the technique. It is therefore proposed that this is addressed as part of future work (Recommendation 1).</p>

Challenge/ Limitation	Impact on Study	Mitigation Strategy
<p>Limited number of archaeological sites surveyed.</p>	<p>The geologies of the three sites surveyed were relatively similar, dominated by gravel deposits. All were agricultural in nature. The effectiveness of Groundhog in more extreme environments such as sandy or granite-dominated regions is not yet known.</p>	<p>The sites selected were chosen based on the amount of existing geophysical data available, ease of access, ease of obtaining the necessary permissions and, in the case of the earlier studies, proximity to the Harwell Campus and University of Reading.</p> <p>Surveying additional sites, including those with distinctly different characteristics (including soil and target types) to those targeted as part of this research, will provide valuable additional data to determine the wider application of the technique. This should be addressed as part of future work (Recommendation 2).</p>
<p>No baseline study to explore the impact of different variables such as target type, substrate type, depth of burial and soil moisture content under controlled conditions.</p>	<p>Limited understanding of the potential impact of these variables on the success of the technique.</p>	<p>Attention was focussed on determining whether gamma radiation surveying methods could generate positive results in the field. If this was found to be repeatedly the case, then further work could be undertaken to understand the observations made.</p>

Challenge/ Limitation	Impact on Study	Mitigation Strategy
<p>Covid-19 pandemic</p>	<p>There was a period of nearly 2 years where it was not possible to undertake fieldwork; either due to controls in place due to the pandemic, or due to the backlog of commercial projects for the Groundhog equipment.</p>	<p>This was largely mitigated by the fact that this research was undertaken on a part-time basis. During this time, it was possible to focus on the literature review and planning a strategy for future fieldwork/ research.</p>
<p>Environmental and archaeological samples for pXRF analysis were not collected from the areas surveyed at Silchester.</p>	<p>pXRF data does not provide a true representation of the variations in concentrations of uranium, thorium and potassium found in the Groundhog data.</p>	<p>This had only a limited impact on the study. The main purpose of this analysis was to gain a broad understanding of the radiological characteristics of materials present at the sites. The data collected was sufficient for this purpose.</p> <p>Looking forward, it will be important to analyse archaeological and environmental samples recovered from the area subject to gamma radiation surveying to aid interpretation of the survey results (Recommendation 3).</p>

Challenge/ Limitation	Impact on Study	Mitigation Strategy
<p>Limited access to the bespoke version of ArcGIS developed by Nuvia for processing Groundhog data.</p>	<p>Delays incurred in processing Groundhog data. Unable to automatically generate count rate distribution maps.</p>	<p>Use of Geoplot for processing data – this was found to be a highly effective tool capable of generating high-quality visualisations. These could be imported into a standard version of ArcGIS to overlay over existing geophysical data to aid interpretation.</p> <p>Count rate distribution maps were generated in Excel. This also enabled the inclusion of a normal distribution curve to aid interpretation.</p>

7.4 Interpretation and Evaluation of Results

Chapters 4, 5 and 6 provide promising early evidence that gamma radiation surveying can offer complementary data to support archaeological investigations. In addition to the delineation of some archaeological targets, the technique has demonstrated the ability to identify historic land boundaries, possible historic variations in land use and transitions in geological conditions. All of these elements may contribute valuable contextual information when characterising a site of archaeological interest.

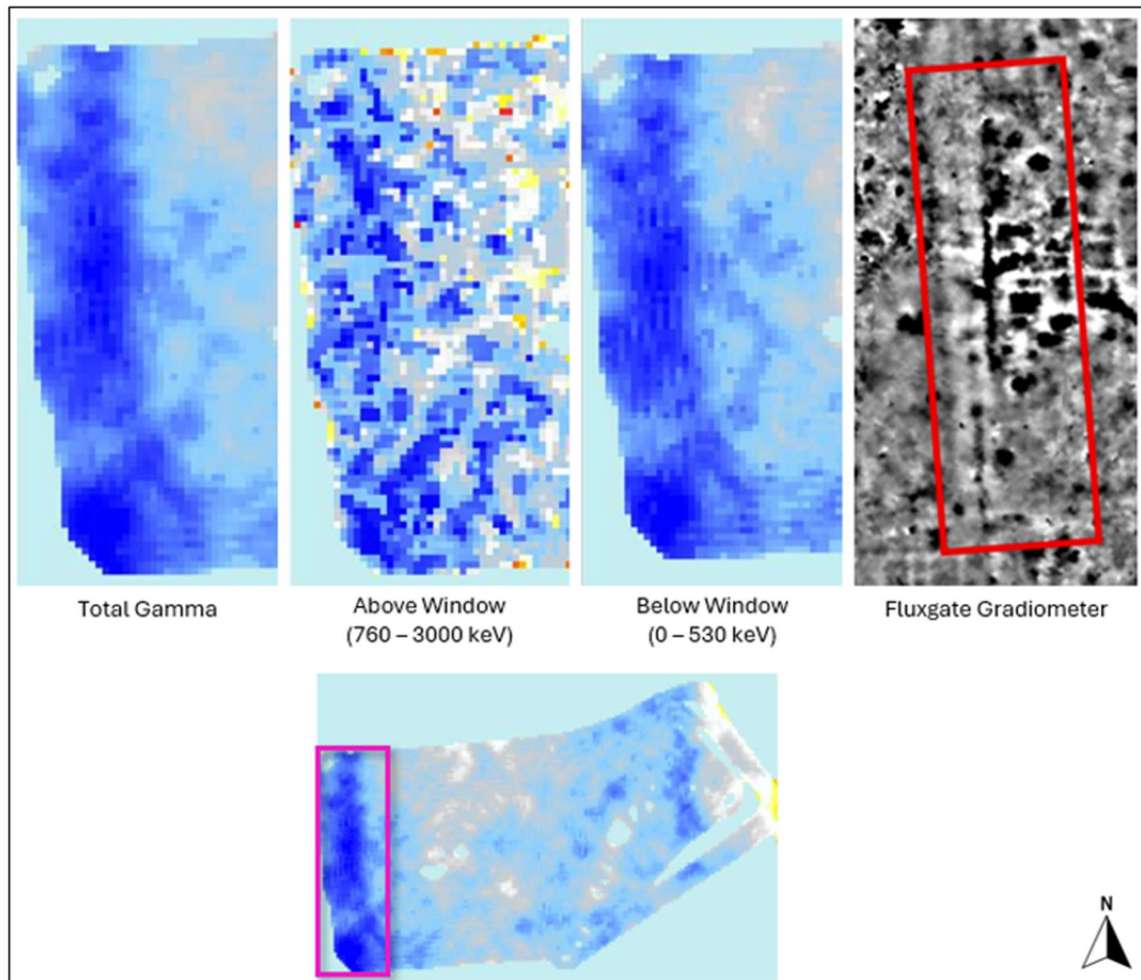
However, as alluded to in the previous sections, the conditions influencing the effectiveness of the technique are not yet fully understood. That the technique appears to more effective at detecting larger features, such as substantial walls (Chapter 4) and roads (Chapter 5) with smaller features such as cremations and inhumations (Chapters 4 and 5) remaining illusive, suggesting that target size is a significant factor.

Initially, it was believed that the amount of interstitial water present in the soil would be a significant contributory factor to the success of the technique. This is due to water's effectiveness at inhibiting gamma radiation and therefore its regular use as shielding material in nuclear facilities, such as in fuel storage ponds (ONR 2023). However, preliminary results from the second survey at Silchester (Chapter 5) suggest that this is not necessarily the case. Both the August 2022 and May 2023 surveys were capable of delineating the road structures, despite differing climatic conditions. This result was unexpected. The August 2022 survey was conducted in warm and dry weather following an extended dry period. These conditions were expected to be ideal for gamma radiation surveying. In contrast, the May 2023 survey followed an extended period of higher than average rainfall. There was a concern that the increased groundwater would act to shield the gamma emissions emanating from the soil from the Groundhog detector, creating a more homogenous gamma radiation distribution map and less clear presentation of anomalies present as observed in the August data. However, this effect was not observed. As the soil in the immediate area around the roads appears to be relatively well draining, it may be that the amount of water present was insufficient to have a significant shielding effect. Further research is recommended to be able to more confidently determine whether soil moisture significantly influences the technique's effectiveness (**Recommendation 4**).

As expected, the presence and absence of certain groups of radionuclides appears to influence the ability to form clearly defined anomalies within the gamma radiation distribution maps. Figure 7.2 presents a close-up view of the anomaly attributable to the main road running through Silchester. The figure shows the visualisations created using the Total Gamma, Above (caesium-137) Window and Below (caesium-137) Window data. The Above Window data generates the lowest quality image, with a lot of 'noise' present, impacting on the clarity of the negative anomaly created by the road. As demonstrated in Table 6.5, this noise may be attributable to radionuclides with higher gamma energy peaks such as potassium-40, bismuth-214 (a daughter in the uranium-238 decay chain) and thallium-208 (daughter in the thorium-232 decay chain). In contrast, the Below Window data provides a gamma radiation distribution map of comparable, if not slightly better, quality to the Total Gamma data. It has therefore been possible to draw out more detail not necessarily visible in the Total data. The negative anomaly in the Total Gamma data appears to be slightly more homogenous when compared to the Below Window image, which appears to show the anomaly becoming less distinctive towards the edges of the road. This may be an effect of the detectors capturing additional gamma rays from the surrounding soil, with incident radiation entering the detector at an angle as well as from directly underneath. Alternatively, this could be indicative of the roads being less well consolidated towards the edges, with greater mixing with the surrounding soil or increased depth. A circular area of slightly increased radioactivity within the road itself, which could indicate a localised change of material type in the road or soil, is slightly better defined in the Below Window image. Similarly, a '>' shaped anomaly to the right of the road also appears to be better defined in the Below Window data.

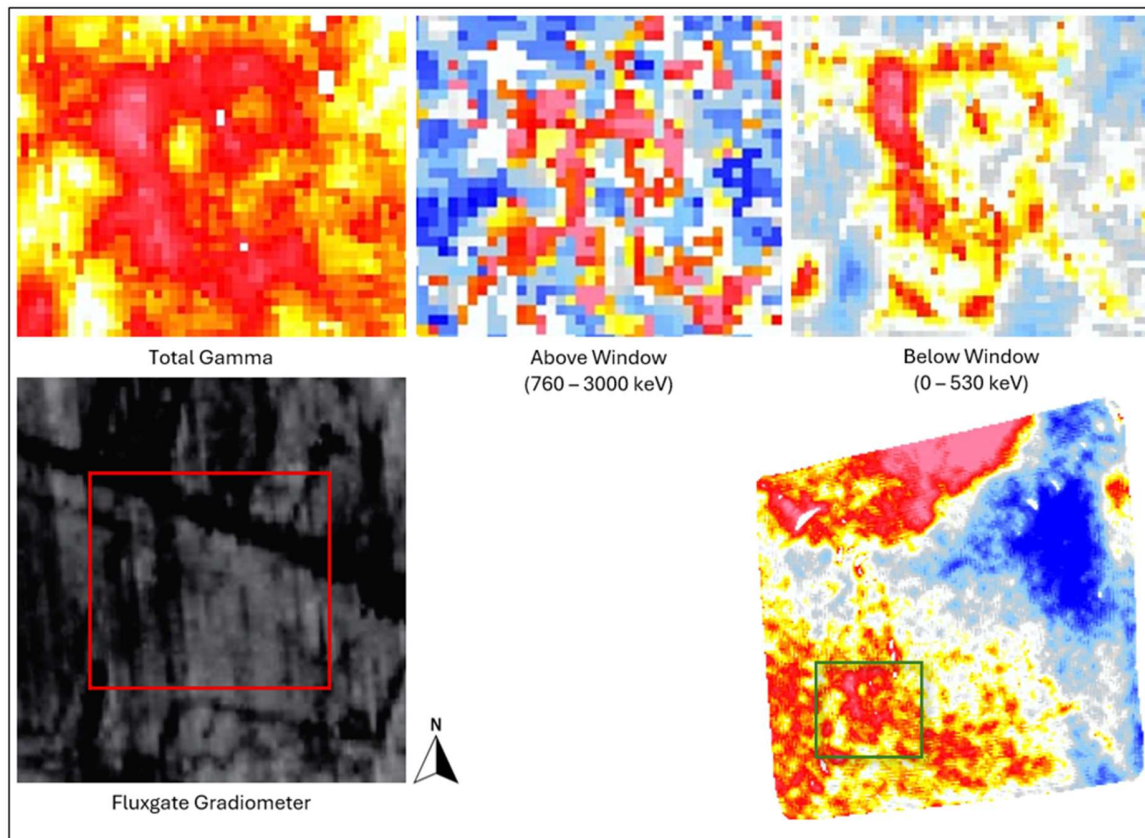
A similar trend is observed in the East Heselton data. Figure 7.3 shows a close-up view of the 'Γ' shaped positive anomaly believed to be part of the ladder settlement. Again, the Above Window data creates the lowest quality image which contains a lot of noise, making the anomaly more difficult to distinguish. In contrast, the Below Window data is particularly effective at drawing out the anomaly – more so than the Total Gamma data. Indeed, the Below Window image gives a more definitive shape to the anomaly, drawing out more detail and possibly also indicating additional anomalies within what appears to be a more square rather than 'Γ' shape. These observations suggest that the feature responsible for creating this anomaly contains elevated concentrations of lower energy radionuclides from the uranium-238 decay chain (including thorium-234, protactinium-234m, radium-226, lead-214 and lead-210) and thorium-232 decay

chain (including actinium-228, lead-212 and thallium-208). It is important to note that even in areas of elevated radioactivity, values remain within normal ranges expected for the region. As observed in the Silchester data, a clear ‘edge’ effect around the out-edges of linear anomaly in the East-Heslerton data is visible, showing a gradual reduction in radioactivity.



Source: Fluxgate Gradiometer Data (Creighton and Fry 2016)

Figure 7.2 – A comparison of the ‘Total Gamma’, ‘Above Window’ and ‘Below Window’ energy window representations of the negative anomaly delineating the main Roman road running through Silchester. All gamma radiation images applied GPS Gap Fill + Wallis Filter.



Source: Fluxgate Gradiometer Data (LRC 2012) and personal data

Figure 7.3 – A comparison of the ‘Total Gamma’, ‘Above Window’ and ‘Below Window’ energy window representations of the positive anomaly associated with the ladder settlement at East Heselton. All gamma radiation images applied GPS Gap Fill + Wallis Filter.

Finally, the burial depth of the target is also expected to have a significant impact on the effectiveness of a gamma radiation survey undertaken at an archaeological site. As shown in Figure 7.4, it is expected that the amount of overburden above a target will result in a progressively weak anomaly, regardless of whether the anomaly created by the target is positive or negative. In the case of a target creating a positive anomaly, increasing the depth of overburden will act to progressively reduce the amount of gamma radiation from the target reaching the detector. This in turn will reduce the contrast between the target and surrounding soil, leading to the creation of a homogenous gamma radiation distribution map. For a target creating a negative anomaly, the increasing amount of overburden, which contains more naturally occurring radioactive material relative to the target, will increase the amount of gamma radiation reaching the detector. Again, this will reduce the measurable contrast, and create a homogenous gamma radiation distribution map.

It is highlighted that the responses presented in Figure 7.4 are indicative only, informed by the findings from this research. To more accurately plot this figure, further research is required to measure detector responses to a known target placed at different depths (**Recommendation 5**).

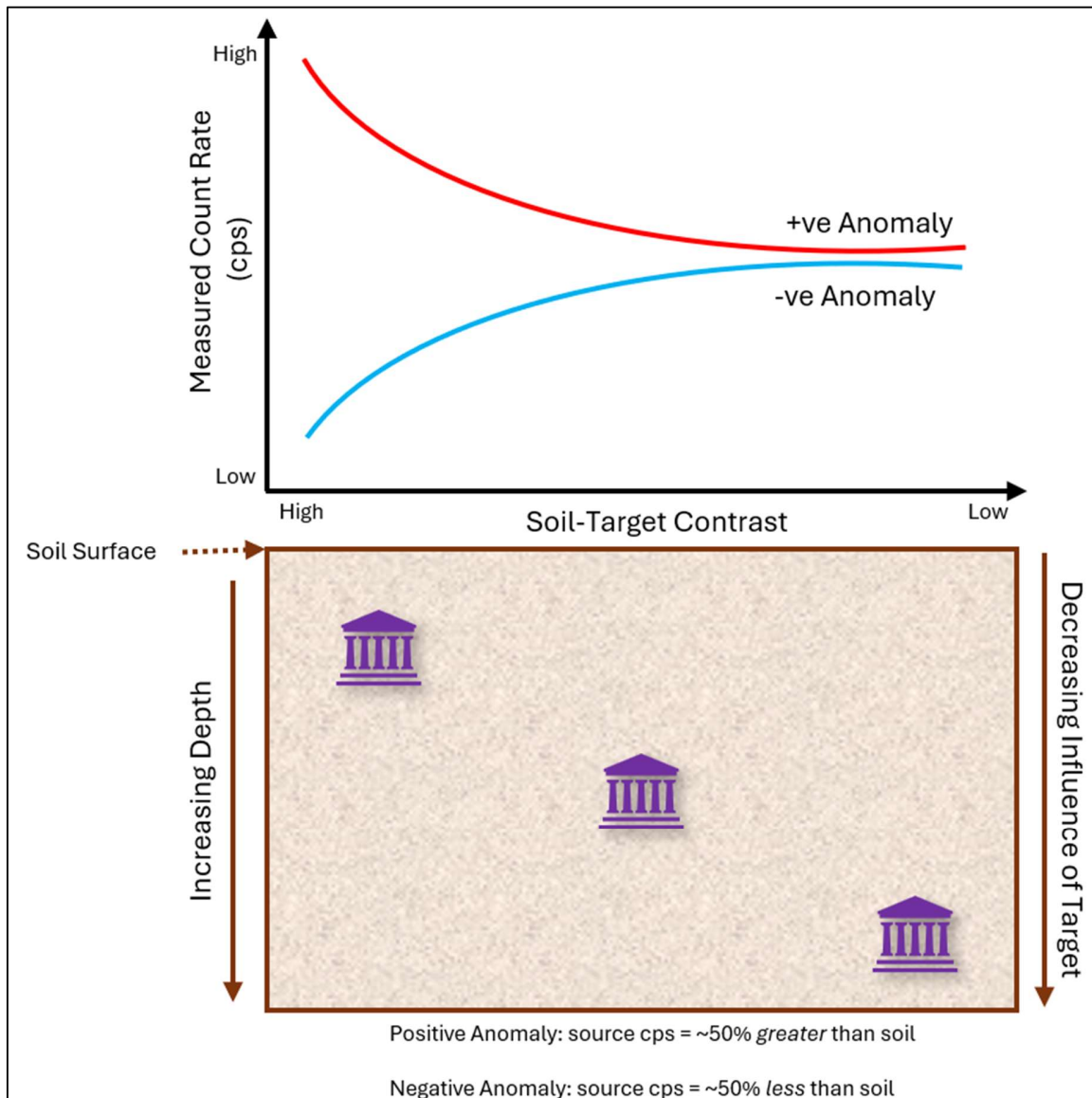


Figure 7.4 – Graphic showing the anticipated impact of burial depth of a point source, containing either a higher or lower concentration of radioactivity relative to the surrounding soil, on the strength of the anomaly generated.

7.5 Implications of this Research and Recommendations for Future Work

This research project provides the first comprehensive study exploring the effectiveness of portable gamma radiation survey methods for the purpose of archaeological investigation. This includes the systematic testing of multiple configurations of the surveying system and the testing of the technique on a range of target types and geologies. In consequence, we have learned that archaeological features are capable of creating both positive and negative anomalies in gamma radiation distribution maps. We are also starting to understand what key factors may be influencing the viability of the technique, including target site, target depth and physical/radiochemical composition. It has also been possible to determine that Total Gamma datasets are capable of generating consistently high quality results, although being able to look at individual energy windows can be of value in some scenarios.

The positive results from this research has several potentially significant implications. Firstly, it is possible that this work has added a new technique to the suite of non-intrusive survey tools available to archaeologies – possibly the first in over 50 years. The technique has the potential to provide additional contextual information, not previously explored, that is unavailable through traditional geophysical methods. Secondly, this research has highlighted the value of cross-discipline knowledge sharing and potential for innovation. For example, it is believed that the work presented here represents the first instance of deploying a system designed within the nuclear industry specifically for the detection and mapping of anthropogenic radioactive contamination in an archaeological context. Finally, there remains further opportunity to explore the efficacy of the technique, expanding into new applications and potentially develop improved techniques and technologies to improve the success of the method.

7.5.1 Recommendations for Future Work

Throughout this discussion, a number of recommendations for future work have been identified.

These are summarised as follows:

- **Recommendation 1** – Completion of repeat surveys at the same site to systematically and accurately test the impact of key variables including:
 - Efficacy in wet and dry conditions.
 - Efficacy of vehicle mounted and hand-held Groundhog surveys on the same target.
 - Impact of surveying with and without collimation on the ability to detect a target – especially those likely to yield minimal contrast.
 - Impact of different sampling densities on gamma radiation distribution map quality.

- **Recommendation 2** – Completion of additional surveys at sites with contrasting geologies and target types relative to those sites covered within this study. The model developed in Chapter 6 (Figure 6.16) can be used to identify optimal target sites.

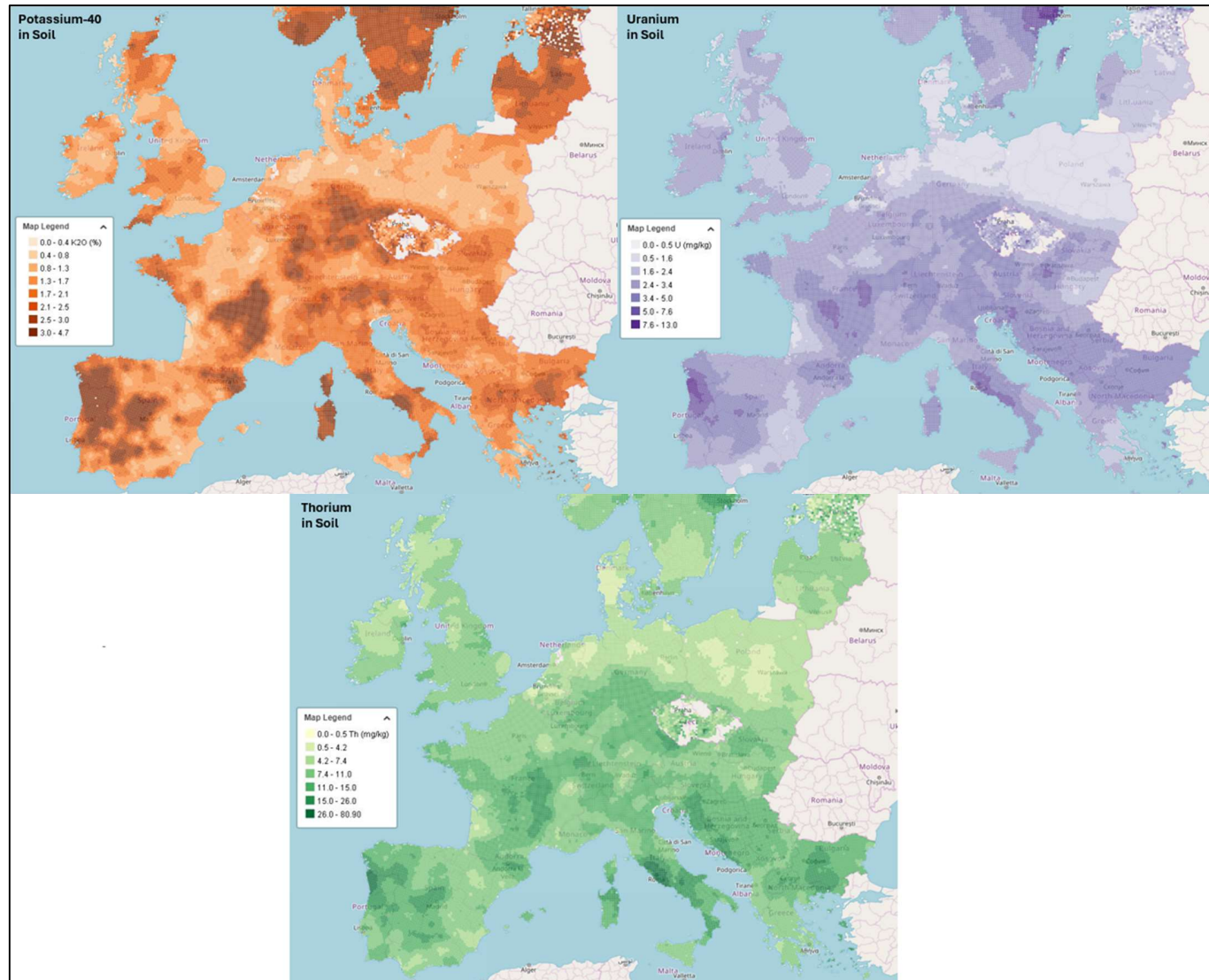
- **Recommendation 3** – Collection and analysis of environmental and archaeological samples collected from the areas subject to gamma radiation surveying to better aid data interpretation.

- **Recommendation 4** – Further work under controlled conditions to determine the impact of soil moisture content on the efficacy of gamma radiation surveys for delineating archaeological targets.

- **Recommendation 5** – Further work under controlled conditions to more accurately determine the impact of target depth on detector response.

In addition to these recommendations, there are other areas that would be beneficial to explore that it has not been possible to cover within the scope of this research project:

- **Use of existing aerial gamma radiation datasets** – Gamma ray spectrometry is increasingly recognised as a valuable tool in various characterisation projects including parent rock and soil mapping, soil organic carbon and peat mapping, plant available potassium mapping, erosion estimation, and the mapping of contamination from mine tailings and other industrial activities (Beamish 2016, van der Veeke, *et. al.* 2021, Loiseau, *et. al.* 2020). In consequence, there is a growing body of published data from extensive aerial surveys that could complement Groundhog data and support the identification of optimal sites for deploying Groundhog as part of future archaeological investigations. As shown in the European Commission’s Joint Research Centre dataset summarised in Figure 7.5, there are several areas in the UK and countries such as Spain, Portugal, Italy and France where radioactivity concentrations in the soil are elevated such that they may be able to offer greater contrasts against any buried archaeological features.
- **Exploring different detector types and sizes** – A study by van der Veeke, *et. al.* (2021), used three different sized thallium activated caesium iodide (CsI(Tl)) detectors on an unmanned aerial vehicle to determine the minimum practical detector size required to map naturally occurring radioactivity accurately, supporting geological characterisation. The study found that larger detectors are capable of collecting more usable data, although survey speed and detector height, as well as method of data processing, also influence data quality. As detector height and survey speed are fixed for Groundhog surveys, and especially for vehicle-mounted surveys, exploring the impact of detector size and type on data quality for archaeological surveys could be insightful.



Source: (EC JRC 2024)

Figure 7.5 – Aerial survey data showing the distribution of Potassium-40, Uranium-238 and Thorium-232 across Europe

7.6 References

Beamish, D. (2016) Mapping the terrestrial gamma radiation dose IN Young, M. E. (ed.) *Unearthed: impacts of the Tellus surveys of the north of Ireland*, Dublin, Royal Irish Academy, DOI: 10.3318/978-1-908996-88-6.ch18

Creighton, J. and Fry, R. (2016) Silchester: changing visions of a Roman town: integrating geophysics and archaeology: the results of the Silchester mapping project, 2005 – 10, Britannia monograph series; no. 28, Society for the Promotion of Roman Studies, ISBN: 9780907764427, pp:486

EC JRC (2024) Radioactivity Environmental Monitoring – Potassium, Uranium and Thorium Concentrations in Soil, <https://remap.jrc.ec.europa.eu/Atlas.aspx#>, European Commission Joint Research Centre (EC JRC) Radioactivity Environmental Monitoring Group, Accessed: 29/06/2024

Loiseau, T. Richer-de-Forges, A. C. Martelet, G. Bialkowski, A. Nehlig, P. and Arrouays, D. (2020) Could airborne gamma-spectrometric data replace lithological maps as co-variates for digital soil mapping of topsoil particle-size distribution? A case study in Western France, *Geoderma Regional*, **22**: 1 – 15, DOI: <https://doi.org/10.1016/j.geodrs.2020.e00295>

LRC (2012) Landscape Research Centre (LRC) Atlas of the Vale of Pickering, www.landscaperesearchcentre.org/atlas/lrc_atlas.html, Accessed: 25/10/2022, Last updated: 2012

ONR (2023) ONR Technical Assessment Guide: Radiation Shielding, NS-TAST-GD-002, Issue 8.1, Published July 2023, Office for Nuclear Regulation (ONR)

van der Veeke, S. Limburg, J. Koomans, R.L. Soderstrom, M. van de Graaf, E. R. (2021) Optimizing gamma-ray spectrometers for UAV-borne surveys with geophysical applications, *Journal of Environmental Radioactivity*, **237**: 1 – 14, <https://doi.org/10.1016/j.envrad.2021.106717>



CHAPTER 8

Conclusion

8 CONCLUSION

8.1 Answering the Research Question

To conclude, I return to the original objectives identified in Chapter 1 of this thesis and demonstrate how each of these objectives have been addressed to answer the overarching research aim and underpinning objectives:

“Some past human activities have created measurable differences in concentrations of naturally occurring gamma radiation emitting radionuclides, enabling detection of buried structures and objects of archaeological interest using portable gamma radiation surveying methods”.

The original objectives and how they have been addressed are as follows:

Objective 1 – Interrogate existing literature to identify the extent of work undertaken to explore the efficacy of using gamma survey methods for archaeological prospection, and key gaps that need to be addressed.

An extensive literature review was conducted with two key functions. The first was to provide necessary background information on several key concepts, recognising the multi-disciplinary nature of this research. In consequence, an overview of naturally occurring radioactivity, radiation detection methods, geophysical survey methods, and mechanisms for generating measurable differences in radioactivity in archaeological targets was provided. The second function of the literature review was to explore the key findings and concepts from analogous studies, with the aim identifying gaps in the published literature, areas for improvement and opportunities for making a new and original contribution to the existing body of knowledge. The literature review highlighted significant gaps in the literature due to the very small number of similar studies, with none utilising portable surveying methods as proposed here. This opened up multiple avenues for research and methodology development.

Objective 2 – Generate datasets through the completion of gamma-ray surveys at various sites, including those of archaeological interest. Surveys will be undertaken using a system known as Groundhog which is well established for use in the nuclear industry.

Comprehensive datasets were generated for the archaeological sites of Silchester, Bisham and East Heselton. All surveys were undertaken using the Groundhog Fusion system. This work was augmented by the pXRF analysis of archaeological and environmental samples from Silchester and East Heselton.

Objective 3 – Analyse generated datasets to test the feasibility of the technique and to classify the types of buried feature that are more amenable to detection via gamma-ray surveys and why.

The raw data was used to generate multiple various outputs to support analysis and establish the efficacy of the technique. This includes gamma radiation distribution maps and count rate distribution graphs. Larger targets, such as roads and ditches produced clear anomalies in the distribution maps, whilst smaller targets did not. The technique also identified possible historic field boundaries and geological characteristics, both providing valuable additional contextual information when characterising an archaeological site.

Creating gamma radiation distribution maps using data from individual energy windows within the Groundhog data, and comparing the output from the Groundhog surveys against the pXRF data helped understand what factors may be influencing the efficacy of the technique. The presence/absence of certain groups of radionuclides present in the targets, mixing of soil and target material, soil moisture content and burial depth were identified as potential factors that could be influencing the effectiveness of the technique.

Objective 4 – Process datasets using commercially available software, testing different methodologies to see which, if any, approaches generate high quality visual outputs.

Groundhog data was processed using both ArcGIS with bespoke applications (created by Nuvia Limited) and the commercially available Geoplot software. Geoplot proved capable of creating high-quality gamma radiation distribution maps capable of drawing out multiple anomalies of

interest. It was found that the Wallis Filter was particularly effective at drawing out features of interest.

Objective 5 – Test multiple variables – e.g. completion of collimated and uncollimated surveys, using Groundhog in both hand-held and vehicle mounted configurations, different geologies and various target types.

The Groundhog system was deployed in both a hand-held and vehicle mounted configuration, demonstrating the method's scalability, repeatability and flexibility. Tests with Groundhog in both collimated and uncollimated configurations showed limited impact on data quality. Targeting various archaeological features from major roads through to cremations and inhumations provided a valuable opportunity to determine which, if any, would be capable of generating measurable differences in naturally occurring radioactivity relative to the surrounding soil. Similarly, deploying the system at different sites across the UK confirmed that the method can be effectively deployed across varying geologies.

8.2 Closing Comments

In conclusion, the studies presented in this thesis have significantly advanced our understanding of the novel application of gamma radiation surveying in support of archaeological prospection, by providing the first comprehensive study utilising portable surveying methods. The research has demonstrated the efficacy of various survey methods in detecting certain archaeological features, and has offered valuable insights into historic land uses and geological transitions that are not visible in traditional geophysical surveys. These combined insights provide valuable contextual information for characterising historical sites. A detailed examination of the generated data sets has yielded unique insights into the mechanisms influencing the technique's effectiveness and has facilitated the development of a new model to help identify optimal sites for further investigation. Finally, this research project has highlighted the value of interdisciplinary collaboration, paving the way for methodological advancements and innovations to be pursued in future research.



APPENDIX 1

Raw Data

APPENDIX 1 - RAW DATA

Raw data from the Groundhog surveys have been captured in Excel spreadsheets to allow others to explore the data.

This data can be accessed via the following link:

<https://www.dropbox.com/scl/fo/ejgfm3zy0b18l06onj7o1/AB5Z7wYMzzT407IzHsgV1eQ?rlkey=wa0877d96050694s3vy6md3xt&st=4mw2dv7s&dl=0>



APPENDIX 2

As Published Papers

APPENDIX 2 – AS PUBLISHED PAPERS

RESEARCH ARTICLE

WILEY

Portable gamma ray spectrometry for archaeological prospection: A preliminary investigation at Silchester Roman Town

Victoria Robinson^{1,2}  | Robert Clark² | Stuart Black¹ | Robert Fry¹ | Helen Beddow²

¹School of Archaeology, Geography and Environmental Science, University of Reading, Reading, UK

²NUVIA Ltd Harwell, Didcot, UK

Correspondence

Victoria Robinson, School of Archaeology, Geography and Environmental Science, University of Reading, Whiteknights Campus, Reading RG6 6UR, UK.

Email: v.a.robinson@pgr.reading.ac.uk

Abstract

Several studies have suggested the potential value in applying gamma radiation surveys to support identification of buried archaeological features. However, the number of previous studies is very small and has yielded mixed results. The true efficacy of the technique is therefore unclear. Here, we report on an alternative survey method that uses Groundhog[®], a portable gamma radiation system with spectrometric capability, to achieve high spatial density monitoring of archaeological sites. The system, which is used extensively in the nuclear industry, was used to carry out preliminary surveys at four different locations within the Silchester Roman Town. Targeting a site for which an extensive amount of archaeological data is available facilitated testing of the method on a range of known target types. Surveys were carried out along 1-m transects at an approximate walking speed of 1 m per second, resulting in the capture of one radiation measurement per square metre. Total gamma radiation, recorded in counts per second, was presented in the form of surface radiation (contour) maps and compared against existing geophysical data. Total gamma counting consists of counting gamma rays, without energy discrimination, that are spontaneously emitted by the material under investigation. The obtained counts represent the total, or gross, gamma contribution from all radionuclides, both natural background series and anthropogenic. Radiation anomalies were identified in two of the four survey sites. These anomalies correlated with features present in the geophysical data and can be attributed to a Temenos wall bounding the temple complex and an infilled clay pit. Early results suggest that this may be a complementary technique to existing geophysical methods to aid characterization of archaeological sites. However, it is believed that data quality could be significantly improved by further increasing spatial resolution. This will be explored as part of future fieldwork.

KEYWORDS

archaeological survey, gamma ray surveying, integrated techniques, natural radioactivity, NUVIA Groundhog[®], Silchester

This is an open access article under the terms of the [Creative Commons Attribution](https://creativecommons.org/licenses/by/4.0/) License, which permits use, distribution and reproduction in any medium, provided the original work is properly cited.

© 2022 The Authors. *Archaeological Prospection* published by John Wiley & Sons Ltd.

1 | INTRODUCTION

The use of non-intrusive survey techniques for the prospection of archaeological targets is well established (Cardarelli & de Filippo, 2009; Columbero et al., 2020; Dick et al., 2015; Gaffney & Gaffney, 2010). They provide an opportunity to undertake timely, resource-effective, non-destructive (and therefore repeatable) data gathering exercises at sites of potential archaeological interest (Barker, 1993). The resultant data can be used to plan targeted intrusive investigations that are more likely to yield finds, minimize environmental disturbance and minimize potential harm to culturally sensitive or protected areas (Barker, 1993).

The most commonly used geophysical surveying techniques can be grouped into three overarching categories—'magnetic', 'electrical' and 'ground-penetrating radar'. It is recognized that there is no single technique within these groups that can be ubiquitously applied to all scenarios (Gaffney & Gaffney, 2010). Rather, consideration must be given to the physical and chemical properties of the suspected target (Gaffney & Gater, 2003) and surrounding substrate, target size (Ruffell & McKinley, 2008) and likely level of overburden. Consideration must be given to nearby infrastructure (such as pipelines, metal fences and cars), which may generate misleading results (Schmidt et al., 2015). By accounting for these variables, it is possible to improve the quality of the data. Targeted selection of the optimal geophysical technique will therefore increase the likelihood of measuring sufficient contrast between the target and surrounding material, minimize the risk of interference from other infrastructure and minimize the risk of false positive and negative results (Milsom & Eriksen, 2011).

Survey data quality can be further improved by utilizing contrasting techniques at the same site. Though more costly and time consuming (Ruffell & McKinley, 2008), such a strategy can minimize the risk of false positives. If contrasting techniques both identify an anomaly in a specific area, it is more likely to be a feature of interest. Comparing the two data sets may highlight less distinctive anomalies that could have otherwise been overlooked. The value of using multiple surveying techniques has been exemplified in multiple studies including those by Creighton and Fry (2016), Halgedahl et al. (2009), Putiška et al. (2014), Trogu et al. (2014) and Zheng et al. (2013).

1.1 | A new geophysical tool

When considering these studies, it may be valuable to think of the available geophysical techniques as tools within a toolbox that can be selected and combined to achieve an optimized solution for archaeological surveys. An alternative non-intrusive survey technique that may offer a valuable contribution to the 'geophysics toolbox' is gamma radiation surveying. The completion of radiation surveys using non-intrusive techniques is already well established in the nuclear industry (IAEA, 1998). They are typically used to identify and characterize anthropogenic contamination in support of reassurance surveys and remediation planning (IAEA, 1998). Rugged, portable systems can

be readily deployed; principally for site characterization and hotspot detection (Davies et al., 2011). Gamma spectrometry techniques have been successfully deployed in multiple geological applications, for example, soil structure characterization or identification of features of interest such as karst structures (Putiška et al., 2014; Reinhardt & Herrmann, 2019). Its use in the field of archaeological prospection is, in contrast, significantly less well established. Only a limited number of studies are currently available in the published literature. The specific techniques applied in this study have not, to the authors' knowledge, been applied in an archaeological context before. This is explored in Section 1.2.

The application of gamma spectrometry in the context of archaeological prospection works on the principle that the compositions of primordial radionuclides, and in particular, K-40, U-238 and Th-232 within archaeological features, are measurably different to that in the surrounding substrate (Moussa, 2001; Sanjuro-Sanchez et al., 2017). This contrast may be attributable to one or more factors including:

- Import of material—Construction materials have, throughout history, been transported over significant distances to a desired location or settlement as exemplified by the Welsh 'blue stones' of Stonehenge (Nash et al., 2020) and Dorset-provenanced Purbeck Marbles of Westminster Abbey (Westminster Abbey, 2020). These imported materials will have a different geochemical composition to the local geology. In some cases, particularly for clays and granites, the radionuclide concentration will be markedly different. Where imported materials are present in sufficient quantities, the difference in gamma signatures should be measurable. This is particularly relevant for construction materials such as clay-fired bricks that are known to concentrate radionuclides during the brickmaking and firing process (Aliyev, 2004; IAEA, 2003).
- Concentration of materials rich in naturally occurring radioactivity—Many historic and ancient structures, from basic houses to places of worship and monuments, used building materials rich in naturally occurring radionuclides. This includes clay bricks that can contain significant concentrations of Ra-226, Th-232 and K-40 (1–200 Bq/kg Ra and Th and 60–2000 Bq/kg K) (IAEA, 2003) and granite, which, in the United Kingdom, can contain 2–770 Bq/kg of U-238 and 2–280 Bq/kg Th-232 (IAEA, 2005). When present in the volumes required for construction, a cumulative effect may be achieved whereby it may be possible to discern a measurable contrast in radioactivity when compared with surrounding areas.
- Industrial activities—Activities such as mining and the processing of ores have been, and continue to be, a notable source of technologically enhanced naturally occurring material (IAEA, 2013). In consequence, historic industrial areas have the potential to generate a measurable contrast to natural background radiation levels.

Extending the application of gamma radiation surveying to an archaeological context could offer several benefits including lack of

susceptibility to interference from modern structures such as fences, pipelines and cables; ability to be deployed on foot (Figure 1a,b) or vehicle mounted (Figure 1c) as required; and ease of deployment and compatibility of output data with traditional geophysical outputs. Further, when deploying a monitoring system with spectrometric capability, specific radionuclides responsible for generating the measured radiation can be identified. By comparing the isotopic composition of an anomaly against the background radiation, it may be possible to identify two distinct material types. This would support a more robust conclusion that the anomaly can be attributable to an archaeological deposit rather than a naturally occurring variation. It is noted that a difference in isotopic composition would only occur where non-local materials are present in the archaeological deposit. For example, if a brick wall was built using local clays, an area of increased radioactivity might be found due to the concentration of the naturally occurring radioactive material. However, the isotopic composition would be comparable with the local source material. If the bricks were imported from elsewhere, a different isotopic fingerprint may be observed.

Some studies have suggested that gamma radiation data can provide valuable insight into the geoarchaeological context of a site. For example, Kozhevnikov et al. (2018) highlighted the value of collecting gamma ray measurements alongside traditional geophysical data during the survey of ancient iron smelting sites in Siberia. In this study, radiation data supported the identification of a rapid change in climatic and/or hydrogeological conditions at the site. This led to a cessation of granitic deposits from the nearby Primorsky Range (Kozhevnikov et al., 2018). This change enabled soil accumulation and vegetation growth over the granitic material, which, due to attenuation by the soil, was characterized by a notable reduction in radioactivity (Kozhevnikov et al., 2018). In a separate study, preliminary findings from Bezuidenhout (2012) suggest that historic human activity at a site may be characterized by a depletion in potassium concentrations. Bezuidenhout's, 2012 study suggests that human activities can enhance the rate of topsoil erosion and expose lower soil layers, which then begin to weather, resulting in the potassium depletion observed.



FIGURE 1 NUVIA Groundhog® system in Uncollimated (a), collimated (b) and vehicle mounted (c) configurations. Source: Personal photographs, NUVIA (2021) [Colour figure can be viewed at [wileyonlinelibrary.com](https://onlinelibrary.wiley.com)]

1.2 | Previous applications of gamma spectrometry in archaeology

The use of the radioactive properties of naturally occurring radionuclides in archaeology dates back to the 1940s and the evolution of radiocarbon dating (Kern, 2020). The technique, which measures residual carbon-14 concentrations in artefacts of typically organic origin, is used to estimate the target's age. The technique has since expanded. An increased number of radionuclides, most commonly uranium, can be measured in a similar way to establish the age of a broader range of materials including those of geological origin (Peppe, 2013).

The application of gamma spectrometry in the field of archaeological prospection is more novel, having only been demonstrated in a small number of studies, including those by Ruffell and Wilson (1998), Moussa (2001), Ruffell et al. (2006), Sanjuero-Sanchez et al. (2017), Aziz et al. (2018) and Kozhevnikov et al. (2018). In each case, static detection systems were used to survey a predefined area with the aim of detecting buried features of interest. Some of these studies, including those by Aziz et al. (2018) and Moussa (2001), yielded positive results. In these two examples, the processed data were successfully used to delineate the position of archaeological features of interest: a granitic Egyptian monument and the foundations of a building, respectively.

Although these preliminary studies suggest that the use of static gamma spectrometry systems may be a viable technique, it is recognized that this can be time consuming. When surveying for naturally occurring radioactivity, count times of up to 6 min per sample can be required in areas depleted in naturally occurring radionuclides to achieve the required measurement precision and data quality (IAEA, 2003; USNRC, 2009). Such an approach, however, will limit the amount of data that can be collected in the available time period.

This study therefore proposes and tests an alternative strategy that utilizes a portable gamma radiation detection system with

spectrometric capability to achieve high spatial density monitoring of archaeological sites. The proposed strategy of collecting a high number of low data resolution (i.e. low ability to distinguish between gamma rays with similar energies) measurements has been used to good effect in the nuclear industry (Davies et al., 2011). Available literature, however, suggests that such an approach has not previously been applied in an archaeological context. The system used in this study, known as Groundhog[®], is developed and owned by NUVIA Limited. It is extensively used for radiation surveys of land, buildings and other infrastructure. Groundhog[®] is a portable system principally comprising a sodium iodide (NaI)-based scintillation detection system with spectrometric capability, survey-grade GPS system and data logger that can be operated in either an uncollimated or collimated configuration (Figure 1). It is capable of continuously recording radiation measurements, at one measurement per second, and global positioning data on an ultra-mobile PC (UMPC). Data are processed to generate multiple visual outputs, including radiation contour maps, spectral distribution graphs and sample maps.

The Groundhog[®] system can be adapted to accommodate a single hand-carried sodium iodide (NaI) detector through to a bank of detectors mounted on a vehicle. It is possible then for a single person to survey tens to multiple thousands of square metres in a day. In consequence, the methodology proposed in this study supports the collection of much larger, high-density data sets over a greater geographical area than has previously been achieved for gamma surveying techniques applied in an archaeological context. This should, in turn, improve the quality and spatial resolution of output data available. Further, the visual outputs generated as a result of these surveys can be easily compared with existing geophysical survey data for the same area, as exemplified in Figures 2, 3, 4 and 5. This will make it easier to test the effectiveness of gamma radiation surveying in this unique context.

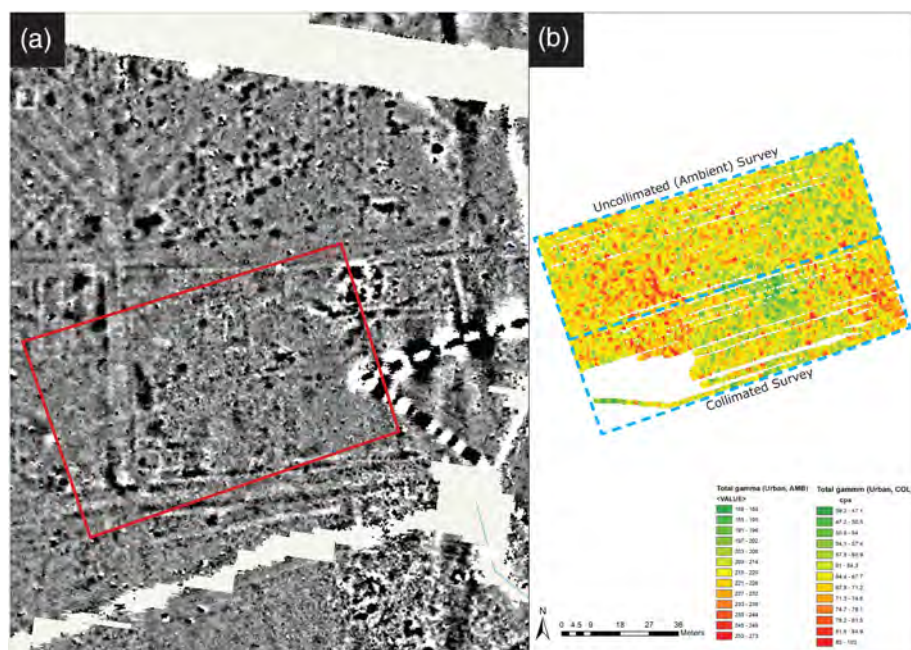


FIGURE 2 Comparison of fluxgate gradiometry data ($\pm 7nT$) (a) against total gamma radiation data (b) collected at the Urban Area (Site A). Both collimated and uncollimated measurements are presented. Radiation data are displayed in cps. No clear anomalies have been identified. An area of increased activity in the bottom right corner of the survey area may be attributable to a modern feature (buried pipe). An area of elevated activity to the left of the survey area broadly aligns with the cross road. However, due to its distribution, it may be a naturally occurring feature. Source: Fluxgate gradiometry data source: Silchester Mapping Project Creighton and Fry (2016) plus own (primary) data [Colour figure can be viewed at wileyonlinelibrary.com]

FIGURE 3 Comparison of fluxgate gradiometry data (± 5 nT) (a) against total gamma radiation data (b) collected at the Cremation/Inhumation Area (Site B). Uncollimated survey data are displayed in cps. No clear anomalies are observable. The area of elevated activity at the top of the survey area is expected to be naturally occurring. Source: Fluxgate gradiometer data source: Silchester Mapping Project, Creighton and Fry (2016), plus own (primary) data [Colour figure can be viewed at wileyonlinelibrary.com]

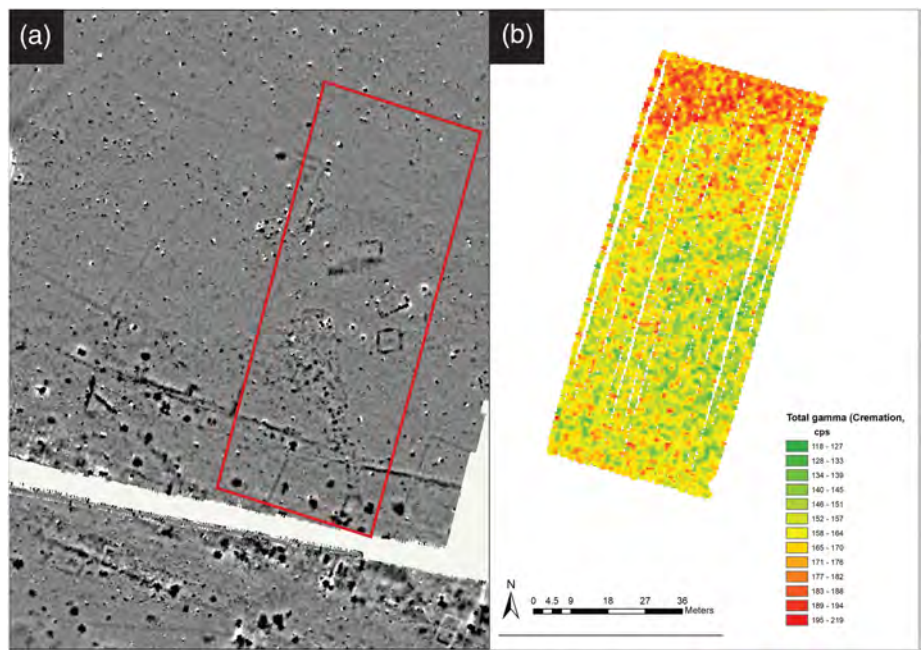
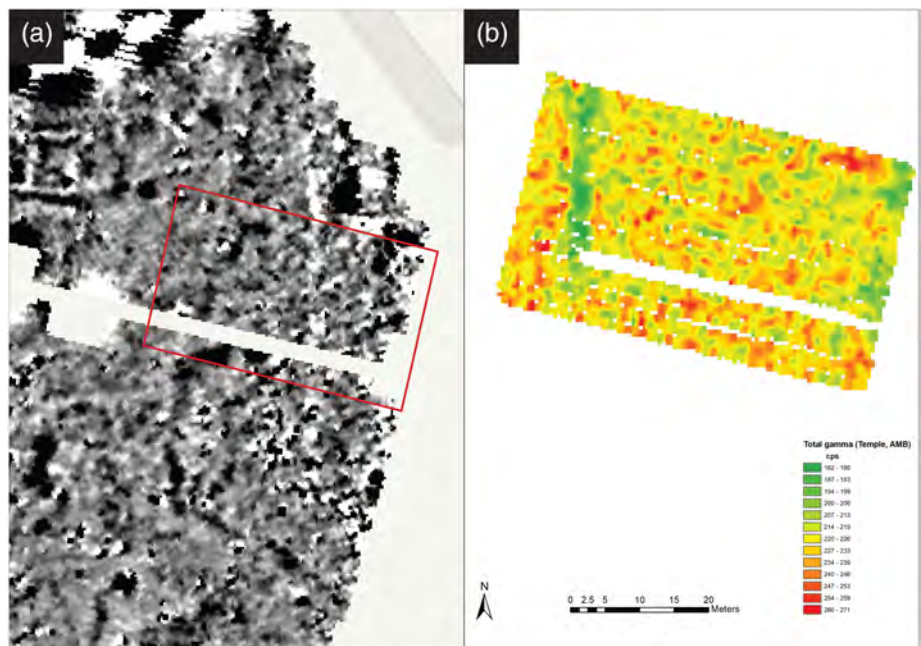


FIGURE 4 Comparison of fluxgate gradiometry data (± 5 nT) (a) against total gamma radiation data (b) collected at the Temple Area (Site C). Uncollimated survey data are displayed in cps. A clear linear anomaly of depleted radioactivity can be seen in the left-hand side of the survey area. This aligns with a feature visible in the fluxgate gradiometry data, which is known to be a Temenos wall. Source: Fluxgate gradiometry data source: Creighton and Fry (2016) Plus own (primary) data [Colour figure can be viewed at wileyonlinelibrary.com]



The overall aim of this investigation is to further explore the effectiveness of radiation surveys in the detection of potential archaeological features of interest and whether it could contribute to the existing range of geophysical surveying techniques available. This will be achieved by building on the findings of previous studies and surveying new sites using the Groundhog[®] system at sites of known archaeological interest. An initial survey using Groundhog[®] has been completed at a well-known archaeological site that has been extensively surveyed using standard geophysical techniques.

2 | STUDY SITE AND EXISTING DATA

This initial study was completed at the site of the Roman town of Silchester (Calleva Atrebatum), which is situated approximately 2 km to the west of the current day village of Silchester, within the United Kingdom. Silchester and the surrounding area sits on a bedrock of London Clay Formation (sandy sedimentary bedrock), which is overlain by the Silchester Gravel Member (sand and gravel of alluvial origin) (BGS, 2019).

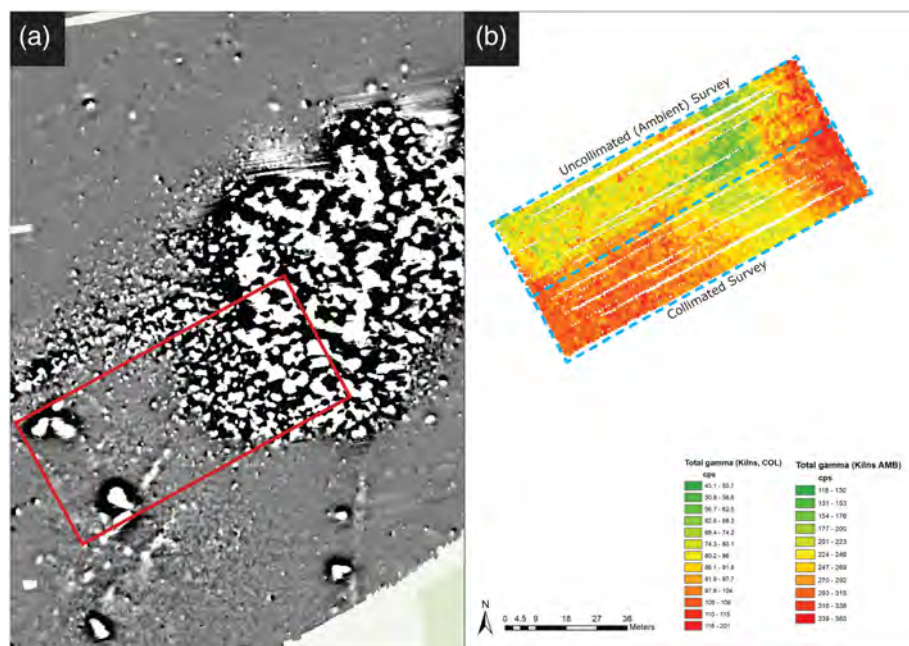


FIGURE 5 Comparison of caesium magnetometry data (+/− 7nT) (a) against total gamma radiation data (b) collected at the Kiln Area (Site D). Both collimated and uncollimated measurements are presented. Radiation data are displayed in cps. An area of depleted radioactivity in the upper half of the Groundhog® survey area aligns with the clear anomaly present in the geophysics data. A ‘P’-shaped anomaly in the bottom left corner of the survey area broadly aligns with one of the kilns but is assumed to be naturally occurring. Source: Fluxgate gradiometry data source: (Linford et al., 2016) plus own (primary) data [Colour figure can be viewed at wileyonlinelibrary.com]

The site has a long history of settlement, with archaeological evidence confirming that Silchester has been occupied since the Iron Age (Creighton & Fry, 2016; Fulford et al., 2006). It evolved into an expansive Roman town covering approximately 0.4 km² (EDINA, 2019) with various distinguishing features including an amphitheatre and town structure that utilized a grid structure comprising discrete blocks or ‘insulae’ (Creighton & Fry, 2016). Occupation continued until its deliberate abandonment in the sixth/seventh centuries (Fulford et al., 2006).

The Silchester site was selected due to the excellent breadth and depth of existing archaeological data available. This derives from extensive programmes of fieldwork and research that have been completed since the early 18th century and continues to this day. Much of these data have been compiled and are accessible through open sources such as the Britannia Monograph Series (SPRS, 2020) and the Archaeological Data Service (ADS, 2021). The history of investigation at Silchester is detailed in Creighton and Fry (2016).

The study targeted four specific areas linked to Silchester Roman Town. These sites were selected as they offered a range of contrasting features/targets and material types, as indicated by previous excavations and geophysical surveys. Each site therefore offered a slightly different condition for the Groundhog® system to test and an opportunity to obtain a range of data across the site. This strategy was adopted with the aim of providing an early indication of efficacy and whether this technique could be pursued in support of archaeological prospection. The targeted survey areas were situated within the following areas:

- Site A—Urban Area (Insula XXXIV)
- Site B—Inhumation/Cremation Area (Close to the West Gate)
- Site C—Temple Area (Insula XXX)
- Site D—Industrial (Kiln) Area (Little London)

Descriptions for each site can be found in Table S1, with a map showing their location in Figure 6.

3 | METHODOLOGY

Surveys were undertaken over 2 days in July 2019, using NUVIA's Groundhog Fusion® system. A manually operated single detector. The detector unit was deployed in both an uncollimated and collimated configuration. As shown in Table S1, Sites A and D were subject to both collimated and uncollimated surveys within the same defined survey area. This approach was applied to test whether use of a collimator, which ensures the detector only captures radiation from the ground directly beneath it, improves data quality, particularly when surveying areas likely to yield poor contrasts relative to background levels. The remaining two sites (Sites B and C) were surveyed in an uncollimated configuration only.

Nuvia's Groundhog probes are subject to annual calibration to ensure they are performing as expected and fit for use, limiting the potential for systematic errors. Calibration is completed in accordance with internal procedures HPP357 (Davies, 2015) and HPI4214 (Clark, 2017). These procedures are based on the National Physics Laboratory's Good Practice Guide 14 (Lee & Burgess, 1999). The calibration process measured the detector's responses against background radiation and a 6-kBq Cs-137 check source for a period of 600 s each. This confirmed that the detector was operating reliably and within acceptable ranges (NUVIA, 2019). The response curve for Cs-137 can be found in Figure S1.

Before the Groundhog® system was deployed on-site, a number of preparatory equipment checks were undertaken at the Harwell office in accordance with NUVIA Method Statement 72736/MS/001 (Beddow, 2019). Key activities included:

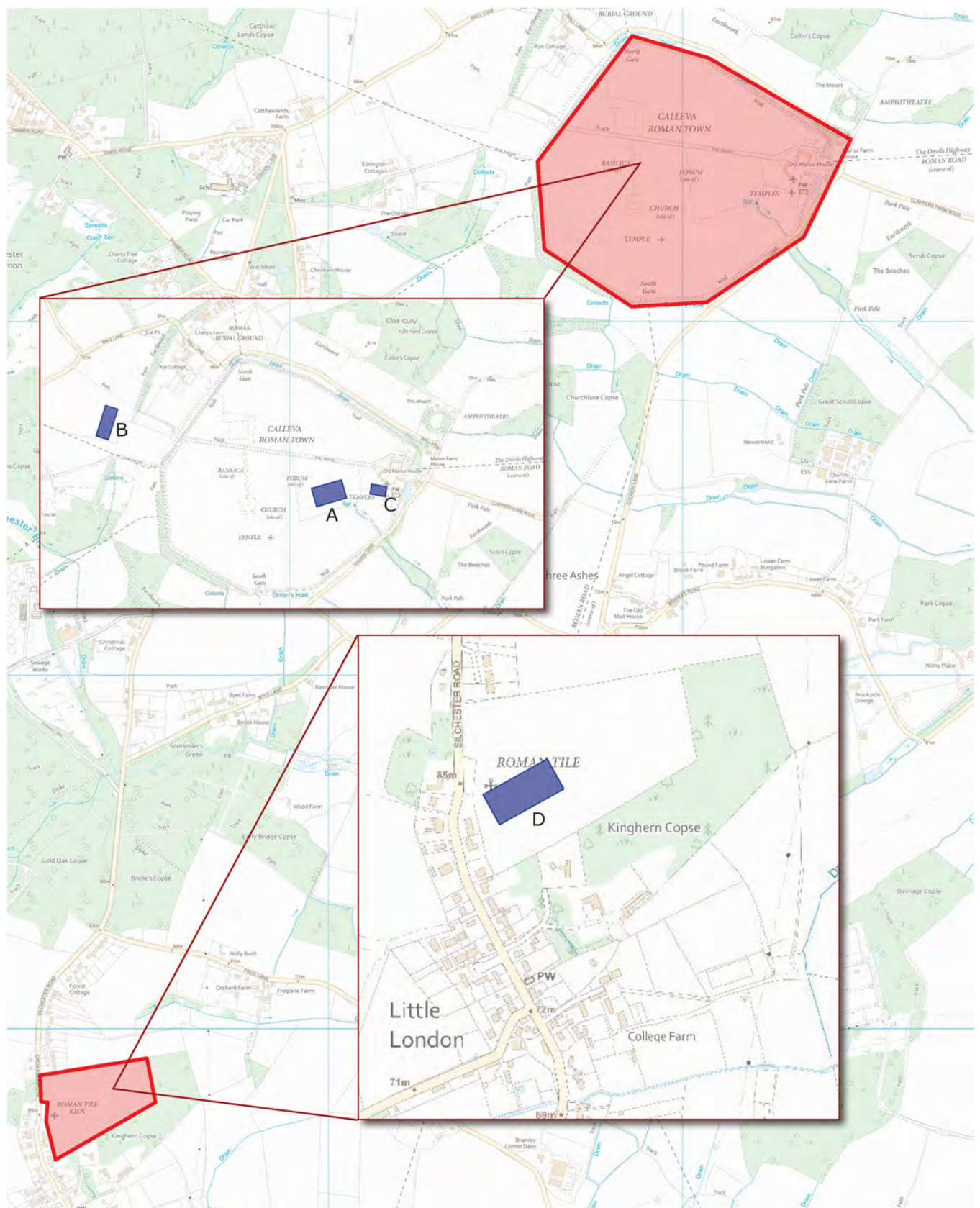


FIGURE 6 Survey locations (a, Urban Area; b, Cremation/Inhumation Site; c, Temple Area; d, Kiln Area) in the context of the site of the Roman town of Calleva Atrebatum (e), Silchester. Source: Adapted from: EDINA DIGIMAP (2019) [Colour figure can be viewed at wileyonlinelibrary.com]

- Ensuring equipment portable appliance test (PAT) labels were present and correct and that dates would not be exceeded in the planned survey period.
- Physical inspection of equipment and cables are in good condition and that batteries are fully charged.
- Functional checks of the individual components of the Groundhog[®] system to ensure the receiver and detector were operating correctly and that the UMPC was recording the resultant data:
 - The UMPC was tested by running the bespoke software and checking that it was operating correctly. Subsequent equipment checks could not be completed until the software was running.
 - The radiation detector was subject to a test to ensure the detector was operating correctly. This was achieved by placing a 10-kBq Cs-137 check source approximately 5 cm from the base of the detector unit. This provides confirmation that the detector is working and that the spectrometer is correctly identifying the 662-keV Cs-137 peak (Please see Supporting Information Figure S1).
 - The GPS unit was tested outside to confirm that a suitable number of satellites were available and that there was a sufficiently strong signal.

Once at the site, a brief walk-down of each survey area was undertaken. This allowed familiarization with the site topography and to identification of any features that may limit accessibility—particularly for the collimator trolley. No significant issues were initially identified.

The predetermined survey areas were delineated using a Leica GS16 GNSS unit. Guide ropes with 1-m transect markers were run across the long edges of the survey area to aid positioning of siting poles used during the survey.

Uncollimated surveys were conducted using the UMPC, and the detector/probe was carried next to the body, arm fully extended to ensure a consistent height of approximately 20 cm between the ground and the detector. The 1-m transects were traversed at an

approximate walking speed of 1 m s^{-1} using the siting poles to ensure the detector remained on target. The UMPC was regularly monitored to ensure a 1 m s^{-1} walking pace was maintained as far as practicable. For the collimated surveys, a dedicated collimator trolley was used (Figure 1b). The collimator comprises a 4.5-cm-thick cylinder made from a coiled lead sheet. It has an aperture of $\sim 18 \text{ cm}$, allowing the fusion probe to slot inside without excessive movement (Figure 7). The base of the probe rests on a thin Perspex sheet set into, and flush with, the base of the trolley. This provides the detector with an unobscured view of the ground directly beneath it. The collimator attenuates gamma radiation from the environment, preventing it from reaching the sides of the probe. This gives the detector directional capability to 'see' only the radioactivity directly beneath it. By reducing the amount of background radiation captured by the detector, it becomes easier to identify more subtle changes in radioactivity levels (NPL, 2014) as might be expected in this context. The UMPC and GPS unit was also secured inside the collimator trolley. This was then pulled along 1-m transects at the same $\sim 1 \text{ m s}^{-1}$ speed used during the uncollimated surveys.

For each survey area, the Groundhog[®] Fusion System was set to take one radiation recording per second. This combined with an approximate surveying speed of 1 m s^{-1} facilitated the capture of radiation measurement for each square metre of the survey area. The survey speed is monitored by the Groundhog[®] system, a visual display on the UMPC which can be monitored by the operator. In addition, an audible alarm will alert the operator if the 1 m s^{-1} speed is exceeded. The regions of interest for this study are those associated with isotopes of potassium, uranium and thorium and their decay products ('daughters').

The captured GPS and radiation data were transferred from the UMPC to a desktop computer for processing. Microsoft Access (v. 16.0.14131.20278) was used to compile the data. Post-processing of the GPS data was undertaken in GrafNav (v. 8.3), supporting improved GPS positioning accuracy. This was supported through the

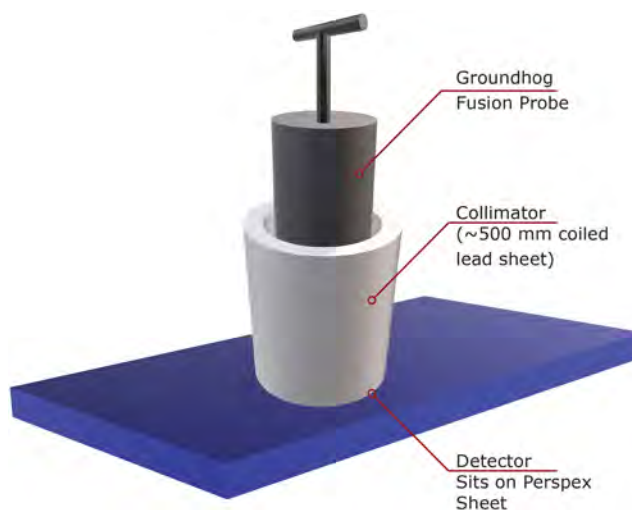


FIGURE 7 Scheme diagram showing the Groundhog[®] detector in its collimated configuration. Source: Drawn by authors [Colour figure can be viewed at wileyonlinelibrary.com]

import of time and date matched data from the Farnborough OS Reference Station (FARB). It was also possible to conduct checks on the completeness of the data. This exercise confirmed that all GPS files were successfully imported and converted to the required format (GNSS to GPB). GPS data quality was excellent across all survey sites, with a general accuracy of <2 cm. Post-processed data were imported to a new project file in ArcGIS (v10.1) as a new layer.

The Groundhog[®] system recorded both total gamma activity across all energies (expressed as counts per second [cps]) and spectral data (recorded in kilo electron volts [keV]). Both data sets were imported into ArcGIS to facilitate data interrogation and surface radiation mapping. The surface radiation (contour) maps support visualization of the radiation data, improving the ease with which features or trends can be identified. Spectral data were analysed in ArcGIS using bespoke tool sets developed by NUVIA. These are described in Davies et al. (2011). Review of the spectral data confirmed that the radiation measurements at each of the four sites were attributable to naturally occurring isotopes of potassium, uranium and thorium. Potassium was identified directly by the gamma radiation emissions of K-40 (1,461 keV). Uranium was identified through the presence of its gamma emitting daughter Bi-214 (1765 keV) and thorium through the presence its daughter Tl-208.

Radiation contour maps were generated for each survey area using interpolated total gamma activity data. Interpolation was achieved using an inverse distance weighting technique with a grid size of 0.5 m and an effective range of 1.5 m. This approach, introduced in a paper by Duggan (1983), uses measured values, in this case total gamma radiation measurements at 1-m spacings, to estimate the gamma radiation levels in the surrounding space (Duggan, 1983). It assumes that each data point has a local influence that reduces proportionately with distance (ESRI, 2022). Although this approach 'hides' small gaps in data coverage, it generates continuous, smooth images of the survey area that are easier to interpret. The contour maps were displayed using a multipart graduated colour scale (green to red). To help draw out features within each of the maps, the number of classes within the scale was adjusted to optimize the data divisions applied. Due to the generally low levels of radioactivity present at all sites, data divisions of 4–6 cps were most effective at drawing

out subtle differences in activity across the sites. The only exception was for the uncollimated measurements for Site D, where data divisions of ~22 cps generated the highest quality images.

Total gamma activity data were also processed to generate count rate frequency distribution graphs for each site. This was achieved by importing the raw data (as comma-separated values) from ArcGIS to Microsoft Excel (v 2106) and generating a series of histograms. These could then be used to identify the most frequently occurring count rates and therefore the natural background radiation for each site.

4 | RESULTS

As shown in Table 1, an average of 1.05–1.74 readings per square metre were recorded at each site, providing a good level of coverage by the Groundhog[®] system. This facilitated the collection of between 2100 and 8800 measurements per site. The sites with the greatest number of measurements collected (Sites A and D) were those where both collimated and uncollimated surveys were undertaken. The only area where notable gaps in survey data were present was Site A (Urban Area), where some areas were not accessible by collimator trolley. This was attributable to deep ruts generated by farm vehicles and an impassable bed of nettles and brambles. These were not immediately obvious during the initial site walk-round. However, it was still possible to survey the majority of the site, providing a good overview of radiological conditions.

Summary statistics for all four sites is provided in Table 1, confirming the total number of measurements taken at each site as well as the minimum, maximum and average total gamma recorded for each site. Further results are discussed on a site-by-site basis below.

Site A- Urban Area

Both collimated and uncollimated surveys were undertaken at Site A as delineated by the blue dotted lines over the radiation contour map in Figure 2. It can be seen that the collimator has significantly reduced the amount of radiation reaching the detector, resulting in much lower total counts overall. The radiation data have been compared against

TABLE 1 Summary survey statistics for Sites A–D, showing the minimum, maximum and average total gamma (counts per second) and total number of measurements taken

Parameter	Site					
	Site A (Urban) Uncollimated	Site A (Urban) collimated	Site B (Inhumation/ Cremation)	Site C (Temple)	Site D (Kiln) Uncollimated	Site D (Kiln) collimated
No. measurements	5255	3470	4189	2136	2678	2,848
Average no. measurements per m ²	1.31	1.74	1.05	1.42	1.07	1.42
Minimum total γ (cps)	163	37	118	158	174	43
Maximum Total γ (cps)	274	102	220	274	367	334
Mean total γ (cps)	217	67	161	223	282	85
Standard deviation	15.61	9.30	15.24	16.82	34.25	18.16

existing fluxgate gradiometer survey data generated by the Silchester Mapping Project (Creighton & Fry, 2016) (Figure 2a). Within Figure 2, it is possible to see the area that was not fully accessible by the collimator trolley due to the thick covering of foliage and disturbed ground. The figure also shows the site to have low levels of background radioactivity. Mean count rates of 67 and 217 cps were recorded for the collimated and uncollimated survey areas, respectively (Table 1).

Count rate frequency distribution graphs for the uncollimated and collimated survey areas (Figure 8a,b) confirm a normal distribution of activity. The uncollimated data (Figure 8b) shows that the most significant part of the frequency distribution and therefore the background radiation for the site is between 215 and 235 cps. This is towards the lower end of the typical range of 200–300 cps observed in the United Kingdom (Davies et al., 2011).

There appears to be no significant difference in data quality between the collimated and uncollimated surveys. In both instances, there are no clear anomalies present that might have been expected due to the presence of clear linear features identified in the fluxgate gradiometry data. This observation is supported by the normal distribution of activity observed in Figure 8. Despite a long history of human occupation and disturbance at the site, the normal distribution of activity at within the survey area is not unexpected. This is due to the relatively small area surveyed, the generally homogenous distribution of trace elements (IAEA, 2005) and the limited mobility of radionuclides such as thorium and uranium (in its reduced form) in soils (Burns & Finch, 1999; Mahmood & Mohamed, 2010).

There is an area of slightly elevated activity in the south-east corner of the survey area, as shown in Figure 2b. This is broadly in the same area as an anomaly, expected to be a modern feature such as a buried pipe, present in the fluxgate gradiometry data. An area of

elevated activity on the west side of the radiological survey broadly aligns with the linear feature present in the fluxgate gradiometry data. However, this is not clearly defined and is likely attributable to normal background radiation.

Site B- Inhumation/Cremation Area

Figure 3 presents the radiation contour map showing gamma radiation survey data for Site B. Only an uncollimated survey was undertaken for this site. As for Site A, these data are compared against existing fluxgate gradiometry data generated as part of the Silchester Mapping Project (Creighton & Fry, 2016) (Figure 3). This figure shows that the site contains consistently low background radioactivity across most of the site. A mean value of 161 cps was recorded, which is lower than the normal range observed for the United Kingdom. This is supported by the count rate frequency graph for this site (Figure 8c), which shows the highest frequency of measurements are in the 155–165 range. The cause of this is unclear. A contributing factor may be the soil type here. Soilscape data (MAGIC Map, 2021) suggest that the soil is characterized by freely draining, slightly acid loamy soil, which is also the case for Sites A and C. In low-pH conditions, radionuclides exhibit increased solubility and are therefore more readily transported from site (IAEA, 2003).

An area of elevated activity is observed at the northern edge of the survey area. However, this does not correlate with any geophysical anomalies and is therefore likely naturally occurring. The lack of anomalies present in the radiation data contrasts with the fluxgate gradiometry data, which identified multiple features of interest. It does however support the data presented in the count rate frequency distribution graph (Figure 8), which shows a normal distribution.

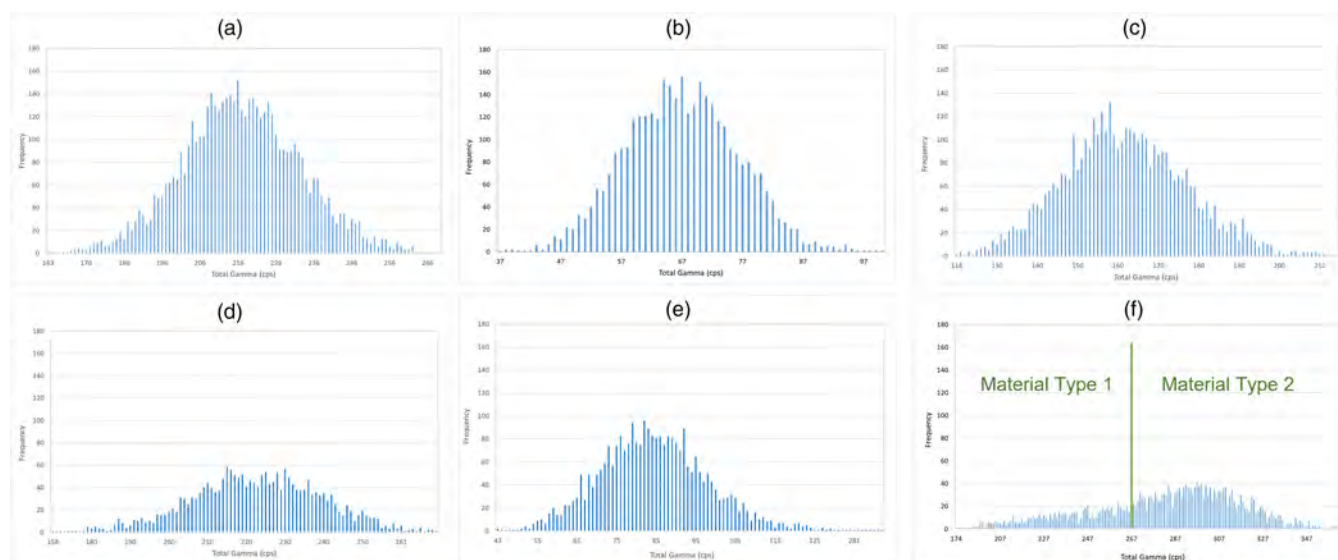


FIGURE 8 Frequency distribution graphs for the Site A (Urban Area), uncollimated (a) and collimated (b); Site B (Cremation/Inhumation Area), uncollimated (c); Site C (Temple Area), uncollimated (d); and Site D (Kilns Area), uncollimated (e) and collimated (f). These charts show a normal distribution of count rates with the exception of the uncollimated data collected for the Kilns Area (e). This graph shows two distinctive activity distributions indicative of two different material types. This differentiation is likely attributable to the former clay pit (which has since been backfilled) in this area (Figures 5 and 9). Source: Own (primary) data [Colour figure can be viewed at [wileyonlinelibrary.com](https://onlinelibrary.wiley.com/doi/10.1002/arp.1859)]

Site C- Temple Area

The gamma radiation survey data generated from an uncollimated Groundhog[®] survey of Site C is presented in Figure 4. This is compared against the existing fluxgate gradiometry data collected as part of the Silchester Mapping Project (Creighton & Fry, 2016) (Figure 4). The small amount of missing radiation survey data visible within this figure is attributable to an existing field boundary fence.

Figure 4 shows a very clear linear anomaly in the gamma radiation data, identified as an area of depleted background radiation with a minimum reading of 161–186 cps, lower than the average of 223 cps recorded for that site. This anomaly aligns perfectly with a linear feature; a Temenos wall that bounds the temple complex, identified in previous work by Fulford et al. (2018). Although a clear anomaly, it is not sufficient in scale to skew the count rate frequency distribution graph that shows a normal distribution for the whole site (Figure 8d). This figure shows the most frequent count rates are in the range of 215–230 cps. This is, as previously observed, consistent with the expected radiation background measurements for a site situated in south-east England.

Site D- Industrial/Kiln Area

As per Site A, both collimated and uncollimated survey methods were applied at Site D. The two areas are clearly delineated in Figure 5. As observed for Site A, the collimator has recorded significantly lower total counts. This figure presents the radiation contour map showing the total gamma radiation measured across Site D. This has been compared against the existing caesium magnetometry data collected as part of the Silchester Environs Project (Linford et al., 2016) as shown in Figure 5. Relative to the other survey areas, Site D appears to have higher levels of background radioactivity with an uncollimated mean of 282 cps and collimated mean of 85 cps. This is the only site to have a different soil type, with the area characterized by 'slightly acid loamy and clayey soils with impeded drainage' (MAGIC Map, 2021). The clay component within the soil here may account for the elevated background activity observed here. Figure 5 reveals a clear anomaly, a

large area of depleted activity, to the north-east of the survey area. A possible 'P'-shaped anomaly can be seen towards the east of the site, which is in a similar location as one of the kilns identified in the geophysics data. However, there is no significant difference between this 'anomaly' and background radiation and is therefore more likely to be attributable to naturally occurring activity.

The larger and most distinctive anomaly in the north-east section of the image shows a well-defined area of lower background radiation, typically in the region of 43–51 cps for the collimated survey area and 177–200 cps for the uncollimated side. When compared with the findings of the caesium magnetometry survey for the same area, it can be seen that this area of depletion closely aligns with a well-defined anomaly present in the caesium magnetometry data. This anomaly can be attributed to an infilled modern clay pit. An Ordnance Survey map from 1912 (Ordnance Survey, 1912) shown in Figure 9 confirms the presence and location of the pit at Site D. This figure shows where the footprint of the pit and the Groundhog[®] survey area overlap and has been detected. An aerial photo taken later in 1947 (Figure 10a) shows the pit as infilled with a well-established stand of trees. This suggests the pit was infilled decades before, with an unknown material of sufficiently different composition to the surrounding material, as to be detectable through both caesium magnetometry and radiation monitoring techniques. Modern satellite images (as exemplified in Figure 10b) show that these trees are no longer present, and hence, an unimpeded Groundhog[®] survey of the area was possible. The satellite image reveals visible patterns/colour variations in the grass cover, further suggesting the pit was backfilled with imported material and/or different soil types. The count rate frequency distribution graphs for the uncollimated and collimated survey data (Figure 8e,f) show normal activity distributions. Review of the uncollimated data (Figure 8e) shows that the most common count rates are in the region of 287–307 cps. As for other survey areas discussed here, this is consistent with the natural background radiation for this region. It is however noted that there is a second distinctive count rate distribution on the left-hand side of Figure 8e, suggesting the presence of a second soil type or other infill material at the site.

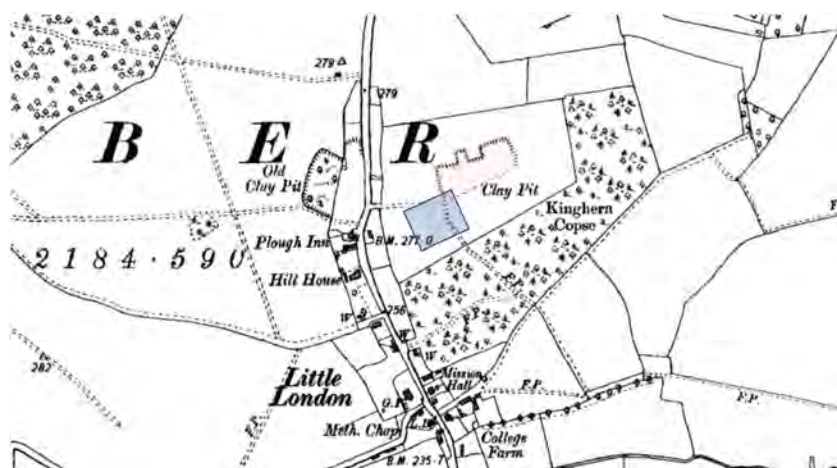


FIGURE 9 Ordnance Survey map from 1912 showing where the kiln survey area (blue square) overlaps the site of a disused modern clay pit (shaded light red). Source: Ordnance Survey (1912) [Colour figure can be viewed at wileyonlinelibrary.com]

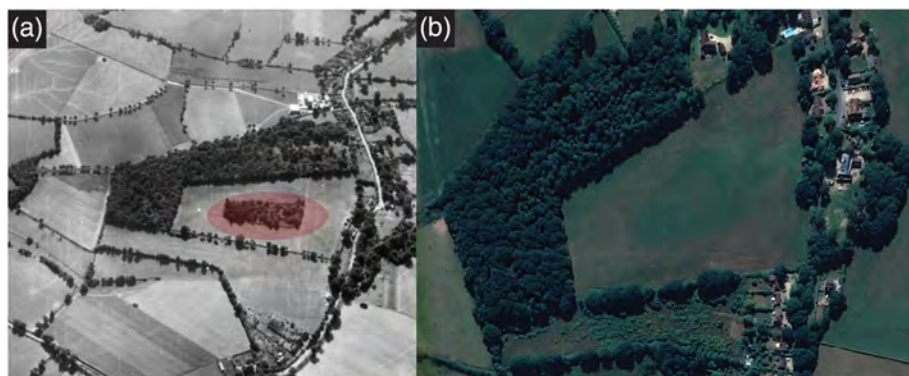


FIGURE 10 (a) 1947 aerial photo showing the site of the Little London clay pit (circled in red) infilled and covered with a well-established tree stand. (b) Modern satellite image of the same site showing absence of the tree stand and revealing a distinct discolouration of the grass covering the former clay pit. Sources: Adapted images from Historic England (2020) and EDINA (2018) [Colour figure can be viewed at wileyonlinelibrary.com]

5 | DISCUSSION

The sites selected for gamma radiation surveying offered four unique conditions for the Groundhog[®] system to test. The data have shown varying levels of success for the efficacy of this technique for the prospection of potential archaeological features of interest.

Site B (Inhumation/Cremation Area) appears to offer the least suitable conditions for this technique in its current configuration, with no radiological anomalies detected. The lack of contrast between the interred remains and surrounding substrate may be attributable to insufficient accumulation of naturally occurring radionuclides through the cremation process or through insufficient accumulation of radioisotopes such as U-238 through the diagenesis of bone as explored in studies such as those by Millard and Hedges (1995), Pike et al. (2002), Farmer et al. (2008), Cid et al. (2014) and Grimstead et al. (2017). Even if some accumulation had occurred, it is unlikely to be in a sufficient concentration as to be detectable against background radiation. Finally, the spatial resolution of the surveys (one measurement per square metre) may be insufficient to delineate the small targets present at this site. This can be attributed to the interpolated values between each of the data points obscuring any subtle variations present. Resurveying the area at a much higher spatial resolution may help overcome this challenge and will be explored during future site surveys with the Groundhog[®] system. Future work planned at the site will also involve the non-destructive analysis of samples of interred remains and surrounding substrate, via high-resolution gamma spectrometry techniques, for detailed comparison. It is anticipated that this will provide a better insight into why no clear anomalies were originally detected.

The results from the survey of Site A (Urban Area) are unclear. When planning this site investigation, it was anticipated that of all the sites surveyed, the urban area would yield the best data (if any). This is because previous geophysical surveys and intrusive investigations have confirmed the presence of large linear structures such as roads and the remains of buildings. It was believed that the construction materials used in these structures would have a sufficiently different radioisotope composition (particularly if made from clays) as to be detectable by the Groundhog[®] system. However, if the construction material was sourced locally, then concentration of the construction material alone may be insufficient to generate a sufficient contrast. A

similar issue was experienced in a study conducted by Sanjuro-Sanchez et al. (2017). Here, radiation surveys were unable to detect any significant differences in the ratios of naturally occurring radionuclides in the remains of Spanish settlements dating back to the late Roman/Medieval period and surrounding soils. This was attributed to the use of local materials in construction and the unusually low concentrations of naturally occurring radioactivity in the area (Sanjuro-Sanchez et al., 2017). For this study, it is anticipated that increasing the spatial resolution of the radiation measurements will help confirm whether the area of elevated activity on the west side of the site is naturally occurring or attributable to the known feature present in that area. It may be possible to provide better definition for the area of elevated activity that broadly aligns with the buried pipe. As for Site B, the intent is to take samples from the targets and surrounding substrate for non-destructive analysis to better understand why targets, clearly visible in other geophysical data, could not be differentiated by Groundhog[®].

The results from Sites C and D (Temple and Kiln Areas, respectively) are more promising. Clearly defined anomalies are visible that correlate closely with features identified within the existing geophysics data. The cause of the depletion in radioactivity observed for the remains of the Temenos wall in Site C is not known. However, it is likely that the wall was built using materials with notably lower concentrations of naturally occurring radionuclides relative to the surrounding soil. Sampling and analysis of soils and any structural material retrieved from the area would help confirm this and will be considered as part of future work. The clearest anomaly associated with the Kiln Area is a significant feature that has been backfilled with imported material with a sufficiently different radioisotope composition as to generate a clear contrast in the survey data.

It is recognized that the large anomaly observed at the Kiln Area is attributable to a modern feature. However, this is still a promising result. It confirms that the presence of material with a sufficiently different composition of naturally occurring radionuclides can be detected if present in a sufficient concentration, as one might expect to find with features such as building foundations, roads or stone monoliths. Although it was initially thought that the small 'P'-shaped anomaly might have been attributed to a kiln, further interrogation of the data suggests that it is a chance occurrence attributable to the

interpolation undertaken on the data. There are two measurements in this localized area in the 116–201 cps (collimated) range, contrasting against the lower surrounding measurements in the 4–86 cps range. The P-shaped feature is therefore more likely a function of the interpolation undertaken that is capturing and exaggerating the two peak measurements. As for the other sites, resurveying this site, targeting the known features at a much higher spatial resolution will help address this uncertainty.

6 | CONCLUSIONS

This preliminary study into the efficacy of using portable radiation survey systems for archaeological prospection has been moderately successful. Although some sites have not yielded positive results, others have clearly identified features of interest that have also been detected using traditional geophysical techniques. The use of gamma radiation surveying may therefore be a useful additional technique in the 'geophysical toolbox'.

The results of this study have raised many questions regarding the cause of the observed anomalies at some sites and why the technique was less effective in others, particularly at Site A where the best results were expected. Further work is required to obtain additional data to address these questions and generate more robust conclusions. There is therefore an intent to revisit the Silchester survey sites to test different configurations and surveying strategies. An area of focus will be increasing spatial resolution of the surveys. The method applied for this study aimed to capture one radiation measurement every square metre, as is applied within the nuclear industry. Due to the size of the targets and limited radiation contrast of targets to surrounding background radiation, this resolution is now believed to be too low. As observed for Site D (Kilns), the lower resolution can result in possibly misleading results due to level of interpolation required to smooth the data. By increasing resolution to one measurement per 0.5 m, or ideally 0.25 m, it is expected that finer interpolation can be achieved by introducing three times as many measurements, improving data quality. Such an approach is expected to draw out smaller anomalies that may currently be obscured. The collection of much larger data sets via a vehicle-mounted system is planned during future fieldwork.

Alternative methods of analysing the data will be explored. One such method proposed is the analysis of Th/K and Th/U ratios within the data. This technique has been used successfully by Ruffell et al. (2006) to more clearly define man-made subsurface structures present in gamma radiation survey data. The ratios of Th/K and Th/U generated clearer images relative to total count or individual isotope measurements Ruffell et al. (2006).

Finally, sampling and analysis of soil and artefacts excavated from the sites will be undertaken. This will help gain a valuable insight into their radiochemical composition and possible reasons behind the varying levels of success at the different sites.

It is envisaged that the lessons learned from repeating the investigations at Silchester will support the development of an optimised

surveying strategy for application at other sites of archaeological interest. This in turn will help establish the efficacy of gamma surveying as a complementary tool within the current array of geophysical techniques.

ACKNOWLEDGEMENTS

This unique investigation was possible thanks to NUVIA Limited, which provided access to the Groundhog[®] Fusion System and supporting software tools. The authors wish to express their thanks and gratitude to the University of Reading for providing access to the Silchester site.

CONFLICT OF INTEREST

The authors declare that there is no conflict of interest.

DATA AVAILABILITY STATEMENT

The data that support the findings of this study are available from the corresponding author upon reasonable request.

ORCID

Victoria Robinson  <https://orcid.org/0000-0002-7610-9884>

REFERENCES

- ADS. (2021). Archaeological data service. <https://www.archaeologydataservice.ac.uk>. <https://doi.org/10.17616/R3MW23> Accessed 15/07/2021
- Aliyev, C. (2004). NORM in building materials. In: IAEA (2004) Naturally Occurring Radioactive Materials (NORM IV): Proceedings of an International Conference Held in Szczyrk Poland, 17–21 May 2004, IAEA-TECDOC-1472.
- Aziz, A., Attia, T., McNamara, L., & Friedman, R. (2018). Application of gamma-ray spectrometry in discovering the granitic monument of King Pepi I: A case study from Hierakonpolis, Aswan, Egypt. *Pure and Applied Geophysics*, 176, 1639–1647. <https://doi.org/10.1007/s00024-018-2036-1>
- Barker, P. (1993). *Techniques of archaeological excavation* (Third ed.). Routledge, Taylor and Francis Group.
- Beddow. (2019). Method statement – Groundhog[®] radiation surveys of land and buildings using portable and vehicle mounted systems. 72736/MS/001, Issue 2, Internal Report for NUVIA Limited UNPUBLISHED.
- Bezuidenhout, J. (2012). Mapping of historical human activities in the Saldanha bay military area. *Scientia Militaria*, 40(2), 89–101. <https://doi.org/10.5787/40-2-998>
- BGS. (2019). Geology of Britain viewer: Silchester, Hampshire. British Geological Society. <http://mapapps.bgs.ac.uk/geologyofbritain/home.html>. Accessed 29/06/2019
- Burns, P. C., & Finch, R. (Eds.) (1999). *Uranium: Mineralogy, geochemistry and the environment* (Vol. 38). Reviews in Mineralogy and Geochemistry. Mineralogical Society of America.
- Cardarelli, E., & de Filippo, G. (2009). Integrated geophysical methods for the characterisation of an archaeological site (Massenzio Basilica) – Roman Forum, Rome, Italy. *Journal of Applied Physics*, 68, 508–521. <https://doi.org/10.1016/j.jappgeo.2009.02.009>
- Cid, A. S. A., Zamboni, R. M., Cardoso, C. B., Muniz, R., Corona, M., Valladares, A., Kovacs, D. L., Macario, L., Perea, K., Goso, D., & Velasco, C. (2014). Na, K, Ca, Mg, and U-series in fossil bone and the proposal of a radial diffusion-adsorption model of uranium uptake. *Journal of Environmental Radioactivity*, 136, 131–139. <https://doi.org/10.1016/j.jenvrad.2014.05.018>

- Clark, R. (2017). Groundhog fusion calibration – Nuvia health physics instruction HPI4214. Internal Report for NUVA Limited UNPUBLISHED.
- Columbero, C. E., Meirano, D., & Sambuelli, L. (2020). Magnetic and radar surveys at Locri Epizephyrii: A comparison between expectations from geophysical prospecting and actual archaeological findings. *Journal of Cultural Heritage*, 42, 147–157. <https://doi.org/10.1016/j.culher.2019.06.012>
- Creighton, J., & Fry, R. (2016). *Silchester: Changing visions of a Roman town: Integrating geophysics and archaeology: The results of the Silchester mapping project, 2005–10*. Britannia Monograph Series, 28. Society for the Promotion of Roman Studies.
- Davies, M. (2015). Health physics procedure HPP357 – Calibration of groundhog detectors. Issue A, September 2015, Internal Report for NUVA Limited UNPUBLISHED.
- Davies, M., Clark, R., & Adsley, I. (2011). High-density gamma radiation spectrometry surveys of contaminated land. Proceedings of the 14th International Conference on Environmental Remediation and Radioactive Waste Management, September 25–29, Reims, France.
- Dick, H. C. P., Sloane, J. K., Carver, B., Wisruewski, J., Haffenden, K. D., Porter, A., Roberts, S., & Cassidy, N. J. (2015). Detection and characterisation of black death burials by multi-proxy geophysical methods. *Journal of Archaeological Science*, 59, 132–141. <https://doi.org/10.1016/j.jas.2015.04.010>
- Duggan, F. (1983). A non-linear empirical prescription for simultaneously interpolating and smoothing contours over an irregular grid. *Computer Methods in Applied Mechanics and Engineering*, 44, 119–125. [https://doi.org/10.1016/0045-7825\(84\)90123-3](https://doi.org/10.1016/0045-7825(84)90123-3)
- EDINA. (2018). Aerial photo of kiln area, high resolution (25 cm) vertical aerial imagery [JPEG geospatial data], scale 1:500, using EDINA aerial Digimap service. <https://digimap.edina.ac.uk>. Accessed on 30th October 2020
- EDINA. (2019). Ordnance survey of Silchester, colour raster (TIFF geospatial data), 1:25,000 scale, using EDINA Digimap ordnance survey service. <https://digimap.edina.ac.uk>. Accessed 19th August 2019
- ESRI. (2022). ArcGIS pro: How inverse distance weighted interpolation works. <https://pro.arcgis.com/en/pro-app/latest/help/analysis/geostatistical-analyst/how-inverse-distance-weighted-interpolation-works.htm>. Accessed 14th January 2022
- Farmer, N., Kathren, R. L., & Christensen, C. (2008). Radioactivity in fossils at the Hagerman Fossil Beds National Monument. *Journal of Environmental Radioactivity*, 99, 1355–1359. <https://doi.org/10.1016/j.jenvrad.2008.02.004>
- Fulford, M., Clarke, A., & Eckardt, H. (2006). *Life and labour in late Roman Silchester: Excavations in insula IX since 1997* (Vol. 22). Britannia Monograph Series. Society for the Promotion of Roman Studies.
- Fulford, M. C., Durham, A., Fry, E., Machin, R., Pankhurst, S., & Wheeler, D. (2018). *Silchester Roman town – The baths 2018*. The University of Reading, Department of Archaeology.
- Gaffney, C., & Gaffney, V. (2010). Through an imperfect filter: Geophysical techniques and the management of archaeological heritage. In D. C. Cowley (Ed.), *Remote sensing for archaeological heritage management*. EAC Occasional Paper No. 5. (pp. 117–127). Europae Archaeologiae Consilium.
- Gaffney, C., & Gater, J. (2003). *Revealing the buried past: Geophysics for archaeologists*. Tempus Publishing Ltd.
- Grimstead, D. N., Clark, A. E., & Rezac, A. (2017). Uranium and vanadium concentrations as a trace element method for identifying diagenetically altered bone in the inorganic phase. *Journal of Archaeological Method and Theory*, 25, 689–704. <https://doi.org/10.1007/s10816-017-9353-z>
- Halgedahl, S. L., Jarrard, R. D., Brett, C. E., & Allison, P. A. (2009). Geophysical and geological signatures of relative sea level change in the upper Wheeler Formation, Drum Mountains, west-central Utah: A perspective into exceptional preservation of fossils. *Palaeogeography, Palaeoclimatology, Palaeoecology*, 277, 34–56. <https://doi.org/10.1016/j.palaeo.2009.02.011>
- Historic England. (2020). Aerial photo of Kinghern Copse and environs, Little London, 1947. Photo reference: EAW011004. <https://www.britainfromabove.org.uk/image/EAW011004>. Accessed 31st October 2020
- IAEA. (1998). Characterization of radioactively contaminated sites for remediation purposes. IAEA-TECDOC-1017. International Atomic Energy Agency (IAEA), Vienna, May 1998.
- IAEA. (2003). Extent of environmental contamination by naturally occurring radioactive material (NORM) and technological options for mitigation. Technical Report Series No. 419. International Atomic Energy Agency, Vienna.
- IAEA. (2005). Natural activity concentrations and fluxes as indicators for the safety assessment of radioactive waste disposal: Results of a coordinated research project. IAEA-TECDOC-1464. October 2005.
- IAEA. (2013). Management of NORM residues. IAEA-TECDOC-1712. International Atomic Energy Agency, Vienna.
- Kern, E. M. (2020). Archaeology enters the ‘atomic age’: A short history of radiocarbon, 1946–1960. *The British Journal for the History of Science*, 53(12), 207–227. <https://doi.org/10.1017/S0007087420000011>
- Kozhevnikov, N. O., Kharinsky, A. V., & Snopkov, S. V. (2018). Geophysical prospecting and archaeological excavation of ancient iron smelting sites in the Barun-Khal valley on the western shore of Lake Baikal (Olkhon region, Siberia). *Archaeological Prospection*, 26, 1–17. <https://doi.org/10.1002/arp.1727>
- Lee, C. J., & Burgess, P. H. (1999). Good practice guide 14, the examination, testing and calibration of portable radiation protection instruments. National Physics Laboratory, Issue 2, First Issued – 1999, Updated – 2014.
- Linford, N., Linford, P., & Payne, A. (2016). Silchester environs project, Little London Roman Tiley, Pamper, Hampshire. Report on Geophysical Survey, July 2015, Research Report Series no. 41-2016, NGR: SU 6226 5971, ISSN: 2059-4453 (online), Historic England.
- MAGIC Map. (2021). Silchester soilscape, map produced by Magic on 27th march 2021 using ordnance survey projection OSGB36, 1:80,000 grid ref.: SU46076249, and Soilscape data from National Soil Resources Institute (polygons showing 27 classes of soil – last updated 01/01/2005).
- Mahmood, Z. U. W., & Mohamed, C. A. R. (2010). Thorium. In D. A. Atwood (Ed.), *Radionuclides in the environment* (Vol. 2010, pp. 247–255). John Wiley and Sons.
- Millard, A. R., & Hedges, R. E. M. (1995). The role of the environment in uranium uptake by buried bone. *Journal of Archaeological Science*, 22, 239–250. <https://doi.org/10.1006/jasc.1995.0025>
- Milsom, J., & Eriksen, A. (2011). *Field geophysics* (Fourth ed.). The Geological Field Guide Series. (pp. 1–32). Wiley-Blackwell.
- Moussa, M. (2001). Gamma-ray spectrometry: A new tool for exploring archaeological sites; a case study from east Sinai, Egypt. *Journal of Applied Geophysics*, 48, 137–142. [https://doi.org/10.1016/S0926-9851\(01\)00077-5](https://doi.org/10.1016/S0926-9851(01)00077-5)
- Nash, D. J., Ciborowski, T., Ullyott, R., Pearson, J., Darvill, M., Greaney, T., Maniatis, S., & Whitaker, K. (2020). Origins of the sarsen megaliths at Stonehenge. *Science Advances*, 6(31), eabc0133. <https://doi.org/10.1126/sciadv.abc0133>
- NPL. (2014). Good practice guide no. 30 – Practical radiation monitoring. Issue 2, National Physical Laboratory, ISSN: 1368-6550.
- NUVIA. (2019). Calibration certificate for groundhog detector GN08. Completed June 2019, Internal Report for NUVA Limited UNPUBLISHED
- NUVIA. (2021). NUVIA UK products: Groundhog®. <https://www.nuvia.co.uk/product/groundhog>. Accessed 21/02/2021
- Ordnance Survey. (1912). Little London, sheet 1:10 560 (county series 2nd revision), scale 1:10560 (TIF file), last updated 1st January 1912,

- ordnance survey, GB. Using: EDINA historic Digimap service. <https://digimap.edina.ac.uk>
- Peppe, D. J. (2013). Dating rocks and fossils using geologic methods. *Nature Education Knowledge*, 4(10), 1.
- Pike, A. W. G., Hedges, R. E. M., & van Calsteren, P. (2002). U-series dating of bone using the diffusion-adsorption model. *Geochimica et Cosmochimica Acta*, 66(24), 4273–4286. [https://doi.org/10.1016/S0016-7037\(02\)00997-3](https://doi.org/10.1016/S0016-7037(02)00997-3)
- Putiška, R., Kušnirak, D., Dostál, I., Lačný, A., Moješ, A., Hók, J., Pasteka, R., Krajňák, M., & Bosansky, M. (2014). Integrated geophysical and geological investigations of karst structures in Kombok, Slovakia. *Journal of Cave and Karst Studies, the National Speleological Society Bulletin*, 76(3), 155–163. <https://doi.org/10.4311/2013ES0112>
- Reinhardt, N., & Herrmann, L. (2019). Gamma-ray spectrometry as a versatile tool in soil science: A critical review. *Journal of Plant Nutrition and Soil Science*, 182, 9–27. <https://doi.org/10.1002/jpln.201700447>
- Ruffell, A., & McKinley, J. (2008). *Geoforensics*. Wiley Blackwell.
- Ruffell, A., McKinley, J., Lloyd, C. D., & Graham, C. J. (2006). Th/K and Th/U ratios from spectra gamma-ray surveys improve the mapped definition of subsurface structures. *Journal of Environmental and Engineering Geophysics*, 11(1), 53–61. <https://doi.org/10.2113/JEEG11.1.53>
- Ruffell, A., & Wilson, J. (1998). Near-surface investigation of ground chemistry using radiometric measurements and spectral gamma ray data. *Archaeological Prospection*, 5, 203–215. [https://doi.org/10.1002/\(SICI\)1099-0763\(199812\)5:4<203::AID-ARP96>3.0.CO;2-D](https://doi.org/10.1002/(SICI)1099-0763(199812)5:4<203::AID-ARP96>3.0.CO;2-D)
- Sanjuro-Sanchez, J., Chamorro, C. A., Alves, C., Sanchez-Pando, J. C., Blanco-Rotea, R., & Costa-Garcia, J. M. (2017). Using in-situ gamma ray spectrometry (GRS) exploration of buried archaeological structures: A case study from north-west Spain. *Journal of Cultural Heritage*, 34, 247–254. <https://doi.org/10.1016/j.culher.2018.05.004>
- Schmidt, A. R., Linford, P., Linford, N., David, A., Gaffney, C. F., Sarris, A., & Fassbinder, J. (2015). *EAC guidelines for the use of geophysics in archaeology: Questions to ask and points to consider, EAC guidelines 2*. Europae Archaeologiae Consilium (EAC), Association Internationale san But Lucratif (AISBL).
- SPRS. (2020). *Britannia monograph series*. Archaeology Data Service, Society for the Promotion of Roman Studies.
- Trogu, A., Ranieri, G., Calcina, S., & Piroddi, L. (2014). The ancient Roman aqueduct of Karales (Cagliari, Sardinia, Italy): Applicability of geophysics methods to finding the underground remains. *Archaeological Prospection*, 21, 157–168. <https://doi.org/10.1002/arp.1471>
- USNRC. (2009). Multi-agency radiation survey and assessment of materials and equipment manual (MARSAME) (NUREG-1575), 'supplement 1'. Office of Nuclear Regulatory Research, US Nuclear Regulatory Commission (USNRC), Washington DC, January 2009.
- Westminster Abbey. (2020). Westminster abbey – History: Architecture. <https://www.westminster-abbey.org/about-the-abbey/history/architecture>, Dean and Chapter of Westminster. Accessed 04/09/2020
- Zheng, W., Li, X., Lam, N., Wang, X., Liu, S., Yu, X., Sun, Z., & Yao, J. (2013). Applications of integrated geophysical method in archaeological surveys of the ancient Shu ruins. *Journal of Archaeological Science*, 40, 166–175. <https://doi.org/10.1016/j.jas.2012.08.022>


SUPPORTING INFORMATION

Additional supporting information may be found in the online version of the article at the publisher's website.

How to cite this article: Robinson, V., Clark, R., Black, S., Fry, R., & Beddow, H. (2022). Portable gamma ray spectrometry for archaeological prospection: A preliminary investigation at Silchester Roman Town. *Archaeological Prospection*, 29(3), 353–367. <https://doi.org/10.1002/arp.1859>

RESEARCH ARTICLE OPEN ACCESS

Radiating Encouragement: Further Investigation Into the Application of Gamma Ray Spectroscopy for Archaeological Prospection at the Roman Town of Silchester

Victoria Robinson^{1,2}  | Stuart Black¹ | Robert Fry¹ | Helen Beddow² | Robert Clark² | Mike Fulford¹

¹School of Archaeology, Geography and Environmental Science, University of Reading, Reading, UK | ²Nuvia Limited, Warrington, UK

Correspondence: Victoria Robinson (v.a.robinson@pgr.reading.ac.uk)

Received: 15 December 2023 | **Revised:** 17 May 2024 | **Accepted:** 28 June 2024

Funding: The authors received no specific funding for this work.

Keywords: archaeological survey | gamma ray surveying | gamma spectrometry | natural radioactivity | Nuvia Groundhog® | Silchester

ABSTRACT

This study builds on a preliminary investigation into the efficacy of gamma radiation surveying as a complementary tool for archaeological prospection. Improved surveying and data processing methods were implemented, including the use of a vehicle-mounted Groundhog surveying system, use of alternative software tools and examination of the impacts of individual radionuclides. The study focuses on a range of targets within *Insulae* VII, XXXV and XXXIII in Silchester Roman town, Hampshire. Targets of interest included a polygonal temple, a house, ditches (including an Iron Age defensive ditch) and several Roman roads. While the survey revealed no measurable differences in the gamma radionuclide content of less substantial structures (such as the temple and house) and the surrounding soil, it successfully delineated major structures. The Roman roads, Iron Age defensive ditch and potentially an indication of a historic field boundary not present in modern records were clearly visible in the generated visualisations. The roads and field boundary appear as distinct linear features of depleted radioactivity. The location of the Iron Age ditch correlates with an area of elevated radioactivity. Notably, the technique not only successfully identified archaeological features but was also able to indicate differences in the properties of similar targets such as variations in road thickness. Further, the gamma radiation data indicates variations in the local geology attributable to historic changes in land use and geochemical composition. This latest study corroborates the findings of the preliminary investigation, demonstrating replicability, scalability and ability to enhance output data quality. Further research, including sampling and non-destructive analysis of materials from the site, is needed to better explain observed results.

1 | Introduction

Multiple geophysical survey methods have been applied on a global scale as a non-destructive method of identifying and analysing features of archaeological interest for over 70 years (Cuenca-Garcia 2018; Jordan 2009; Wynn 1986). As noted by Jordan (2009), an extensive amount of data has been accrued over this period, demonstrating the successful application of these techniques in supporting archaeological investigations. However, the effectiveness of each method is dependent on the

ability to measure clear differences in the physical properties of potential targets and surrounding substrate and susceptibility to interference from modern features (Gaffney and Gater 2011; Milsom and Eriksen 2011; Ruffell and McKinley 2008). Selection of an optimal geophysical technique most likely to yield significant contrasts must therefore be managed on a site-by-site basis. Consideration must be given to the physical characteristics of anticipated targets, the surrounding substrate, target size and presence of modern features that could cause interference (Gaffney and Gater 2011; Ruffell and McKinley 2008).

This is an open access article under the terms of the [Creative Commons Attribution](https://creativecommons.org/licenses/by/4.0/) License, which permits use, distribution and reproduction in any medium, provided the original work is properly cited.

© 2024 The Author(s). *Archaeological Prospection* published by John Wiley & Sons Ltd.

To improve data fidelity, multiple geophysical survey methods measuring different physical properties, and with different susceptibilities, can be applied. Multiple studies demonstrating the effectiveness of using complementary geophysical methods for the prospection and mapping of archaeological sites are available in the published literature. Key benefits associated with the application of complementary geophysical techniques at a site include improving the accuracy of data interpretation and increasing the amount of data that can be retrieved to characterise a site beyond merely establishing the presence and position of archaeological features. This first point is exemplified in a study by Cuenca-Garcia (2018). Here, multiple geophysical techniques were consistently applied to three contrasting sites of archaeological interest across Scotland. Techniques included fluxgate gradiometer, electromagnetic induction, ground-penetrating radar (GPR) and earth resistance surveys (Cuenca-Garcia 2018). Geochemical analysis of soil samples taken from each site was also undertaken to aid geophysical data interpretation (Cuenca-Garcia 2018). The selected sites contained known targets including a Viking Longhouse, Iron Age ditches and Neolithic/Bronze Age closures. The findings from the study highlighted the benefits of implementing complementary techniques. This is best demonstrated in data from the survey of the Viking Longhouse. The Fluxgate Gradiometer survey was unable to detect the target through the deep windblown sands but was able to detect midden deposits that may have otherwise been missed (Cuenca-Garcia 2018)—a false negative conclusion. In contrast, the GPR and electromagnetic methods were capable of measuring the contrast between the longhouse and surrounding substrate (Cuenca-Garcia 2018). The study highlights the value of such an approach in regions with more challenging geologies for archaeological prospection and in particular those with significant heterogeneity in the soil overburden which can have the effect of shielding responses or creating noise in the output data.

Indeed, the author notes that in areas where significant variability exists, ‘surveys based on a single technique ... have a high chance of being disappointing ...’ (Cuenca-Garcia 2018, 70). A later paper by Porcelli et al. (2020) further highlights the importance of utilising multiple datasets to aid interpretation. Within this paper, Porcelli et al. (2020) refers to a GPR survey of Tutankhamun’s tomb, undertaken to confirm an earlier theory that it may be part of a larger tomb infrastructure belonging to Queen Nefertiti. This preliminary GPR survey appeared to confirm this theory, with the findings published as the ‘discovery of the century’ (Porcelli et al. 2020). However, two subsequent GPR surveys covering the same area, including one undertaken by the original authors, showed that this original conclusion was incorrect and that there were no further features of interest (Porcelli et al. 2020)—a false positive result. This second paper highlights the potential vulnerability of using a single technique and how even different datasets using the same technique can lead to conflicting conclusions.

A study by Simon et al. (2015) highlights the value of integrating different geophysical techniques to improve site characterisation, recognising that a single technique will only be able to generate data on one specific parameter of the site. In this study, the authors applied a combination of geophysical

techniques to investigate a Neolithic site in Thessaly, Greece. Techniques gainfully employed included magnetic surveys, electrical tomography and GPR (Simon et al. 2015). The combination of techniques yielded data with greater interpretive value. Useful insights into the presence and location of Neolithic structures, depth profiles of these features and indications of the geomorphology and sediment diversity of the area were provided (Simon et al. 2015). Further, the techniques applied facilitated a proportionate approach to surveying and the ability to gain the most amount of information possible within resource constraints. Magnetic and electrical methods enabled the efficient and effective surveying of a substantial area at a useful resolution (Simon et al. 2015). GPR, a higher resolution technique, could then be applied to much smaller areas, targeting features most likely to benefit from this higher resolution (Simon et al. 2015).

In summary, the application of multiple geophysical techniques in archaeological prospection follows a philosophy similar to that of James Lovelock’s insightful Gaia theory; that when these different complex techniques are applied cooperatively, the value of the combined data should be greater ‘than the sum of its parts’ (Lovelock 2000). Building on this philosophy, the authors of this paper aim to assess an alternative nonintrusive survey method’s effectiveness in archaeological prospection and its ability to contribute to this multitechnique approach. Specifically, the use of portable gamma radiation systems to measure any contrasts in concentrations of naturally occurring radioactivity in archaeological targets and the surrounding substrate. If successful, the use of gamma surveying methods could add to the existing ‘toolbox’ of nonintrusive archaeological prospection methods and may even facilitate improved interpretation of acquired data.

This research is the first reporting of a vehicle-mounted gamma radiation survey conducted at an archaeological site, for the purpose of prospection, available within the published literature. Our study successfully demonstrates the repeatability and scalability of the method, as well as an ability to apply multiple processing methods to generate high quality visual outputs that are novel, and that show significant promise for archaeological and land-use investigations.

2 | Building on a Preliminary Investigation at Silchester

Following an earlier study, the authors published findings from a preliminary investigation exploring the efficacy of using gamma radiation surveying methods to support the identification of buried archaeological features (Robinson et al. 2022). This approach is based on the principle that naturally occurring radioactive material is ubiquitous in the environment (IAEA 2023) and that human activity can cause measurable changes in the concentrations of this radioactivity. This includes, for example, importing and depositing (construction) materials from other locations, using clays which are naturally rich in naturally occurring radionuclides to make bricks (Aliyev 2004; IAEA 2003) and other industrial activities. The study focussed on targets within Silchester Roman Town. This location was selected due to the extensive geophysical and archaeological data available for the site

(Creighton and Fry 2016; Fulford 2021). This provided a valuable opportunity to compare gamma surveying data against this existing and well-understood information.

In the preliminary study (Robinson et al. 2022), gamma radiation surveys were undertaken using a hand-held gamma surveying system in both a collimated and uncollimated configuration to target four small areas across the site. Each contained a different target type. The system used was a Groundhog® Fusion system, developed, owned and operated by Nuvia Limited. The Groundhog® Fusion system (subsequently referred to here as Groundhog®) is part of a family of rugged, portable gamma radiation detection systems with spectrometric capability. The key components of Groundhog® used for this study are presented in Section 4. The system can be deployed in various configurations including collimated, uncollimated, vehicle mounted (using a bank of gamma detectors) or hand-held (single gamma detector). Groundhog® systems are traditionally used in the nuclear industry for mapping out anthropogenic radioactive contamination in the environment.

Results using a hand-held gamma detector from this earlier investigation at Silchester showed varying results. Gamma radiation data from two of the areas: an 'urban' site from the centre of the Roman Town and an area containing cremations/inhumations from just outside the Late Roman Town walls, failed to distinguish any archaeological features (Robinson et al. 2022). However, the other two sites, a temple area in the east side of the site and an industrial area in nearby Little London, yielded positive results. Here, the Groundhog® system was able to identify man-made features (both archaeological and more modern) that were also visible within extant fluxgate gradiometer and GPR data. Features identified included a Temenos wall/ditch bounding a Roman temple and an infilled clay pit (Robinson et al. 2022). The results suggested that gamma radiation surveys could be used to support the identification of some buried archaeological features and could add value to a multi-method geophysical approach to a site's identification and interpretation. Completion of this pilot study highlighted a number of opportunities for potentially improving the quality and efficiency of survey outputs. This included improving the scalability of the technique by using Nuvia's vehicle-mounted Groundhog® system and applying different data processing methods. This paper presents the results of work testing these variables.

2.1 | Aspects for Further Investigation

Completion of the first set of gamma surveys highlighted several opportunities for further work to test:

- Whether the findings from the first study could be replicated for other analogous targets,
- Whether the technique could be scaled up to cover a larger area within a similar period of time and
- Methods for improving the quality of processed data used for interpretation.

Two subsequent surveys were therefore undertaken at a different location within Silchester's boundary walls. The new location offered analogous targets, including the Roman road

infrastructure, a 16-sided temple structure and a major defensive Iron Age Ditch to test replication. Scalability was tested through the deployment of the vehicle-mounted Groundhog® system, which is capable of operating three gamma detector units simultaneously and, using a traversing speed of ~1 m/s, is able to cover approximately 1.4–2 ha/day. The collected data for this paper was processed using Geoplot 4 (Geoscan Research), enabling further experimentation with data processing. Finally, data from the two surveys were normalised with the intent of integrating the two datasets.

3 | Current Study Site and Existing Data

The study site is situated within the Roman Town of Silchester (Callewa Atrebatum) (Figure 1). The town is located approximately 2 km to the west of the current day village of Silchester, Hampshire, in south-east England. The site has a long history of occupation, dating back to the Iron Age (Fulford 2021). Indeed, one of the targets selected for this study is an Iron Age ditch that formed part of a large defensive enclosure, encompassing an area of ~38 ha (Fulford 2021). The positioning of the later Roman town broadly aligns with this enclosure (Fulford 2021). The Roman town of Silchester hosted various buildings and supporting infrastructure, from domestic dwellings to workshops, shops, temples and road networks (Creighton and Fry 2016; Fulford 2021). The roads divided the town into *insulae*, each generally containing a mixture of building types. It was this diversity of target type, combined with the extensive geophysical and archaeological data already available for the site that cemented Silchester as an optimal case study for this research project. These data have been acquired from over 150 years of systematic excavations at the site, starting principally with Reverend James Joyce in the 1860s (Creighton and Fry 2016) and decades of geophysical survey initiated in the 1950s (Creighton and Fry 2016).

The targets selected for this study are located across *Insulae* VII and XXXV to the west and *Insulae* XXXIII and XXXII to the east.

3.1 | *Insulae* VII and XXXV

The first survey location (Area 'A'), outlined in red in Figure 2, is a 0.6 ha area spanning *Insulae* VII and XXXV and contains three targets of interest (Figure 2). The first target is an anomaly broadly circular in shape, identified as a temple of stone construction, including ironstone quoins (Fulford 2021; Ward 1911). This feature comprises two concentric shapes: the outer being a 16-sided polygonal wall and an inner circular structure with a total maximum diameter of ~20 m (Creighton and Fry 2016). Although the foundations of this temple have previously been described as 'slight' (Creighton and Fry 2016), they produce a clear circular anomaly in the fluxgate gradiometer (Figure 2) and GPR data. The latter suggesting a depth of 1.57 and 0.23 m below the soil surface (Linford, Linford, and Payne 2019). It was therefore hoped that the structure would be substantial enough to support detection of a contrast in naturally occurring radioactive material relative to the surrounding substrate. In addition to the temple, there is '*Insula* VII House 4', an eight-roomed house (Creighton and Fry 2016),

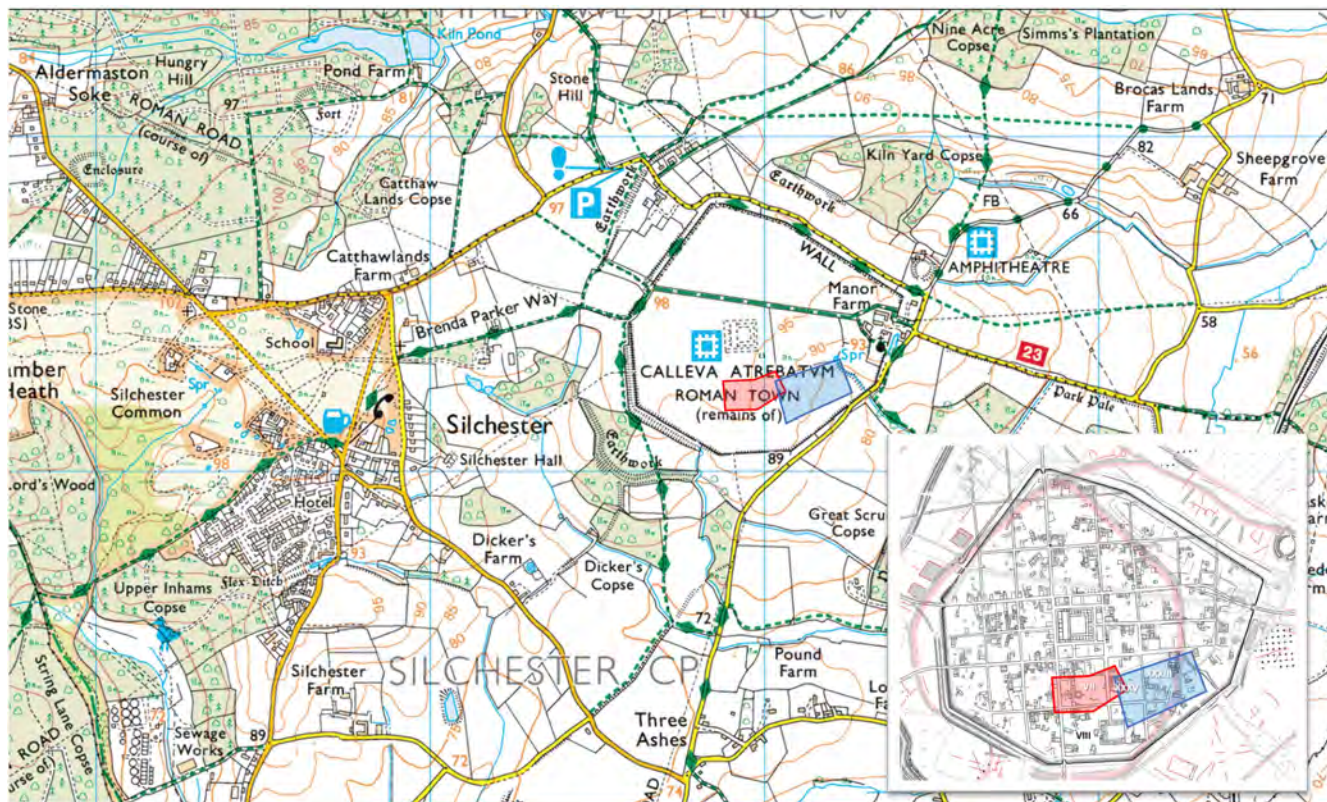


FIGURE 1 | Survey areas 1 and 2, outlined in red and blue, respectively, in the context of Silchester Roman Town and surrounding area (Digimap 2023). Inset: *Insulae* covered by the survey area.

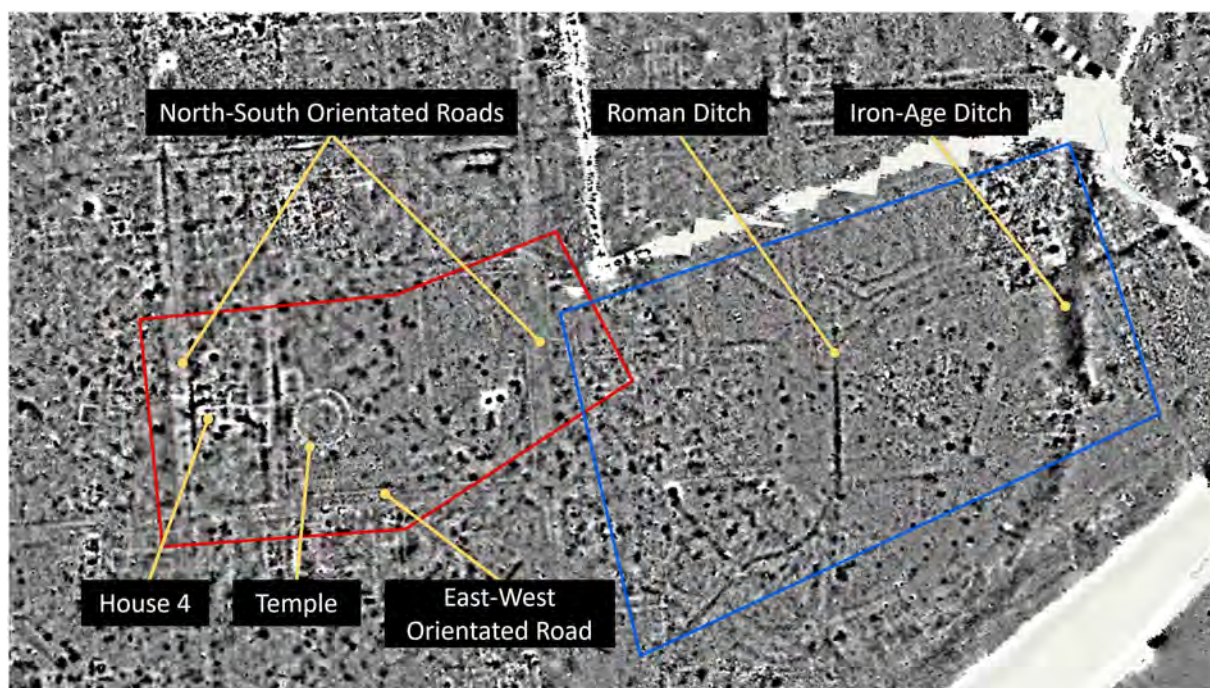


FIGURE 2 | Close-up view of the survey areas overlaying the fluxgate gradiometer data (+/- 7nT—black high to white low). The figure shows the targets present within Area A (outlined in red) and Area B (outlined in blue).

and sections of road in both north–south and east–west orientations. One of these roads is the major north–south road of the town, linking its North and South Gates (Fulford 2021). It is understood that House 4, as per other buildings on site, is

predominantly of flint rubble construction with brick corner stones (Creighton and Fry 2016) and therefore of more typical construction to other buildings in the Town compared to the temple. It was identified as a good target for the gamma

radiation survey due to its shallow depth (approximately 30 cm below ground level) and its ability to generate a prominent magnetic anomaly in the extant Fluxgate Gradiometer data (Creighton and Fry 2016; Linford, Linford, and Payne 2019). The roads appear to be located at similar depths to the temple, as suggested by GPR data (Linford, Linford, and Payne 2019). The roads predominantly consist of compacted gravel extracted from quarries west of the Roman Town (Fulford 2021). The roads and temple targets were of particular interest to the authors. In the previous study by Robinson et al. (2022), the roads in *Insula XXXIV* failed to generate a measurable difference in gamma emissions relative to the surrounding substrate. The authors wished to explore whether these findings would be repeated for roads in a different area of the Silchester site or if different behaviours would be observed. The temple structure provided a novel target type of significant size to further test the efficacy of the Groundhog system.

3.2 | *Insulae XXXIII*

A larger ~1.4 ha area (Area 'B'), outlined in blue in Figure 2, was targeted in an adjacent space spanning *Insulae XXXIII* and *XXXII* (Figure 2). This site was selected due to the presence of two key features clearly present within the extant geophysics data: a large (Iron Age) defensive ditch running down the east of the survey area and a suspected Roman ditch for a drain or water supply (Figure 2). The Iron Age ditch was excavated in 2019 which demonstrated that it terminates at 4.8 m below the ground surface (Fulford et al. 2019). The ditch was selected for this study as it is analogous to targets clearly visible in the previous study: the ditch features associated with the temenos wall and the infilled clay pit. The Roman ditch offered a clear linear feature which turns into a long sweeping curve at the southern end of the survey area. It introduces a new target type to this research project and an opportunity to further test the efficacy of this technique.

It is noted that both study areas also contain other features such as large pits, wells, minor roads and structures that may also form targets of interest. However, due to their smaller size, they are less likely to generate significant contrasts in background radioactivity compared to the surrounding soil.

4 | Methodology

4.1 | Overview of Equipment Used

The use of a vehicle-mounted system facilitated the simultaneous operation of three Groundhog[®] gamma detector units. The Groundhog[®] units each contain a 76 mm × 76 mm sodium iodide (NaI) scintillation type gamma detector and spectrometer. The NaI detectors have an operating energy range of approximately 15–3000 keV. The units are linked to a mapping grade GPS unit and data logger in the form of an ultra-mobile personal computer (UMPC). One gamma spectrum measurement is recorded by the system every second, along with the corresponding positioning data.

With the deployment of three detectors in the vehicle-mounted system, it is possible to achieve the simultaneous collection of

three gamma radiation measurements per second, with each gamma detector spaced 1 m apart. This contrasts significantly with the hand-held system's capacity for collecting one gamma radiation measurement per second, highlighting the enhanced efficiency afforded by the vehicle-mounted configuration.

4.2 | Site Surveys

Vehicle-mounted surveys were completed on 18 August 2022 and 16 May 2023. The second survey was originally unplanned and undertaken to fill in a substantial gap in the data on the eastern side of the survey area as a result of a GPS signal failure on the original survey (Area B) (Figure 4).

In advance of each deployment of the vehicle-mounted system, the three Groundhog[®] detector units were subject to full calibration, in accordance with Nuvia procedures. These annual calibration checks are essential to ensure that each unit is performing as expected and fit for purpose, thereby reducing the risk of introducing systematic errors. The Nuvia procedures are based on the National Physics Laboratory's Good Practice Guide 14 (Lee and Burgess 2014). The calibration process measured the gamma detectors' responses against background gamma radiation and a 5.72 kBq Cs-137 check source for a period of 600 s each. This confirmed that the gamma detectors were operating within acceptable ranges and therefore generating reliable data. The calibration checks confirmed that the detectors had an efficiency (i.e., the ratio of light pulses generated by the NaI crystal relative to the number of gamma rays emitted by the check source) of ~18 counts per second (cps) in the Cs-137 (662 keV) photopeak and net value of 3.17 cps which is well within the acceptable range of 2.93–3.24 cps. It was further confirmed that the detectors were operating with an energy resolution (i.e., the detector's ability to differentiate between energy peaks in a spectrum) of 7% at full width half maximum (FWHM) amplitude. Again, this was within the acceptable range of 6.50%–8.00%.

On the morning of each survey, the Groundhog[®] system was subject to additional equipment function checks. These were undertaken in accordance with Nuvia's internal Method Statement. Key activities included:

- Vehicle safety checks.
- Ensuring equipment has been subject to the necessary electrical safety checks.
- Visual checks of equipment and cables to ensure they are in good physical condition and that batteries have full charge.
- Functional checks of the Groundhog[®] system to ensure the GPS receiver and gamma radiation detectors were operating correctly. This included checking the responses of the detector unit, checking functionality of the necessary software tools, and that the GPS unit was receiving a sufficiently strong signal.

As the survey areas were located in a large open field, a detailed walk-round was not required. It could be seen that there were no obstructions or hazards that could impact on vehicle access.

It was however noted that one small area close to the Iron Age ditch was heavily rutted. While it was acknowledged that this would not impact on vehicle progress, suddenly dropping into a deep rut could trigger an 'excess speed' alarm on the UMPC. It could also potentially shock the NaI crystals of the detector units, leading to an erroneous measurement.

To facilitate the vehicle survey, the three gamma radiation detectors and GPS antenna were fixed in place using a mounting frame attached to the front of the Land Rover (Figure 3). The frame ensures that the detectors are securely positioned 1 metre apart at a consistent height of ~30 cm. The corners of the targeted survey areas, shown in Figure 2, were marked out with siting poles positioned using a Leica GS16 RTK GNSS unit.

The vehicle surveys were completed by driving around the perimeter of one of the predetermined survey areas and gradually working inwards towards the centre, following the tyre tracks of the previous circuit to avoid introducing gaps in the measurements. Several passes of the centre of each survey area were made due to the turning circle of the vehicle. A constant slow speed of approximately 1 m s^{-1} was maintained by placing the vehicle in first gear on a low transfer case setting ('low range'), thereby avoiding the need to apply acceleration. Maintaining this speed facilitated the collection of at least one gamma radiation measurement per square metre for each detector. This speed, combined with the simultaneous use of three detectors

simultaneously enabled the collection of three radiation measurements every second, covering an area of three square metres. On completion of one survey area, the vehicle was relocated to the second predefined survey area (August 2022 survey only) and the process repeated.

4.3 | Data Processing

During the August 2022 and May 2023 surveys, gamma radiation and GPS measurements were automatically logged on the UMPC set up in the cab of the vehicle. At the end of each survey, these data were transferred to a stand-alone desktop computer for quality checks and preliminary processing.

As per the previous study, Microsoft Access (v. 16.0.14131.20278) was used to compile the data, with post-processing to improve the quality of location data undertaken in GrafNav (v. 8.3). RINEX data from the Hartley Wintney (HART) OS Reference Station was used for differential correction. Further quality checks, including checks on the completeness of the data, highlighted the significant gap in the August 2022 data within Area B. Later investigation showed that this affected an area of $\sim 5500 \text{ m}^2$ (Figure 4), nearly a third of the eastern portion of the survey area, for which corresponding gamma data could not be plotted. These missing data informed the decision to resurvey the eastern side of the survey area to fill in this gap (Area B).



FIGURE 3 | View of the Nuvia survey vehicle, fitted with three Groundhog® Detectors and GPS system secured to the front. The detectors are spaced 1 m apart and positioned ~20 cm above ground level.

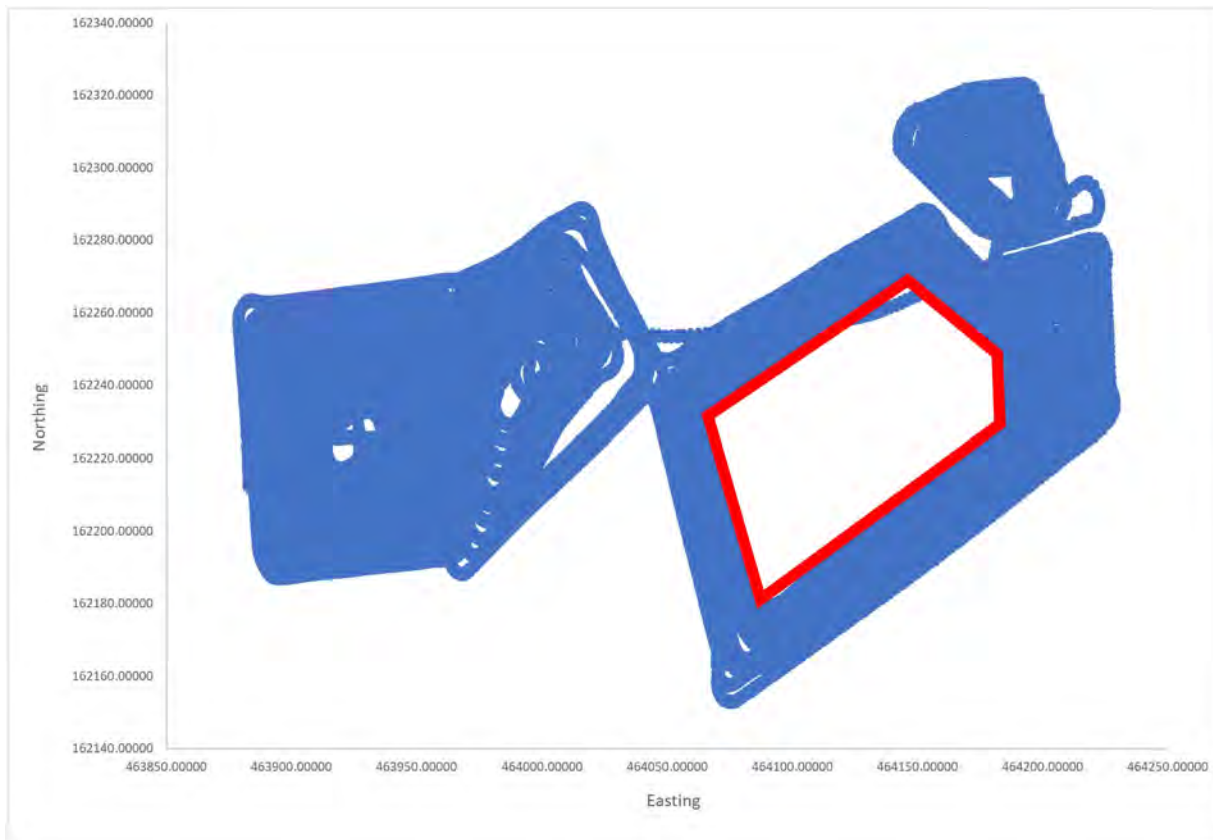


FIGURE 4 | Plot of the GPS/gamma radiation data points (blue) collected during the August 2022 survey, highlighting the area affected by missing GPS data (outlined in red).

With the exception of the missing GPS points, the remainder of the August 2022 and subsequent May 2023 positional data was excellent, achieving centimetre accuracy. Finally, quality checks also highlighted seven erroneous gamma radiation measurements in the May 2023 data. These values were an order of magnitude higher than the average readings in the dataset. The anomalous data points can be attributed to a physical shock to one of the NaI crystals in a detector unit, likely due to driving over the ruts or contacting tufts of long grass. It is considered improbable for measurements exceeding 3000 cps to occur naturally in an area with typical background radioactivity for the region. Notably, these elevated readings affected only one detector at a time. If there was a point source of elevated radioactivity in the ground, we would expect multiple detectors to record similarly high values. In consequence, these erroneous measurements were removed from the dataset.

Finally, both the August 2022 and corrected May 2023 datasets were exported as dBase database (.dbf) files for further processing.

The original strategy for processing the data was to combine the August 2022 and May 2023 datasets to create a single set of visualisations. This was accomplished using the Geoplot software tool (version 4). However, this was found to be non-viable. The data could not be integrated, with areas of overlapping measurements obscuring any potential anomalies present. As shown in Figure 5, the overlaid measurements actually created false positives, showing linear features that were attributable to vehicle movements.

To establish the cause of this incompatibility, gamma radiation measurements from two areas of overlap were samples (Figure 6) and subject to a two-tailed *t*-test, assuming unequal variances. The hypothesised mean difference was set at 0, assuming that there would be no significant difference in background gamma radiation measurements. A significance value of 0.05 was also set. As shown in Table 1, both sample areas confirm that the two datasets are significantly different, with *p* values of <0.05. After identifying a significant difference, the August 2022 data, which demonstrated a higher mean background gamma radiation value, were normalised against the May 2023 data. Multiple normalisation methods were applied, including subtracting the minimum value from each entry in the combined dataset and dividing by the range, dividing all values by the mean of the August 2022 and May 2023 mean values and dividing by mean and median values. None of these approaches addressed the problem. Consequently, a decision was made to process the August and May datasets separately, with resultant visualisations combined post-processing.

In the preliminary study by Robinson et al. (2022), gamma radiation data heatmaps were created exclusively in a bespoke add-on of ArcGIS, managed by Nuvia Limited. These heatmaps allowed the authors to identify anomalies that aligned with known archaeological features. However, for the purposes of this research project, a different software solution, Geoplot (version 4) was selected to plot the gamma data and create the visualisations. This choice not only enabled the exploration of alternative processing methods but also offered opportunities for enhancing image quality.

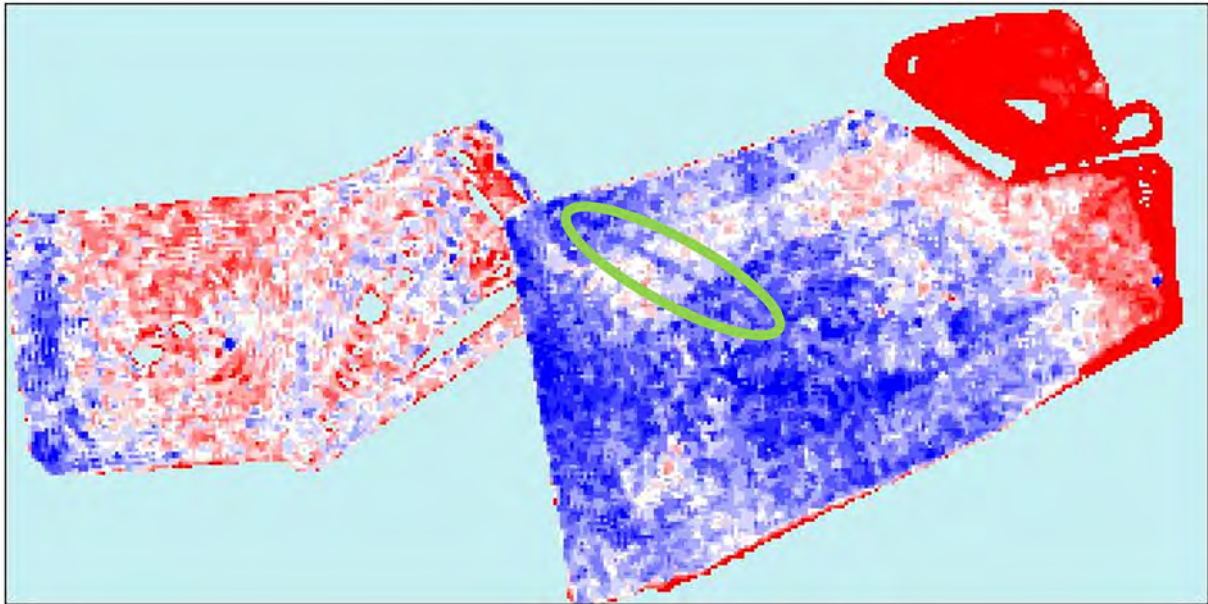


FIGURE 5 | Preliminary attempt at creating visualisations by combining the August 2022 and May 2023 datasets. This shows how the overlaid data are obscuring any anomalies and indeed creates false positives as highlighted in the green oval.



FIGURE 6 | Plot of the GPS/gamma radiation data points collected during the August 2022 and May 2023 surveys. Areas 1 and 2 denote where data were sampled for statistical analysis.

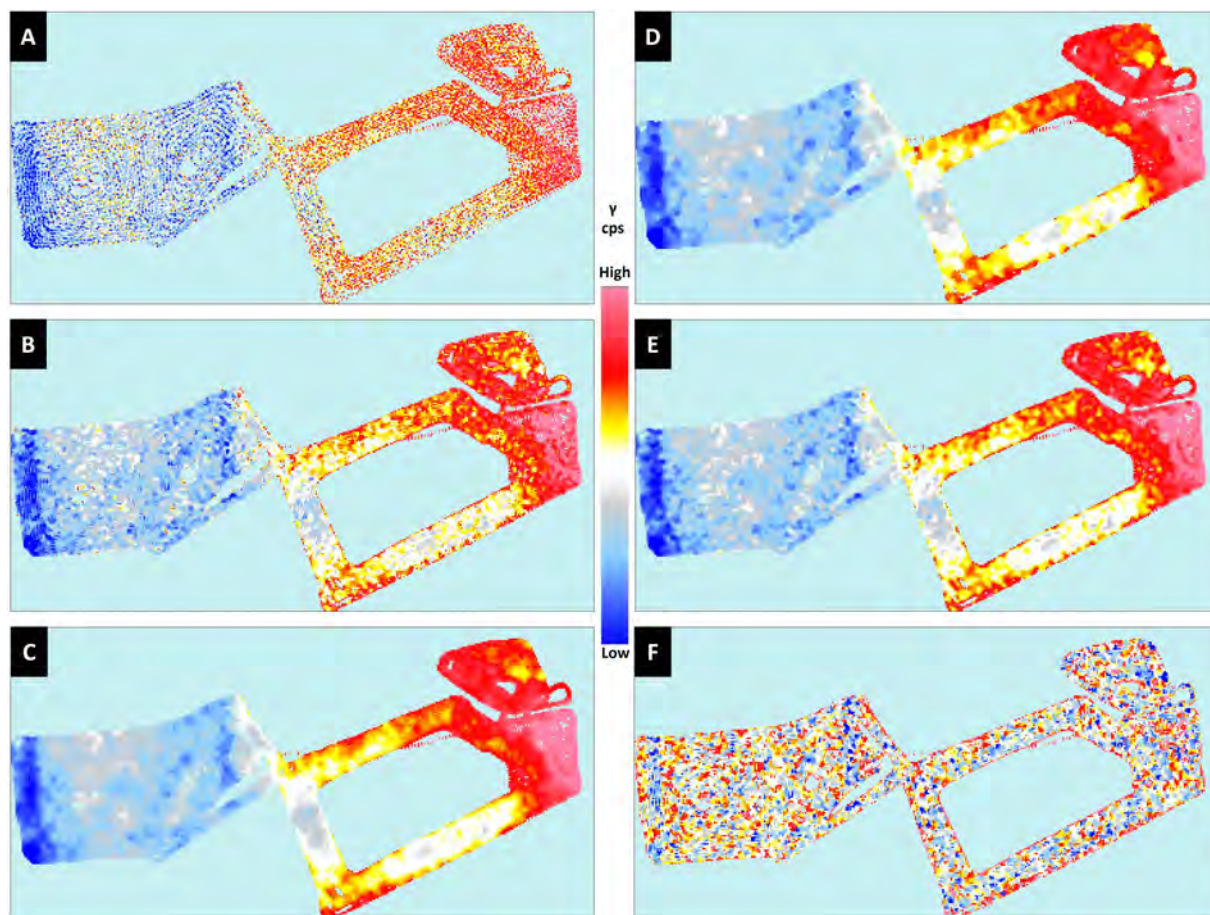
Further, this approach utilised a widely used software programme that does not require bespoke add-ons, improving accessibility.

Geoplot 4 offers a broad range of processing tools to enhance image quality. Work was therefore undertaken to explore which tools, or combination of tools, would generate the best quality

visualisations. Different processing tools were applied to the total gamma counts per second recorded during both the August 2022 and May 2023 surveys. Care was taken to achieve an optimal balance between enhancing image quality to draw out features and excessively altering the output, reducing fidelity to the original datasets. Colour palette 09 (± 2 standard deviations) was

TABLE 1 | Results from a two-tailed *t*-test for subsets of overlapping data from the August 2022 and May 2023 surveys as shown in Figure 6.

Parameters	Area 1		Area 2	
	Aug 22	May 23	Aug 22	May 23
Mean (cps)	225	189	237	199
Variance (cps)	310	239	359	259
Observations	3171	3264	2404	2950
Hypothesised mean difference	0		0	
<i>df</i>	6276		4727	
<i>t</i> stat	87.11		77.69	
$p(T \leq t)$ one-tailed	0.000		0.000	
<i>t</i> critical one-tailed	1.65		1.65	
$p(T \leq t)$ two-tailed	0.000		0.00	
<i>t</i> critical two-tailed	1.96		1.96	

**FIGURE 7** | Impact of different Geoplot processing tools on image quality for August 2022 total gamma counts (cps). The methods presented here are 'No Processing' (A), 'GPS Gap Fill' (B), Wallis Filter + GPS Gap Fill (C), Median Filter + GPS Gap Fill (D), Low Pass Filter + GPS Gap Fill (E) and High Pass Filter + GPS Gap Fill (F). The Wallis Filter + GPS Gap Fill (C) was identified as the preferred processing method.

found to be the most compatible with all processing methods to highlight the features of interest.

As a baseline, a single application of GPS Gap Fill was applied to the data. Subsequently, different data enhancement and

smoothing filters (either a single application or combination of Wallis, median, low pass and high pass filters) were tested on the raw dataset, (Figure 7). The Wallis filter was found to optimise and enhance potential archaeological features within the dataset without overly smoothing the data.

Interrogation of the output images identified the combination of ‘Wallis Filter + GPS Gap Fill’ as the optimal method for processing the data. It created a smooth image capable of drawing out features of interest without excessive deviation from the raw data (Figures 7 and 9). This method was therefore applied to all subsequent processing.

Expanding on the data processing methods applied in the preliminary Silchester study (Robinson et al. 2022), the authors completed a more comprehensive analysis by investigating the specific impact of individual radionuclides on the observations from the ‘total gamma counts’ visualisations. Targeted radionuclides included both naturally occurring primordial radionuclides, namely, potassium-40, uranium-238 and thorium-232, and the anthropogenic caesium-137. Further, the authors examined energy windows that aggregated measurements falling below the caesium-137 energy range (‘Below Window’) and above it (‘Above Window’). Targeting of these individual radionuclides was achieved by importing data from individual regions of interest into Geoplot. The ability to explore the impact of individual radionuclides has the exciting potential to offer additional interpretive value for more traditional geophysical surveys of archaeological deposits. By generating visualisations for each radionuclide, it may be possible to make inferences on the materials used on the construction of features identified as being of archaeological interest. For example, elevated concentrations of uranium and thorium may indicate the presence of granitic features, whereas concentrated areas of depleted radioactivity across all radionuclides may suggest features comprising sedimentary rock such as flint. More broadly, the behaviours of individual radionuclides may help characterise the geological history of the area, as evidenced in studies such as that undertaken by Kozhevnikov, Kharinsky, and Snopkov (2018).

As illustrated in Table 2, each radionuclide can be identified through its characteristic energy range. When a gamma radiation measurement is registered by a detector, it is assigned to the corresponding energy window. It is further noted that where

TABLE 2 | Regions of interest subject to interrogation via Geoplot.

Region of interest	Energy range (keV)
Total gamma	0–3000
Potassium (K) (via ^{40}K)	1400–1600
Uranium (U) (via ^{214}Bi)	1600–1900
Thorium (Th) (via ^{208}Tl)	2500–3000
Caesium (Cs) (via ^{137}Cs)	581–740
Below (^{137}Cs) window	0–530
Above (^{137}Cs) window	760–3000

Note: Each gamma ray photon emitted by a decaying radionuclide has a specific energy, typically measured in keV. This energy is unique to the source radionuclide (IAEA 2017). The energies of these gamma photons therefore act as a fingerprint, supporting the characterisation of radioactive material. Where there are multiple radionuclides present that emit gamma ray photons with similar energies, it may be difficult to differentiate between them, depending on the resolution of the detector used. For example, the radionuclides Pb-214, which emits gamma ray photons with energies of 295 and 351 keV, and Bi-214, which emits gamma ray photons of 609 and 665 keV (IAEA 2008), would fall in the Cs-137 region of interest of 581–740 keV, as shown in the above table for the Groundhog NaI gamma detectors.

radionuclides do not undergo decay through emission of gamma photons, a proxy daughter radionuclide that emits gamma photons is used, as shown in Table 2.

5 | Results

The use of the vehicle-mounted Groundhog® system significantly increased the area that could be practically surveyed in a day. In the preliminary study by Robinson et al. (2022), where Groundhog® was deployed in a hand-held configuration, a total of ~16 000 m² was surveyed over a 2-day period. As shown in Table 3, approximately 23 500 m² was surveyed in a single day in August 2022, using the vehicle-mounted system. It is acknowledged that the efficiency of the hand-held surveys was impacted by the need to relocate between survey areas and the need to set up transect guides at each site. However, even once this inefficiency has been accounted for, it can be seen that the vehicle-mounted system significantly improves the scale of survey achievable. This supports the well-established findings from the commercial application of the Groundhog® system where it is known that a typical hand-held survey can cover hundreds to thousands of square metres (~15 000 readings per person/day) to tens of thousands of square metres per day (>50 000 readings per day).

Using the vehicle-mounted system also yielded a slight improvement in measurement density, increasing from a mean density of 1.3 measurements per square metre using the hand-held system (Robinson et al. 2022) to a mean of 2.2 measurements per square metre using the vehicle-mounted system as shown in Table 3. This improvement is attributable to the degree of overlap achieved during each pass of the Land Rover. This outlines the summary statistics for the August 2022 and May 2023 surveys, as well as those from the July 2019 survey of the Urban Area (Robinson et al. 2022), which is analogous in terms of target

TABLE 3 | Summary statistics for the August 2022 and May 2023 surveys shown against the July 2019 Urban Area survey for comparison.

Parameter	August 2022	May 2023	July 2019
Total area surveyed (m ²)	~23 500	~18 000	~4000
Total No. measurements	44 161	45 168	5255
Average No. readings/m ²	1.9	2.5	1.3
Minimum total gamma (cps)	132	124	163
Maximum total gamma (cps)	310	264	274
Mean total gamma (cps)	212	186	217
Standard deviation	24	16	16

Note: This highlights the improved survey density achieved by the vehicle-mounted system.

Source: July 2019 data are taken from Robinson et al. (2022).

types to the current survey areas. The total number of measurements recorded during each survey and minimum, maximum and mean readings collected are presented. Notably, the data from the May 2023 survey exhibit a closer resemblance to the July 2019 survey data than to the August 2023 data, the latter being collected during an extreme, high-temperature weather event. The two-tailed *t*-test applied to the datasets (Table 1) confirmed that the differences in the values observed for the August 2022 and May 2023 surveys are statistically significantly different.

5.1 | Total Gamma Emissions

Figure 7 presents the visualisations generated through the processing of total gamma counts recorded during the August 2022 survey. This figure reveals the impact of applying different processing tools on data quality.

The total gamma dataset from August 2022 identified two clear feature types within the survey area. These are clearly visible in both the raw data (Figure 7A) and processed data (Figure 7C–F). The first relates to the presence of linear features on the western extent of each dataset associated with Area A. There are two distinctive north–south aligned features and a less well-defined east–west feature running along the bottom of the area. These anomalies align very closely with known Roman roads clearly visible in the fluxgate gradiometer data (Figure 2). These linear features are present as areas of depleted radioactivity. The second feature of note is the clear transition from an area of generally low background radioactivity (~130–190 cps) in Area A, to a gradual increase in Area B, peaking at ~250–300 cps on the far eastern side of Area B. This observation is confirmed in the count rate distribution graph (Figure 8) which shows that gamma data from the August 2022 survey are not normally distributed. The chart demonstrates a bias towards lower counts per second, which will be influenced by the missing data from Area B where higher counts dominate. The transition from an area of lower background radioactivity in Area A to higher background radioactivity in Area B aligns with a historic field boundary running down the centre of the survey area. The

localised area of elevated radioactivity in the far eastern side of Area B may be suggestive of a change in the hydrogeological conditions. These findings are explored further in Section 5.

It is recognised that none of the data processing methods were able to delineate the circular anomaly of the temple or the features of House 4, which were the other key features of interest in this area. This may be anticipated, given the comparatively less substantial structures of these features relative to the roads and considering the survey's spatial resolution. However, it is noteworthy that there is also an absence of any localised areas of either depleted or elevated levels of radioactivity that could be associated with these structures.

Visualisations generated for the May 2023 data that focussed solely on Area B are presented in Figure 9. As observed for the August figures, it is evident that various anomalies can be identified. Notably, two linear features are visible to varying degrees in all images: one running north to south and the other running east to west. These features, which appear as areas of depleted background radioactivity, again correspond closely to Roman roads as depicted in the existing fluxgate gradiometer data (Figure 2). Interestingly, the May 2023 visualisations reflect the same localised area of radioactivity present in the far east side of Area B, as observed in the August 2022 data. Again, this is reflected in the count rate distribution graph for May 2023 (Figure 8), which suggests data are not normally distributed, with a bias towards moderate count rates. It is noted that the area containing the highest concentrations of radioactivity on the far right of the images broadly aligns with the Iron Age Oppida bordering the area.

Again, not all features of interest visible in the Fluxgate Gradiometer data are present in the gamma radiation heat maps. In particular, there is no indication of the presence of the smaller ditch or culvert running through the centre of this survey area.

As might be expected, those filters capable of smoothing the data and drawing out weaker features have yielded the best results for both datasets. Notably, the Wallis (Figures 7C and 9C), median (Figures 7D and 9D) and low pass (Figures 7E and 9E)

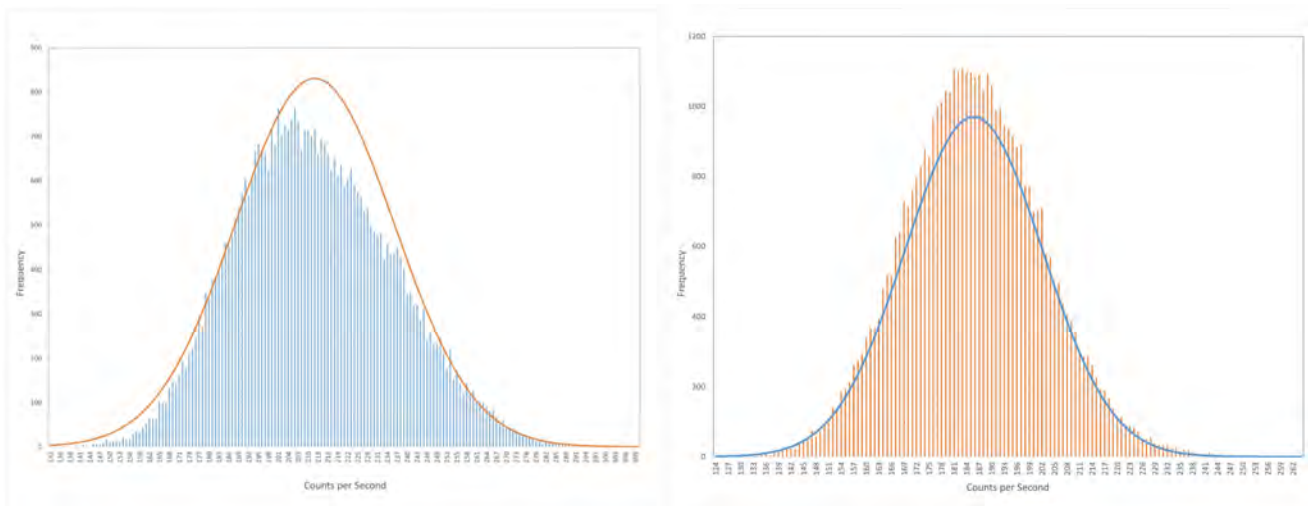


FIGURE 8 | Count rate distribution graphs for the August 2022 (left) and May 2023 (right) datasets. The August 2022 chart indicates that the background radioactivity is not normally distributed.

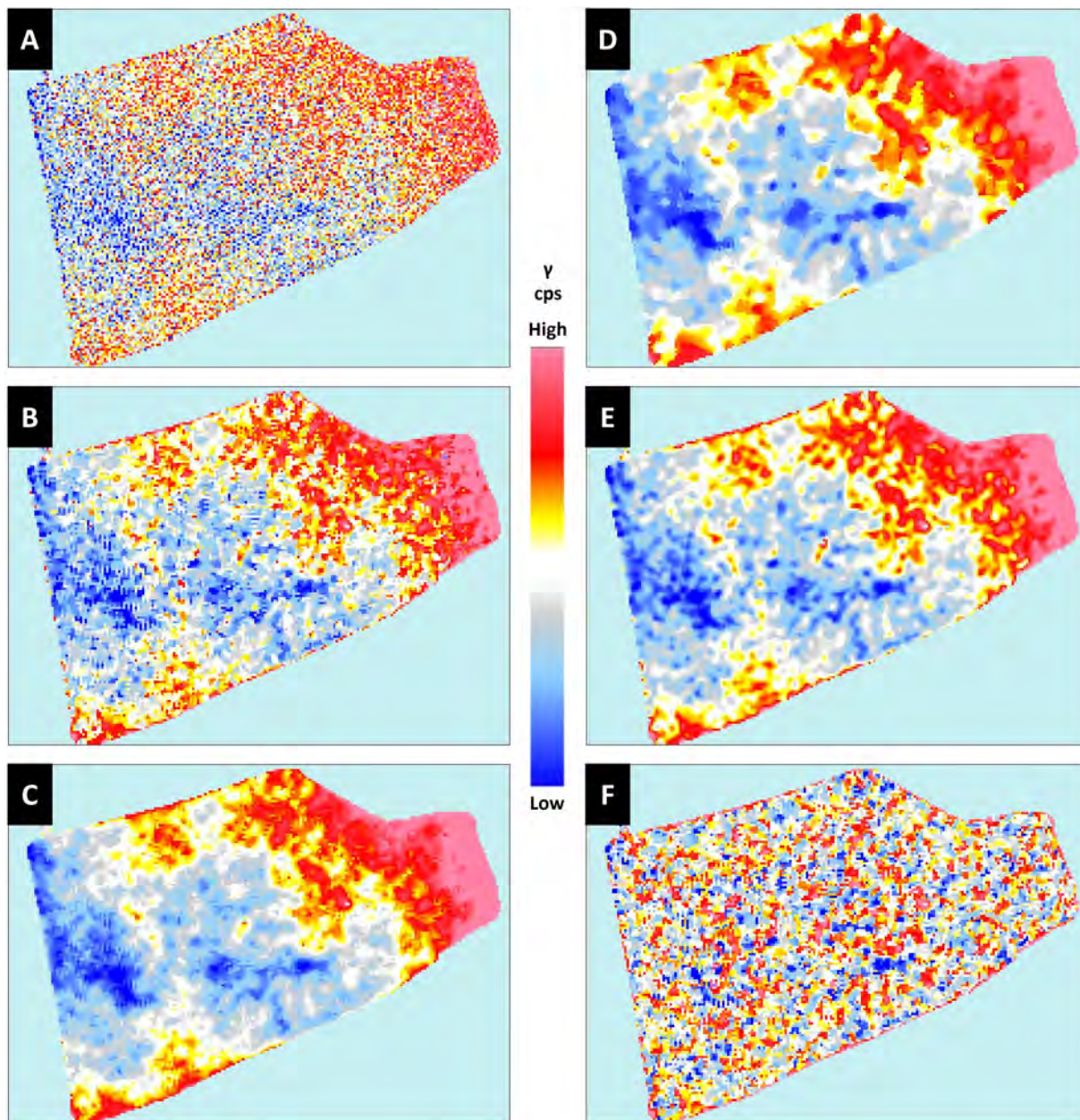


FIGURE 9 | Impact of different Geoplot processing tools on image quality for May 2023 total gamma counts (cps). The methods presented here are 'No Processing' (A), 'GPS Gap Fill' (B), Wallis Filter + GPS Gap Fill (C), Median Filter + GPS Gap Fill (D), Low Pass Filter + GPS Gap Fill (E) and High Pass Filter + GPS Gap Fill (F). The Wallis Filter + GPS Gap Fill (C) was identified as the preferred processing method.

filters have effectively reduced the 'noise' present and drawn out the linear features of the Roman roads without obscuring any detail. In contrast, the high pass filter that acts to remove low-frequency large-scale spatial detail (Geoscan 2014) has had a negative impact on image quality, obscuring features otherwise visible (Figures 7F and 9F).

5.2 | Understanding the Impact of Individual Radionuclides

Figures 10 and 11 provide visualisations for the contributions of individual radionuclides within the August 2022 and May 2023 surveys, respectively. Interestingly, visualisations for the

potassium, thorium and caesium energy window data collected during the August 2022 survey (Figure 10A,C,D) reflect the findings of the total gamma count data; that count rates increase as you move eastwards across the survey areas.

For both the August 2022 and May 2023 surveys, the roads are faintly visible within the potassium energy window (Figures 10A and 11A), albeit to a lesser degree in the August 2022 figures. This may be due to the generally higher number of counts attributable to potassium in the May survey, making any shielding effects from the roads more prominent.

Uranium and thorium appear to be broadly uniformly distributed across the survey areas in both the August 2022

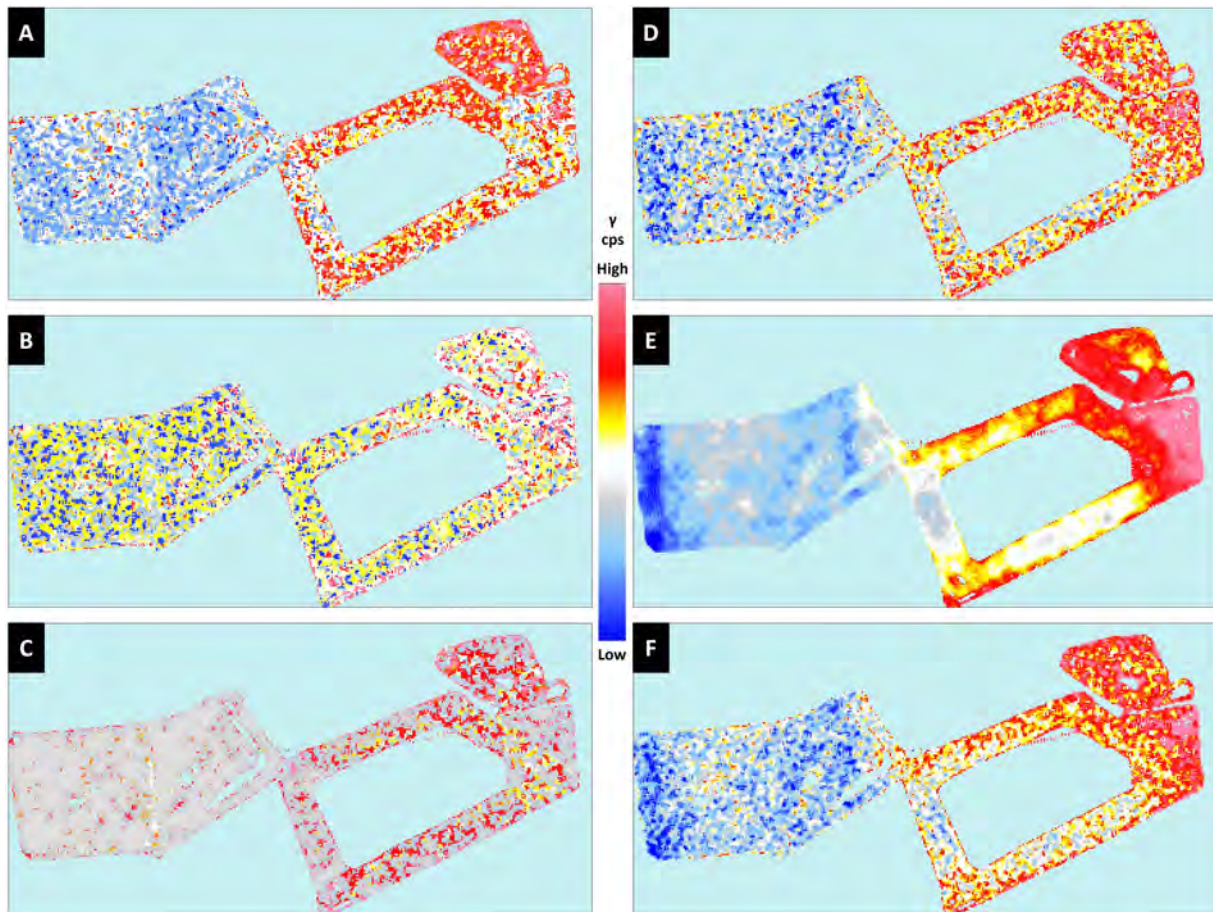


FIGURE 10 | Application of the Wallis Filter+GPS Gap Fill to the following regions of interest within the August 2022 dataset, as per Table 2: potassium (A), uranium (B), thorium (C), caesium (D), below window (E) and above window (F).

(Figure 10B,C) and May 2023 (Figure 11B,C), with no anomalies visible.

The linear features of the Roman roads are visible in the caesium data in the August 2022 visualisation (Figure 10D) and to a lesser extent in May 2023 (Figure 11D).

Data extracted from the ‘below window’ (Figures 10E and 11E) and ‘above window’ (Figure 11E,F) energy windows show that the contrast for the roads are most prominent here. The below window visualisations generate the highest quality images, even though it covers the smallest energy range (0–530 keV, relative to the 730–3000 keV emissions captured in the ‘above window’ dataset). This is in part attributable to the detector capturing gamma rays emitted from a range of naturally occurring radionuclides with similar energies including Pb-214 (with gamma photon energies of 52.2, 241.9, 295.2 and 351.9 keV), Ra-226 (with a gamma photon energy of 186.2 keV) and U-238 (with gamma photon energies of 49.5 and 113.5 keV) (IAEA 2008). Further, it is noted that NaI detectors of the dimensions used within the Groundhog® system (76 mm × 76 mm) are particularly efficient in this energy window (Mirion 2023).

Figures 10 and 11 suggest that potassium and caesium have the greatest impact on the visibility of any subsurface features.

However, it is acknowledged that it is the total gamma counts that provide the best quality images overall. This is particularly well demonstrated in Figures 12 and 13 that show the combined August 2022 and May 2023 total gamma visualisations overlaying the Fluxgate Gradiometer data of Creighton and Fry 2016. These figures clearly show the alignment of the Roman roads between the two types of data. Figure 13 also provides an overlay of building outlines for further context. This confirms the absence of other key features such as the temple.

6 | Discussion

The surveys undertaken as part of this latest study underpin the findings of the preliminary investigation completed by Robinson et al. (2022). They have confirmed that portable gamma surveying methods can be effective at identifying features of archaeological interest. This is achieved by detecting measurable differences in concentrations of naturally occurring radioactive material present in or above archaeological targets and surrounding soil. However, as for the preliminary study, the August 2022 and May 2023 surveys have yielded mixed results.

Neither of the buildings or the thin linear Roman trench within *Insulae VII, XXXV* or *XXXII* were capable of generating

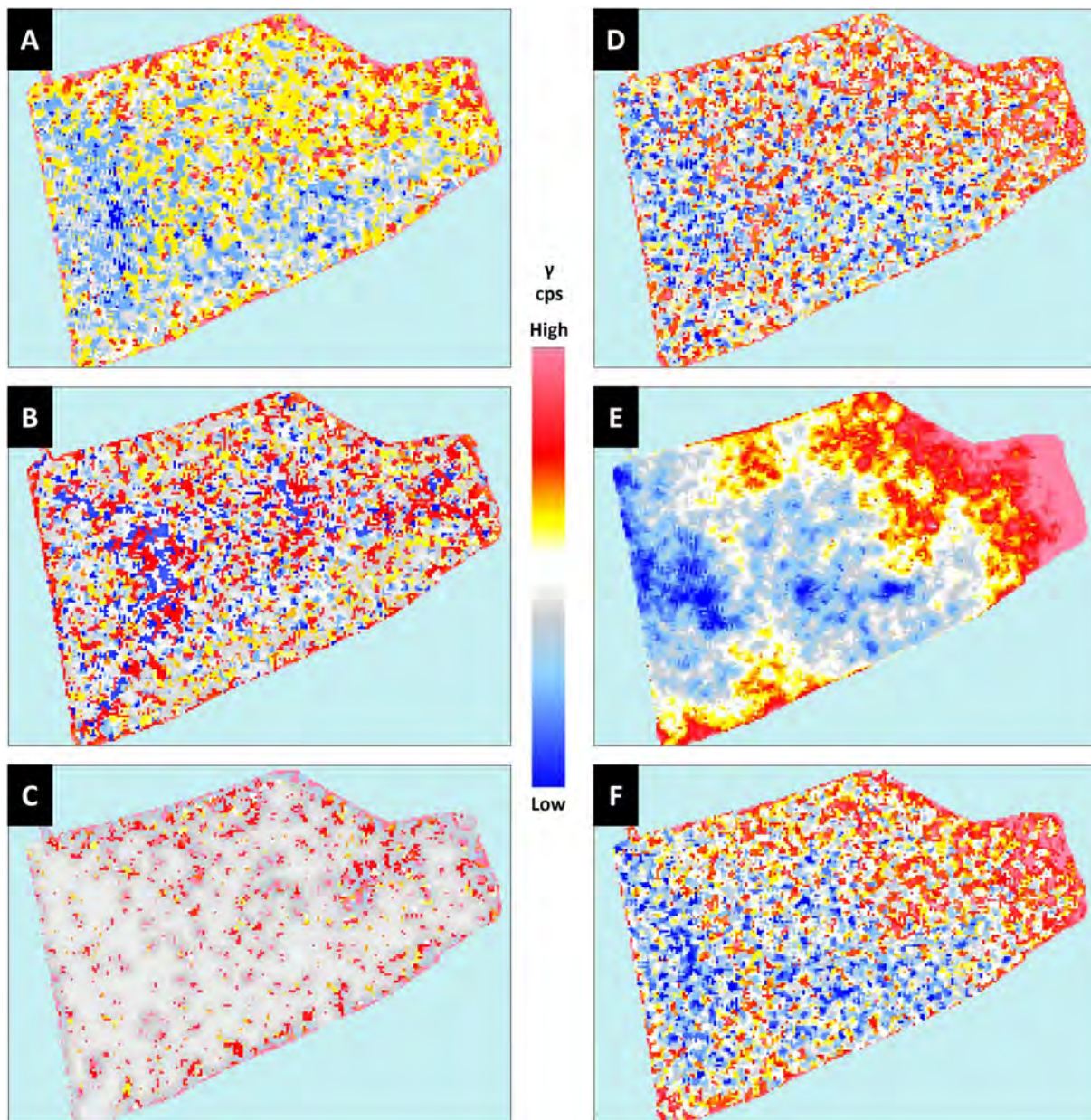


FIGURE 11 | Application of the Wallis Filter+GPS Gap Fill to the following regions of interest within the May 2023 dataset, as per Table 2: potassium (A), uranium (B), thorium (C), caesium (D), below window (E) and above window (F).

measurable contrasts in radioactivity as to be distinguished in the visualisations. This reflects the findings of the preliminary study which also failed to delineate the outlines of known buildings. It is possible that this is attributable to the less robust structures of these buildings, reducing their ability to create a sufficient contrast in background gamma radiation measurements. This effect may be exacerbated by the resolution of the surveys. Alternatively, it is possible that the materials of construction have a similar gamma radionuclide composition to the surrounding soil than observed for the roads. While the difficulty in clearly delineating these less substantial features may be expected for these reasons, it is interesting that there are no general areas of localised increased or decreased counts attributable to the disturbance caused by this past activity. Further work is therefore planned to explore this finding through collection and analysis of samples of building materials and soils.

A welcome finding of this latest study was the ability to delineate road structures. This was not achieved in the preliminary study. In both the August 2022 and May 2023 data, roads appear as areas of low background radioactivity. Particular attention is drawn to the roads visible in the August 2022 ‘total gamma’ visualisations (Figure 7). In all iterations of this image, Silchester’s primary north–south road, visible on the left-hand side of each image, is the most prominently featured, followed by a secondary north–south road to the right. In contrast, the east–west road is showing a very weak contrast and is incomplete in the gamma data. This variability is absent in the Fluxgate Gradiometer data shown in Figure 2. It is suggested that variations in the observed gamma radionuclide content of the roads may be indicative of varying thicknesses of road material which possesses a lower concentration of radioactive material relative to the surrounding soil. Consequently, it shields the gamma radiation emitted from

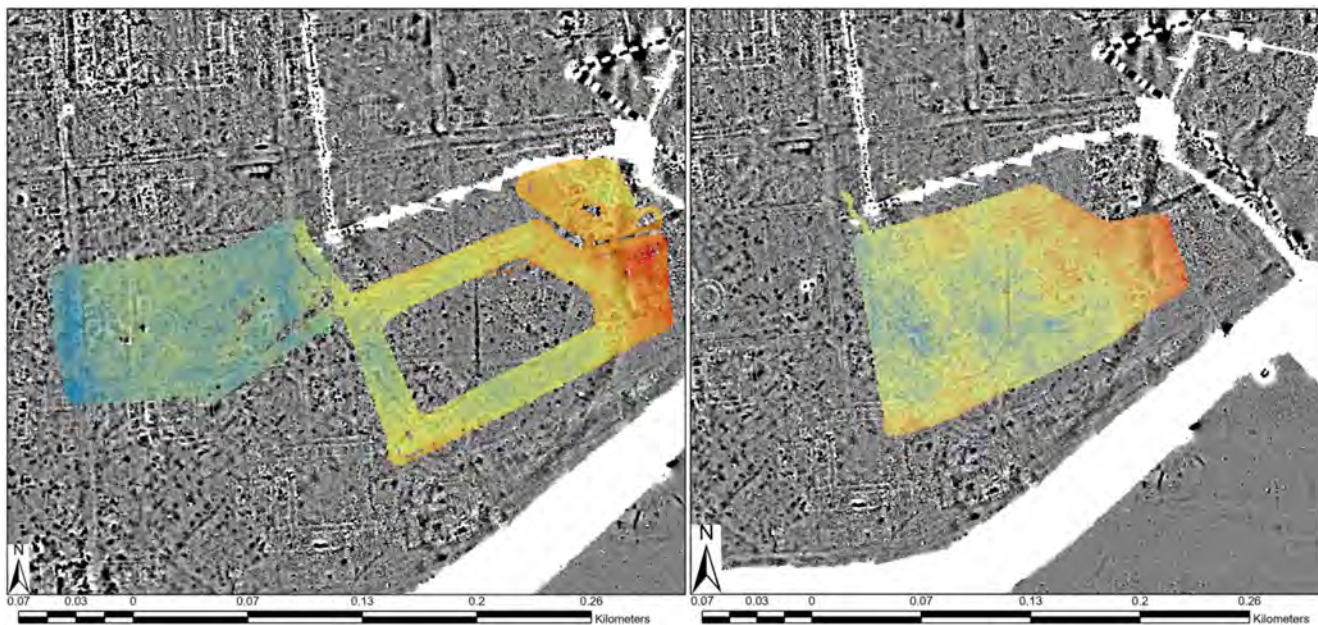


FIGURE 12 | August 2022 (left) and May 2023 (right) Geoplotted-processed data overlaid on existing Fluxgate Gradiometer data, demonstrating the alignment of observed anomalies. Gamma radiation data has been set at 25% transparency to reveal underlying anomalies.

Source: Fluxgate Gradiometer Data from Creighton and Fry (2016).

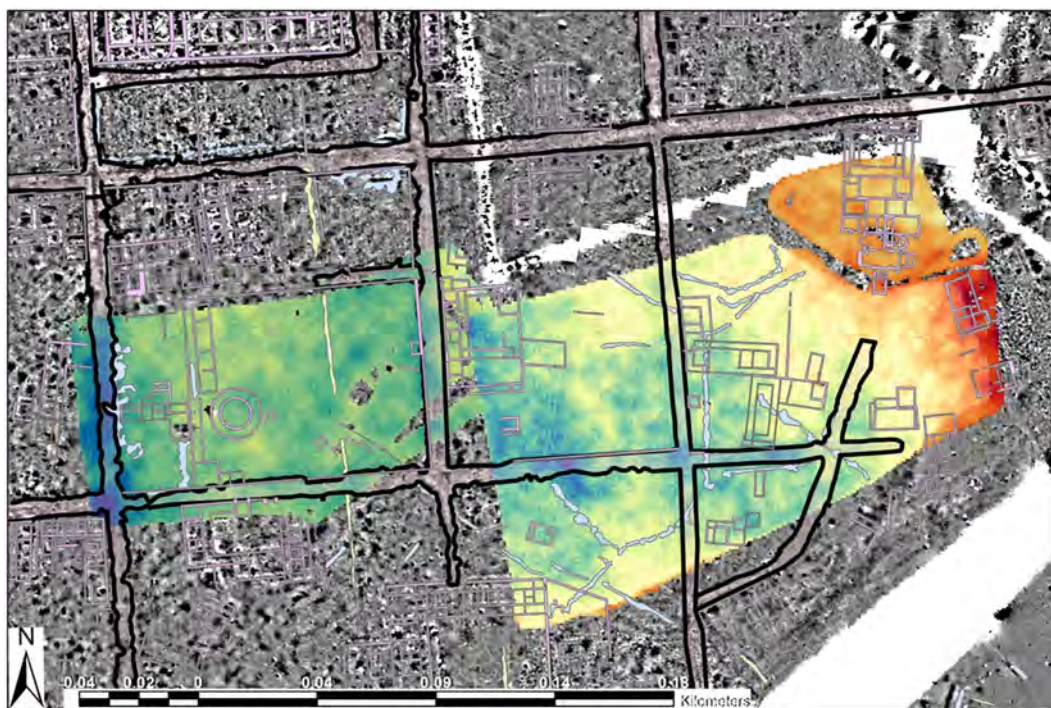


FIGURE 13 | Combined August 2022 and May 2023 Geoplotted-processed data overlaid on existing Fluxgate Gradiometer data, with previously mapped features overlaid demonstrating alignment of the anomalies in the gamma radiation data with known features. Overlaid data include the Antiquaries Great Plan (pink lines), the Fluxgate Gradiometer interpretation of the roads (black outlines), positive linear features in the Fluxgate Gradiometer data (blue lines) and historic field boundary from 1759 (red dotted line).

the underlying soil to a different extent. This is supported by the work of Fulford, Clarke, and Pankhurst (2024) who note that the main north–south road is a substantial structure, measuring up to 7.6 m in width and approximately 1 m in thickness. In contrast, the east–west road is up to 6 m wide and 0.85 m thick

(Fulford, Clarke, and Pankhurst 2024). Another factor contributing to the observed variations in the gamma radionuclide content of the roads is the extent of material consolidation. Previous excavations revealed that the materials comprising the main north–south road had become cemented together, presenting a

more solid mass (M. Fulford, personal communication). This increased consolidation, combined with the increased thickness in the road material, may have enhanced the shielding effect. The cause of this cementation process is unknown but may be attributable to the heavy use of this street and its accommodation of carts carrying substantial loads of up to 500 kg (M. Fulford, personal communication). This discovery suggests that portable gamma radiation data collected as part of an archaeological investigation could aid interpretation of traditional geophysical survey outputs, enhancing the value of other nonintrusive surveys. This is particularly relevant when it is recognised that in the fluxgate gradiometer dataset, the clear delineation of the roads is largely attributable to the accompanying roadside ditches, rather than the deposition of the flint and gravel itself.

In addition to the linear anomalies attributable to the roads, another feature of interest is the transition from an area of lower radioactivity in Area A to higher activity in Area B. This is clearly visible in the August 2022 survey data (Figure 7). The point of transition, where Areas A and B connect, aligns closely with a historic field boundary visible in a 1759 plan of Silchester, as depicted in Figure 13. This boundary may be indicative of differing land uses that have caused changes in soil chemistry or composition, which in turn has influenced the adsorption/retention of radionuclides. This field boundary may also be visible in the gamma radiation data. In the May 2023 survey, there is a north–south aligned linear feature, present as an area of depleted radioactivity, running along the left-hand edge of the survey area (Figure 9). Specifically, this appears to be attributable to localised reductions in concentrations of potassium, thorium and caesium (Figure 11). As shown in Figure 13, this linear anomaly does not align with any of the Roman roads but does closely follow the 1759 boundary. It is noted that this boundary is not present in the later 1841 tithe map for the area (Hampshire Archives 2023a). However, the accompanying Tithe Award identifies the area within which the gamma radiation survey data sits as the ‘Watch Field and the Nine Acres’ (Hampshire Archives 2023b). The area to the right of the 1759 field boundary is approximately nine acres in size. This further suggests that the two sides of this field remained distinct for an extended period, even though the physical field boundary was no longer present.

The area containing the highest levels of radioactivity, running along the right-hand edge of Area B is present in both the August 2022 and May 2023 data. This aligns closely with the location of the Iron Age ditch and an area prone to waterlogging.

The waterlogged area aligning with the Iron Age ditch is expected to have a different chemistry to the adjacent soil. This difference can influence the behaviour of naturally occurring radionuclides present. For example, uranium in soils is commonly found as a mobile form of UO_2 in its U (VI), particularly in slightly basic to acidic soils (Smedley and Kinniburgh 2023). However, under strongly reducing conditions, the uranium can be reduced to its U (IV) state, leading to its precipitation as an immobile form of UO_2 or otherwise become sorbed onto the surface of soil particles (Smedley and Kinniburgh 2023), thereby increasing uranium concentrations in the soil. The waterlogged area at Silchester could provide such conditions.

Further, this area is rich in clay deposits, contributing to waterlogging. The Iron Age defensive ditch is cut into London Clay, eventually becoming infilled with a mixture of clays and anthropogenic deposits, including brick and organic materials (M. Fulford, personal communication). The location of the elevated radioactivity coincides with an area where the gravel capping over the London Clay had been eroded away (M. Fulford, personal communication). The presence of these clay deposits increases the chance of accumulating radionuclides such as caesium-137 which adsorbs strongly to clay particles (Ritchie 1998). The authors intend to further characterise this area as part of ongoing research to gain a better understanding of the geochemical properties of the area and how these properties vary across the site profile.

The equipment failure during the August 2022 survey and requirement to resurvey the eastern side of the site provided an additional opportunity to explore the impact of changing soil moisture content on the effectiveness of portable gamma surveying, recognising the potential for shielding from interstitial water. The August 2022 survey was conducted in what may be considered optimal ground conditions, minimal soil moisture following an extended period of very low rainfall and high temperatures. Indeed, evidence suggests that this was the fourth driest summer on record (McCarthy 2022). This contrasts with the meteorological conditions in May 2023, where the first half of the month saw rainfall levels exceed the mean value for the period 1991–2020 for the same month (Met Office 2023). As a result, soil moisture content and therefore potential for increased gamma radiation shielding was much higher in May. It might therefore be expected that the May 2023 survey would yield lower quality results. However, as seen in Figures 7 and 9, groundwater in this case does not appear to have a significant impact on data quality, with road structures clearly visible in both conditions. However, it is noted that this survey has resulted in generally lower levels of radioactivity recorded overall, which is expected to be attributable to a degree of shielding by interstitial water. It is recognised that this result in isolation is insufficient to draw any meaningful conclusions on this aspect, and therefore, further research is required to fully understand the impact of groundwater conditions on gamma survey data quality in archaeological applications.

In addition to the aspects identified for further investigation already discussed, it is acknowledged that there are still multiple other areas that require further exploration. This includes conducting surveys at different locations to explore the impact of varying geologies, testing the responses of different target types (e.g., considering materials of construction, size and burial depths) and the completion of surveys in more controlled conditions to facilitate better control of individual variables.

7 | Conclusions

This study has provided a valuable opportunity to further challenge the viability of portable gamma surveying as a contributory tool for nonintrusive archaeological prospection. This has been achieved by:

1. Testing the replicability of the technique by surveying areas containing analogous target types to the preliminary study completed by the authors;
2. Testing scalability of the technique by applying a vehicle-mounted Groundhog® system; and
3. Exploring alternative data processing methods to improve the quality of the visualisations used to identify anomalies that could be attributable to archaeological features of interest.

Completion of this latest suite of gamma radiation surveys has confirmed that the method can be successfully scaled to encompass a much larger survey area without compromising data quality. As per the preliminary investigation, the latest surveys have yielded mixed results with the Groundhog® system successfully delineating some known archaeological features such as Roman roads, while failing to detect others such as buildings. Interestingly, the types of targets detectable have not been consistent between the two studies. In the preliminary study, roads and buildings could not be identified whereas ditches created clear anomalies. In this latest study, roads were consistently capable of generating anomalies within the gamma radiation data, whereas this was less successful for the ditches. Where the area of elevated radioactivity aligns with the Iron Age ditch, there is some uncertainty as to whether the anomaly can be attributed to the ditch itself or if it is indicative of ground disturbance associated with past excavations.

The strength of the anomalies associated with each road may indicate variations in either the depth of road material or construction materials, suggesting that gamma radiation data could aid interpretation of other geophysical survey outputs. This strengthens the argument that portable gamma surveying can add value to nonintrusive archaeological investigations.

There is notable uncertainty regarding the causes of some of the observed outcomes. This uncertainty relates to the absence of measurable differences in gamma radiation levels present in/over archaeological targets (identified as being strong candidates) and surrounding soils and the discrepancy in the types of targets discernible in the preliminary and current investigations. Consequently, additional investigations and research is imperative if these uncertainties are to be adequately addressed. This will be achieved through the direct radiochemical analysis of samples of soil and target material and surveying of new archaeological sites.

The use of an alternative software tool, Geoplot, has provided a valuable opportunity to apply different processing tools to enhance the quality of visualisations generated. This was successful, with the Wallis filter, in particular, being able to draw out features of interest without deviating too far from the raw data.

The ability to investigate the influence of individual radionuclides on the results observed has also produced interesting insight and may aid interpretation of the total gamma visualisations. This includes identifying areas of ground disturbance

indicative of previous excavation works. It is believed that this area also warrants further explanation.

Overall, this latest study has proven to be a successful progression of the preliminary investigation confirming that portable gamma surveying methods can identify archaeological features of interest. However, further work is now required to better understand what types of features are most amenable to this technique and how it can be most effectively applied.

Acknowledgements

This unique investigation was possible thanks to Nuvia Limited who provided access to the Groundhog® fusion vehicle-mounted system and supporting software tools. The authors wish to express their thanks and gratitude to Ben Kolosowski and the University of Reading for permitting and facilitating access to the Silchester site and to Anthony Sweeney for helping to set up the equipment at Silchester.

Conflicts of Interest

The authors declare no conflicts of interest.

Data Availability Statement

The data that support the findings of this study are available from the corresponding author upon reasonable request.

References

- Aliyev, C. 2004. "NORM in Building Materials." In *IAEA (2004) Naturally Occurring Radioactive Materials (NORM IV): Proceedings of an International Conference Held in Szczyrk Poland, 17–21 May 2004*, IAEA-TECDOC-1472. Vienna Austria: IAEA.
- Creighton, J., and Fry, R. 2016. *Silchester: Changing Visions of a Roman Town: Integrating Geophysics and Archaeology: The Results of the Silchester Mapping Project, 2005-10*, Britannia Monograph Series; vol. 28, Hampshire, UK: Society for the Promotion of Roman Studies. ISBN: 9780907764427.
- Cuenca-Garcia, C. 2018. "Soil Geochemical Methods in Archaeogeophysics: Exploring a Combined Approach at Sites in Scotland." *Archaeological Prospection* 26, no. 1: 57–72. <https://doi.org/10.1002/arp.1723>.
- Digimap. 2023. Silchester Overview, PDF Map, Scale 1:10000, Projection: British National Grid (EPSG:27700), OS Master Map, March 2023, Ordnance Survey Using Digimap Ordnance Survey Collection. Created 22 October 2023. <https://digimap.edina.ac.uk/>
- Fulford, M. 2021. *Silchester Revealed: The Iron Age and Roman Town of Calleva*. Havertown: Windgather Press. ISBN: 9781911188865.
- Fulford, M., A. Clarke, J. Eaton, et al. 2019. *Silchester Roman Town: The Baths 2019*. Reading, UK: Department of Archaeology, University of Reading.
- Fulford, M., A. Clarke, and N. Pankhurst. 2024. *Silchester Insula IX. Oppidum to Roman City, c. A.D. 85-125/50. Final Report on the Excavations 1997–2014*, London, Society for the Promotion of Roman Studies. Britannia Monograph 37.
- Gaffney, C., and J. Gater. 2011. *Revealing the Buried Past: Geophysics for Archaeologists*. Gloucestershire, UK: Tempus Publishing Ltd.
- Geoscan. 2014. Geoplot Version 3.0 for Windows: Datasheet Issue 13, GPW300_13 PPX2, June 2014. Accessed October 2023. Created June 2014, http://www.geoscan-research.co.uk/Geoplot3_v13_Data_Sheet.pdf.

- Hampshire Archives. 2023a. Plan of the Parish of Silchester in the County of Hants 1841. Accessed October 2023.
- Hampshire Archives. 2023b. Apportionment of the Rent-Charge in Lieu of Tithes in the Parish of Silchester in the County of Southampton (sic), Published by Routledge London 1841. Accessed October 2023.
- IAEA. 2003. *Extent of Environmental Contamination by Naturally Occurring Radioactive Material (NORM) and Technological Options for Mitigation*, Technical Report Series No. 419, International Atomic Energy Agency, Vienna.
- IAEA. 2008. *Handbook of Nuclear Data for Safeguards: Database Extensions, INDC (NDS)534*. Vienna: International Atomic Energy Agency.
- IAEA. 2017. *In Situ Analytical Characterization of Contaminated Sites Using Nuclear Spectrometry Techniques, Review of Methodologies and Measurements*, IAEA Analytical Quality in Nuclear Applications Series No. 49, International Atomic Energy Agency, Vienna.
- IAEA. 2023. Radiation in Everyday Life. Vienna: International Atomic Energy Agency (IAEA). Accessed 21 January 2023. <https://www.iaea.org/Publications/Factsheets/English/radlife>.
- Jordan, D. 2009. "How Effective Is Geophysical Survey? A Regional Review." *Archaeological Prospection* 16: 77–90. <https://doi.org/10.1002/arp.348>.
- Kozhevnikov, N. O., A. V. Kharinsky, and S. V. Snopkov. 2018. "Geophysical Prospection and Archaeological Excavation of Ancient Iron Smelting Sites in the Barun-Khal Valley on the Western Shore of Lake Baikal (Olkhon Region, Siberia)." *Archaeological Prospection* 2018: 1–17. <https://doi.org/10.1002/arp.1727>.
- Lee, C. J., and P. H. Burgess. 2014. *Good Practice Guide 14, The Examination, Testing and Calibration of Portable Radiation Protection Instruments*. NPL, Middlesex, UK: National Physics Laboratory (NPL) Issue 2, First Issued—1999, Updated—2014.
- Linford, N., P. Linford, and A. Payne. 2019. *Silchester Roman Town Hampshire: Report on Geophysical Surveys June 2009, March 2014 and July 2015*, Research Report No. 85-2019. Portsmouth, UK: Historic England, ISSN: 2059-4453.
- Lovelock, J. 2000. *Gaia: A New Look at Life on Earth*. Oxford, UK: Oxford University Press. ISBN: 9780192862181.
- McCarthy, M. 2022. "Guest Post: A Met Office Review of the UK's Record-Breaking Summer in 2022." *Carbon Brief*. Accessed 17 August 2023 Last Updated: 28/09/2022. <https://www.carbonbrief.org/guest-post-a-met-office-review-of-the-uks-record-breaking-summer-in-2022/>.
- Met Office. 2023. May 2023 Monthly Weather Report. Accessed October 2023. Last Updated: May 2023. https://www.metoffice.gov.uk/binaries/content/assets/metofficegovuk/pdf/weather/learn-about/uk-past-events/summaries/mwr_2023_05_for_print.pdf.
- Milsom, J., and A. Eriksen. 2011. *The Geological Field Guide Series: Field Geophysics*. 4th ed. Sussex, UK: Wiley-Blackwell.
- Mirion. 2023. *Gamma and X-Ray Detection*. Harwell, UK: Mirion Technologies. Accessed 10 December 2023, <https://www.mirion.com/discover/knowledge-hub/articles/education/nuclear-measurement-fundamental-principle-gamma-and-x-ray-detection>.
- Porcelli, F., L. Sambuelli, C. Comina, et al. 2020. "Integrated Geophysics and Geomatics Surveys in the Valley of the Kings." *Sensors (Basel, Switzerland)* 20, no. 6: 1552. <https://doi.org/10.3390/s20061552>.
- Ritchie, J. C. 1998. "¹³⁷Cs Use in Estimating Soil Erosion—30 Years of Research." In *IAEA (1998) Use of ¹³⁷Cs in the Study of Soil Erosion and Sedimentation, IAEA-TECDOC-1020*. Vienna: International Atomic Energy Agency.
- Robinson, V., R. Clark, S. Black, R. Fry, and H. Beddow. 2022. "Portable Gamma Ray Spectrometry for Archaeological Prospection: A Preliminary Investigation at Silchester Roman Town." *Archaeological Prospection* 29, no. 3: 353–367. <https://doi.org/10.1002/arp.1859>.
- Ruffell, A., and J. McKinley. 2008. *Geoforensics*. New Jersey, USA: Wiley-Blackwell.
- Simon, F. X., T. Kalayci, J. C. Donati, C. Cuenca-García, M. Manataki, and A. Sarris. 2015. "How Efficient Is an Integrative Approach in Archaeological Geophysics? Comparative Case Studies From Neolithic Settlements in Thessaly (Central Greece)." *Near Surface Geophysics* 13, no. 6: 633–643. <https://doi.org/10.3997/1873-0604.2015041>.
- Smedley, P. L., and D. G. Kinniburgh. 2023. "Uranium in Natural Waters and the Environment: Distribution, Speciation and Impact." *Applied Geochemistry* 148: 105534. <https://doi.org/10.1016/j.apgeochem.2022.105534>.
- Ward, J. 1911. *Romano-British Buildings and Earthworks, Chapter 10, Volume 24 of Antiquary's Books*. North Yorkshire, UK: Methuen & Company Limited. ISBN: 0598613269, 9780598613264.
- Wynn, J. C. 1986. "A Review of Geophysical Methods in Archaeology." *Archaeology* 1, no. 3: 245–257. <https://doi.org/10.1002/gea/3340010302>.